Diss. ETH No. 20066

New Rhenium-Catalyzed Reactions: From Asymmetric Hydrogenation to Trifluoromethylation

A dissertation submitted to
ETH ZÜRICH

for the degree of
DOCTOR OF SCIENCES

presented by
OSCAR ESTEBAN MEJIA VARGAS
Master of Sciences - Chemistry, National University of Colombia
born on February 2th, 1981
citizen of Colombia

accepted on the recommendation of
Prof. Dr. Antonio Togni, examiner
Prof. Dr. Christophe Copéret, co-examiner

Zürich, 2011

A mis padres y a mi hermano

"Chemie ohne Katalyse ist wie ein Schwert ohne Griff, eine Kerze ohne Licht oder eine Glocke ohne Klang."

"Chemistry without catalysis is like a sword without a hilt, a candle without light or a bell without sound."

Alwin Mittasch

"Какой-то математик сказал, что наслаждение не в открытии истины, но в искании ее."

"Some mathematician has said that enjoyment lies in the search for truth, not in the finding it."

Лев Толстой (Анна Каренина)
Leo Tolstoy (Anna Karenina)

Table of Contents

Acknowledgements - Agradecimientos i
Abstract iii
Zusammenfassung vii

1. General Introduction 1
  1.1. The Discovery of Rhenium 1
  1.2. Chemistry of Rhenium Compounds 3
    1.2.1. Rhenium species with formal negative oxidation states 3
    1.2.2. Rhenium(0) 4
    1.2.3. Rhenium(I) 5
    1.2.4. Rhenium(II) 6
    1.2.5. Rhenium(III) 7
    1.2.6. Rhenium(IV) 9
    1.2.7. Rhenium(V) 10
    1.2.8. Rhenium(VI) 11
    1.2.9. Rhenium(VII) 12
  1.3. Applications of Rhenium Complexes in Catalysis 15
    1.3.1. C-C Bond forming reactions 17
    1.3.2. C-N Bond forming reactions 21
    1.3.3. C-O Bond forming reactions 23
    1.3.4. Hydrosilylations 24
    1.3.5. Hydrogenations and dehydrogenations 27
    1.3.6. Oxygen transfer reactions and oxidations 30
    1.3.7. Olefin metathesis 33
  References 36

2. Asymmetric Transfer Hydrogenation 41
  2.1. Introduction 41
    2.1.1. Ferrocenylphosphine ligands of the Josiphos family 42
  2.2. Synthesis and Characterization of the Complexes 43
    2.2.1. Ligand synthesis 43
    2.2.2. Synthesis of rhenium(I) derivatives 44

*2.2.3. Synthesis of rhenium(V) derivatives of the type [ReOX$_3$(**2**)] (X = Cl, Br)* 50
2.2.4. Synthesis of other rhenium(V) derivatives with Josiphos ligands 61
2.2.5. Synthesis of rhenium(V)-oxotrichloride derivatives with other diphosphine ligands 64
2.3. Transfer Hydrogenation of Ketones 65
2.3.1. Method development 65
2.3.2. Mechanistic considerations 69
2.4. Conclusion 72
References 73

3. Chiral Rhenium Hydrido Complexes and Catalytic Hydrogenation 77
3.1. Introduction 77
3.1.1. Pigiphos ligands 78
3.2. Synthesis and Characterization of the Complexes 79
3.2.1. Ligand synthesis 79
3.2.2. Synthesis of rhenium(I) derivatives of ***19a*** 79
3.2.3. Synthesis of rhenium(V)-oxo derivatives 83
*3.2.4. Synthesis of the rhenium(III) derivatives [ReCl$_3$(**19**)] (**23**)* 84
3.2.5. Synthesis of rhenium(V) and -(VII) polyhydrides 86
3.3. Reactions of the Rhenium Polyhydrides with Brønsted Acids and Hydride Scavengers 95
3.4. Catalytic Hydrogenation of Dimethyl Itaconate 98
3.4.1. Development of the method 98
3.4.2. Mechanistic considerations 99
3.5. Conclusion 101
References 102

4. Aromatic Trifluoromethylation 105
4.1. Introduction 105
4.1.1. Trifluoromethylation 105
4.1.2. Methyltrioxorhenium (MTO) 108
4.2. Rhenium-Catalyzed Aromatic Trifluoromethylation 110
4.2.1. Reaction discovery and development: a case of serendipity 110
4.2.2. Substrate screening and reaction scope 112

4.3. Mechanistic Studies 115

4.3.1. ^{17}O NMR 115

4.3.2. Time dependant ^{19}F NMR 117

4.3.3. EPR 120

4.3.4. Deuterium kinetic isotope effect 124

4.3.5. UV-Vis 125

4.3.6. Mechanistic proposal 126

4.4. Conclusion 127

References 128

5. General Conclusion and Outlook 131

6. Experimental Part 133

6.1. General Methods 133

6.1.1. Starting materials 133

6.1.2. Analytical methods and instruments 134

6.2. Asymmetric Transfer Hydrogenation (Chapter 2) 135

6.2.1. Synthesis of ligands and complexes 135

6.2.2. Transfer hydrogenation catalysis 156

6.3. Chiral RheniumHydrido Complexes and Catalytic Hydrogenation (Chapter 3) 158

6.3.1. Synthesis of ligands and complexes 158

6.3.2. Hydrogenation catalysis 167

6.4. Aromatic Trifluoromethylation (Chapter 4) 168

6.4.1. Trifluoromethylation catalysts 168

6.4.2. Mechanistic studies 177

References 179

7. Appendix 181

7.1. Crystallographic Information 181

7.1.1. Experimental details 181

7.1.2. Crystallografic data and tables 181

7.2. Publications 197

7.3. Participations in Conferences and Symposia 197

7.4. Curriculum Vitae 199

Acknowledgements - Agradecimientos

In the first place I want to tank my Doktorvater, Prof. Antonio Togni for giving me the opportunity to join his group in Zürich, for believing in me and for being always willing to help me and guide me through the sometimes obscure path of research. Herzlichen Dank, grazie mille!

Andrea Sachs, our incredibly efficient secretary, deserves here a special Danksagung, not only for always being ready to solve my small problems with the Swiss bureaucracy, but also for having always, no matter what, a smile on her face. Danke schön!

Special tanks to Prof. Antonio Mezzetti for all the advices and interesting discussions (not only in the realms of chemistry). I'd also like to thank him for the wonderful opportunity to be his Teaching Assistant. Grazie!

To Dr. Benoît Pugin from Solvias AG, thanks not only for generously providing us with some compounds, but also, and specially, for his help, guidance and insightful advices during my brief time in Basel. Merci vielmal!

To Prof. Christophe Copéret for being my co-examiner, for the proof-reading and correction of this text and for his useful advices. Merci beaucoup!

To the ETH staff that in a way or another helped me to accomplished my research and made possible my way through my PhD. Thanks to Dr. Heinz Rüegger†, Dr. Aitor Moreno and Dr. Réne Verel for their help with the NMR and to Dr. Gustavo Santiso for his help with the X-ray. Herzlichen Dank to Dr. Reinhard Kissner for his invaluable help with the EPR and UV experiments. Also thanks to the people in the MS-service and in the Schalter, specially to Carmela Pansino.

To all of the former and current members of the Togni and Mezzetti groups for the help and patience during all these years. Thanks to Barbara for her support in the NMR and to the "Crystallographic people" Pietro, Raphael, Katrin and Elli. I'm specially thankful to my closest lab-mates and friends, Jamal, Jan, Tina, Aline, Laurence, Peter, Elli and Vasek. To all of them,

thanks for making my time in ETH a bit less traumatic. Merci, vďaka, Danke, gracias, díky!!

To my students, Nikolas Huwyler, Marco Kobelt and Pascal Engl for joining me in this adventure, for doing part of the job and for having me as their Advisor. To my "Praktikum" students, specially Diana Andina, Johanes Boshkow, Julian Bleich, Lukas Bregy, Céline Capelli and (last but not least) Laura & Lyndsey Hendriks, not only for cooking some of my compounds, but specially for the nice time we had together.

Un agradecimiento de todo corazón a toda mi gente linda que a lo largo de todos estos años me acompañó por el sinuoso y pedregoso camino que hoy me ha traído hasta este punto. Juan, Rafa, Lucho, Eliza, Marija (хвала!), Gustavo y Fernando. Gracias por su amistad y sobretodo por estar siempre ahí, cuando los necesité. A Luisa, gracias por su compañía, su amor, su alegría y por ser como es; de no ser por ella, la historia hubiera sido diferente. De nuevo a ellos, ¡gracias totales!

A la familia Fischer, Elsa, Joaquín, Nicole Tatiana y Mónica, no sólo por acogerme en su hogar sino también por hacerme sentir que tengo una familia en Suiza. No me alcanzarían las palabras para expresar toda mi gratitud, así que la resumo en un inmenso "Gracias".

Gracias también, por supuesto, a la gente que me hizo posible dar el salto transatlántico; a mi primer mentor, Prof. Ricardo Fierro por mostrarme el camino de la Química Organometálica y al Prof. Luca Fadini, por convencerme de que sí es posible. A ambos muchas gracias por sus enseñanzas, por creer en mí y en últimas, por traerme hasta aquí.

Por último, para cerrar con broche de oro, quiero agradecer a mi familia, mi papá, mi mamá y mi hermano, a quienes debo lo que soy y donde estoy. Este pequeño trabajo, y lo que éste representa, es dedicado a ellos porque es un logro suyo, no mío, el que yo esté cumpliendo este sueño. ¡Mil y mil gracias!

Abstract

The present doctoral dissertation describes the synthesis and characterization of new rhenium complexes and their application as catalysts in different homogeneous transformations, i. e. asymmetric hydrogenation, transfer hydrogenation and trifluoromethylation.

The first part (chapter 2) describes the synthesis and characterization a series of new rhenium complexes containing chiral ferrocenyldiphosphine ligands of the Josiphos family, starting from commercially available rhenium sources. All the complexes are air- and moisture-stable in various oxidation states and with different accompanying ligands such as halides, hydrides, oxo, alkoxo, nitrido and CO.

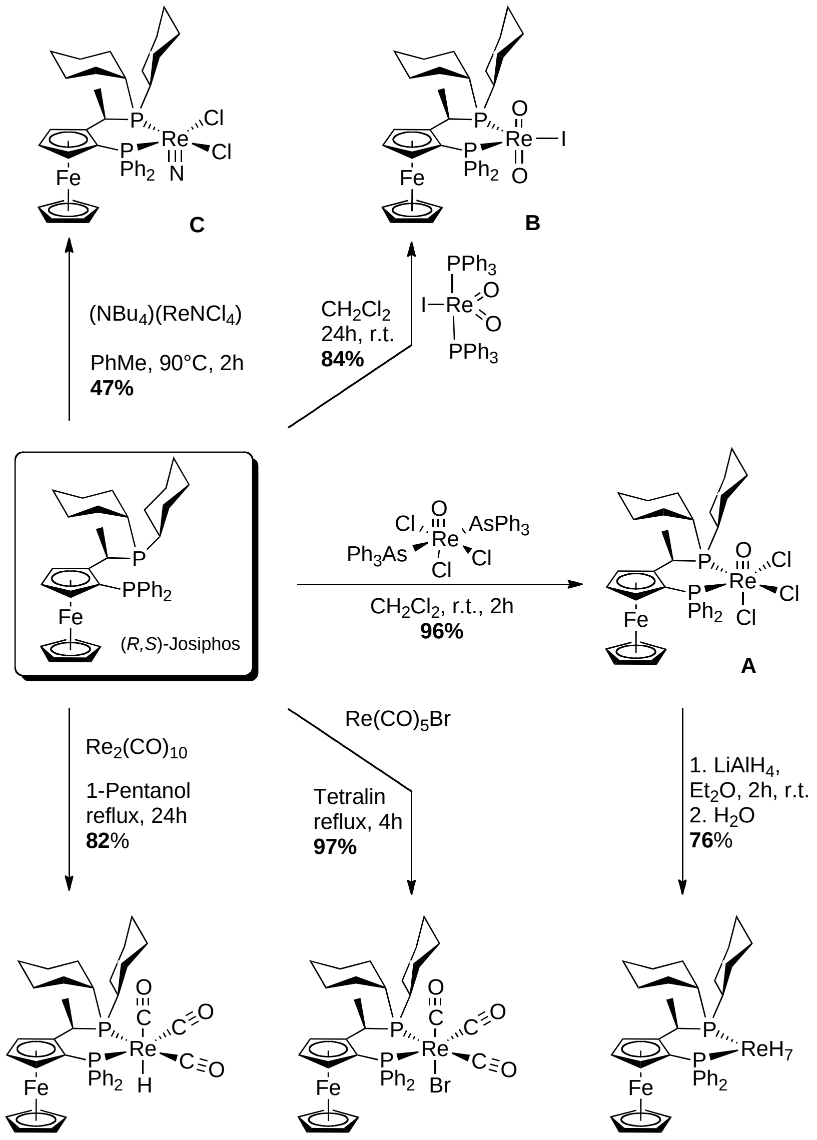
C
B
A
(R,S)-Josiphos
(NBu4)(ReNCl4)
PhMe, 90°C, 2h
47%
CH2Cl2
24h, r.t.
84%
CH2Cl2, r.t., 2h
96%
Re2(CO)10
1-Pentanol
reflux, 24h
82%
Re(CO)5Br
Tetralin
reflux, 4h
97%
1. LiAlH4,
Et2O, 2h, r.t.
2. H2O
76%

The Re^V oxo (like **A**, also with different alkyl and aryl substituents at phosphorus and **B**) and nitrido (**C**) complexes showed to be active catalysts in the asymmetric transfer hydrogenation of ketones using 2-propanol as the hydrogen source in the presence of substoichiometric amounts of TEA. The reaction proceed cleanly with good to excellent yields (50-99 %) but still with moderate enantioselectivity (up to 58 %ee). A plausible reaction mechanism is proposed.

In the second part (chapter 3), the synthesis of several rhenium complexes containing chiral tridentate ferrocenyltriphosphine ligands of the Pigiphos family is discussed.

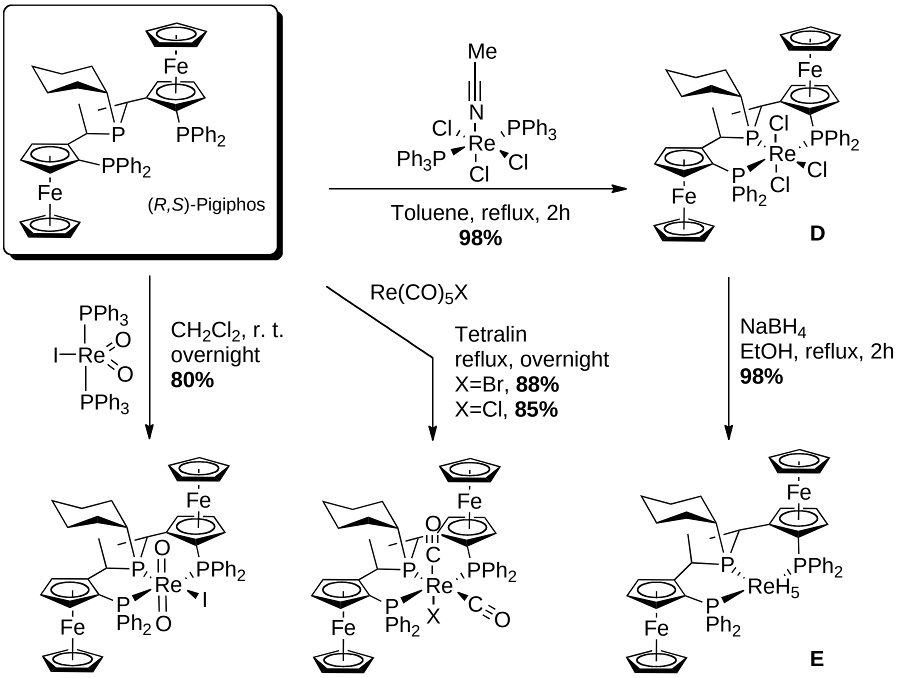

The paramagnetic Re^{III} complex $[ReCl_3(Pigiphos)]$ (**D**) was synthesized by reaction of $[ReCl_3(NCMe)(PPh_2)_2]$ with the ligand Pigiphos. The Re^V polyhydride complex $[ReH_5(Pigiphos)]$ (**E**) was synthesized by reaction of **D** with an excess of $NaBH_4$ in refluxing ethanol. Both compounds were characterized by X-Ray diffraction techniques and complex **E** by variable temperature NMR experiments indicating than it is in fact a classic polyhydride. The polyhydride complex readily reacts with both Brønsted acids and hydride scavengers to give the corresponding cationic tetrahydride species $[ReH_4(Pigiphos)]^+$ which showed to be active in the catalytic hydrogenation of dimethyl itaconate.

In the third part (chapter 4) the discovery and development of a novel methodology for the direct trifluoromethylation of both activated and unactivated arenes and heteroarenes (N-, O- and S- based) is presented. It uses the benziodoxolone-based trifluoromethylating reagent **F** and methyltrioxorhenium (MTO) as catalyst. Only a small excess of substrate and 5-10% of catalyst are required.

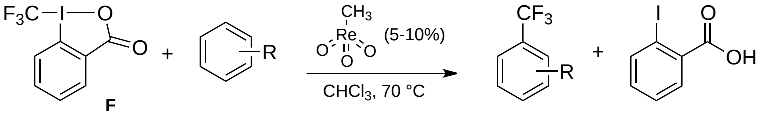

To the best of our knowledge, this is the direct aromatic trifloromethylation procedure with the broadest substrate scope so far (R = alkyl, aryl, silyl, alkoxy, amino, acyl, halogen, ciano, nitro). NMR, EPR and KIE experiments suggest a radical mechanism triggered by the rhenium-catalyzed oxidation of the aromatic moiety by an activated form of **F**.

Zusammenfassung

Die vorliegende Doktorarbeit befasst sich mit der Synthese und der Charakterisierung von neuen Rhenium-Komplexen und ihrer Anwendung als Katalisatoren der Hydrierung (asymmetrische Hydrierung und Transferhydrierung) so wie in der aromatischen Trifluoromethylierung.

Das erste Teil (Kapitel 2) beschreibt die Synthese und Charakterisierung einer Reihe von Komplexen mit dem chiralen zweizähnigen Ferrocenylphosphin-Ligand *Josiphos*, die aus im Handel erhältlichen Rhenium-Quellen hergestellt wurden.

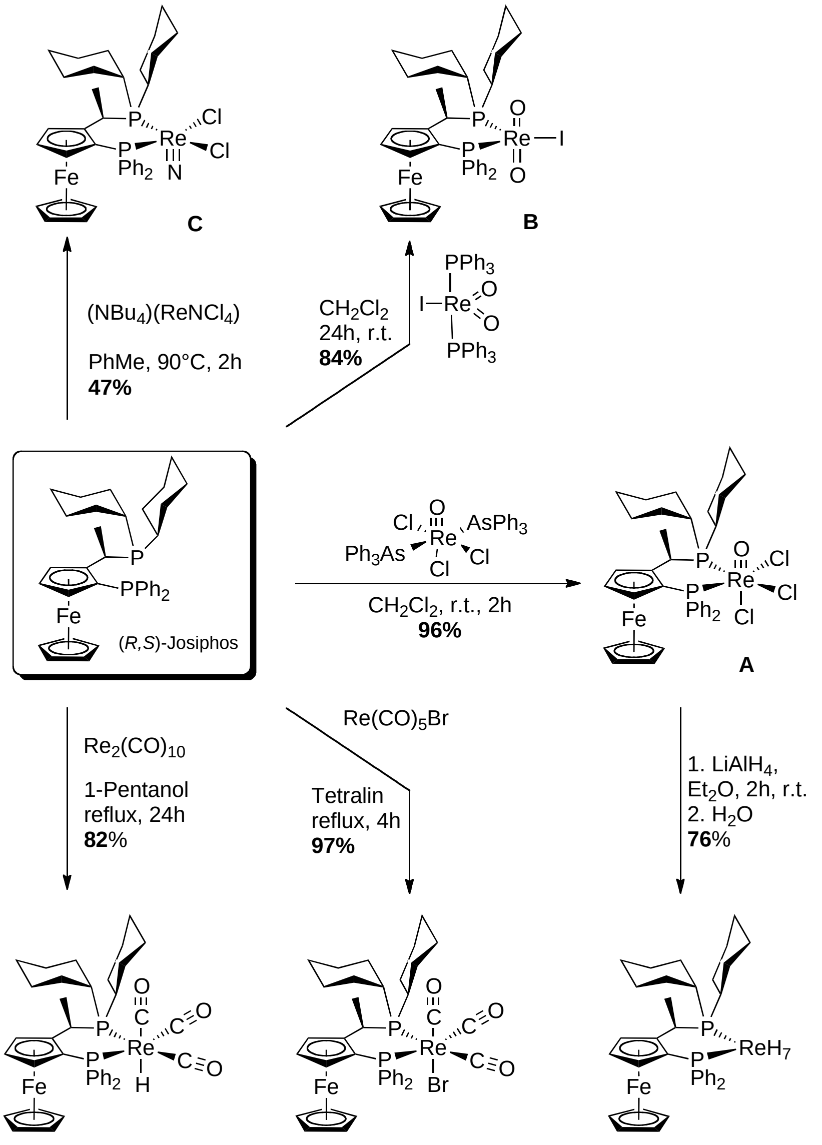
C
B
(NBu4)(ReNCl4)
PhMe, 90°C, 2h
47%
CH2Cl2
24h, r.t.
84%
(R,S)-Josiphos
CH2Cl2, r.t., 2h
96%
A
Re2(CO)10
1-Pentanol
reflux, 24h
82%
Re(CO)5Br
Tetralin
reflux, 4h
97%
1. LiAlH4,
Et2O, 2h, r.t.
2. H2O
76%

Alle Komplexe sind luft- und feuchtigkeitsbeständig in verschiedenen Oxidationsstufen (I, III, V und VII) und mit verschiedenen begleitenden Liganden wie Halogenide, Hydride, Oxo, Alkoxo, Nitrido und CO.

Die Rhenium(V)-oxo (wie **A**, mit verschiedenen Resten am P und **B**) und der Nitrido-Komplex **C** sind aktive Katalysatoren in der asymmetrischen Transferhydrierung von Ketonen mit 2-Propanol als Wasserstoffquelle. Die Reaktion benötigt die Zugabe einer Base (Triethylamin) in unterstöchiometrischer Menge. Die Umwandlung läuft sauber und mit guten bis exzellenten Ausbeuten (50-99%) ab, jedoch mit mittelmäßiger Enantioselektivität. In diesem Teil wird ebenfalls ein möglicher Reaktionsmechanismus vorgeschlagen.

Im zweiten Teil der Dissertation (Kapitel 3) werden Synthese und Charakterisierung von mehreren Rhenium-Komplexen mit dem chiralen dreizähnigen Ferrocenylphosphin-Ligand *Pigiphos* präsentiert. Der paramagnetische Re^{III}-Komplex [ReCl$_3$(Pigiphos)] (**D**) wurde durch Reaktion von [ReCl$_3$(NCMe)(PPh$_3$)$_2$] mit dem Ligand *Pigiphos* hergestellt.

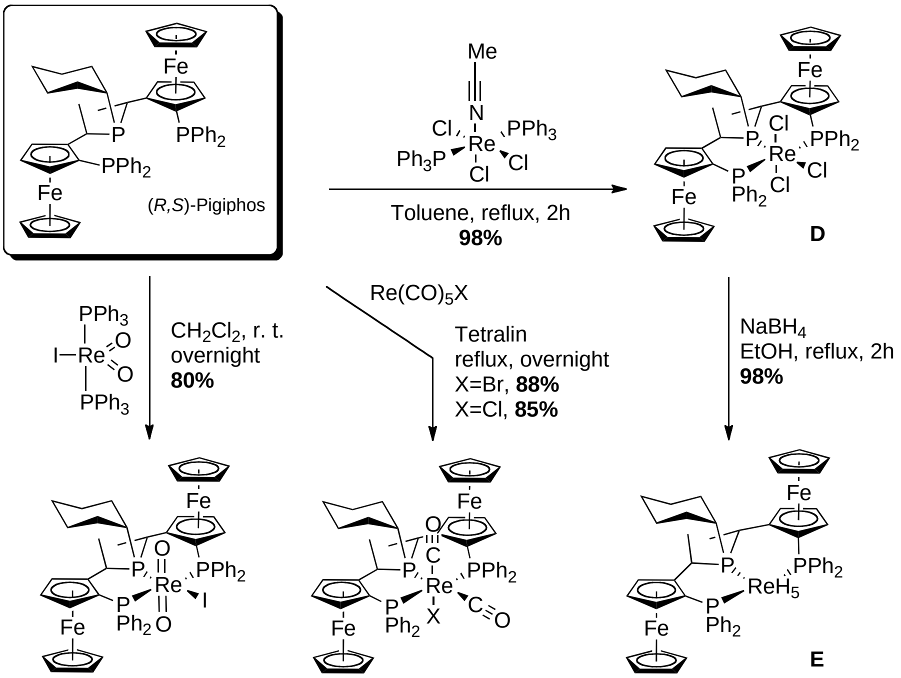
(R,S)-Pigiphos
Fe
P
PPh2
Me
N
Cl
PPh3
Re
Ph3P
Cl
Toluene, reflux, 2h
98%
D
PPh3
I–Re
O
CH2Cl2, r. t.
overnight
80%
Re(CO)5X
Tetralin
reflux, overnight
X=Br, 88%
X=Cl, 85%
NaBH4
EtOH, reflux, 2h
98%
Ph2
I
C
O
X
ReH5
E

Komplex **D** wurde durch Zugabe von NaBH$_4$ in kochendem Ethanol zum Pentahydrido-Komplex [ReH$_5$(Pigiphos)] (**E**) umgesetzt. Beide Komplexe wurden durch Röntgenbeugungsmethoden charakterisiert. Mittels temperaturabhängiger NMR-Experimente wurde bewiesen, dass Komplex **E** ein klassisches Polyhydrid ist. Der Polyhydrid-Komplex **E** reagiert sowohl mit starken Brønsted-Säuren als auch mit Hydrid-Fängern vollständig ab, und wird in die kationische, aktivierte Form $[ReH_4(Pigiphos)]^+$ überführt. Letztere erwies sich als aktiv in der katalytischen Hydrierung von Itaconsäuredimethylester.

Im dritten Teil (Kapitel 4) wird die Entdeckung und Entwicklung einer neuen Methode zur direkten Trifluoromethylierung aktivierter und unaktivierter Arene und Heteroarene (N-, O- und S-haltige) präsentiert. Die Reaktion benötigt stoichiometrische Mengen des benziodoxolonartigen Reagenz **F** und Methyltrioxorhenium (MTO) als Katalysator. Nur ein kleiner Überschuss Edukt und 5 - 10% Katalysatorzugabe sind dazu erforderlich.

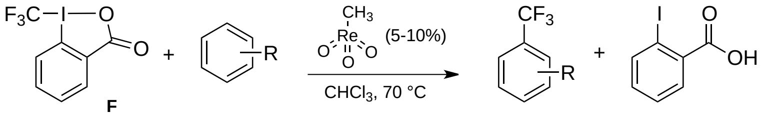

Nach heutigem Wissen, ist dies die direkte aromatische Trifluoromethylierungsmethode mit dem größten Anwendungsbereich (R = Alkyl, Aryl, Silyl, Alkoxy, Amino, Acyl, Halogen, Cyano, Nitro). NMR-, EPR- und KIE-Experimente deuten auf einen Radikalketten-Mechanismus hin, der durch die Rhenium-katalysierte Oxidierung des aromatischen Rests ausgelöst wird.

1. General Introduction

The purpose of this chapter is to introduce the reader in the fascinating and frequently overlooked chemistry of rhenium compounds, their properties and multiple applications in catalysis, a field that has been growing in the last decades. In the first part, a brief historical perspective is presented including the discovery and the main classes of rhenium compounds with focus on their coordination chemistry and their chemical behavior. The second part deals with the main applications of rhenium complexes in homogeneous catalysis. Applications of rhenium complexes in heterogeneous catalysis, medicinal chemistry, materials and molecular sensors will not be discussed since they are out of the scope of this work.

1.1. The Discovery Rhenium

By the time when D. Mendelejeff published his early version of the Periodic Table in 1869,[1] he didn't realized that there should be a "hole" under manganese corresponding to two missing elements, namely technetium and rhenium. Years after, in 1871, he mended the oversight and included the holes in his table calling them *Ekamangan* (Tc), and *Dwimangan* (Re) from the Sanskrit Eka = the first and Dwi = the second.[2] However, he was still dubious about their existence and suggested that the missing places under Mn could be occupied (as in his previous system) by Ru and Os and that the elements to find were then the *Ekaeisene*, under Fe. Five decades after Mendelejeff's work, there were already hypotheses saying that these holes were not "ausfüllbar" (prone to be filled) and hence, that the *Ekamangane* did not exist at all.[3]

In 1908 Masataka Ogawa, a Japanese chemist working under the supervision of Sir William Ramsay at the University College in London, found a new element during his X-ray studies of thorianite from Ceylon (today's Sri Lanka) and Japanese molybdenite. Ogawa (and Ramsay) thought it was the missing element 43 (technetium) and gave it the name *Nipponium* after Japan's name in Japanese. He continued his investigations on nipponium in his homeland without success so his claim was soon discarded. Years after, in 1930 (short before his death) he realized that his nipponium was in fact the newly discovered element 75 (vide infra), but it was already too late to claim priority on the discovery. His later results never were published and nipponium was regarded for almost one century as a myth.[4]

In 1925, two German chemists, Walter Noddack and Ida Tacke (the later eventually became Frau Noddack), managed to isolate for the first time element 75 from a Russian platinum ore and characterized it by X-ray spectroscopy.[5] They also claimed the discovery of element 43 but this could never be confirmed, since not even they were able to reproduce their own experiments.[6] The Noddacks, with a high dose of nationalism, proposed then the names *Rhenium* for element 75 after the Rhine river and *Masurium* for element 43 after the Masuria region in east Prussia (today Poland). In order to assess the chemical and mechanical properties of the newly discovered *Re*, they isolated 1.042 g of pure metal from 660 kg of Norwegian molybdenite (MoS_2). With the help of two technicians and 4000 kg of nitric acid, they digested the ore within 40 days and after successive cycles of concentration, precipitation of molybdenum as phosphate and sulfite, reduction under H_2 flow (at 1000 °C), oxidation with O_2 flow (150 °C), and sublimation, they isolated the metal as the volatile rhenium heptoxide which was then reduced, oxidized, resublimated and reduced again to afford the pure material with 77% yield.[7]

Rhenium is one of the scarcest elements in both earth crust and the solar system.[8] With a concentration around 0.0007 ppm in earth's crust,[9] it shows a strong contrast with the chemically akin molybdenum which is the third most abundant transition metal after iron and titanium. It is also dispersedly distributed so there are not sufficient concentrations anywhere to allow their extraction as the main commodity being then commercially obtained as a by-product of the molybdenum industry. It is estimated that the total world reserves on Re are ca. 1000 tons of which 70% are in the U.S.A. and 20-25% in Chile.[8] In 1995, the first pure rhenium mineral, namely *Rheniite* (rhenium sulfide) was found in samples of pyroclastic debris from the Kudriavy volcano on Iturup island in the Pacific ocean.[10]

1.2. Chemistry of Rhenium Compounds

The chemistry of rhenium is characterized by its large number of easily accessible oxidation states, eleven in total, from -3 to 7, all of them represented by a considerable number of species. Since several comprehensive reviews are available in the literature[8-9, 11] only general comments and selected examples for each class will be given here.

1.2.1. Rhenium species with formal negative oxidation states

The chemistry of this class of compounds is relatively underdeveloped, having their main representative examples in the rhenium carbonyl clusters. The most important molecular compound is the anion $[Re(CO)_5]^-$, obtained by reduction of $Re_2(CO)_{10}$ with Na/Hg. It serves as nucleophile in the synthesis of clusters with Re-C, Re-Re and Re-M bonds.[11c] Further reduction to $[Re(CO)_4]^{-3}$, a d^{10} species with a formal oxidation state of -3, is possible with Na in HMPA.[11e] As many other metal pentacarbonyls, the anion $[Re(CO)_5]^-$ exhibits a trigonal bipyramidal geometry. It was recently confirmed by X-ray structural analysis of the complex $[Yb(THF)_6][Re(CO)_5]_2$ (see Figure 1), prepared by the direct reaction of Yb metal and $Hg[Re(CO)_5]_2$ in THF.[12]

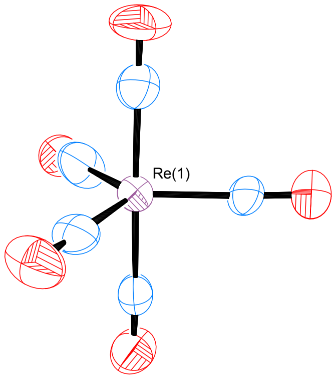

Figure 1. ORTEPIII diagram for the crystal structure of one of the $[Re(CO)_5]^-$ anions in $[Yb(THF)_6][Re(CO)_5]_2$. The second anion and the cationic moieties are omitted for clarity. Thermal ellipsoids with 50% probability.[12]

One interesting example of the reactivity of $[Re(CO)_5]^-$ is its reaction with $[M(CO)_6]^+$ (M = Mn, Re) which proceeds via nucleophilic attack to a CO ligand followed by a fast two-electron/one CO transfer reaction followed by SET and coupling to give binuclear products (Scheme 1).[13]

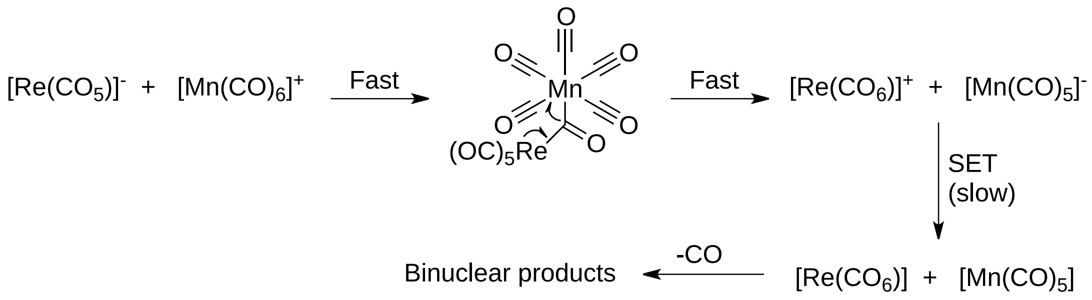

Scheme 1

1.2.2. *Rhenium(0)*

From all the known rhenium complexes, those of Re^0 are the rarest and are virtually limited to carbonyl derivates, $[Re_2(CO)_{10}]$ being the simplest example in which the two rheniumpentacarbonyl fragments are held together by a Re-Re single bond (Figure 2).[14] It can be synthesized by carbonylation of Re_2O_7, by reduction of $ReCl_5$ or K_2ReCl_6 under CO pressure,[11e] or simply by reduction of ammonium perrhenate with DIBAL-H at atmospheric CO pressure.[15] The intermetallic bond can be cleaved by photolysis to give reactive radical 17-electron species.[11b, 11d] The CO ligands can be easily replaced under thermal or photolytic conditions by tertiary phosphines, arsines, silanes, pyridines and isocyanides.

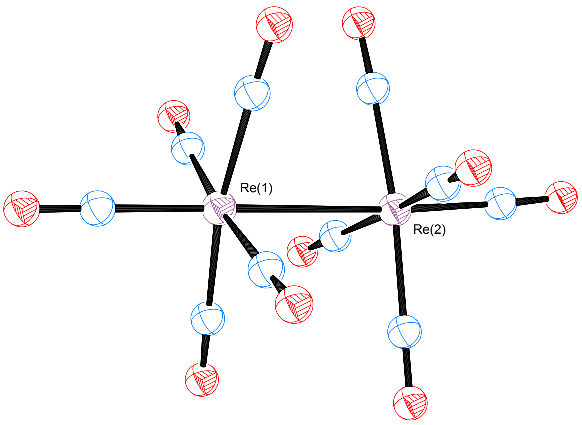

Figure 2. ORTEPIII diagram for the Crystal structure of $[Re_2(CO)_{10}]$. The molecule has an approximate D_{4d} symmetry.[14]

Photochemical induced substitutions do not occur through the $[Re(CO)_5]$ radical as it was first suggested but from the photointermediate $[Re_2(CO)_9]$; nevertheless, Re-Re bond breaking may always occur.[11e] An alternative route that avoids the intermetallic bond cleavage is the PdO catalyzed decarbonylation and ligand substitution, which in the case of $[MnRe(CO)_{10}]$ is site-selective.[16]

1.2.3. *Rhenium(I)*

The most important compounds of this class are polycarbonyls, specially those containing the *fac*-$[Re(CO)_3]^+$ fragment since their derivatives are fairly stable and can be prepared in aqueous solutions, leading to a broad spectrum of applications in radioimaging and radiotherapeuthics, as models for the corresponding Tc complexes, and in luminescence. An important precursor to access this chemistry is $[ReBr(CO)_3(THF)]_2$, easily prepared by refluxing $ReBr(CO)_5$ in THF.[17] This dinuclear compound has no intermetallic bond, being the two Re atoms bridged by Br ligands (Figure 3).[18]

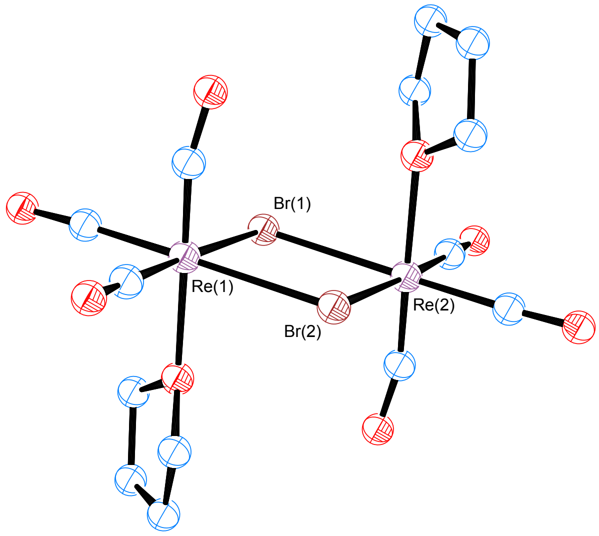

Figure 3. ORTEPIII diagram for the crystal structure of $[ReBr(CO)_3(THF)]_2$. The molecule has an approximate C_{2h} symmetry.[18]

Another entry into this chemistry are the halide derivatives of the type $[Re(CO)_5X]$ (X = H, Cl, Br, I, F, CH_3) which can be prepared by oxidative cleavage of $[Re_2(CO)_{10}]$ with X_2 (X = Cl, Br, I, H). Thermal substitution of the carbonyl ligands by mono-, bi-, or tridentate ligands (neutral or uninegative) leads to most of the chemistry of rhenium(I) complexes. An alternative, more specific (monodecarbonylation) route is the PdO catalyzed ligand substitution.[19] The vast majority of such derivatives has been prepared in order to study their photophysical properties or as models of technetium compounds for radiochemical applications. Conversely, relatively few reactivity studies have been published.[11c]

1.2.4. *Rhenium(II)*

Complexes of rhenium in the formal oxidation state +2 (with a d^5 configuration) are relatively rare. They are more reactive than their $\mathrm{Mn^{II}}$ counterparts, and often disproportionate easily to thermodynamically more stable $\mathrm{Re^{III}}$ and $\mathrm{Re^{I}}$ species. In order to reduce the electronic density at the metal center, soft donor ligands with π-acceptor capabilities are required. Thus, the coordination chemistry of $\mathrm{Re^{II}}$ is governed mainly by phosphines and other π-binding ligands such as isocyanides.[11b]

A considerable part of the molecules known in this oxidation state are those including the $[Re_2X_4]$ core (X = Cl, Br) in which the two rhenium atoms are triply bonded with an electron rich $\sigma^2\pi^4\delta^2\delta^{*2}$ electronic configuration.[11a] The crystal structure of a representative example of this group, $[Re_2Cl_4(dppm)_2]$, is presented in Figure 4.[20]

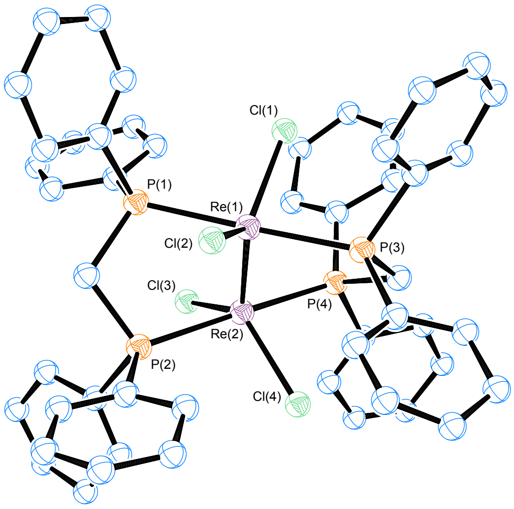

Figure 4. ORTEPIII diagram for the crystal structure of $[Re_2Cl_4(dppm)_2]$.[20]

In contrast to the abundant examples of carbonyl Re^I compounds, the access to 17-electron mononuclear Re^{II} derivatives has been elusive, due in part to their reactive nature and to the resistance to oxidation displayed by the Re^I complexes.[11c] Only recently, Alberto and co-workers presented "a convenient entry into rhenium(II) chemistry", namely the complex $[ReBr_4(CO)_2]^{2-}$, an air-stable synthon which easily undergoes substitution reactions with mono-, bi- and tridentate ligands. The crystal structure of one of such complexes, $[ReBr_2(bipy)(CO)_2]$, is presented in Figure 5.[21]

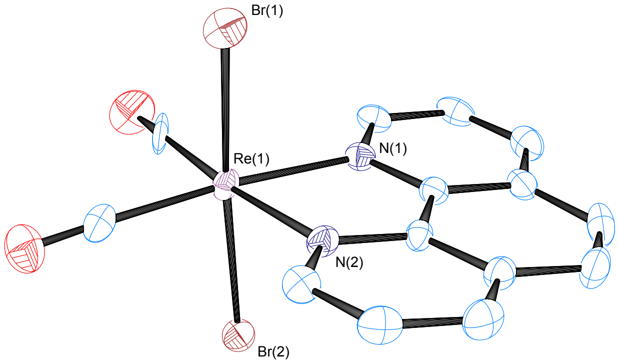

Figure 5. ORTEPIII diagram for the crystal structure of $[ReBr_2(bipy)(CO)_2]$. Thermal ellipsoids are presented with 50% probability.[21]

These complexes, due to their inherent paramagnetism and their open-shell electronic configuration are of high interest in magnetochemistry and have potential, yet unexplored, applications in catalysis.[21]

1.2.5. Rhenium(III)

The d^4 configuration of the rhenium center can be effectively stabilized by good σ-donor or π-acceptor ligands and hence, the number of derivatives in this oxidation state is quite numerous. The majority of these complexes are fairly stable against hydrolysis, making them suitable for radiomedicinal studies (as models of the target Tc analogues).[11d] Phosphine ligands, generally accompanied by halides, are predominating in the coordination chemistry of Re^{III} compounds. Complexes of the type ReX_3L_3 (L = alkyl or aryl phosphines or arsines) constitute an important class in the coordination chemistry of mononuclear Re^{III} derivatives, usually prepared by reduction of rhenium(V) precursors ($[ReOCl_3(PPh_3)_3]$ or $[ReOCl_2(OEt)(PPh_3)_3]$) in HX in the presence of L, or by ligand substitution from a suitable precursor like $[ReCl_3(MeCN)(PPh_3)_2]$.[11a]

Perhaps the most important class of Re^{III} compounds are those containing the quadruply bonded Re_2^{6+} core, not only due to their rich chemistry but thanks to their historical significance. Since the quadruple Re-Re bond in $[Re_2Cl_8]^{2+}$ was the first of this kind to be observed, it opened up a new field of study and constituted, no doubt, a breakthrough in the field of inorganic chemistry.

After several year of stirred debate and confusing reports coming from the Russian literature in the late fifties,[22] Kuznetzov and Koz'min published in 1963 the first X-ray structural determination of the aforementioned anion, a square prism formed by eight chlorine atoms with the two rhenium centers lying within the resulting cube. In this report, the authors mention only briefly that the valence electrons of rhenium should take part in the formation of a Re-Re bond.[23] It was only in 1964 that Cotton and co-workers unveiled the quadruple nature of the Re-Re bond, possessing a $\sigma^2\pi^4\delta^2$ electronic configuration.[24] The crystal structure of the dirhenium core from $[1,6\text{-}C_6H_{12}N_2H_6]^{2+}[Re_2Cl_8]^{2-}$ is presented in Figure 6.[25]

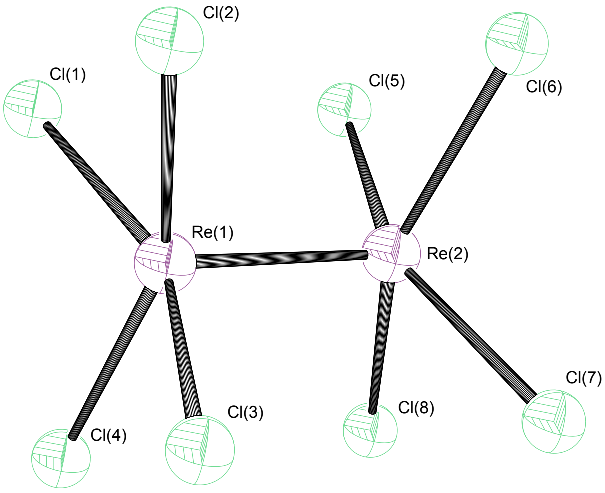

Figure 6. ORTEPIII diagram for the crystal structure of $[1,6\text{-}C_6H_{12}N_2H_6]^{2+}[Re_2Cl_8]^{2-}$. The cation has been omitted for clarity. The molecule has an approximate D_{4h} symmetry.[25]

The successive replacement of the chlorine atoms by phosphine ligands gives rise to several isomeric complexes of the types [$ReCl_4(PR_3)_4$], [$ReCl_5(PR_3)_3$] and [$ReCl_6(PR_3)_2$], which are either monocationic, neutral or monoanionic species. Complexes of these types display a triple bond between the Re centers.[26] Upon reaction with bidentate phosphines of large bite angles, interesting observations have been made. One case is the synthesis of [Re_2Cl_6(dppf)] in which, the symmetrical dirhenium core undergoes intramolecular disproportionation in a way that, formally Re^{II} and Re^{IV} centers are joined by a quadruple bond as in the parent complex, with the chelating ligand in a *trans* situation (see Figure 7).[26]

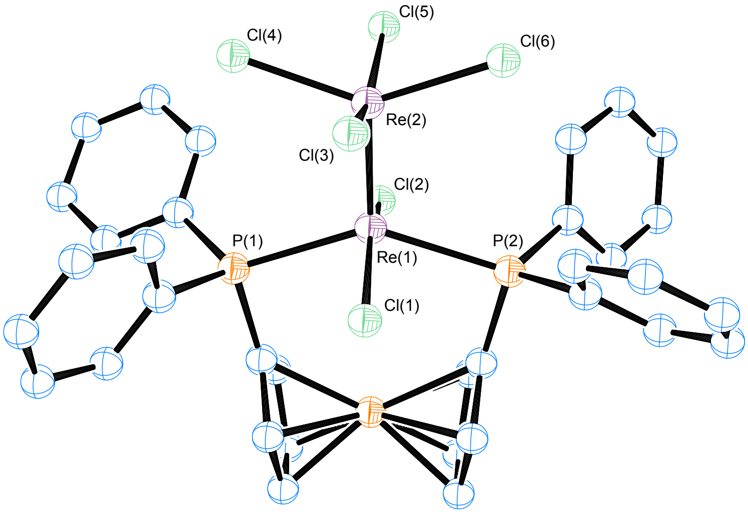

Figure 7. ORTEPIII diagram for the crystal structure of [Re_2Cl_6(dppf)].[26]

1.2.6. *Rhenium(IV)*

The most representative species in this oxidation state are halides of the type [ReX_4L_2], [ReX_5L]$^-$ and [ReX_6]$^{2-}$.[11a] Typical L in this chemistry are neutral monodentate or chelate ligands with P (phosphines), O (ethers), N (nitriles and isothiocianate), S (tioethers) and As (arsines) as donor atoms.[11b] Rhenium(IV) compounds hydrolyze readily in the presence of water and show already the tendency to form Re-oxo bonds, a typical feature of the higher oxidation states, V, VI and VII. Contrary to their low oxidation state congeners, Re^{IV} complexes are not prone to form metal-metal bonds, being the triple-bonded nonahalodirhenate(IV) anions [Re_2X_9]$^-$ a notable exception.[11a]

Convenient precursors to access the chemistry of Re^{IV} complexes are salts of the type K_2ReX_6 (X = Cl, Br), which upon heating in aqueous HX in the presence of tetrahydrothiophene (THT) give the stable complexes *trans*-$[ReX_4(THT)_2]$,[27] which are as well useful starting points for the preparation of further Re^{IV} complexes. Interestingly, the THF analog displays a *cis*-arrangement.[28] An illustrative example of one of such complexes is the chelato complex $[ReCl_4(18\text{-crown-}6)]$, presented in Figure 8.[29]

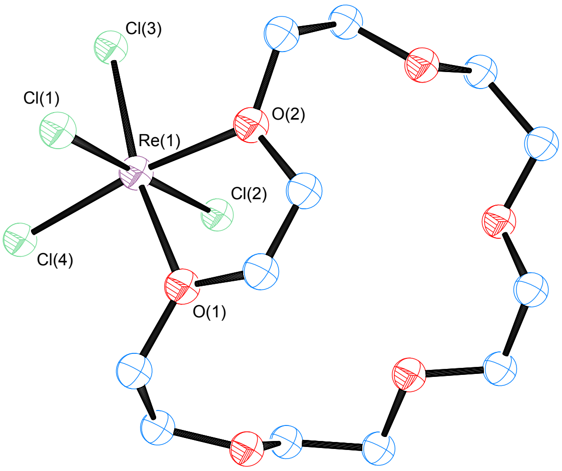

Figure 8. ORTEPIII diagram for the crystal structure of $[ReCl_4(18\text{-crown-}6)]$.[29]

1.2.7. *Rhenium(V)*

Complexes of the oxidation state +5 are, by far, the most numerous in rhenium chemistry. This could be attributed to the high stability of the rhenium(V)-oxo, -nitrido and -imido cores, the most representative of this class. The prevalence of this multiple bonded ligands (O^{2-}, N^{3-} and RN^{2-}) is due to their excellent π-donor capabilities, able to stabilize high oxidation states.[11b] Rhenium(V) complexes of the types $[ReOX_5]^{-2}$, $[ReOX_4L]^{-}$, $[ReOX_3L_2]$, $[ReO_2X_4]^{3-}$, $[ReO_2L_4]^{+}$, $[(ReOX_2L_2)_2O]$, $[ReNX_2L_3]$ and $[Re(NR)X_3L_3]$ are typically octahedral,[8] although due to the strong *trans*-influence of the aforementioned ligands, strongly tetragonaly distorted six-coordinated complexes or five-coordinated species with square-pyramidal geometry are often encountered. For example, in *mer*-$[ReOCl_3(PPh_3)_2]$, the chlorine atom *trans* to the oxo ligand can be easily replaced by alcohols to give *mer*-$[ReOCl_2(OR)(PPh_3)_2]$ (R = alkyl or aryl).[30] With few exceptions, Re^{V}

complexes are diamagnetic, containing a spin-paired *d*^{2} configuration or show a slightly temperature-dependent paramagnetism.[11b] Perhaps the most versatile precursors for the preparation of Re^V derivates (via ligand substitution) are those of the types [ReEX$_3$L$_2$] (E = O, N; X = Cl, Br; L = phosphines, arsines) and [ReEX$_4$]$^-$.[11a, 11b, 31] They are stable to bench conditions and readily accessible from perrhenate salts.[30-32] The crystal structure of one of these complexes, namely *mer*-[ReOCl$_3$(PPh$_3$)$_2$] is presented in figure 9.[33]

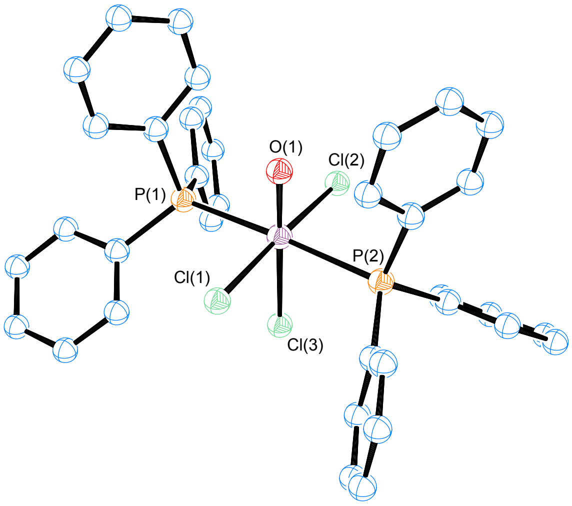

Figure 9. ORTEPIII diagram for the crystal structure of *mer*-[ReOCl$_3$(PPh$_3$)$_2$].[33]

Another important starting material (although less versatile) for the synthesis of rhenium(V) complexes, specially those without the oxo, nitrido or imido ligands is the highly reactive ReCl$_5$. In the solid state, the metal center avoids the penta-coordination by forming a bridged dimer in which two ReCl$_6$ octahedra share a common edge.[34] For the rhenium(V) chloride, it has been said, the reactions are "numerous and complex"[8] heavily dependant on the nature of the ligands, the solvents and the reaction conditions.[35] It can thus undergo simple ligand substitution, reduction to rhenium(IV) species, hydrolysis and disproportionation.[8]

1.2.8. Rhenium(VI)

This kind of complexes, with a *d*^{1} electronic configuration are one of the most unstable among the plethora of rhenium compounds, paralleling the behavior of osmium(VII) but in strong contrast to its lighter isoelectronic congener tungsten(V).[8] They are frequently observed as intermediate species in the reduction of rhenium(VII) complexes or in the oxidation of rhenium(V) precursors, and are prone to undergo further redox reactions.[11b] The Re^{VI} center can be stabilized by strong donor ligands such as terminal oxo or nitrido groups.[11a, 11b] The octahedral coordination is preferred although species with coordination numbers from four to eight are known.[8]

Perhaps the most prominent representatives of this oxidation state are the oxo and nitrido tetrahalide derivatives of the types $[ReOX_4]$ and $[ReNX_4]^-$ (X = Cl, Br) which display a distorted square pyramidal geometry in which the multiply bonded oxo or nitrido ligand occupies the apical position. They tend to adopt six-fold coordination by intramolecular association in the solid state[8] or by coordination with monodentate ligands.[36] A representative example is $[NBu_4][ReNCl_4]$, a common precursor to several nitrido complexes, which can be easily synthesized by reduction of tetrabutylammonium perrhenate with sodium azide in the presence of HCl (see Figure 10).[31]

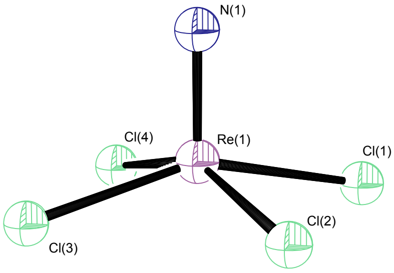

Figure 10. ORTEPIII diagram for the crystal structure of $[NBu_4][ReNCl_4]$. The cation is omitted for clarity.[31]

1.2.9. Rhenium(VII)

As expected, just by following the periodic trends, the redox potentials of rhenium, in the third row, are lower than those for manganese and technetium. As a consequence, the low oxidizing nature of Re^{VII} species allows the development of a rich coordination chemistry.[11b] The high stability of the perrhenate ion, $[ReO_4]^-$, added to the fact that this is precisely the way in which rhenium is industrially isolated from molybdenum ores, makes it the most popular (and cheapest) starting material in rhenium chemistry. Perrhenate salts with virtually all metal cations are known. All of them have an exceptional stability, which descends with the increase of the cationic charge.[8] Alkylammonium salts can be readily prepared by extraction of perrhenate with alkylamines into organic solvents, being those the preferred choice for non-aqueous preparations.

The highly volatile polymeric Re_2O_7 is also a common precursor for numerous rhenium complexes. It dissolves readily in (wet) organic solvents and in water to give perrhenic acid solutions from which metal perrhenates may be prepared. In its yellow crystalline form, polymeric Re_2O_7 consists of sheets made of tetrameric rings of octahedral $[ReO_6]$ and tetrahedral $[ReO_4]$ units.[8] This polymeric structure can be easily cleaved by donor solvents to give single $[Re_2O_7]$ units with two free coordination sites which can form complexes of the type $[Re_2O_7L_2]$ with both mono and bidentate ligands.[11b] Isolated "perrhenic acid", resulting from hydrolysis of Re_2O_7, is actually $[Re_2O_7(H_2O)_2]$ (Figure 11).[37]

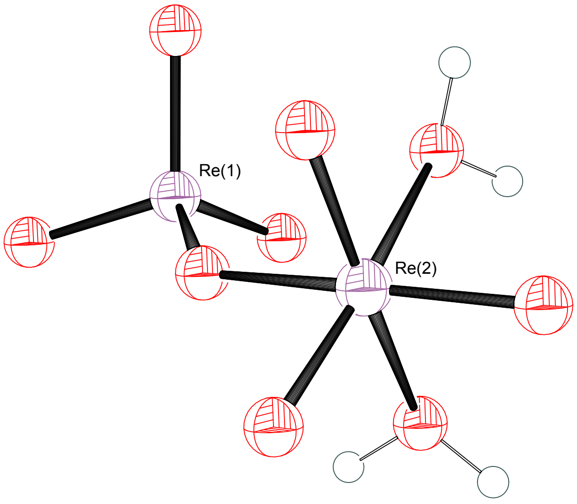

Figure 11. ORTEPIII diagram for the crystal structure of $[Re_2O_7(H_2O)_2]$ (diglyme solvate). The solvent molecules are omitted for clarity.[37]

Rhenium organyl oxo and peroxo derivates constitute an important field of study in the chemistry of Re^{VII}. Trioxides of the type $RReO_3$ (R = alkyl, aryl) have been thoroughly studied and have found several applications in material science and catalysis during the last three decades.[38] From this family, the most prominent member is the simplest one, methyltrioxorhenium, CH_3ReO_3, usually abbreviated as MTO (Figure 12).[39]

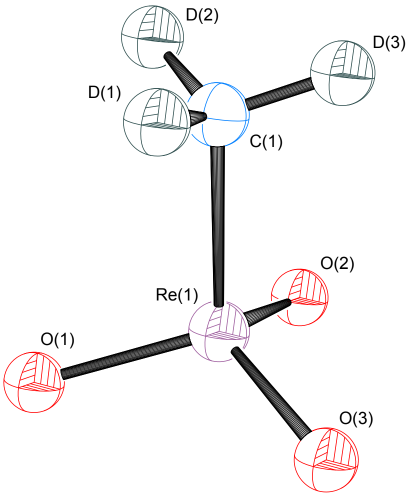

Figure 12. ORTEPIII diagram for the crystal structure of CD_3ReO_3, MTO (powder neutron diffraction).[39]

MTO was first synthesized in 1979 by Beattie and Jones,[40] and regarded only as a laboratory's curiosity until Herrmann and co-workers developed an efficient synthesis[41] (which has been further improved[42]) and started a systematic study of its properties and applications in catalysis. MTO has become one of the most versatile oxidation catalysts in organic chemistry.[38] Further information on its structure, properties and uses is presented in Chapter 4 of this work.

Apart from the complexes with "hard" multiply bonded ligands such as O^{2-}, N^{3-} and NR^{2-} which dominate the coordination chemistry or rhenium(VII), other prominent examples of Re^{VII} complexes are also worth mentioning. Metallic rhenium reacts with fluorine gas to yield a mixture of ReF_6 and ReF_7, but under 3 atm of F_2 at 400 °C (in a nickel container for several hours) it leads to pure ReF_7.[43] This remarkable compound is the only thermally stable heptafluoride of the transition metals. It can be stored indefinitely at room temperature (in sealed vials) or be heated at 400 °C for several hours without decomposition. It also shows no reaction when heated at 500 °C under several bars of oxygen pressure for several hours.[43] Its spectroscopical properties are consistent with a D_{5h} symmetry with the seven (highly disordered) fluorine atoms around the metal center in a pentagonal bipyramidal geometry.[8]

Perhaps the most fascinating rhenium(VII) complex is the enneahydridorhenate (or *nonahydride*) anion $[ReH_9]^{-2}$, one of the few examples of nonacoordinated complexes and also the first homoleptic metal polyhydride to be isolated. It was initially prepared by the reduction of potassium perrhenate with metallic potassium in an aqueous ethylendiamine solution.[44] The compound was first reported as a rhenide, $KRe(H_2O)_4$ but the Re^{-I} nature of the complex was soon discarded when, by means of ^1H NMR, the presence of a metal hydride was confirmed.[45] The definitive evidence to unveil the molecular structure and composition of K_2ReH_9 was provided by the neutron diffraction studies by Abrahams and co-workers, who found that the anion displays the geometry of a tricapped trigonal prism (point group symmetry D_{3h}).[46] The crystal structure of $K_2[ReH_9]$ is presented in Figure 13.[47]

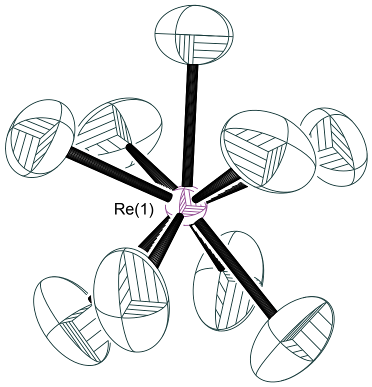

Figure 13. ORTEPIII diagram for the crystal structure of $K_2[ReH_9]$ (neutron diffraction). Potassium cations are omitted for clarity. Thermal ellipsoids with 50% probability.[47]

1.3. Applications of Rhenium Complexes in Catalysis

Due to the rich variety of stable, easily accessible rhenium complexes, in different oxidation states and bearing different kinds of ligands, rhenium-catalyzed organic reactions have witnessed a significant development in the last three decades. In spite of its scarcity, several rhenium complexes are commercially available and the price of rhenium metal is still lower than that of ruthenium, rhodium, palladium, platinum and gold, all of them very important in metal-catalyzed reactions.[48]

In 1926, only one year after the discovery of rhenium, it was already claimed that the catalytic activity of MnO_2 on the decomposition of $KClO_3$ was in fact due to the presence of small amounts of element 75 (detected by X-ray spectroscopy).[49] Not long after that, in 1929, the Noddacks patented the use of catalysts containing rhenium as metal, oxide or salt for several oxidation reactions using oxygen or air.[50] Since then, the number of reports on rhenium-catalyzed reactions has being growing steadily (see Chart 1) although, if compared with other transition metals, this field is still in its infancy.

Chart 1. Number of publications under the keyword "Rhenium catalysis" (as indexed in CAS).

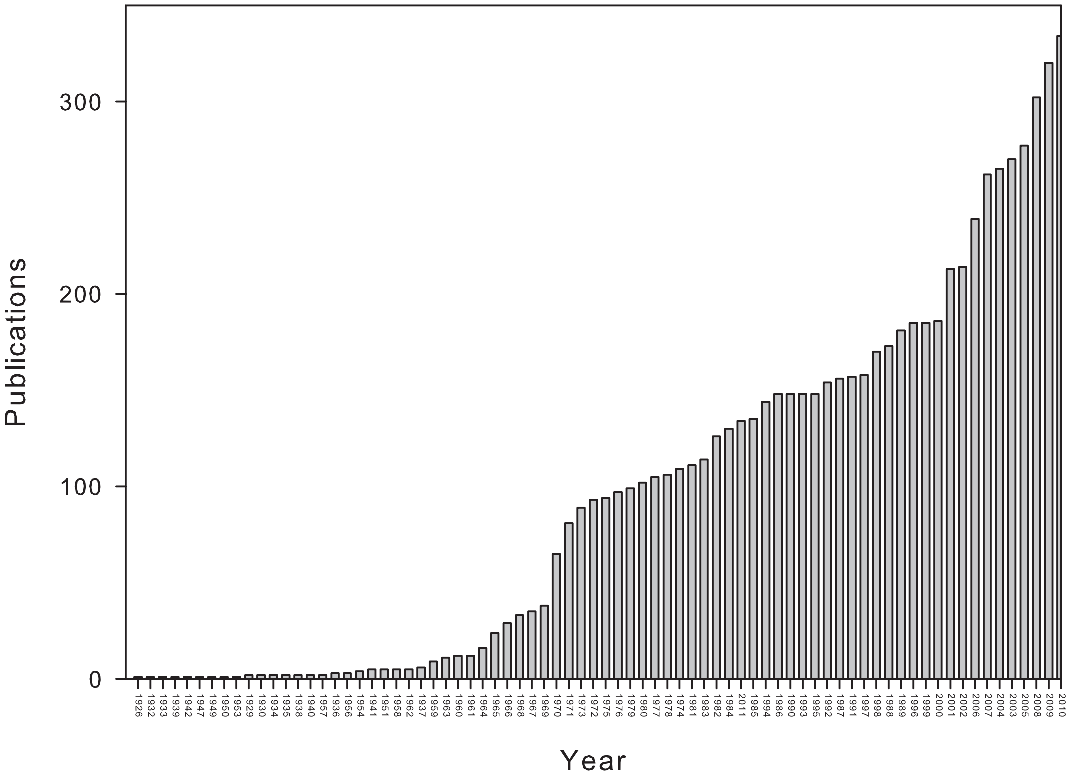

For the year 2010, the CAS database lists only 334 publications under the topic "rhenium catalysis", while for the same year the number of reports for other precious metals is: Ru 2141, Rh 1789, Pd 5187, Ir 821, Pt 3827 and

Au 2002. There is, undoubtedly, still a lot to discover and to be learned in the realm or rhenium catalysis. As early as 1968, a survey on the incipient field of rhenium catalysts appeared.[51] A couple of comprehensive reviews on rhenium catalysis have been published in recent years[38b, 48, 52] and hence only selected examples will be presented here.

1.3.1. C-C Bond forming reactions

A number of rhenium complexes, as other transition metal compounds, are good Lewis acids and consequently are active catalysts in Friedel-Crafts alkylations and arylations. In 1966 Tsuji and co-workers reported that $ReCl_5$ could catalyze (among other reactions) the alkylation and arylation of benzene and toluene at 50 °C using catalytic amounts of the rhenium complex (see scheme 2) .[53]

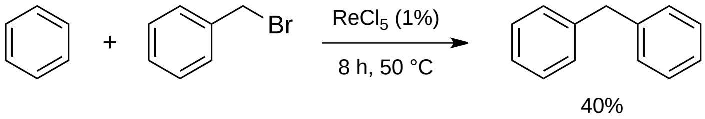

Scheme 2

Low-valent rhenium carbonyl complexes also display hard Lewis acidity. This fact has been exploited by several groups to promote Friedel-Crafts type reactions in a catalytic manner.[48, 52] Kusama and Narasaka reported the preparation of indanone and tetralone derivatives by intramolecular acylation catalyzed by $[Re(CO)_5Br]$ (Scheme 3).[54]

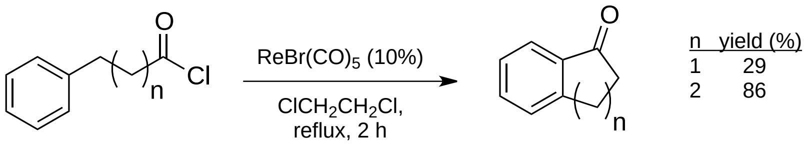

n	yield (%)
1	29
2	86

Scheme 3

As the added catalyst is a coordinatively saturated 18-electron species, it was postulated (and demonstrated) that the actual catalyst is the 16-electron complex $[Re(CO)_4Br]$, product of the thermal decarbonylation of

$[Re(CO)_5Br]$. The active intermediate was trapped by addition of triphenylphosphine to the reaction mixture and recovered as $[Re(CO)_4Br(PPh)_3]$.[54]

Nucleophylic addition to carbonyl compounds, Knoevenagel condensations, Mukaiyama aldol reactions, Michael additions and other related transformations have also been effectively achieved with the use of rhenium catalysts.[48] An interesting example is the asymmetric phenyl transfer from organozinc compounds to aldehydes reported by Bolm and co-workers using a planar chiral η^5-cyclopentadienylrhenium(I)tricarbonyl complex as catalyst (see Scheme 4). The authors claim that the enhanced Lewis acidity of the $[Re(CO)_3]$ moiety compared with the corresponding ferrocene analogues is responsible for their improved catalytic performance.[55]

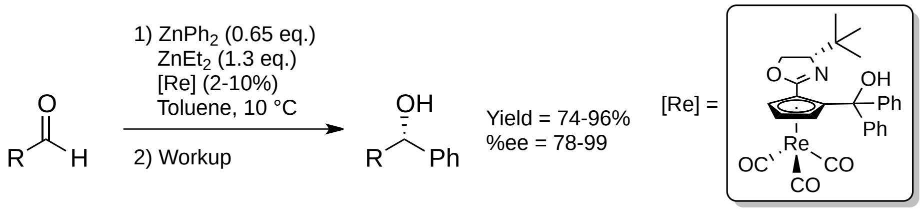

Scheme 4

Apart from the popular rhenium carbonyl complexes, other Re^I species like *cis*-$[ReH(N_2)(PMe_2Ph)_4]$ and its enolate derivatives have been shown to catalyze Knoevenagel and Michael reactions under mild conditions.[56]

During the last decade, Kuninobu, Takay and co-workers have intensively explored the use of rhenium(I) carbonyl complexes in several novel and interesting transformations, most of them based on C-H activation and C-C cleavage processes.[48] In 2005 this group reported the synthesis of indene derivatives by [3+2] annulation of aromatic aldimines with acetylenes via C-H bond activation catalyzed by $[ReBr(CO)_3(THF)]_2$[57] (Figure 3). The first reaction step is the coordination of the imine nitrogen to the rhenium center followed by the formation of the *ortho*-metallated imine via C-H bond activation. Then the alkyne is inserted into the strongly polarized Re-C bond of the aryl-rhenium intermediate, not into the M-H bond as normally observed in the case of ruthenium or rhodium. The ring-closing step occurs via intramolecular nucleophilic attack of the carbon atom attached to Re to the carbon atom of the imine. The final step of the catalytic cycle is a reductive elimination followed by an isomerization to give the final product (see Scheme 5).[48]

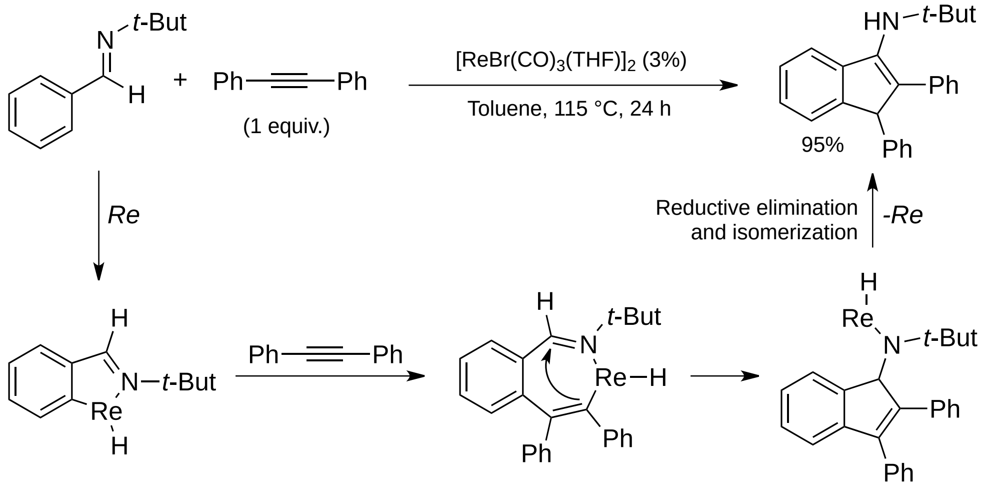
N
t-But
H
+
Ph
Ph
(1 equiv.)
[ReBr(CO)3(THF)]2 (3%)
Toluene, 115 °C, 24 h
HN
t-But
Ph
95%
Ph
Re
Reductive elimination
and isomerization
-Re
H
N
t-But
Re
H
Ph
Ph
H
N
t-But
Re
H
Ph
Ph
H
Re
N
t-But
Ph
Ph

Scheme 5

The prolific Japanese group has also developed, among other reactions,[48] the synthesis of bicyclo[3.3.1]nonene derivatives via ring expansion of cyclic β-keto esters with terminal alkynes[58] and the formation of multisubstituted aromatic rings by single C-C bond cleavage (retro-aldol reaction) of β-keto esters in the presence of alkynes,[59] both transformations catalyzed by $[ReBr(CO)_3(THF)]_2$. More recently, they reported the regioselective alkylation of phenols catalyzed by $[Re_2(CO)_{10}]$[60] and the diastereoselective synthesis of aminoindanes by the reaction of aromatic imines with allenes in the presence of the complex $[ReH(CO)_4]_n$ (Scheme 6).[61]

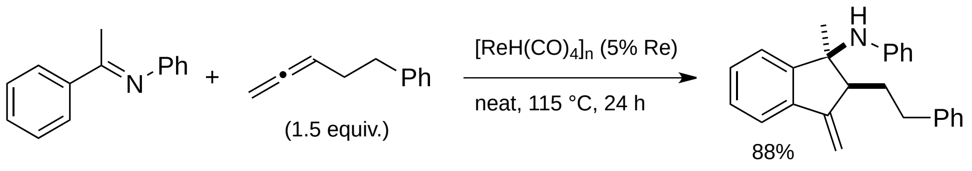
N
Ph
+
Ph
(1.5 equiv.)
[ReH(CO)4]n (5% Re)
neat, 115 °C, 24 h
H
N
Ph
Ph
88%

Scheme 6

In 2007 Kwong and co-workers reported the catalytic asymmetric cyclopropanation of alkenes with ethyl diazoacetate (EDA) using chiral bipyridine and terpyridine rhenium(I)-tricarbonyl complexes of the type [ReL(CO)$_3$(MeCN)]OTf (L = chiral C_2-symmetric chelating pyridine ligand). The reaction mechanism is still unclear but the authors propose the intermediacy of carbene complexes (Scheme 7).[62] This reaction is analogous to the aziridinations and epoxidations reported by Espenson and his group (vide infra).

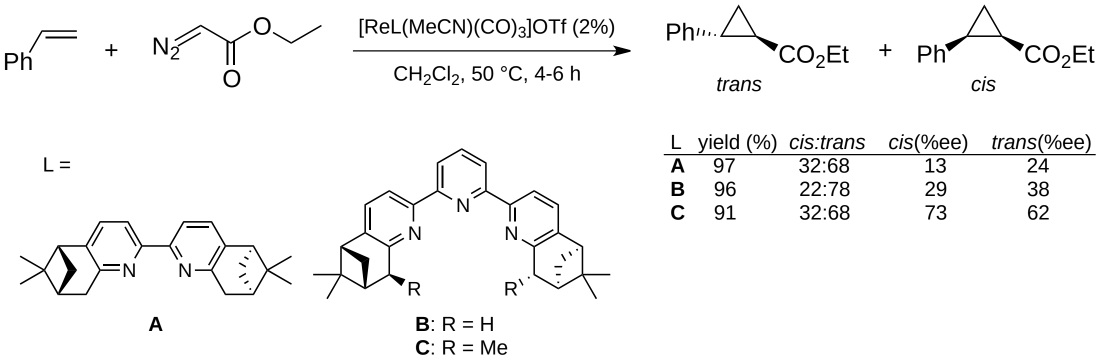
[ReL(MeCN)(CO)3]OTf (2%)
CH2Cl2, 50 °C, 4-6 h
Ph
N2
O
CO2Et
trans
cis
L =
N
R
A
B: R = H
C: R = Me

L	yield (%)	*cis:trans*	*cis*(%ee)	*trans*(%ee)
A	97	32:68	13	24
B	96	22:78	29	38
C	91	32:68	73	62

Scheme 7

One of the few examples of rhenium-catalyzed C-C bond formation reactions using high-valent Re^{V} complexes as catalyst was reported in 2003 by Toste and co-workers, namely the coupling of propargyl alcohols and allyl silanes to produce 1,5-enynes. The catalyst in this case is the air- and moisture-stable oxo-complex [ReOCl$_3$(dppm)] (Scheme 8). The high stability of this complex even allows catalyst recovery and reuse without significant detriment in activity.[63]

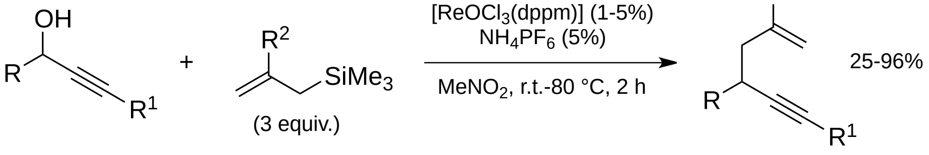
OH
R
R1
+
R2
SiMe3
(3 equiv.)
[ReOCl3(dppm)] (1-5%)
NH4PF6 (5%)
MeNO2, r.t.-80 °C, 2 h
R2
R
R1
25-96%

Scheme 8

The versatile Re^{VII} complex methyltrioxorhenium, MTO (Figure 12), catalyzes the Diels-Alder reaction of α-β-unsaturated ketones or aldehydes with several dienes in water, faster and more selectively than in organic solvents. The ability of MTO to bind weakly and reversibly the dienophile or diene is the key of success for this reaction (see Scheme 9).[64]

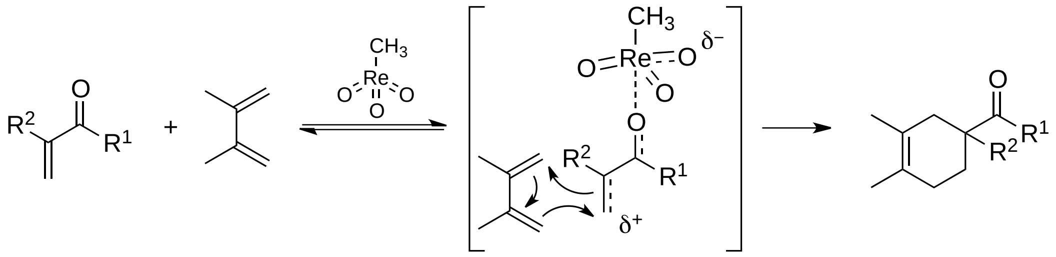

Scheme 9

Olefin metathesis, a very important, formally C-C bond forming reaction, due to its special nature will be treated separately (see section 1.3.7).

1.3.2. C-N Bond forming reactions

Intramolecular hydroamination of alkynes has been studied to some extent by Müller, Yan and co-workers using group 7-12 transition metal complexes.[65] They developed a series of rhenium(I)tricarbonyl triflato complexes with different pyridine ligands, which showed different catalytic activities depending on the ligand used and the solvent (Scheme 10). These catalysts are advantageous compared to early- and late-transition metal catalysts since they are more stable to air and moisture.[66]

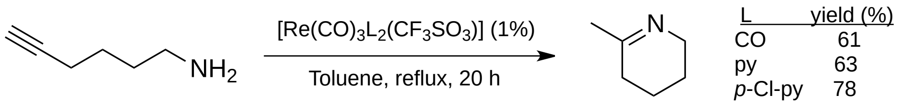

L	yield (%)
CO	61
py	63
p-Cl-py	78

Scheme 10

Espenson and Zhu reported the synthesis of aziridines by reaction of aromatic imines with ethyl diazoacetate (EDA) using MTO as catalyst (Scheme 11). This reaction proceeds cleanly with exclusion of air and under mild conditions, giving the *trans* isomer as only product. The authors propose the intermediacy of a carbenoid rhenium complex (structure **A** in Scheme 12).[67]

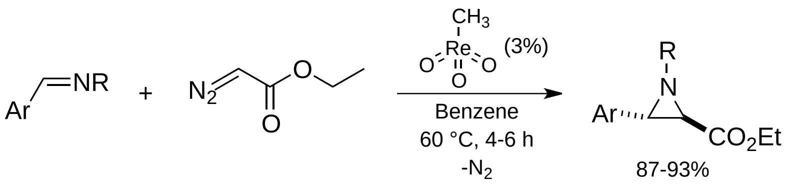

Scheme 11

The same group also reported the conversion of amines into glycine esters by reaction with EDA using MTO as catalyst. The reaction is completed after one hour at room temperature with a catalyst loading of only 0.4%.

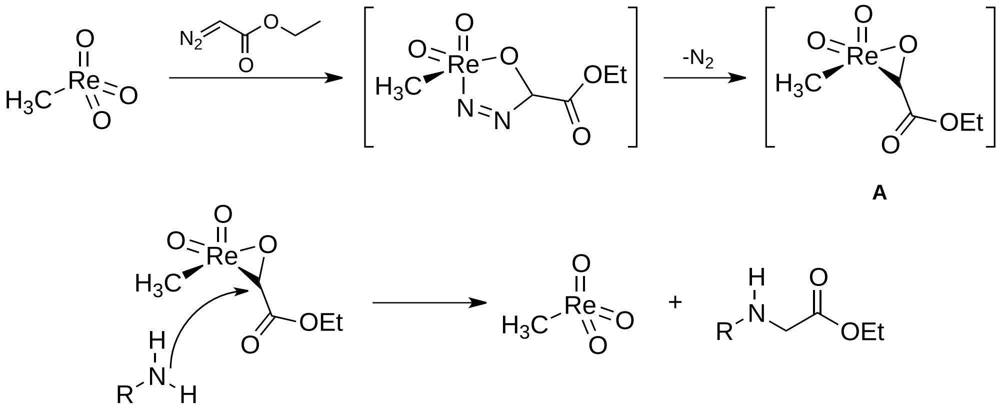

Scheme 12

The proposed reaction mechanism (Scheme 12), as for the aziridination, requires the formation of a carbenoid intermediate (**A**) which upon nucleophilic attack from the amine forms the glycine ester and regenerates the catalyst.[68] With the same catalyst, the synthesis of secondary amines from primary aromatic alcohols and various amines has been carried out with high yields at room temperature.[69]

In 2005 Toste and co-workers described the synthesis of propargylamines by coupling propargyl alcohols with tosylamines using [ReOCl$_3$(dppm)] as catalyst. This regioselective transformation opened a novel approach to the synthesis of nitrogen-containing heterocycles as exemplified by the same authors with the synthesis of the marine product Pentabromopseudilin, a potent Lipoxygenase inhibitor, and its analogues (Scheme 13).[70]

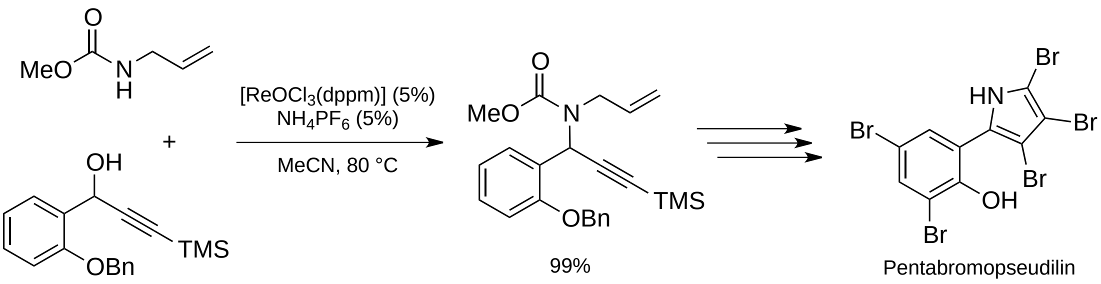

Scheme 13

1.3.3. *C-O Bond forming reactions*

A practical method for the synthesis of ethers is the catalytic dehydration of alcohols. Espenson and his group developed a novel procedure for the synthesis of both symmetric and asymmetric dibenzyl ethers in moderate to high yields, using MTO as catalyst. This systems display high activities only with secondary aromatic alcohols.[69]

A more general and highly selective method for the etherification of benzyl alcohols was reported in 2005 by Hua and co-workers, using [ReBr(CO)$_5$] as catalyst in the presence of air (Scheme 14). It has been postulated that the actual catalyst is the rhenium(III)-oxo species [ReBrO(CO)$_4$].[71]

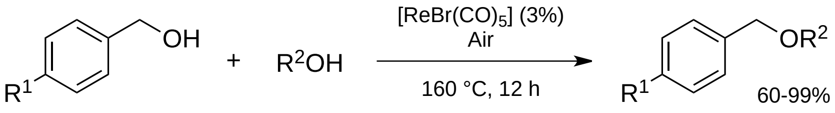

Scheme 14

In 2003 Toste's group reported an efficient *sp*^{3}-C-O bond forming reaction, namely the coupling of propargylic alcohols with simple alcohols using the same rhenium(V)-oxo catalyst as for the propargylic amination ([ReOCl$_3$(dppm)], Scheme 13).[70] Thanks to the high stability of the catalyst this transformation gives high yields under mild conditions without the exclusion of air or moisture (Scheme 15).[72]

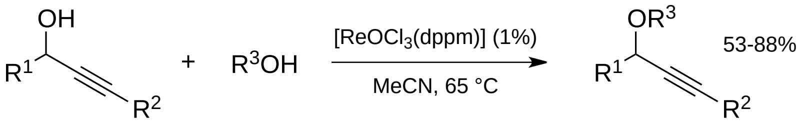

Scheme 15

Espenson and Zhu reported the reaction of EDA with aldehydes and ketones catalyzed by MTO to produce epoxides in moderate to good yields (Scheme 16).[68] This reaction is analogous to the aziridination reported by the same group (Scheme 11).[67] With this system, when phenols or alcohols are used as substrates, the corresponding ethers are obtained, also in good yields.[68]

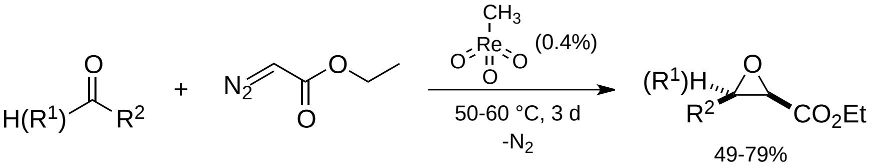

Scheme 16

1.3.4. Hydrosilylations

The rhenium-catalyzed addition of silanes to C-C and C-X (X = O, N) double bonds has been subject of intense research in the last lustrum. Several different rhenium complexes, most of them high-valent, have been used effectively in this transformations, displaying high activities and selectivities.

Hua and co-workers provided one of the few examples of Si-H addition to double bonds catalyzed by low-valent rhenium complexes. They studied the hydrosylilation of styrenes using various rhenium(I) and (0) complexes as catalysts to afford selectively the corresponding *anti*-Markovnikov adducts. From the tested catalysts [ReBr(CO)$_5$] yielded the best results (Scheme 17).[73]

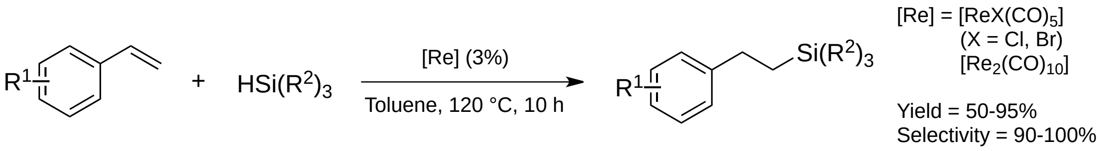

Scheme 17

In a seminal publication, Toste and co-workers reported the hydrosylilation of aldehydes and ketones using the air- and moisture-tolerant rhenium(V)-dioxo complex $[ReO_2I(PPh_3)_2]$ under mild conditions (Scheme 18). This new one-step reduction-protection method tolerates a wide range of functional groups such as amino, cyano, nitro, aryl halo, ester and alkene.[74] This transformation, formally a reduction, is conceptually interesting since it "reverses" the traditional role of high-valent metal-oxo complexes, typically used as oxidants.

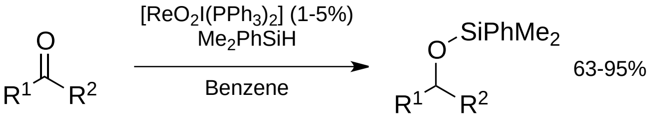

Scheme 18

The unprecedented mechanism for this reaction was thoroughly studied experimentally[75] and supported by DFT calculations.[76] It proceeds as follows: 1) [2+2] addition of the Si-H bond across one of the rhenium-oxo bonds to give $[Re(I)(O)(H)(OSiR_3)(PPh_3)_2]$; 2) coordination of the carbonyl to the resulting rhenium(V)-hydrido intermediate preceded by dissociation of one phosphine ligand; 3) reduction of the C-O double bond by insertion into the Re-H bond to yield a siloxyrhenium alkoxide complex; 4) re-coordination of the free phosphine ligand and concomitant liberation of the product by transfer of the silyl group from the siloxy ligand to the alkoxy ligand via a formal retro-[2+2] reaction (Scheme 19).[75] What makes this mechanistic proposal unprecedented is that, contrary to the widely accepted mechanism first proposed by Chalk and Harrod,[77] the activation of the Si-H bond is not made via oxidative addition to the metal center.

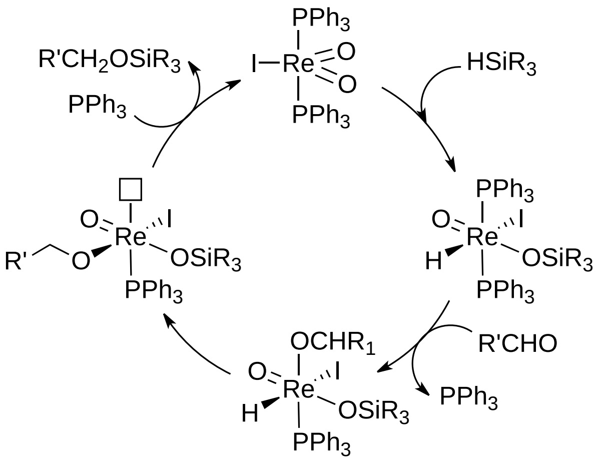
PPh3
I—Re
O
O
PPh3
HSiR3
R'CH2OSiR3
PPh3
O
Re
I
H
OSiR3
R'CHO
OCHR1
R'
PPh3

Scheme 19

Abu-Omar and co-workers reported a series of cationic rhenium(V) complexes, highly active as catalysts for the hydrosylilation of aldehydes and ketones at room temperature (Scheme 20).[78] They found out a σ-bond metathesis mechanism in which the organosilane is activated through the formation of a η^2-R_3SiH complex and without the involvement of a metal hydride. They also demonstrated that their mono-oxo complexes do not undergo addition of the silane across the Re-X multiple bond (X = O, N). These results are in strong contrast with the mechanism found by the Toste group. They even claimed that "the postulated mechanism for *cis*-$Re(O)_2I(PPh_3)_2$ is likely to be the exception rather than the rule for hydrosilylation reactions catalyzed by high-valent oxorhenium complexes".[79]

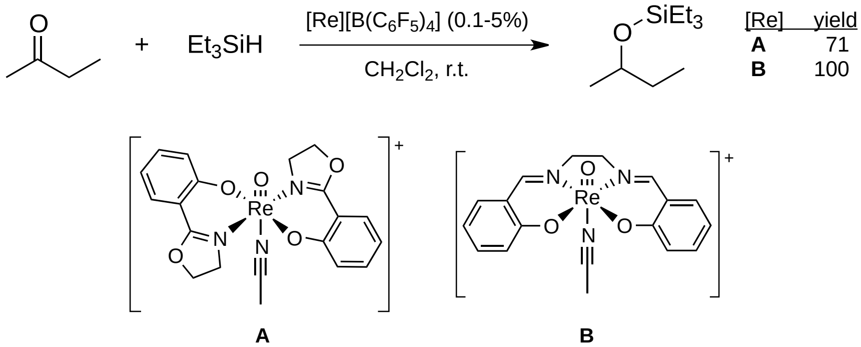
+
Et3SiH
[Re][B(C6F5)4] (0.1-5%)
CH2Cl2, r.t.
SiEt3
O
[Re] yield
A 71
B 100
Re
N
O
+
A
B

Scheme 20

The enantioselective version of this reaction was reported recently by Toste using chiral, non racemic, rhenium(V)-oxo complexes with cianobis(oxazoline) ligands (Scheme 21). These complexes catalyze efficiently the hydrosilylation of imines and ketones in high yields and with high enantioselectivities. The reaction conditions are mild and the cautious exclusion of moisture is not necessary thanks to the pronounced stability of the catalysts.[80]

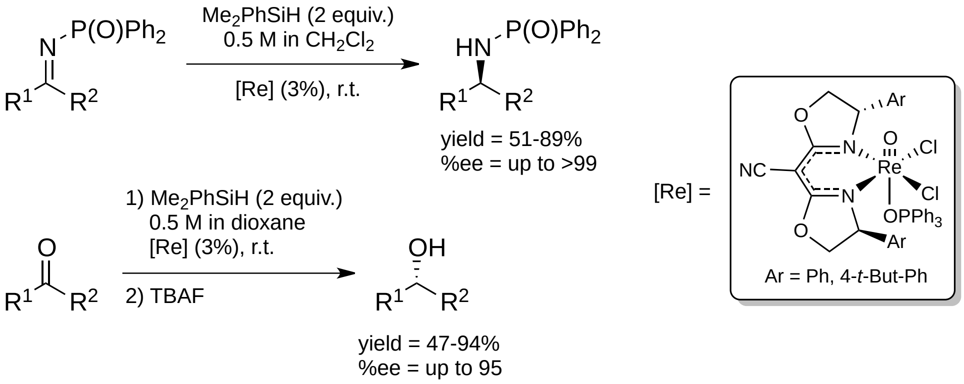
P(O)Ph$_2$
N
R^1
R^2
Me$_2$PhSiH (2 equiv.)
0.5 M in CH$_2$Cl$_2$
[Re] (3%), r.t.
HN
P(O)Ph$_2$
yield = 51-89%
%ee = up to >99
O
1) Me$_2$PhSiH (2 equiv.)
0.5 M in dioxane
[Re] (3%), r.t.
2) TBAF
OH
yield = 47-94%
%ee = up to 95
[Re] =
NC
Re
Cl
OPPh$_3$
Ar
Ar = Ph, 4-*t*-But-Ph

Scheme 21

1.3.5. Hydrogenations and dehydrogenations

In July 1930 the Bataafsche Petroleum, a Dutch company, patented the use of rhenium sulfides for the production of liquid hydrocarbons by destructive hydrogenation of "carbonaceous materials", i. e. coal, lignin, asphalt, tar, cellulose, etc.[81] This is the first mention in the literature of a rhenium hydrogenation catalyst. In August of the same year, Tropsch and Kassler reported some catalytic properties of rhenium metal, showing its ability to hydrogenate ethylene and carbon monoxide, albeit in low yields.[82] In the late thirties Platonow and his group in Leningrad (today's St. Petersburg) studied the capabilities of rhenium metal in the hydrogenation of several substrates[83] and also in the dehydrogenation of alcohols.[84] During the subsequent two decades, the research in rhenium catalysis stood relatively still, due principally to the warfare (WW2). In the late fifties and sixties this area flourished again, mainly thanks to the work of Broadbent and his group in Utah who developed various rhenium-catalyzed processes for both hydrogenation and dehydrogenation.[85] These new catalysts (specially rhenium oxides, sulfides and selenides) were highly selective for carbonyl, nitro and olefin groups and showed a remarkable resistance to poisoning.[51]

Apart from a short communication from the late sixties describing the hydrogenation of olefins catalyzed by $ReCl_5$ in the presence of $SnCl_2$ in polar solvents,[86] the actual incursion of rhenium complexes in the realm of homogeneous catalysis only took place in the eighties, with the work of Belousov and his group. They reported the use of high-valent rhenium complexes, with mono- and bidentate phosphine ligands, in the hydrogenation of 1-hexene. The highest catalytic activities were found for the complexes $[ReOX_3(PPh_3)_2]$ (X = Cl, Br) and $[ReOBr_3(dppe)]$.[87] Later, in 1990, the same Russian group described the hydrogenation of nitro compounds catalyzed by rhenium(V)-oxo-halide complexes with thiourea and phosphine ligands.[88] In 2000, Ryashentseva and Borisova extended the applicability of rhenium(V) complexes with thiourea derivatives for the hydrogenation of cyclohexene.[89]

The groups of Royo and Calhorda, both in Portugal, published in 2008 the first report on rhenium-catalyzed alkyne hydrogenation. They used high-valent Re^{V}- and Re^{VII}-oxo complexes to selectively reduce alkynes to alkenes in quantitative yields. Under similar conditions, these catalysts were also capable of reducing sulfoxides to sulfides (Scheme 22).[90]

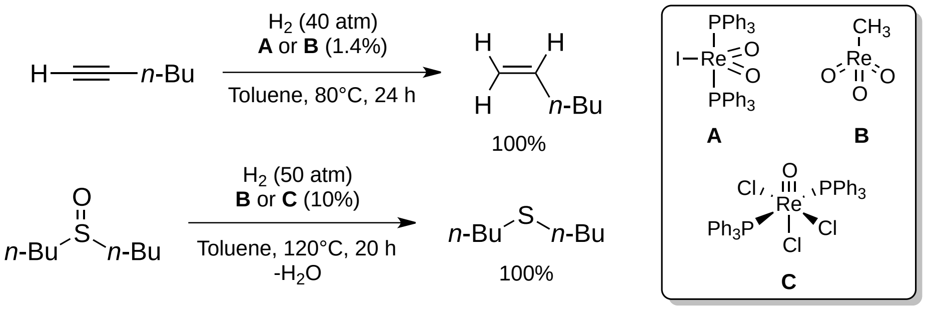

Scheme 22

Very recently, Berke and co-workers reported outstanding results in alkene hydrogenation using the highly active rhenium(I)-mononitrosyl hydride complexes presented in Scheme 23. Initial experiments on the hydrogenation of alkenes using complexes of the type $[Re(H)_2(\eta^2C_2H_4)(NO)(PR_3)_2]$ (**A**, Scheme 23) under hydrogen pressure (68-70 bar) afforded the corresponding alkanes in good to excellent yields (up to 100%) but with moderate activities (TOF up to 47 h^{-1}).[91] A much more efficient system for the hydrogenation of olefins was developed by the same group using five-coordinate rhenium(I) complexes of the general formula $[ReBrH(NO)(PR_3)_2]$ (**B**, Scheme 23). With the aid of Lewis acids as co-catalysts, they obtained high conversions (up to quantitative) and exceptionally high activities (TOF up to 56000 h^{-1}), comparable to those of Ir, Rh or Ru catalysts, ranking it among the best transition-metal catalysts for hydrogenations.[92]

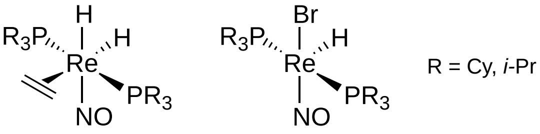

A **B**

Scheme 23

Concerning rhenium-catalyzed asymmetric hydrogenations, very little has been done. There is actually only one report, a somewhat obscure patent, that describes the asymmetric reduction of α,β-unsaturated carboxylic acids in the presence of rhenium halides and a chiral diphosphine ligand.[93]

In 1980 Baudry, Ephritikhine and Felkin observed that bis(phosphine)rhenium heptahydrides $[ReH_7(PAr_3)_2]$ were capable of dehydrogenate linear and cyclic alkanes stoichiometrically via C-H bond activation to afford selectively the corresponding mono alkenes.[94] The French group then developed the catalytic version of this reaction using an olefin as the hydrogen acceptor. The reaction conditions were mild (30-80 °C) but the catalysts were not very efficient (up to 9 turnovers).[95] The proposed reaction mechanism is depicted in Scheme 24.[96] The first step is the thermal (or photochemical) dehydrogenation of the rhenium(VII)-heptahydride to produce the coordinatively unsaturated rhenium(V) species $[ReH_5(PAr_3)_2]$. The next step is the insertion of the added olefin into one Re-H bond, followed by a reductive elimination to give the highly reactive intermediate

$[ReH_3(PAr_3)_2]$. This rhenium(III) species oxidativelly adds the alkane substrate to afford $[ReH_4R(PAr_3)_2]$ which undergoes β-hydride elimination, regenerating the pentahydride and releasing the product.

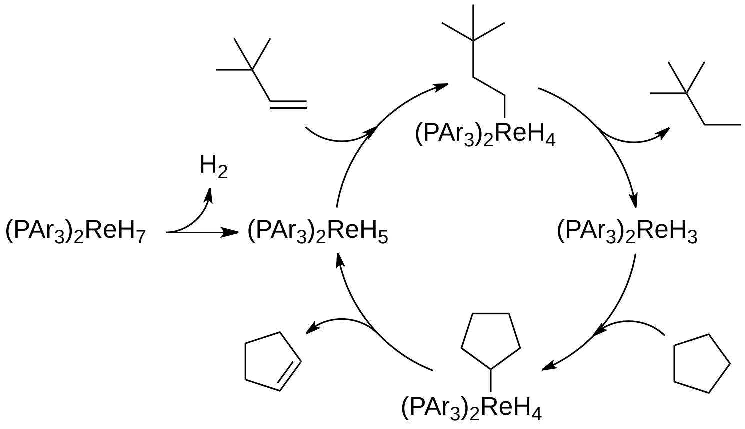

Scheme 24

A decade later, Crabtree improved the system by obviating the addition of the hydrogen acceptor, removing the produced hydrogen simply by reflux of the solvent or by bubbling an inert gas through the reaction mixture. In his experiments, among other precious metals, he used the rhenium(V) pentahydride $[ReH_5(triphos)]$. This new method had a broader scope than those published before.[97]

1.3.6. Oxygen transfer reactions and oxidations

Probably the main use of rhenium complexes in catalysis is precisely as oxidants and oxygen atom transfer reagents in several organic transformations. The most important class among these complexes, are rhenium(VII) oxides and peroxides for which it has been said, they are the most versatile oxidation catalysts in organic chemistry.[38b] About two decades ago, the potential use of rhenium complexes in catalytic oxidations was still not recognized, which is somehow surprising since its neighbors, tungsten and osmium, form exceptional epoxidation and oxidation catalysts.[98] Thanks to the arduous work of Herrmann and his group in Munich, the enormous usefulness of MTO and its peroxo derivatives has been successfully exploited for the catalytic oxidation of several substrates.[38]

The most meticulously studied catalytic oxidation reaction using rhenium(VII) oxides as catalysts, specially MTO, is olefin epoxidation.[99] The system MTO/H_2O_2 is highly active at room temperature and even at -30 °C, using catalyst loadings as low as 0.2%. Contrary to several metal-based epoxidation catalysts, MTO do not decompose H_2O_2. One proposed mechanistic pathway is depicted in Scheme 25.[38b]

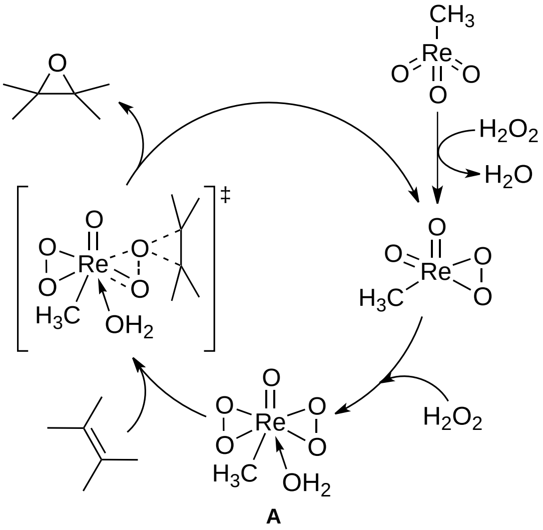

Scheme 25

The first step in the reaction mechanism is the formation of a monoperoxo complex which reacts further with H_2O_2 to give the bisperoxo complex [Re(CH_3)(O_2)(O)] (**A**, Scheme 25) which has been isolated as a solvato adduct and fully characterized.[100] The next step is the attack of the electron-rich double bond to a peroxidic oxygen to form the corresponding epoxide.[38] The addition of Lewis bases like pyridine or quinuclidine enhances the selectivity towards epoxidation, suppressing the diol formation.[99]

The catalytic system MTO/H_2O_2 has been applied successfully for the oxidation of alkanes, alkynes, aromatic compounds, sulfur compounds, phosphines, arsines, stibines, organonitrogen compounds, halide ions, etc.[38a] The deep understanding of their reactivity and mechanisms, acquired through Herrmann's research, has served as model for the study of other metal-oxide catalysts.[38b]

Gable and co-workers have comprehensively studied the catalytic oxygen atom transfer (OAT) reactions from epoxides to phosphines to give the corresponding alkenes with retention of configuration, using rhenium(VII) oxides of the type [$ReLO_3$] (L = Cp*, tris(3,5-dimethylpirazolyl)hydridoborate).[101] The catalytically active species is proposed to be a rhenium(V) intermediate of the type [$ReLO_2$] resulting from the abstraction of an oxygen atom by the added phosphine. This highly electron-deficient species can then deoxygenate the epoxide substrate, to give the alkene product (Scheme 26).[101a]

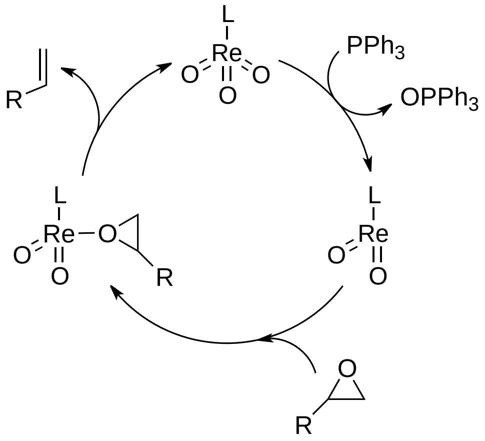

Scheme 26

Catalytic OAT reactions have also been effectively promoted by rhenium(V)-oxo complexes with bidentate oxazoline- and thiazoline-derived ligands.[11f] For example, Abu-Omar reported the fast reduction of perchlorate with sulfides to afford the corresponding sulfoxides under mild conditions using [$ReO(hoz)_2L$]OTf (hoz = 2-(2'-hydroxyphenyl)-2-oxazoline, L = H_2O, MeCN) as catalysts.[102] The reaction mechanism is outlined in Scheme 27. The kinetics of such transformations are extremely fast, approaching even enzymatic activities.[102] In a first step, the oxygen donor (in this case perchlorate) coordinates to the coordinatively unsaturated rhenium(V) monooxo complex [$ReO(hoz)_2L$]$^+$ which is then oxidized to a rhenium(VII) dioxo species. The oxygen acceptor reacts with the resulting Re^{VII} intermediate which gets reduced to the initial Re^V complex, affording the OAT product and closing the catalytic cycle.

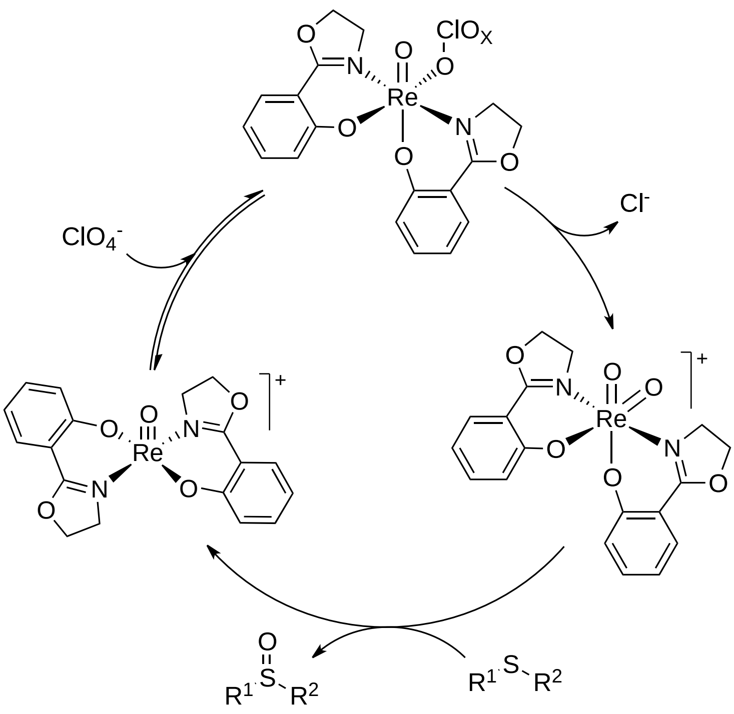

Scheme 27

1.3.7. *Olefin metathesis*

Not long after the discovery of metal-catalyzed olefin metathesis in the late fifties by Eleuterio, using heterogeneous group VI metal oxide catalysts,[103] the high activity of rhenium oxides in this transformation was recognized. In 1966 Howman and Turner (BP Chemicals) patented the system Re_2O_7/Al_2O_3 as an effective catalyst for olefin metathesis under mild conditions.[104] Along with molybdenum and tungsten, rhenium belongs to the most active metals in "classical" heterogeneous olefin metathesis systems.[105] However, the poor understanding of the nature of the active sites (structure **A** in Scheme 28 is the proposed active species in Re_2O_7/Al_2O_3) and governing mechanisms of these systems somewhat hampered the research directed towards their improvement.[106]

More than twenty years after the work of Calderon, who in 1967 reported the first homogeneous version of the reaction using a mixture of WCl_6 and $EtAlCl_2$ in ethanol,[107] Schrock and his team prepared in 1990 the first well-defined rhenium complex active in olefin metathesis.[105, 108] This compound, namely [Re(C-*t*-Bu)(CH-*t*-Bu)(OCMe(CF_3)$_2$)$_2$] (**B**, Scheme 28),[108a] although active, did not exhibit metathesis rates comparable to those of Mo and W and, furthermore, it showed high sensitivity to deactivation by acidic (and other) impurities and substrate inhibition (for example with ester-containing olefins).[108b]

In 2001, Coperét and Basset tackled the problem by grafting of [Re(C-*t*-Bu)(CH-*t*-Bu)(CH$_2$-*t*-Bu)$_2$] on silica to obtain the well-defined Silica(O)-[Re(C-*t*-Bu)(CH-*t*-Bu)(CH$_2$-*t*-Bu)] species (**C**, Scheme 28).[109] This supported catalyst showed to be more efficient than the best of its molecular counterparts, readily catalyzing the metathesis of functionalized olefins without additional co-catalysts.[110]

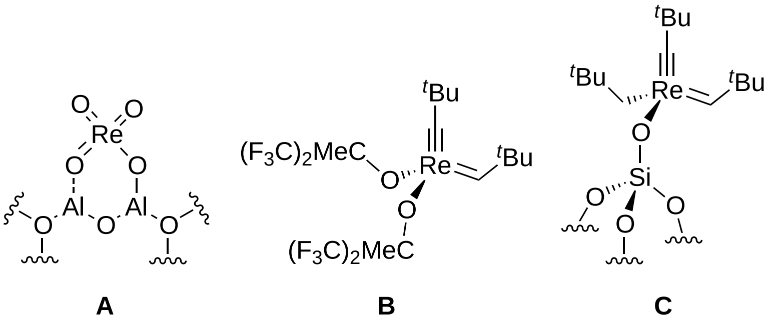

Scheme 28

The feasible synthesis of an effective homogeneous rhenium catalysts for these processes was questioned in 2003 by Schrock: "It remains to be seen whether well-defined rhenium complexes that are highly active for olefin metathesis in solution can be prepared".[111] The answer to Schrock's doubts was soon found by Berke in 2006 who, with his low-valent rhenium-nitrosyl complexes, obtained unprecedented activities in ROMP reactions.[112] These rhenium dinitrosyl-biphosphine complexes (**A**, Scheme 29), [Re(NO)$_2$(PR$_3$)$_2$][BAr$^F_4$] (R = Cy, *i*-Pr), are prepared by hydride abstraction from [ReH(NO)$_2$(PR$_3$)$_2$] and can be easily converted in the corresponding benzylidene derivatives (**B**, Scheme 29) which, in turn, showed almost no catalytic activity. The proposed, rather complex, reaction mechanism has been thoroughly studied and supported by experimental and theoretical evidence. This system is only suitable for ROMP of strained, non-functionalized cyclic olefins like norbornene. No activity was observed in the metathesis of simple linear olefins.[112]

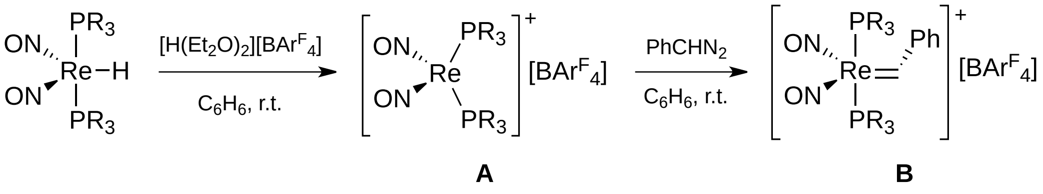
PR3
ON
Re–H
ON
PR3
[H(Et2O)2][BArF4]
C6H6, r.t.
+
[BArF4]
PhCHN2
C6H6, r.t.
Ph
A
B

Scheme 29

References

[1] D. Mendelejeff, *Zeitschr. f. Chem.* **1869**, 405-406.

[2] D. Mendelejeff, *Ann. d. Chem. u. Pharm.* **1871**, *VIII. Suplementband*, 133-229.

[3] W. Prandtl, A. Grimm, *Z. Anorg. Allg. Chem.* **1923**, *136*, 283-288.

[4] H. K. Yoshihara, *Spectrochim. Acta, Part B* **2004**, *59*, 1305-1310.

[5] I. Tacke, W. Noddack, O. Berg, *Naturwissenschaften* **1925**, *26*, 567-574.

[6] R. Zingales, *J. Chem. Educ.* **2005**, *82*, 221-227.

[7] J. Noddack, W. Noddack, *Z. Anorg. Allg. Chem.* **1929**, *183*, 353-375.

[8] G. Rouschias, *Chem. Rev.* **1974**, *74*, 531-566.

[9] N. Greenwood, A. Earnshaw, *Chemistry of the Elements*, 2 ed., Butterworth-Heinemann, Oxford, **1998**.

[10] M. A. Korzhinsky, S. I. Tkachenko, K. I. Shmulovich, Y. A. Taran, G. S. Steinberg, *Nature* **1994**, *369*, 51-52.

[11] a) K. A. Conner, R. A. Walton, in *Comprehensive Coordination Chemistry, Vol. 4* (Eds.: G. Wilkinson, R. Gillard, J. A. McCleverty), Pergamon, **1987**, pp. 125-203; b) U. Abram, in *Comprehensive Coordination Chemistry II, Vol. 5*, Second ed. (Eds.: J. A. McCleverty, T. J. Meyer), Elsevier, **2003**, pp. 271-402; c) B. Royo, C. C. Romão, in *Comprehensive Organometallic Chemistry III, Vol. 5* (Eds.: R. H. Crabtree, D. M. P. Mingos), Elsevier, **2007**, pp. 855-960; d) J. O'Connor, in *Comprehensive Organometallic Chemistry II, Vol. 6* (Eds.: E. W. Abel, F. G. A. Stone, G. Wilkinson), Pergamon, Oxford, **1995**, pp. 167-229; e) C. C. Romão, in *Encyclopedia of Inorganic Chemistry*, John Wiley & Sons, Ltd, **2006**; f) A. J. L. Pombeiro, M. F. C. Guedes da Silva, R. H. Crabtree, in *Encyclopedia of Inorganic Chemistry*, John Wiley & Sons, Ltd, **2006**.

[12] P. V. Poplaukhin, X. Chen, E. A. Meyers, S. G. Shore, *Inorg. Chem.* **2006**, *45*, 10115-10125.

[13] Y. Zhen, J. D. Atwood, *J. Am. Chem. Soc.* **1989**, *111*, 1506-1508.

[14] M. R. Churchill, K. N. Amoh, H. J. Wasserman, *Inorg. Chem.* **1981**, *20*, 1609-1611.

[15] S. Top, P. Morel, M. Pankowski, G. Jaouen, *J. Chem. Soc. Dalton Trans.* **1996**, 3611-3612.

[16] P. Johnston, G. J. Hutchings, N. J. Coville, *J. Am. Chem. Soc.* **1989**, *111*, 1902-1903.

[17] D. Vitali, F. Calderazzo, *Gazz. Chim. Ital.* **1972**, *102*, 587-596.

[18] F. Calderazzo, I. P. Mavani, D. Vitali, I. Bernal, J. D. Korp, J. L. Atwood, *J. Organomet. Chem.* **1978**, *160*, 207-222.

[19] A. E. Leins, N. J. Coville, *J. Organomet. Chem.* **1991**, *407*, 359-367.

[20] T. J. Barder, F. A. Cotton, K. R. Dunbar, G. L. Powell, W. Schwotzer, R. A. Walton, *Inorg. Chem.* **1985**, *24*, 2550-2554.

[21] F. Zobi, L. Kromer, B. Spingler, R. Alberto, *Inorg. Chem.* **2009**, *48*, 8965-8970.

[22] F. A. Cotton, C. A. Murillo, R. A. Walton, in *Multiple Bonds between Metal Atoms*, Third ed. (Eds.: F. A. Cotton, C. A. Murillo, R. A. Walton), Springer Science and Business, New York, **2005**, pp. 1-15.

[23] V. G. Kuznetzov, P. A. Koz'min, *J. Struct. Chem.* **1963**, *4*, 49-55.

[24] F. A. Cotton, N. F. Curtis, C. B. Harris, B. F. G. Johnson, S. J. Lippard, J. T. Mague, W. R. Robinson, J. S. Wood, *Science* **1964**, *145*, 1305-1307.

[25] F. Albert Cotton, J. H. Matonic, D. d. O. Silva, *Inorg. Chim. Acta.* **1995**, *234*, 115-125.

[26] N. D. Reddy, P. E. Fanwick, R. A. Walton, *Inorg. Chem.* **2001**, *40*, 1732-1733.

[27] I. M. Gardiner, M. A. Bruck, P. A. Wexler, D. E. Wigley, *Inorg. Chem.* **1989**, *28*, 3688-3695.

[28] L. M. Engelhardt, B. N. Figgis, A. N. Sobolev, P. A. Reynolds, *Aust. J. Chem.* **1996**, *49*, 489-496.

[29] D. W. von Gudenberg, G. Frenzen, W. Massa, K. Dehnicke, *Z. Anorg. Allg. Chem.* **1995**, *621*, 525-530.

[30] N. P. Johnson, C. J. L. Lock, G. Wilkinson, J. L. Booker, R. J. Thompson, in *Inorganic Syntheses, Vol. 9* (Ed.: S. Y. Tyree), McGraw-Hill, **1967**, pp. 145-148.

[31] U. Abram, M. Braun, S. Abram, R. Kirmse, A. Voigt, *J. Chem. Soc. Dalton Trans.* **1998**, 231-238.

[32] J. Chatt, G. J. Leigh, D. M. P. Mingos, R. J. Paske, *J. Chem. Soc. (A)* **1968**, 2636-2641.

[33] A.-M. Lebuis, A. Beauchamp, *Can. J. Chem.* **1993**, *71*, 441-449.

[34] K. F. Mucker, G. S. Smith, Q. Johnson, *Acta Cryst.* **1968**, *B24*, 874-879.

[35] a) D. A. Edwards, R. T. Ward, *J. Chem. Soc. (A)* **1970**, 1617-1620; b) H. Gehrke, G. Eastland, *Inorg. Chem.* **1970**, *9*, 2722-2725.

[36] W. Noh, G. S. Girolami, *Dalton Trans.* **2007**, 674-679.

[37] W. A. Herrmann, J. D. G. Correia, F. E. Kühn, G. R. J. Artus, C. C. Romão, *Chem. Eur. J.* **1996**, *2*, 168-173.

[38] a) C. C. Romão, F. E. Kühn, W. A. Herrmann, *Chem. Rev.* **1997**, *97*, 3197-3246; b) F. Kühn, W. Herrmann, in *Structure and Bonding, Vol. 97* (Ed.: B. Meunier), Springer Berlin / Heidelberg, **2000**, pp. 213-236.

[39] W. A. Herrmann, W. Scherer, R. W. Fischer, J. Bluemel, M. Kleine, W. Mertin, R. Gruehn, J. Mink, H. Boysen, *J. Am. Chem. Soc.* **1995**, *117*, 3231-3243.

[40] I. R. Beattie, P. J. Jones, *Inorg. Chem.* **1979**, *18*, 2318-2319.

[41] W. A. Herrmann, J. G. Kuchler, J. K. Felixberger, E. Herdtweck, W. Wagner, *Angew. Chem.* **1988**, *100*, 420-422.

[42] W. Herrmann, A. Rost, J. Mitterpleininger, N. Szesni, S. Sturm, R. Fischer, F. Kühn, *Angew. Chem. Int. Ed.* **2007**, *46*, 7301-7303.

[43] J. G. Malm, H. Selig, *J. Inorg. Nucl. Chem.* **1961**, *20*, 189-197.

[44] J. B. Bravo, E. Griswold, J. Kleinberg, *J. Phys. Chem.* **1954**, *58*, 18-21.

[45] A. P. Ginsberg, J. M. Miller, J. R. Cavanaugh, B. P. Dailey, *Nature* **1960**, *185*, 528-529.

[46] S. C. Abrahams, A. P. Ginsberg, K. Knox, *Inorg. Chem.* **1964**, *3*, 558-567.

[47] W. Bronger, L. à. Brassard, P. Müller, B. Lebech, T. Schultz, *Z. Anorg. Allg. Chem.* **1999**, *625*, 1143-1146.

[48] Y. Kuninobu, K. Takai, *Chem. Rev.* **2010**, *111*, 1938-1953.

[49] J. G. F. Druce, *Continental Met. & Chem. Eng.* **1926**, *1*, 111-112.

[50] I. Noddack, W. Noddack*, Vol. B01J23/36*, Siemens AG, Germany, **1929**.

[51] W. H. Davenport, V. Kollonitsch, C. H. Kline, *Ind. Eng. Chem.* **1968**, *60*, 10-19.

[52] R. Hua, J.-L. Jiang, *Curr. Org. Syn.* **2007**, *4*, 151-174.

[53] J. Tsuji, T. Nogi, M. Morikawa, *Bull. Chem. Soc. Jpn.* **1966**, *39*, 714-716.

[54] H. Kusama, K. Narasaka, *Bull. Chem. Soc. Jpn.* **1995**, *68*, 2379-2383.

[55] C. Bolm, M. Kesselgruber, N. Hermanns, J. P. Hildebrand, G. Raabe, *Angew. Chem. Int. Ed.* **2001**, *40*, 1488-1490.

[56] M. Hirano, M. Hirai, Y. Ito, T. Tsurumaki, A. Baba, A. Fukuoka, S. Komiya, *J. Organomet. Chem.* **1998**, *569*, 3-14.

[57] a) Y. Kuninobu, A. Kawata, K. Takai, *J. Am. Chem. Soc.* **2005**, *127*, 13498-13499; b) Y. Kuninobu, Y. Nishina, A. Kawata, M. Shouho, K. Takai, *Pure Appl. Chem.* **2008**, *80*, 1149-1154.

[58] Y. Kuninobu, J. Morita, M. Nishi, A. Kawata, K. Takai, *Org. Lett.* **2009**, *11*, 2535-2537.

[59] Y. Kuninobu, H. Takata, A. Kawata, K. Takai, *Org. Lett.* **2008**, *10*, 3133-3135.

[60] Y. Kuninobu, T. Matsuki, K. Takai, *J. Am. Chem. Soc.* **2009**, *131*, 9914-9915.

[61] Y. Kuninobu, P. Yu, K. Takai, *Org. Lett.* **2010**, *12*, 4274-4276.

[62] C.-T. Yeung, P.-F. Teng, H.-L. Yeung, W.-T. Wong, H.-L. Kwong, *Org. Biomol. Chem.* **2007**, *5*, 3859-3864.

[63] M. R. Luzung, F. D. Toste, *J. Am. Chem. Soc.* **2003**, *125*, 15760-15761.

[64] Z. Zhu, J. H. Espenson, *J. Am. Chem. Soc.* **1997**, *119*, 3507-3512.

[65] T. E. Müller, M. Grosche, E. Herdtweck, A.-K. Pleier, E. Walter, Y.-K. Yan, *Organometallics* **1999**, *19*, 170-183.

[66] L. L. Ouh, T. E. Müller, Y. K. Yan, *J. Organomet. Chem.* **2005**, *690*, 3774-3782.

[67] Z. Zhu, J. H. Espenson, *J. Org. Chem.* **1995**, *60*, 7090-7091.

[68] Z. Zhu, J. H. Espenson, *J. Am. Chem. Soc.* **1996**, *118*, 9901-9907.

[69] Z. Zhu, J. H. Espenson, *J. Org. Chem.* **1996**, *61*, 324-328.

[70] R. V. Ohri, A. T. Radosevich, K. J. Hrovat, C. Musich, D. Huang, T. R. Holman, F. D. Toste, *Org. Lett.* **2005**, *7*, 2501-2504.

[71] Y. Liu, R. Hua, H.-B. Sun, X. Qiu, *Organometallics* **2005**, *24*, 2819-2821.

[72] B. D. Sherry, A. T. Radosevich, F. D. Toste, *J. Am. Chem. Soc.* **2003**, *125*, 6076-6077.

[73] W.-G. Zhao, R. Hua, *Eur. J. Org. Chem.* **2006**, 5495-5498.

[74] J. J. Kennedy-Smith, K. A. Nolin, H. P. Gunterman, F. D. Toste, *J. Am. Chem. Soc.* **2003**, *125*, 4056-4057.

[75] K. A. Nolin, J. R. Krumper, M. D. Pluth, R. G. Bergman, F. D. Toste, *J. Am. Chem. Soc.* **2007**, *129*, 14684-14696.

[76] L. W. Chung, H. G. Lee, Z. Lin, Y.-D. Wu, *J. Org. Chem.* **2006**, *71*, 6000-6009.

[77] A. J. Chalk, J. F. Harrod, *J. Am. Chem. Soc.* **1965**, *87*, 16-21.

[78] a) E. A. Ison, E. R. Trivedi, R. A. Corbin, M. M. Abu-Omar, *J. Am. Chem. Soc.* **2005**, *127*, 15374-15375; b) E. A. Ison, J. E. Cessarich, G. Du, P. E. Fanwick, M. M. Abu-Omar, *Inorg. Chem.* **2006**, *45*, 2385-2387.

[79] G. Du, P. E. Fanwick, M. M. Abu-Omar, *J. Am. Chem. Soc.* **2007**, *129*, 5180-5187.

[80] a) K. Nolin, R. Ahn, Y. Kobayashi, J. Kennedy-Smith, F. Toste, *Chem. Eur. J.* **2010**, *16*, 9555-9562; b) K. A. Nolin, R. W. Ahn, F. D. Toste, *J. Am. Chem. Soc.* **2005**, *127*, 12462-12463.

[81] N. V. de Bataafsche Petroleum Maatschappij*, Vol. GB 358180*, Bataafsche Petroleum, Great Britain, **1930**.

[82] H. Tropsch, R. Kassler, *Ber. Dtsch. Chem. Ges. B* **1930**, *63*, 2149-2151.

[83] M. S. Platonow, S. B. Anissimow, W. M. Krascheninnikowa, *Ber. Dtsch. Chem. Ges. B* **1935**, *68*, 761-765.

[84] M. S. Platonow, S. B. Anissimow, W. M. Krascheninnikowa, *Ber. Dtsch. Chem. Ges. B* **1936**, *69*, 1050-1053.

[85] H. S. Broadbent, *Ann. N. Y. Acad. Sci.* **1967**, *58*, 58-71.

[86] A. P. Krushch, A. E. Shilov, *Kinet. Katal.* **1969**, *10*, 466.

[87] V. M. Belousov, T. A. Palchevskaya, O. M. Negomedzyanova, K. V. Kotegov1, *React. Kinet. Catal. Lett.* **1985**, *28*, 41-46.

[88] V. M. Belousov, T. A. Palchevskaya, L. V. Bogutskaya, L. A. Zyuzya, *J. Mol. Cat.* **1990**, *60*, 165-172.

[89] M. A. Ryashentseva, L. V. Borisova, *Russ. Chem. Bull. Int. Ed.* **2000**, *49*, 1732-1734.

[90] P. M. Reis, P. J. Costa, C. C. Romão, J. A. Fernandes, M. J. Calhorda, B. Royo, *Dalton Trans.* **2008**, 1727-1733.

[91] A. Choualeb, E. Maccaroni, O. Blacque, H. W. Schmalle, H. Berke, *Organometallics* **2008**, *27*, 3474-3481.

[92] Y. Jiang, J. Hess, T. Fox, H. Berke, *J. Am. Chem. Soc.* **2010**, *132*, 18233-18247.

[93] W. D. Klobucar, C. H. Kolich, T. Manimaran*, Vol. 5187136*, Ethyl Corporation, Richmond, Va., United States, **1993**.

[94] a) D. Baudry, M. Ephritikhine, H. Felkin, *J. Chem. Soc., Chem. Commun.* **1980**, 1243-1244; b) D. Baudry, M. Ephritikhine, H. Felkin, *J. Chem. Soc., Chem. Commun.* **1982**, 606-607; c) D. Baudry, M. Ephritikhine, H. Felkin, J. Zakrzewski, *J. Chem. Soc., Chem. Commun.* **1982**, 1235-1236; d) D. Baudry, M. Ephritikhine, H. Felkin, J. Zakrzewski, *Tetrahedron Lett.* **1984**, *25*, 1283-1286.

[95] D. Baudry, M. Ephritikhine, H. Felkin, R. Holmes-Smith, *J. Chem. Soc., Chem. Commun.* **1983**, 788-789.

[96] N. Aktogu, D. Baudry, D. Cox, M. Ephritikhine, H. Felkin, R. Holmes-Smith, J. Zakrzewski, *Bull. Soc. Chim. Fr.* **1985**, 381-385.

[97] T. Aoki, R. H. Crabtree, *Organometallics* **1993**, *12*, 294-298.

[98] K. A. Jørgensen, *Chem. Rev.* **1989**, *89*, 431-458.

[99] W. A. Herrmann, R. W. Fischer, M. U. Rauch, W. Scherer, *J. Mol. Cat.* **1994**, *86*, 243-266.

[100] a) W. A. Herrmann, J. D. G. Correia, G. R. J. Artus, R. W. Fischer, C. C. Romão, *J. Organomet. Chem.* **1996**, *520*, 139-142; b) W. A. Herrmann, R. W. Fischer, W. Scherer, M. U. Rauch, *Angew. Chem. Int. Ed. Engl.* **1993**, *32*, 1157-1160.

[101] a) K. P. Gable, E. C. Brown, *J. Am. Chem. Soc.* **2003**, *125*, 11018-11026; b) K. P. Gable, E. C. Brown, *Organometallics* **2000**, *19*, 944-946; c) K. P. Gable, F. A. Zhuravlev, A. F. T. Yokochi, *Chem. Commun.* **1998**, 799-800.

[102] M. M. Abu-Omar, *Chem. Commun.* **2003**, 2102-2111.

[103] H. S. Eleuterio*, Vol. 3074918*, Du Pont, United States of America, **1963**.

[104] E. J. Howman, L. Turner*, Vol. 1105563*, British Petroleum Company, Great Britain **1966**.

[105] R. Toreki, R. R. Schrock, *J. Am. Chem. Soc.* **1990**, *112*, 2448-2449.

[106] C. Copéret, *New J. Chem.* **2004**, *28*, 1-10.

[107] N. Calderon, H. Y. Chen, K. W. Scott, *Tetrahedron Lett.* **1967**, *8*, 3327-3329.

[108] a) R. Toreki, R. R. Schrock, W. M. Davis, *J. Am. Chem. Soc.* **1992**, *114*, 3367-3380; b) R. Toreki, G. A. Vaughan, R. R. Schrock, W. M. Davis, *J. Am. Chem. Soc.* **1993**, *115*, 127-137.

[109] M. Chabanas, A. Baudouin, C. Copéret, J.-M. Basset, *J. Am. Chem. Soc.* **2001**, *123*, 2062-2063.

[110] M. Chabanas, C. Copéret, J.-M. Basset, *Chem. Eur. J.* **2003**, *9*, 971-975.

[111] R. R. Schrock, in *Handbook of Metathesis, Vol. 1* (Ed.: R. H. Grubbs), Wiley-VCH, Weinheim, **2003**, p. 20.

[112] C. M. Frech, O. Blacque, H. W. Schmalle, H. Berke, C. Adlhart, P. Chen, *Chem. Eur. J.* **2006**, *12*, 3325-3338.

2. Asymmetric Transfer Hydrogenation

2.1. Introduction

In search for new, more versatile, environmentally friendlier or "greener" chemical processes, transfer hydrogenation reactions have become an attractive alternative to the classical reduction with molecular hydrogen due to their high selectivity, mild reaction conditions and operational simplicity.[1] Depending on the nature of the metal and the ligands used, the mechanism of these processes could be classified in two main classes: direct H transfer or "metal-templated" and "hydride mediated" process.[1b].

The most popular hydrogen sources are 2-propanol,[2] formic acid[3] and the azeotropic mixture formic acid/triethylamine.[4] The metal complexes used to catalyze these transformations are limited to Rh,[2-3, 5] Ru,[4, 6] Ir,[5, 7] Ni,[8] and more recently Os[9] and Fe.[10] The ligands used in asymmetric transfer hydrogenation feature different architectures and donor atoms including oxygen, sulphur, nitrogen and phosphorus in different combinations and in bi-, tri- and tetradentate fashions.[1b]

Probably due to its scarcity,[11] the coordination chemistry of rhenium remains underdeveloped as compared to other transition metals. Nevertheless, in the last decade it has gained growing popularity as catalyst in different processes.[12] Since it is less expensive than rhodium or iridium and due to its unique chemistry,[13] rhenium-catalyzed reactions are an interesting field of exploration. In the field of rhenium-catalyzed asymmetric synthesis, the pioneering work of Toste on enantioselective hydrosilylation of ketones and imines[14] and that of Kwong in asymmetric cyclopropanation of alkenes[15] using chiral Re^V and Re^I catalysts standalone. Other important achievements in the rhenium-catalyzed reduction of carbonyls have been reported by Abu-Omar[16] and Royo.[17] For a most comprehensive perspective in rhenium-catalyzed reactions, see section 1.3.

A special class of ligands used in transfer hydrogenation reactions are bi-, tri-, or tetradentate ferrocenylphosphines,[6b, 18] which were only moderately successful until Baratta and co-workers reported outstanding results (enantioselectivity and TONs)[9, 19] by using Josiphos ligands (Scheme 1), some of the most successful in asymmetric catalysis and hence one of the so called "privileged ligands".[20] They have been widely used in several applications in research laboratories both in academia and industry.[20b]

In this chapter, the synthesis and characterization of a series of new rhenium complexes in different oxidation states with chiral bidentate ferrocenylphosphine ligands of the Josiphos family will be presented and discussed. Rhenium(V)-oxo and -nitrido complexes were successfully used as catalysts for the asymmetric transfer hydrogenation of ketones. A plausible reaction mechanism is also proposed.

2.1.1. Ferrocenylphosphine ligands of the Josiphos family

Bis-cyclopentadienyl iron or Ferrocene, discovered in 1951 by Kealy and Pauson,[21] has found uncountable applications in many areas of synthesis, materials and polymer sciences. Its remarkable stability and the plethora of methods to readily incorporate it into more complex structures, have led to the development of several molecules and materials with unique features.[22] A consequence of the famous "sandwich-like" structure of ferrocene, first conceived by Wilkinson[23] (who in 1973 got the Nobel prize in chemistry for this insightful thought), is that by 1,2- or 1,3-disubstitution a planar chiral motif is obtained which in turn could be potentially synthesized in enantiomerically pure form.[24] Perhaps the most popular method for the synthesis of such enantiomerically pure (or enriched) ferrocene derivatives exhibiting planar chirality is based on a diastereoselective *ortho*-lithiation followed by reaction with a suitable electrophile. This methodology was developed by Ugi and co-workers using a stereogenic amine fragment as a diastereoselective *ortho*-directing functionality.[25] This compound, (*R*)-[1-(dimethylamino)ethyl]ferrocene, typically called Ugi's amine, was used by Hayashi, Kumada, and co-workers*.* to prepare the first chiral ferrocenylphosphines, nicknamed *pfa* (phosphino-ferrocenyl-amine) (**1**) from which the dimethylamino group could be easily replaced by nucleophilic substitution with full retention of configuration.[26] This method was elegantly exploited by Togni to synthesize several chiral ferrocenyldiphosphines (**2**) by reaction of **1** with different secondary phosphines (see Scheme 1). These compounds showed outstanding performance as chelating ligands in various asymmetric transformations.[27] The first of them to be synthesized, (*R*)-1-[(S_P)-2-(diphenylphosphino)ferrocenyl]ethyldicyclohexylphosphine (**2a**) was called *Josiphos* after Josi Puleo, the technician who actually first prepared it. Nowadays the name is used for the whole family of ligands. The most remarkable feature of this procedure is that the two phosphine substituents are introduced in separate consecutive steps, conferring high modularity to the system and the possibility to fine-tune the steric and electronic properties of the ligands.

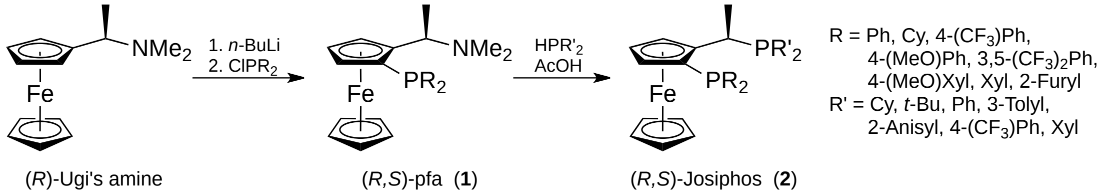
NMe2
Fe
1. n-BuLi
2. ClPR2
NMe2
PR2
Fe
HPR'2
AcOH
PR'2
PR2
Fe
R = Ph, Cy, 4-(CF3)Ph, 4-(MeO)Ph, 3,5-(CF3)2Ph, 4-(MeO)Xyl, Xyl, 2-Furyl
R' = Cy, t-Bu, Ph, 3-Tolyl, 2-Anisyl, 4-(CF3)Ph, Xyl
(R)-Ugi's amine
(R,S)-pfa (1)
(R,S)-Josiphos (2)

Scheme 1

Several complexes containing Josiphos ligands have been prepared with various metals including Pd, Ir, Rh, Ru, Cu, Pt and W. These complexes have been successfully used in different asymmetric transformations like enantioselective reductions of C=C, C=O and C=N bonds, hydroborations, hydrophosphinations, hydroaminations, hydrocarboxylations, allylic alkylations, Michael additions, Heck reactions, isomerizations, ring-opening reactions, etc. Comprehensive reviews covering all these catalytic applications in both academia and industry, as well as synthetic and structural aspects of Josiphos ligands, are available in the literature.[20b, 28]

2.2. Synthesis and Characterization of Complexes

2.2.1. Ligand synthesis

Ferrocenyldiphosphine ligands of the Josiphos family were synthesized by a slight modification of the reported procedure.[27] The common precursor in all cases was the comercially available (*R*)-Ugi's amine[25b] which in a first step is selectively *orto*-lithiated and the resulting ferrocenyllithium derivate allowed to react with the corresponding secondary chlorophosphine to give the (*R,S*)-pfa intermediate (**1**). The dimethylamino moiety is then substituted by the corresponding secondary phosphine to give the desired Josiphos ligand (**2**) (see Scheme 1). In this work only the "classic" Josiphos (R = Ph, R' = Cy, **2a**) and the commercially unavailable analogues were synthesized. All other ferrocenyldiphosphine ligands were purchased from Solvias AG. Ligand **2l** (R = CF_3) was synthesized and kindly provided by R. Koller.[29]

2.2.2. Synthesis of rhenium(I) derivatives

The chemistry of rhenium(I) complexes is governed by the ubiquitous $[Re(CO)_3]^+$ core. These kind of complexes are air- and moisture stable- and large number of examples have been prepared (see section 1.2.3.). Strange enough, their application as catalysts are virtually limited to the most simple ones, namely $[ReX(CO)_3]$ (X = Cl, Br, H) and $[ReBr(CO)_3(THF)]_2$[12b] (see section 1.3.). One notable exception is the work of Kwong and co-workers in the asymmetric cyclopropanation of alkenes with rhenium(I) tricarbonyl catalysts containing chiral bi- and tri-dentate ligands with nitrogen donor atoms (see section 1.3.1., Scheme 7). To the best of our knowledge, no complexes of the type $[ReX(CO)_3L_2]$ with chiral bi-dentate phosphines have been used in catalysis. Besides, actually only one such complexes has been published, $[ReMe(CO)_3($*S,S*-chiraphos$)]$, but without any catalytic application.[30]

Encouraged by this precedent, we decided to undertake the synthesis of rhenium(I)-tricarbonyl complexes containing chiral ferrocenyldiphosphine ligands of the Josiphos family and test their activity in asymmetric catalysis. The first one of these complexes to be synthesized was $[ReBr(CO)_3($**2a**$)]$ (**3**). It was prepared by thermal decarbonylation of the commercially available $[ReBr(CO)_5]$ in the presence of the chelating biphosphine ligand. It was obtained by adapting the procedure reported by Bond and co-workers for the synthesis of $[M(CO)_2(P_2P')X]^{+/0}$ (M = Mn, Re; X = Cl, Br; P_2P' = η^3-$Ph_2P(CH_2)_2P(Ph)(CH_2)_2PPh_2$).[31] Due to the high temperature required to accomplish the ligand substitution,[31] we decided to use tetralin (1,2,3,4-tetrahydronaphthalene) as solvent. After completion of the reaction the product was separated from the high-boiling-point solvent by passing the reaction mixture trough a plug of silica using *n*-hexane as eluent. The same method was employed for the synthesis of the chlorine analog [ReCl(CO)$_3$(**2a**)] (**4**) (Scheme 2).

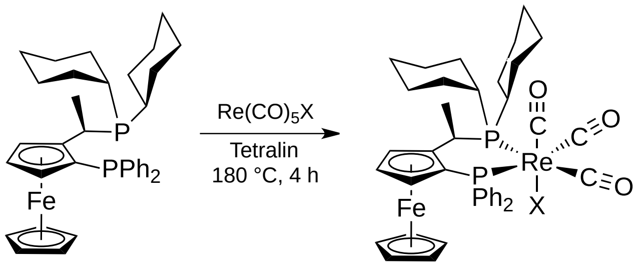

2a

X	Comp.	Yield(%)
Br	**3**	97
Cl	**4**	74

Scheme 2

Both complexes **3** and **4** were obtained in good yields, which, considering the harsh reaction conditions, speaks for the high stability not only of the compounds, but also of the Josiphos ligand. In both cases, a considerable excess of one of both possible isomers *endo* or *exo* (according to the relative position of the halide ligand with respect to the unsubstituted Cp ring) was obtained (for an explanation to this preference see below). The preferential formation of one isomer could be easily confirmed in the ^{31}P NMR spectra. In both cases, two major doublet peaks are observed, accompanied by another set of doublets corresponding to the minor isomer (see Figure 1).

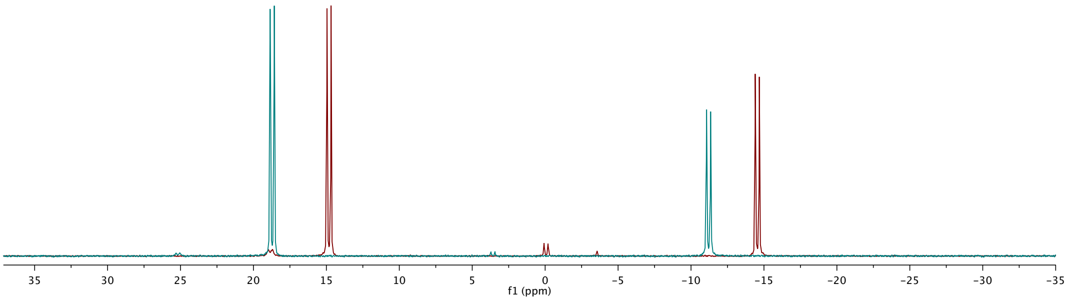

Figure 1. ^{31}P NMR spectra (101.3 MHz, CD$_2$Cl$_2$) for complexes **3** (red) and **4** (green).

Direct comparison of the ^{31}P NMR spectra showed the same splitting pattern between both complexes, being the bromine analog **3** low-field shifted due to the lower electronegativity of Br. X-Ray structure analysis of compound **3** revealed that the major isomer is *endo*-[ReBr(CO)$_3$(**2a**)] (Figure 2). Thanks to the strong structural similarity between **3** and **4**, it is reasonable to assume that the same isomer is also preferentially formed for the chloride analog **4**.

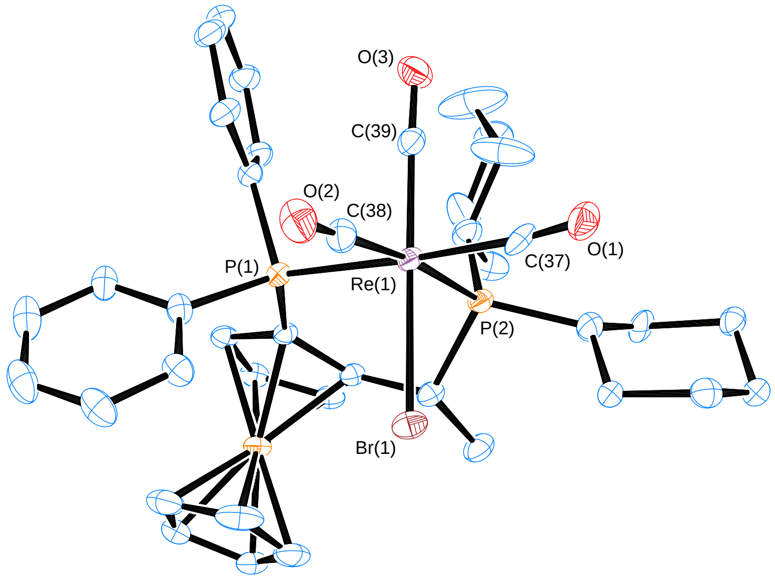

Figure 2. ORTEPIII drawing of the crystal structure for complex **3**. Ellipsoids at 50% probability. Relevant distances and angles (Å and deg.): Re-P(1) 2.4820(7), Re-P(2) 2.5206(7), Re-Br 2.6767(4), Re-C(37) 1.955(3), Re-C(38) 1.945(3), Re-C(39) 1.907(2), C(37)-O(1) 1.136(4), C(38)-O(2) 1.139(3), C(39)-O(3) 1.131(3). P(1)-Re-P(2) 87.43(2), C(39)-Re-Br 174.46(8)

The fact that only the *cis* isomers, with the halide ligand in apical position, are obtained can be easily explained by simple orbital symmetry arguments. It has been observed and demonstrated that the CO ligands in [MX(CO)$_5$] (M = Mn, Re; X = Cl, Br, I) complexes *cis* to the halide are more labile that the one in the *trans* position. Since the halide is less π accepting than carbonyl, the CO group *trans* to it has less "competition" for either the d_{xz} or d_{yz} orbitals, having a more effective back-bonding from the metal and hence, a stronger M-CO bond. Conversely, the *trans* CO ligands compete with each other for the same set of orbitals making them more labile to substitution.[32]

The possible reaction mechanism for the formation of complexes **3** and **4** is depicted in Scheme 3. The first step is the thermal decarbonylation *cis* to the halide to produce the reactive pentacoordinated 16-electron species **A**. This reactive intermediate can display either C_{4v} (square pyramidal) or C_{3v} (trigonal bipyramidal) symmetry, the later being most likely.[32b] Intermediate **A** reacts fast with the bidentate ligand to give the coordinatively saturated monosubstituted complex **B**. *Cis* labilization of another CO ligand leads to the pentacoordinated intermediate **C** with a pseudo-square pyramidal geometry.[32b] Considering that the incoming phosphine ligand is a poorer π acceptor than CO, the *cis* labilizing effect arises from the stabilization of the transition state by P compared with CO in the *cis* position.[32b] Rapid nucleophilic attack from the hanging ligand P leads to the formation of product **D**.

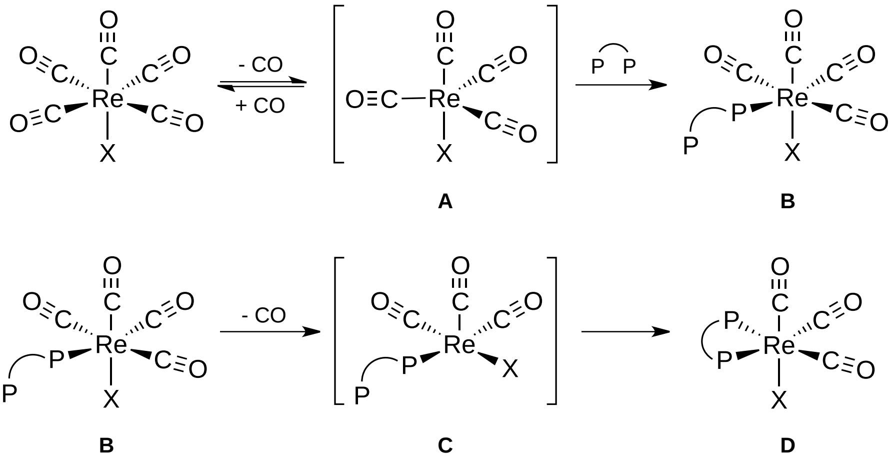

Scheme 3

It is important to note that intermediate **C** is chiral, and should adopt a preferred configuration in order to, after coordination of the hanging L, form preferentially one isomer, either *endo* or *exo.* This is in fact the case and the *endo* isomer is favored, thanks to the chirality of the Josiphos ligand. The *endo*/*exo* ratios for both complexes are different, namely 8:1 for **3** while for **4** it is 30:1. This difference is probably due to the highest reactivity of the chlorinated intermediate **C** than its brominated analog. The faster reaction with the incoming nucleophile reduces the chances for the fluxional pentacoordinated intermediate to isomerize, contrary to the most polarizable, less electronegative bromine-containing analog which reacts slower.[32b]

The synthesis of the corresponding hydride analog [ReH(CO)$_3$(**2a**)] (**5**) followed a slightly different approach (Scheme 4). Reaction of the rhenium(0) precursor [Re$_2$(CO)$_{10}$] with ligand **2a** in 1-pentanol led to the formation of the product presumably through intermediacy of the reactive [ReH(CO)$_5$].[33]

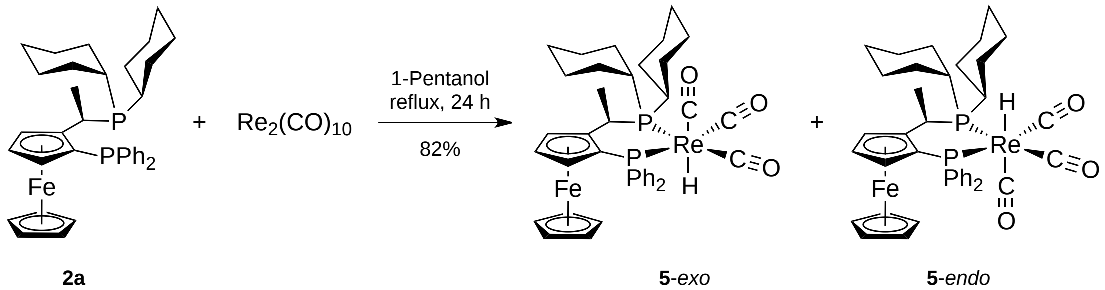

Scheme 4

As for the halide complexes **3** and **4**, product **5** was obtained as a mixture of two isomers but contrary to the formers, only a small excess of 2:1 of one of them is observed. By analogy, the preferential formation of the *endo* isomer could be assumed. The ^{1}H NMR spectrum of mixture **5** is presented in Figure 3. The signals for the hydride protons possess the expected low-field shift, typical for this kind of complexes.[33] They appear as doublet of doublets arising from the coupling with the two non-equivalent phosphorus atoms of the ligand. Another set of two peaks of small intensity also appear in the same region and with the same coupling pattern. Due to the fact that CO ligand exchange is made almost exclusively at the *cis* positions, it is very unlikely that these peaks correspond to the other two "missing" isomers resulting from substitution *trans* to the hydride. Those could be also attributed to conformational isomers but this assumption has not been further investigated. In the ^{31}P NMR spectrum also two set of signals were observed, two pairs of doublets, as expected (Figure 3).

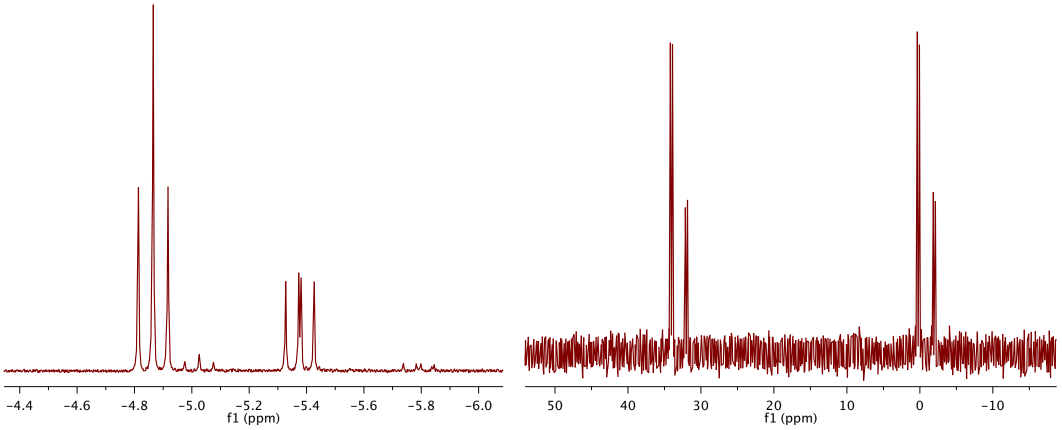

Figure 3. ^{1}H NMR (left, 500 MHz, CD_2Cl_2. Only the hydride region is presented) and ^{31}P NMR (right, 101.3 MHz, CD_2Cl_2) spectra of complex **5** (mixture of isomers).

In order to unleash the reactivity of these kind of complexes, it is first necessary to generate the coordinatively unsaturated 16-electron moiety $[Re(CO)_3L]^+$. This has been accomplished by protonation of the corresponding hydride,[34] or by ligand (hydride or halide) abstraction with MeOTf.[35] The high Lewis acidity of the cationic rhenium(I) core precludes the easy formation of pentacoordinated products, obtaining instead the corresponding (η^2-H_2)- or (OTf-*κO*)-adducts, both of considerable stability.[34-35] The reaction of either **3** or **5** with MeOTf at low temperature leads to the almost quantitative formation of the same product, presumably $[Re(CO)_3(OTf\text{-}\kappa O)]$ (**6**) (Scheme 5).

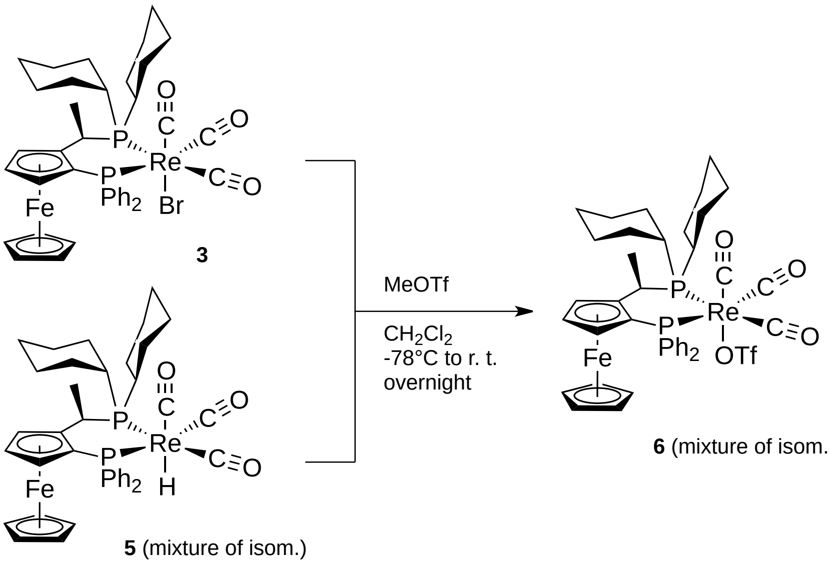

Scheme 5

The formation of the new complex **6** could be evidenced by ^{31}P NMR (Figure 4). After reaction or **3** or **5** with MeOTf, the doublet peaks of the parent complex disappear almost completely and two new sets of peaks appear. This two pairs of doublets could be then attributed to the corresponding *endo* and *exo* isomers. Attempts to isolate and characterize this reactive product were, unfortunately, unsuccessful. The poor characterization of the activated complex (**6**) and the impossibility to obtain a single isomer, discouraged us to pursue any catalysis attempts with these complexes.

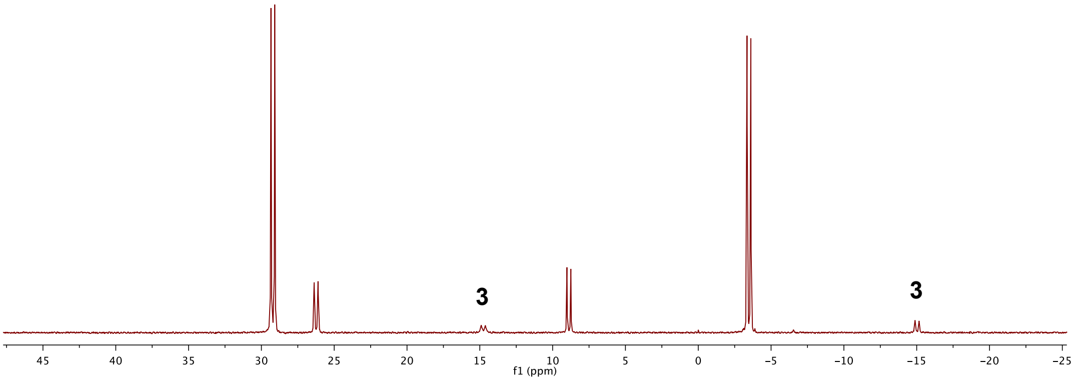

Figure 4. ^{31}P NMR spectrum (101.3 MHz, Tol-D_6) spectra of complex **6** (mixture of isomers). The peaks corresponding to unreacted **3** are marked.

*2.2.3. Synthesis of rhenium(V) derivatives of the type [ReOX_3(**2**)] (X = Cl, Br)*

The parent oxotrihalobis(triphenylarsine)rhenium(V) complexes, *mer*-[$ReOX_3(AsPh_3)_2$] (X= Cl, Br), were synthesized following the reported procedures[36] but using $KReO_4$ instead of $HReO_4$ as starting material (Scheme 6).

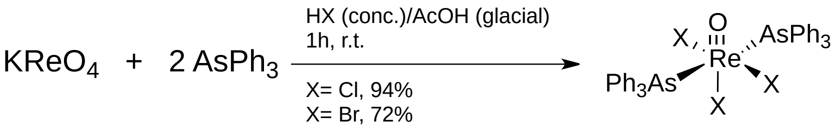

Scheme 6

These arsine complexes reacted readily with Josiphos ligands **2** in CH_2Cl_2 at room temperature to give the corresponding *fac*-[$ReOX_3$(**2**)] complexes (**7**, Table 1) in a procedure analogous to the one reported by Parr.[37] As depicted in Scheme 7, the coordination of the chiral diphosphine ligands to the rhenium centre gives a mixture of the two isomeric products, *endo*-**7** and *exo*-**7**. This was confirmed by X-Ray diffraction (see below).

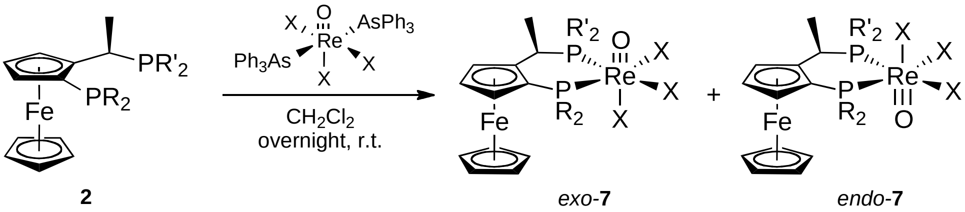
PR'2
PR2
Fe
2
X
O
AsPh3
Re
Ph3As
X
X
CH2Cl2
overnight, r.t.
R'2
P
O
X
Re
P
X
R2
X
Fe
exo-7
+
R'2
X
P
X
Re
P
X
R2
O
Fe
endo-7

Scheme 7

Table 1. Complexes of the type [ReOX_3(**2**)] (**7**).

Complex (**7**)	R	R'	X	Yield (%)
a	Ph	Cy	Cl	94
b	Cy	Ph	Cl	78
c	Ph	Adamantyl	Cl	85
d	Ph	3,5-$(Me)_2$Ph	Cl	71
e	Cy	Cy	Cl	73
f	Ph	*t*-But	Cl	97
g	Cy	*t*-But	Cl	85
h	Cy	3,5-$(CF_3)_2$Ph	Cl	16
i	3,5-$(Me)_2$Ph	Cy	Cl	>99
j	*t*-But	Ph	Cl	72
k	Ph	Cy	Br	97
l	CF_3	Cy	Cl	87

It was observed that upon ligand substitution on *mer*-[ReOX_3($AsPh_3$)$_2$], the *endo*- isomer is produced first (kinetic product) and it slowly isomerizes in solution to the more stable *exo*- isomer (thermodynamic product) (see Figure 5). The lability of the P-Re bonds in the *endo*- complex is evidenced in the ^{31}P

NMR spectra by their broad peaks, as a consequence of this dynamic behavior. All complexes were obtained in good yields except **7h** which contains trifluoromethylated substituents on the phosphorus. This compromises not only the donor and coordinating abilities of the ligand due to its electron-withdrawing properties, but also confers additional steric demand. The complexes are solids stable to air and moisture and can be stored for several months at room temperature without apparent decomposition. They decompose slowly in solution (in non-degassed solvents) to give oxidation products (see below)

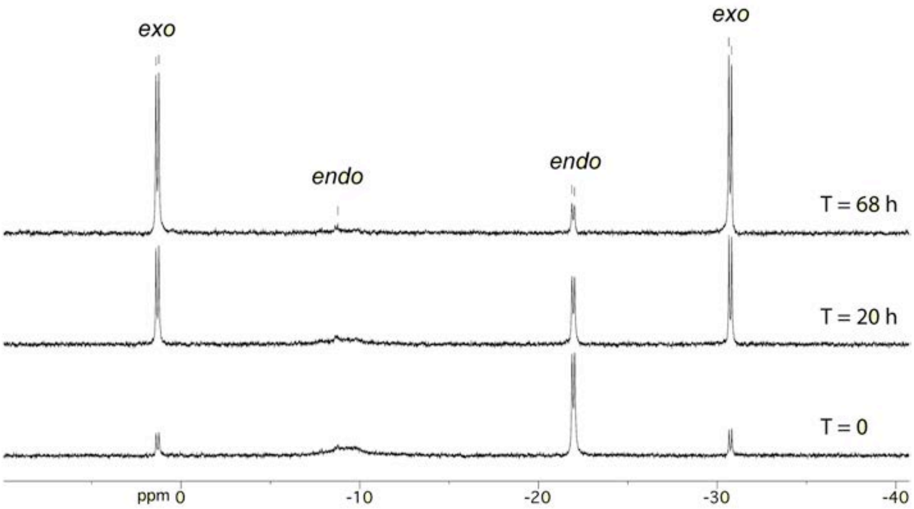

Figure 5. Time dependent ^{31}P NMR spectra (101.2 MHz, r. t., $CDCl_3$) for complex **3d**.

X-Ray quality single crystals of *exo*-**7-** (Figure 6), *exo*-**7d** (Figure 7), *exo*-**7e** (Figure 9), *endo*-**7f** (Figure 10), **7g** (both isomers, figure 11) *exo*-**7i**, (Figure 13) and *exo*-**7l-** (Figure 14) were obtained by slow diffusion of *n*-hexane, diethylether or benzene layered over a solution of the corresponding compounds in dichloromethane or chloroform. Since all these complexes present analogous structures, the analysis of the general properties and geometry will be only made for *exo*-**7a**.

The geometry around the Re centre is distorted octahedral with a *fac-cis* configuration. One of the main features of the structure is the small angle O-Re-Cl_{trans} of 170.46(12) Å with the oxygen atom bent towards the bidentate ligand as reported for other Re^V diphosphine mono-oxo complexes.[37-38] This is due to the electronic repulsion between the Re-O moiety and the negatively charged chloride ligands.[38b] The short Re-O bond distance (1.685(4) Å) is in good agreement with other complexes of this kind[39] and is better described as a triple bond (one σ bond and two π bonds), clearly shorter than a double bond with a theoretical value of 1.86 Å.[38a, 40] The reason for the increased bond order is the overlap of both p_x and p_y oxygen orbitals with the rhenium d_{xz} and d_{yz} orbitals (z axis through the Re-O bond). The two *d* electrons would then occupy the nonbonding d_{xy} orbital[39] explaining the observed diamagnetism of the complexes.[40]

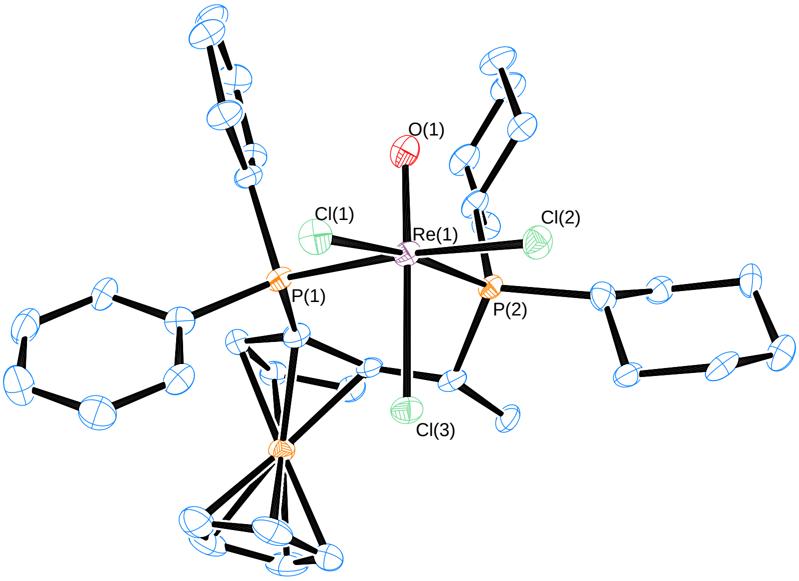

Figure 6. ORTEPIII drawing of complex *exo*-**7a**•(CD_2Cl_2)•(C_6H_6). Solvent molecules are omitted for clarity. Ellipsoids at 50% probability. Relevant distances and angles (Å and deg.): Re-P(1) 2.4604(13), Re-P(2) 2.4875(12), Re-O 1.685(4), Re-Cl(1) 2.4024(12), Re-Cl(2) 2.3972(13), Re-Cl(3) 2.4143(13), P(1)-Re-P(2) 89.05(4), O-Re-Cl(3) 170.46(12).

The crystal structure for complex *exo*-**7d** features two molecules in the asymmetric unit, both corresponding to the *exo* isomer but with different conformation on the six-member ring formed by the chelating ligand and the metal center (Figure 7). A superimposition of both structures shows clearly the marked difference between them (Figure 8). This change in conformation, which results in a shift of the metal center of 0.971 Å, arises from the pronounced steric demand of the xylyl moieties on the phosphine.

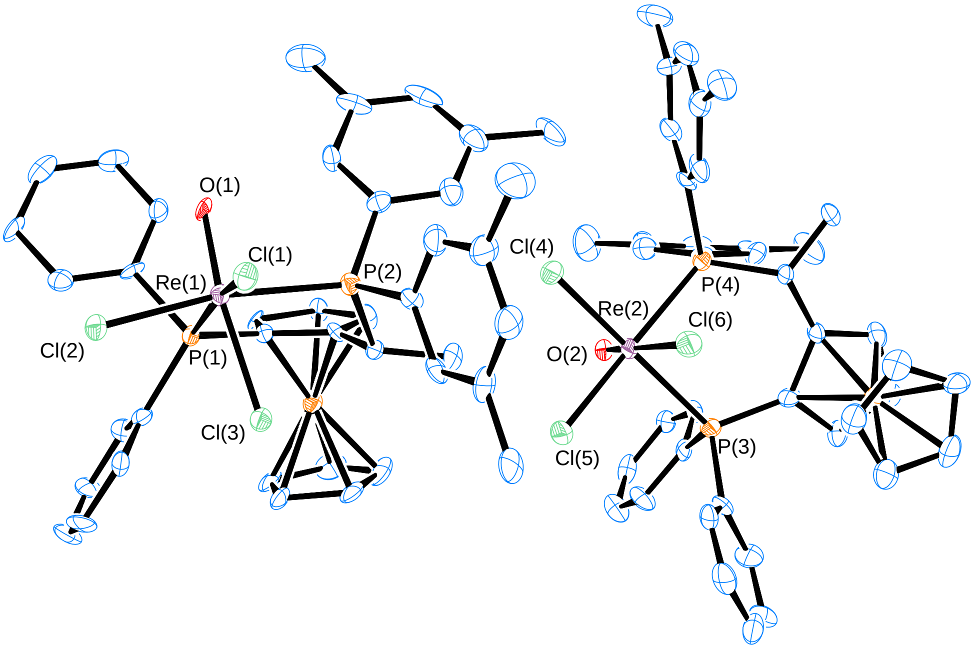

Figure 7. ORTEPIII drawing of complex *exo*-**7d**•(CDCl$_3$)$_n$. The number of solvent molecules in the unit cell is ca. six. Solvent molecules are omitted for clarity. Ellipsoids at 50% probability. Relevant distances and angles (Å and deg.): Re(1)-P(1) 2.464(2), Re(1)-P(2) 2.479(2), Re(1)-O(1) 1.689(5), Re(1)-Cl(1) 2.3712(19), Re(1)-Cl(2) 2.386(2), Re(1)-Cl(3) 2.4120(19), P(1)-Re(1)-P(2) 92.99(7), O(1)-Re(1)-Cl(3) 167.33(18), Re(2)-P(3) 2.466(2), Re(2)-P(4) 2.470(2), Re(2)-O(2) 1.666(5), Re(2)-Cl(4) 2.385(2), Re(2)-Cl(5) 2.382(2), Re(2)-Cl(6) 2.46(2), P(3)-Re(2)-P(4) 90.37(7), O(2)-Re(2)-Cl(6) 169.42(19).

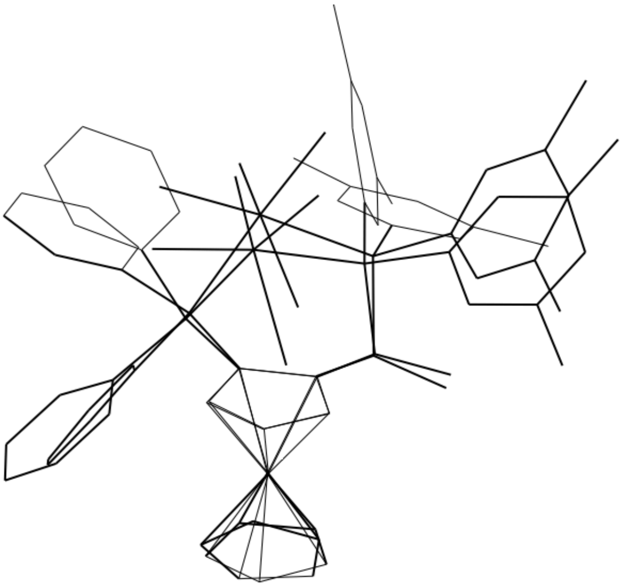

Figure 8. MacMoMo drawing of the superimposition of both molecules in the asymmetric unit of complex *exo*-**7d**•(CDCl$_3$)$_n$.

Single crystals of complex **7e**, which contains only cyclohexyl substituents on the phosphorus atoms, showed to correspond to a single isomer (*exo*, Figure 9).

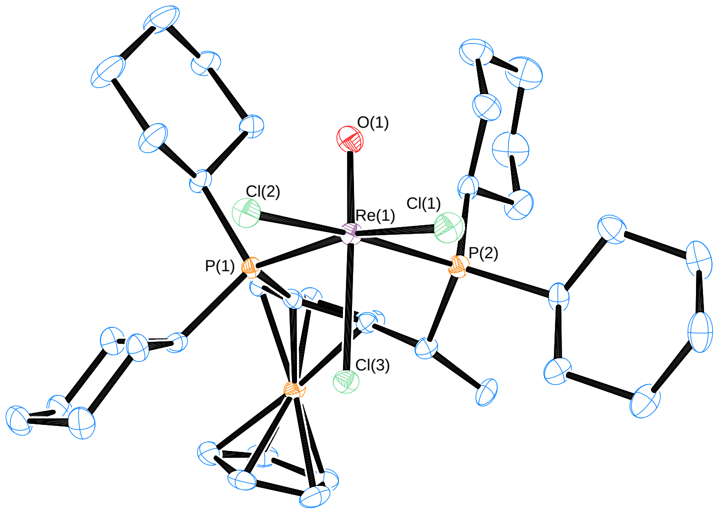

Figure 9. ORTEPIII drawing of complex *exo*-**7e**. Ellipsoids at 50% probability. Relevant distances and angles (Å and deg.): Re-P(1) 2.4884(10), Re-P(2) 2.4919(11), Re-O 1.670(3), Re-Cl(1) 2.3674(10), Re-Cl(2) 2.4006(10), Re-Cl(3) 2.4396(10), P(1)-Re-P(2) 92.24(3), O-Re-Cl(3) 169.23(10).

Interestingly, and in contrast to the above presented results, single crystals of complex **7f** were obtained only for the *endo* isomer (Figure 10). An "intermediate" situation was found for complex **7g** in which both *endo* and *exo* imomers crystallize together in the same unit cell (Figure 11). The superimposition of both structures shows that they are indeed very similar, having the same conformation in the six-member ring formed by the metal and the chelating ligand. The only important differences lay in the conformation of the cyclohexyl rings and in the angle O-Re- Cl_{trans}, having the *endo* isomer a more pronounced deviation from linearity and hence a more congested steric situation (see Figure 12). Taking this observation into account, The decrease of steric demand would be the driving force for the observed isomerisation process (vide supra).

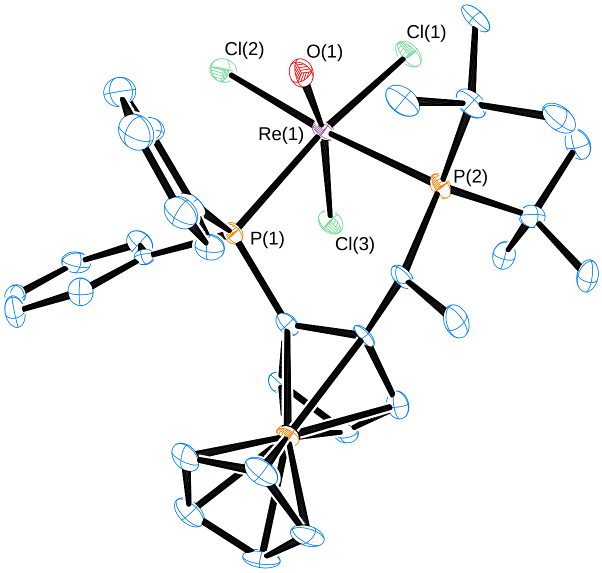

Figure 10. ORTEPIII drawing of complex *endo*-**7f**•($CDCl_3$). Solvent molecules are omitted for clarity. Ellipsoids at 50% probability. Relevant distances and angles (Å and deg.): Re-P(1) 2.4622(16), Re-P(2) 2.5836(17), Re-O 1.676(5), Re-Cl(1) 2.3780(16), Re-Cl(2) 2.4234(16), Re-Cl(3) 2.3929(15), P(1)-Re-P(2) 90.99(5), O-Re-Cl(3) 167.61(16).

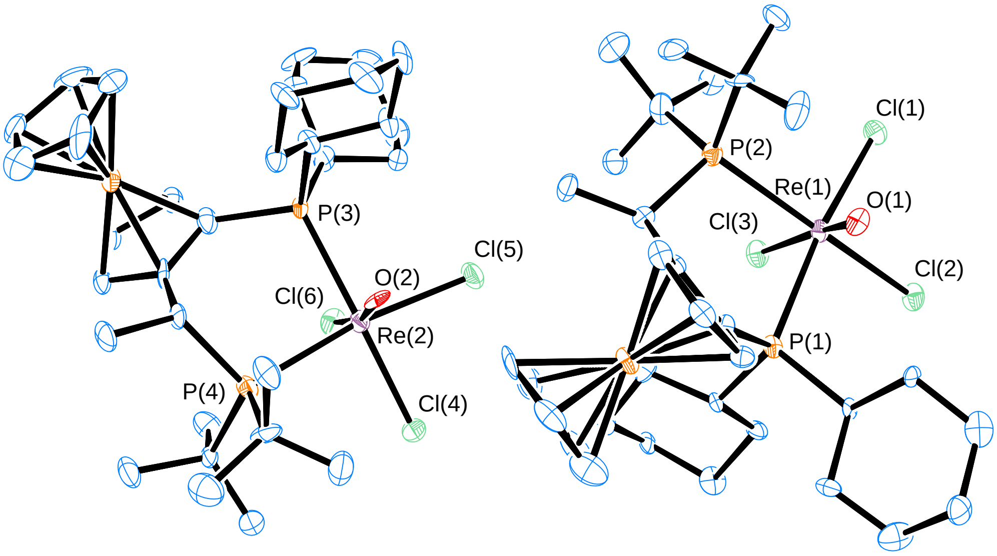

Figure 11. ORTEPIII drawing of complex **7g**. Ellipsoids at 50% probability. The asymmetric unit consist of both *endo*- (left) and *exo*- (right) isomers. Relevant distances and angles (Å and deg.): *exo*-isomer Re(1)-P(1) 2.493(3), Re(1)-P(2) 2.578(3), Re(1)-O(1) 1.707(8), Re-Cl(1) 2.393(3), Re-Cl(2) 2.395(3), Re-Cl(3) 2.385(3), P(1)-Re(1)-P(2) 95.63(10), O(1)-Re(1)-Cl(3) 171.1(3). *endo*-isomer Re(2)-P(3) 2.458(3), Re(2)-P(4) 2.579(3), Re(2)-O(2) 1.751(8), Re(2)-Cl(4) 2.363(3), Re(2)-Cl(5) 2.414(3), P(3)-Re(2)-P(4) 95.13(9), O(2)-Re(2)-Cl(6) 167.0(3).

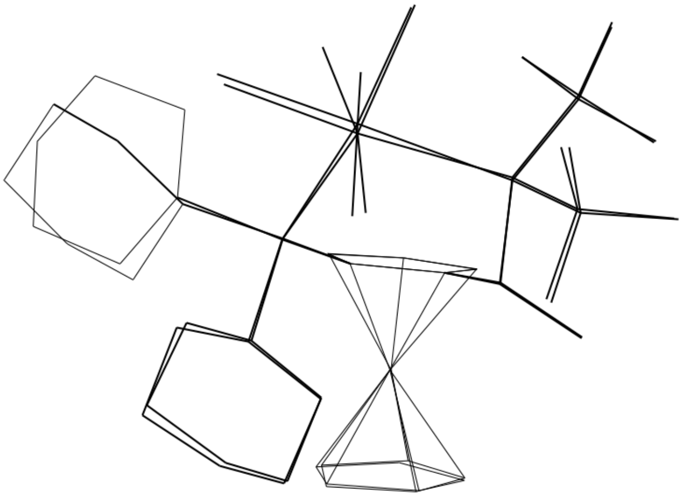

Figure 12. MacMoMo drawing of the superimposition of both molecules in the asymmetric unit of complex **7g** (*endo* and *exo*).

Single crystals of complex *exo*-**7i** were also obtained. It possesses the same distorted octahedral structure as the above mentioned complexes. It is important to note that the ligand used for this synthesis, **2i**, is neither commercially available, nor published, so it was synthesized for the first time in this work.

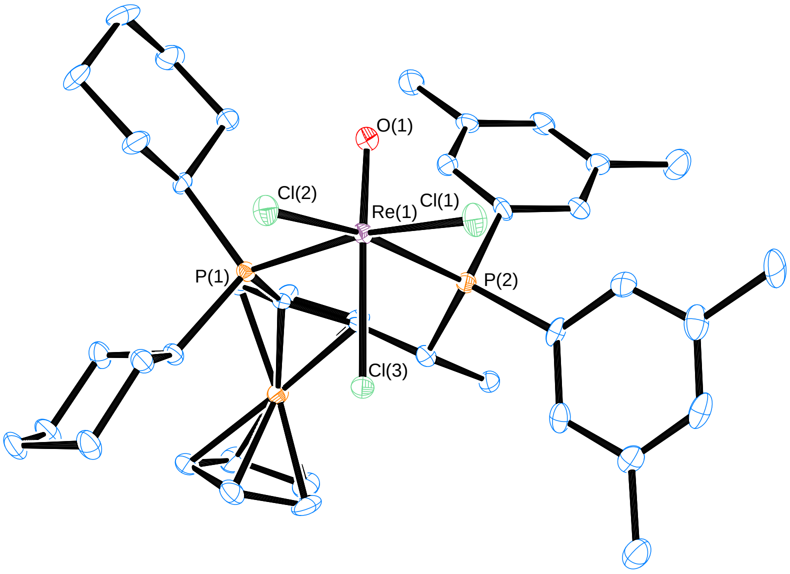

Figure 13. ORTEPIII drawing of complex *exo*-**7i**•(CD_2Cl_2). Solvent molecules are omitted for clarity. Ellipsoids at 50% probability. Relevant distances and angles (Å and deg.): Re-P(1) 2.4880(12), Re-P(2) 2.4691(11), Re-O 1.681(3), Re-Cl(1) 2.3799(11), Re-Cl(2) 2.3767(11), Re-Cl(3) 2.4503(11), P(1)-Re-P(2) 94.57(4), O-Re-Cl(3) 164.49(11).

The last member of this family of complexes for which single crystals suitable for X-ray analysis were obtained was **7l**, which contains the bistrifluoromethylated ligand **2l**. The structure corresponds to the *exo* isomer (Figure 14).

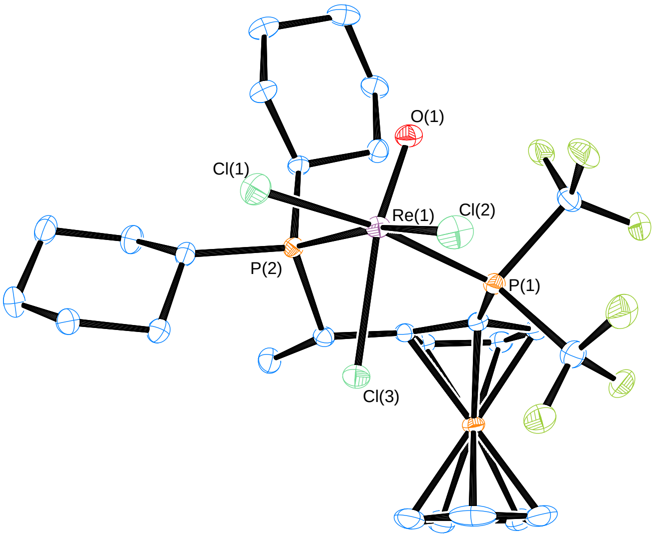

Figure 14. ORTEPIII drawing of complex *exo*-**7l**. Ellipsoids at 50% probability. Relevant distances and angles (Å and deg.): Re-P(1) 2.4173(7), Re-P(2) 2.5067(7), Re-O 1.680(2), Re-Cl(1) 2.3532(7), Re-Cl(2) 2.3792(6), Re-Cl(3) 2.4217(7), P(1)-Re-P(2) 92.05(2), O-Re-Cl(3) 163.19(7).

Attempts to crystallize the tribromo derivative **7k** under non-inert conditions gave as a result the oxidation product [ReOBr$_4$(**2a**(OPPh$_2$)-κ*O*)] (**8**, Figure 15) in which the neutral Re^{VI} [ReOBr$_4$] moiety is coordinated with the mono-oxidised form of the Josiphos ligand. Rhenium(VI) complexes are rare and often very reactive.[41] In this case, the Re^{VI} center is stabilized by the strongly bonded oxo group (Re-O = 1.612(7) Å) and the weakly bonded phosphine oxide ligand (Re-O = 2.127(7) Å). The mechanism of formation of **8** is still unclear but considering the fact that the [Re^{V}O]$^{+3}$ core is a redox-active unit and could serve as an oxo-transfer agent,[42] it is likely for the oxidation of the phosphine ligand to be achieved by intramolecular oxygen transfer rather than by reaction with O$_2$ in solution. The same result was obtained during the crystallization of **7c**, in which case the corresponding Re^{VI} derivative [ReOCl$_4$(**7c**(OPPh$_2$)-κ*O*)] (**9**, Figure 16) was isolated.

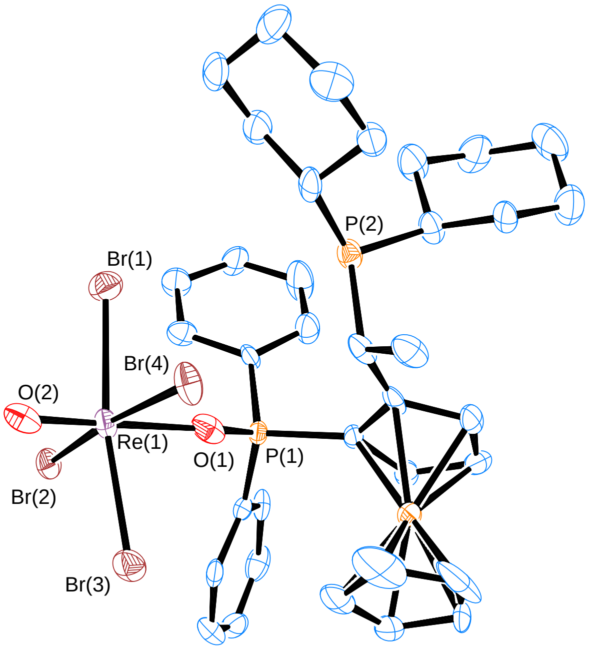
Br(1)
P(2)
Br(4)
O(2)
Re(1)
O(1)
P(1)
Br(2)
Br(3)

Figure 15. ORTEPIII drawing of complex **8**•(CD_2Cl_2). Solvent molecules are omitted for clarity. Ellipsoids at 50% probability. Relevant distances and angles (Å and deg.): Re-O(1) 2.127(7), Re-O(2) 1.612(7), P(1)-O(1) 1.522(7), O(1)-Re-O(2) 178.0(3).

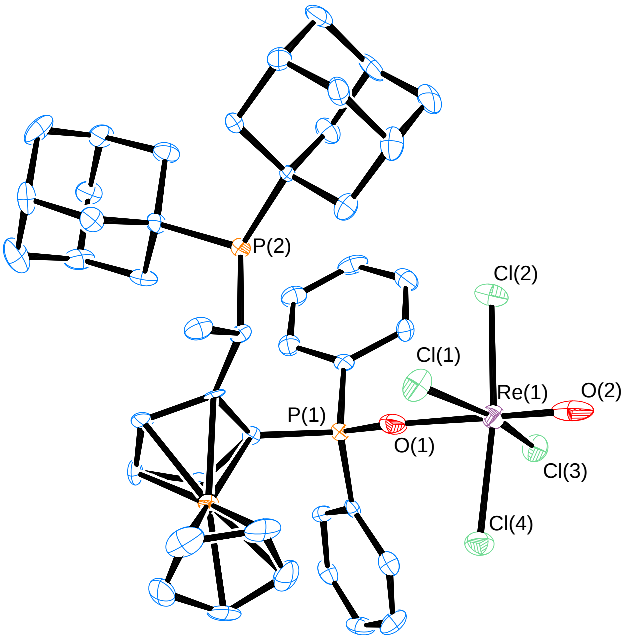
P(2)
Cl(2)
Cl(1)
Re(1)
O(2)
P(1)
O(1)
Cl(3)
Cl(4)

Figure 16. ORTEPIII drawing of complex **9**•2(CD_2Cl_2). Solvent molecules are omitted for clarity. Ellipsoids at 50% probability. Relevant distances and angles (Å and deg.): Re-O(1) 2.127(6), Re-O(2) 1.587(8), P(1)-O(1) 1.530(6), O(1)-Re-O(2) 179.0(3).

In spite of the apparent similarity between these complexes ([ReOCl$_3$(**2**)], **7**), all having the same metal core [ReOCl$_3$] in a pseudo-octahedral geometry and all forming a six-membered ring upon the *cis* coordination of the chelating diphosphine, they display significant differences in terms of conformation. Comparison of the solid-state structures for the different complexes (**7**) reflects clearly the absence of conformational rigidity of the Josiphos scaffold (a particularity of this ligand family pointed out by Togni *et al.*[20b]). By simple examination of the graphic superimposition of the crystal structures (Figure 17) it appears clear that, changing the substituents on the phosphorus atoms leads not only to (very) different steric (and electronic) situations around the metal center, but also results in a pronounced change on the conformation of the six-membered metallacycle, shifting the rhenium center from an *exo* (above) to an *endo* (below) position with respect to the plane defined by the substituted cyclopentadienyl ring.

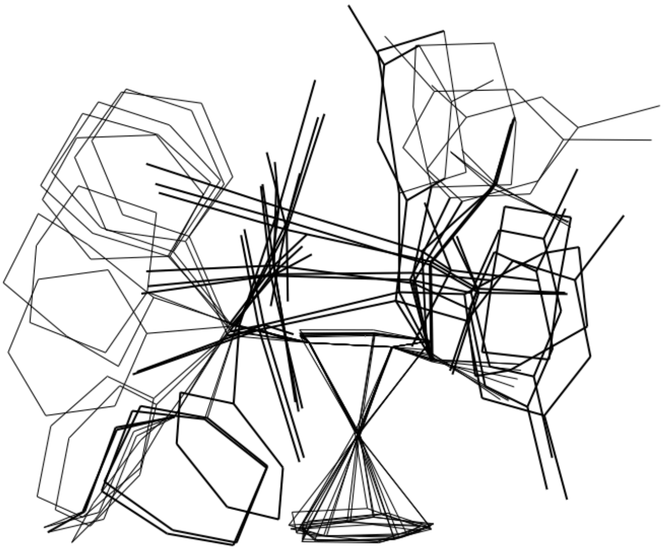

Figure 17. MacMoMo drawing of the superimposition of the crystal structures of complexes **7a**, **7d** (both conformers), **7e**, **7f**, **7g** (*endo* and *exo*) and **7i**.

In order to quantify these structural differences, the conformational analysis introduced by Togni *et al.* was used.[20b] As a parameter of comparison, the torsion angles $\alpha1$ and $\alpha2$ were chosen (see Chart 1). Angle $\alpha1$ refers to the torsion around the Cp-P^1 bond which defines the relative orientation of the *exo* substituent on P^1 with respect to the plane of the Cp ring. Angle $\alpha 2$ refers to the torsion around the Cp-C(Me)P^2 bond which in turn defines the relative position of the methyl group on the chiral side chain bearing P^2 with respect to the same Cp ring.

Chart 1. Conformational space of complexes of the type [$ReOCl_3$(**2**)], **7**. M = $ReOCl_3$.

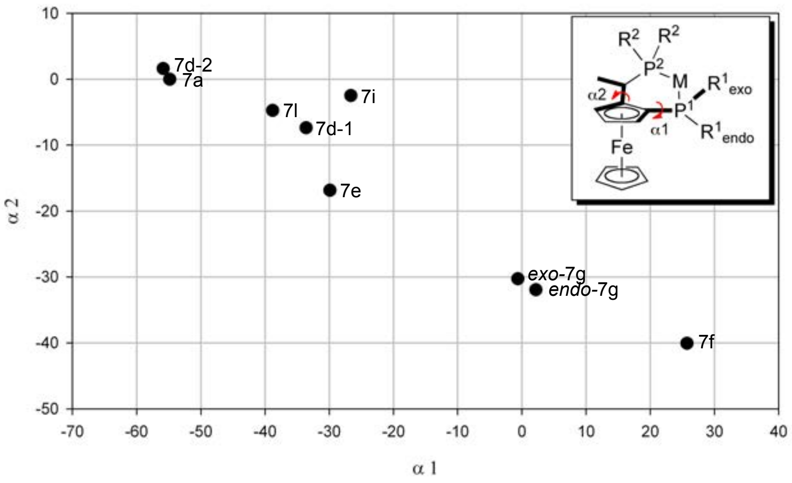

It appears also clear that there is no conformational preference among these structures, displaying $\alpha 1$ angles within a range of ca. 80 degrees and $\alpha 2$ angles within a range of ca. 40 degrees. This analysis shows a higher "similarity" on the conformation involving the side chain bearing the carbon-centered chirality, a trend already observed when comparing several metal complexes with Josiphos ligands.[20b]

2.2.4. Synthesis of other rhenium(V) derivatives with Josiphos ligands

The dioxo derivate [ReO_2I(**2a**)] (**10**) was synthesized in an analogous procedure by simple ligand substitution of the parent complex [$ReO_2I(PPh_3)_2$] with the bidentate ligand **2a** at room temperature in dichloromethane (Scheme 8). The elemental analysis of the resulting paramagnetic compound confirms the proposed stoichiometry, having the two oxo ligands in a *trans* configuration due to the required *cis* chelation of the biphosphine ligand. Unfortunately, X-ray quality crystals of **10** could not be obtained to confirm this assumption. However, analysis of the FT-IR spectra of **10** suggests that the ReO_2 moiety has indeed a *trans* configuration, showing the corresponding stretching band at 790.73 cm^{-1}, very close to the reported value for analogous compounds around 785 cm^{-1} [43] and very distant from the value of 923 cm^{-1} observed for *cis*-dioxo-*trans*-diphosphino complexes analogous to the rhenium precursor.[40]

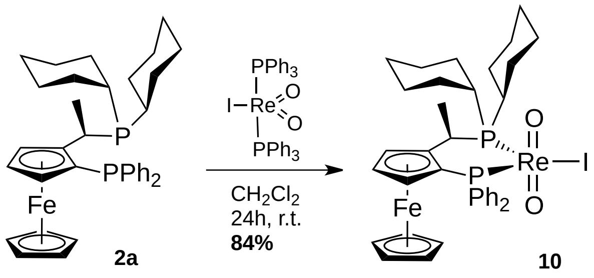
PPh3
I–Re O O
PPh3
CH2Cl2
24h, r.t.
84%
P
PPh2
Fe
2a
P
P
Ph2
Re—I
O
O
Fe
10

Scheme 8

The nitrido complex [ReNCl$_2$(**2a**)] (**11**), was synthesized from [NBu$_4$][ReNCl$_4$] and the biphosphine ligand **2a** by adapting the procedure reported by Duatti[44] (Scheme 9). It was also obtained as a mixture of the *endo*- and *exo*- isomers and upon crystallization single crystals of *endo*-**11** were obtained, so its structure was confirmed by single crystal X-ray analysis (Figure 18).

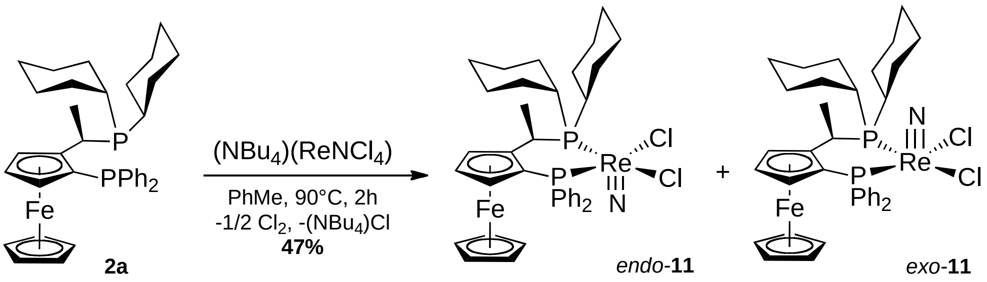
(NBu4)(ReNCl4)
PhMe, 90°C, 2h
-1/2 Cl2, -(NBu4)Cl
47%
P
PPh2
Fe
2a
P
P
Ph2
Re
Cl
Cl
N
Fe
endo-11
+
N
P
P
Ph2
Re
Cl
Cl
Fe
exo-11

Scheme 9

Complex *endo*-**11** exhibits a distorted tetragonal pyramidal geometry around the Re centre with the nitrido ligand in the apical position. The rhenium atom is displaced 0.447 Å from the mean plane P(1)-P(2)-Cl(1)-Cl(2) towards the nitrido ligand as previously observed for other rhenium-nitrido complexes with chelating diphosphines.[44] Both complexes **10** and **11** are coordinativelly unsaturated 16-electron complexes, which could be advantageous when using them as catalyst since a coordination position is available from the beginning and the prior activation of the complex could be avoided. This feature, however, showed no impact on the catalytic performance (vide infra).

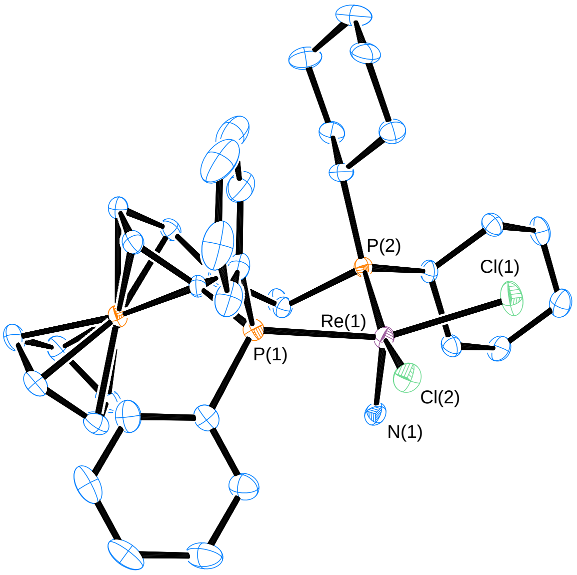

Figure 18. ORTEPIII drawing of complex *endo*-**11**•(CD_2Cl_2). Solvent molecules are omitted for clarity. Ellipsoids at 50% probability. Relevant distances and angles (Å and deg.): Re-P(1) 2.3985(9), Re-P(2) 2.4152(9), Re-N 1.679(3), Re-Cl(1) 2.3879(9), Re-Cl(2) 2.4107(8), P(1)-Re-P(2) 91.45(3).

In an attempt to improve the synthesis of complex **11** (yield and selectivity), an alternative route was tried, adapting the procedure of Sullivan for the synthesis of [$ReNCl_2(PPh_3)_2$]. It consists in the reaction of [$ReOCl_3(PPh_3)_2$] with hydrazine salts in the presence of triphenylphosphine in wet ethanol, to yield the desired product along with $OPPh_3$.[45] In our case, the reaction of precursor **7a** under these conditions (Scheme 10) did not afford the expected product (**11**), but only an ethoxo-derivative, [$ReOCl_2$(EtO)(**2a**)], **12**, whose structure was confirmed by X-ray analysis (Figure 19).

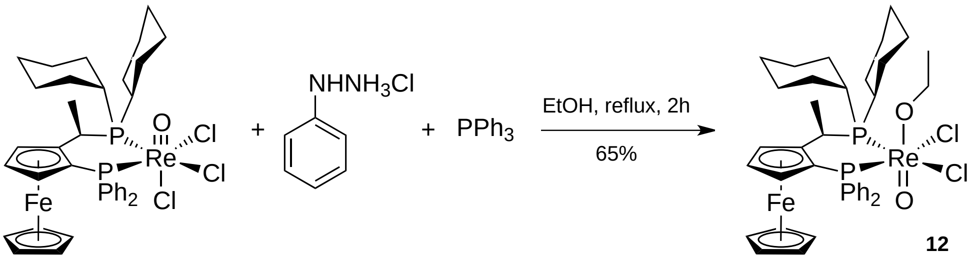

Scheme 10

This finding was not completely unexpected since the alcoholysis of rhenium(V)-oxotrihalide complexes under similar conditions has been already reported.[36]

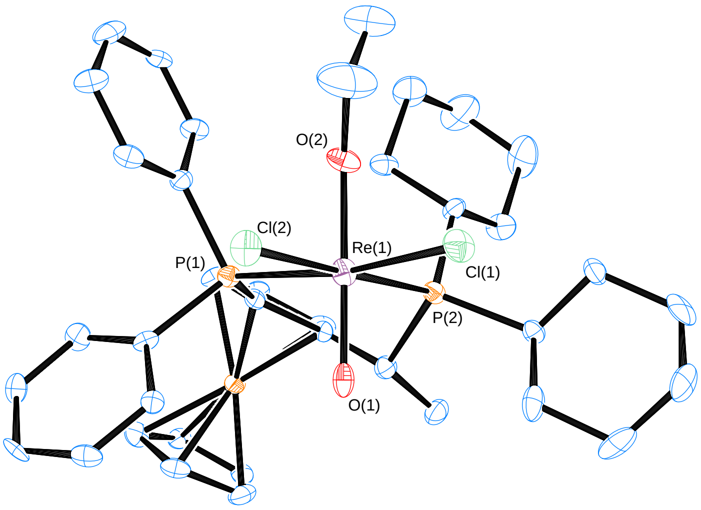

Figure 19. ORTEPIII drawing of complex **12.** Ellipsoids at 50% probability. Relevant distances and angles (Å and deg.): Re-P(1) 2.458(2), Re-P(2) 2.457(2), Re-O(1) 1.757(6), Re-O(2) 1.864(6), Re-Cl(1) 2.428(2), Re-Cl(2) 2.449(2), P(1)-Re-P(2) 92.35(7), O(1)-Re-O(2) 176.4(3).

Complex **12** exhibits a slightly distorted octahedral geometry containing a *trans*-oxo-alkoxo unit typical for this kind of complexes.[38a, 46] The Re-oxo distance (1.757(6) Å) is longer than in the parent complex *exo*-**7a** but still shows significant triple bond character. The Re-O(alkoxy) distance (1.864(6) Å) suggests strong π-donation so it can be regarded as a double bond. Another remarkable structural feature of complex **12** is its inverted configuration relative to the parent complex *exo*-**7a**, having the terminal oxo ligand in the *endo* position.

2.2.5. Synthesis of rhenium(V)-oxotrichloride derivatives with other diphosphine ligands

Using the same general procedure as for the synthesis of complexes **7** (Scheme 7), three more complexes were synthesized using chelating diphosphines other than Josiphos (Scheme 11), namely [ReOCl$_3$(**13a**)] (**14**) and [$ReOCl_3$(**13b**)] (**15**) using ligands from the Walphos family, and [$ReOCl_3$(**16**)][37] (**17**) using *S*-BINAP. The complexes were obtained in high yields and in the case of **14** and **15** one major isomer was obtained (>90%). However, their configuration was not determined since single crystals suitable to X-ray analysis could not be obtained.

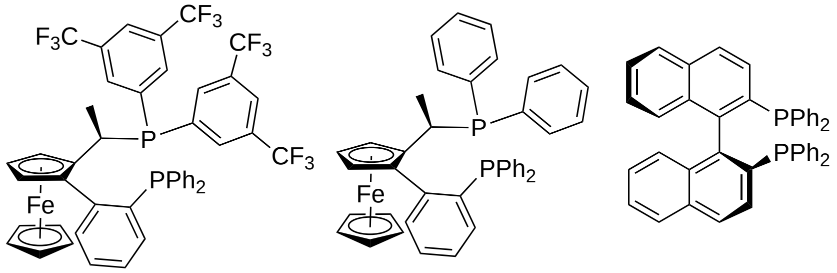

13a **13b** **16**

Lig.	Comp.	Yield (%)
13a	**14**	>99
13b	**15**	66
16	**17**	82

Scheme 11

2.3. Transfer Hydrogenation of Ketones

2.3.1. Method development

With the Re complexes in hand, their catalytic activity in the transfer hydrogenation of ketones was tested using acetophenone as the model substrate. In a typical procedure, a certain amount of catalyst (ca. 1% mol) was dissolved in dry 2-propanol under argon atmosphere along with one equivalent of acetophenone. Then a base was added (ca. 10%) and the mixture was heated overnight. For the selection of the best conditions complex **7a** and other Re^V complexes were used as catalysts (Table 2).

Table 2. Results for the transfer hydrogenation of acetophenone under different reaction conditions.

Entry[a]	Catalyst	Base	Time (h)	Temp. (°C)	Yield (%)[b]	ee[c] (%)
1	**7a**		12	80	0	-
2	**7a**	K_2CO_3[d]	12	80	50	11(*S*)
3	**7a**	K_2CO_3[d]	48	80	99	rac.
4	**7a**	iPrONa	21	80	67	rac.

5	**7a**	$(iPr)_2NEt$	20	80	76	17(*S*)
6	**7a**	NEt_3	24	80	83(75)	17(*S*)
7	**7a**	NEt_3	48	25	0	-
8	**7a**	NEt_3	48	40	(46)	19(*S*)
9[e]	**17**	NEt_3	20	80	15	rac.
10[f]	$[ReOCl_2(PPh_3)_2]$	NEt_3	20	80	0	-
11	**7a** (in situ)	NEt_3	20	80	92	14(*S*)

[a] Reaction conditions: Conc. of substrate 0.4M; ca. 1% of catalyst; 8% of base [b] Calculated by integration of the signals in ^{1}H NMR. Numbers in brackets correspond to isolated yields. [c] Determined by chiral HPLC (see experimental part). [d] Excess (ca. 20-fold). [e] Complex synthesized as reported previously.[37] [f] Synthesized as reported previously.[47]

The addition of a base proved crucial since a lack of it (Table 2, entry 1) resulted in no product formation. When potassium carbonate was used (Table 2, entries 2 and 3) good conversion was obtained but with loss of enantioselectivity. The same effect was observed with the addition of sodium isopropoxide (Table 2, entry 4). This could be due to decomposition of the complex, generating different active species without the chiral ligand. When triethylamine (TEA) was used instead, moderate enantioselectivities were obtained. The same selectivity was observed when bulkier diisopropylethylamine was added, although in lower yield (Table 2, entry 5).

The reaction temperature also had a dramatic effect on the reaction yield. When the reaction was run at 25 °C (Table 2, entry 7) no conversion was observed. At 40 °C, a yield of only 46% was obtained after two days while at 80 °C a yield of 80% was obtained (Table 2, entry 6). When other Re^V complexes were used as catalysts, namely *mer*-$[ReOCl_3(PPh_3)_2]$ and **17**, the results were not satisfactory, giving no conversion with the former (Table 2, entry 10) and low conversion and no selectivity with the latter (Table 2, entry 9). When the catalyst was synthesized *in situ*, mixing equimolar amounts of *mer*-$[ReOX_3(AsPh_3)_2]$ and the Josiphos ligand (**2a**) in 2-propanol prior to the addition of the ketone, similar results were obtained as when the isolated complex was used (Table 2, entry 11). Having selected the best conditions for the asymmetric transfer hydrogenation of acetophenone with complex **7a** (Table 2, entry 6), the catalytic performance for the other Re^V complexes was assessed. The results are summarized in Table 3.

Table 3. Results for the transfer hydrogenation of acetophenone catalyzed by rhenium(V) complexes with ferrocenyldiphosphine ligands.

Entry[a]	Catalyst	Yield (%)[b]	ee[c] (%)	Entry[a]	Catalyst	Yield (%)[b]	ee[c] (%)
1	**7b**	96	37(*R*)	11	**7j**	4	23(*S*)
2	**7b[d]**	96	37(*R*)	12	**7k**	95	15(*S*)
3	**7c**	79(35)	8(*S*)	13[f]	**7k**	49	20(*S*)
4	**7d**	50(31)	12(*R*)	14	**10**	97	11(*S*)
5	**7e**	97(85)	10(*R*)	15[f]	**10**	25	20(*S*)
6	**7f**	92	19(*R*)	16	**10**[d]	93	11(*S*)
7	**7g**	89	30(*R*)	17	**11**	88	15(*R*)
8	**7h**	70	55(*R*)	18[f]	**11**	6	15(*R*)
9	**7h**[d]	97	43(*R*)	19	**14**	0	-
10[e]	**7i**	67	52(*R*)	20	**15**	0	-

[a] Reaction conditions: Conc. of substrate 0.4M; ca. 1% of catalyst; 8% of TEA; 80 °C, 20 h. [b] Calculated by integration of the signals in ^{1}H NMR. Numbers in brackets correspond to isolated yields. [c] Determined by chiral HPLC (see experimental part). [d] Made *in situ*. [e] 14 hours. [f] 40°C

In general, good to excellent yields were obtained for the rhenium-catalyzed transfer hydrogenation of acetophenone with the different complexes containing ligands of the Josiphos type. The only exception was for complex **7j** (Table 3, entry 11) due probably to the steric hinderance imparted by the bis-*t*-butylphosphine moiety on the ferrocene. Complexes **14** and **15** containing ligands of the Walphos type showed to be inactive (Table 3, entries 19 and 20) .

It is important to note that in spite of the fact that all complexes contain ligands with the same absolute configuration (R,S_p), the stereochemical outcome of the reaction changes depending on the nature and relative position of the organic residues on the P atoms. Complex **7a** (R = Ph, R' =

Cy) gives preferentially the *S*-isomer (17 %ee, Table 2, entry 6) while its "inverted" analog **7b** (R = Cy, R' = Ph) gives an excess of the *R*-isomer (37 %ee, Table 3, entry 1). The same effect was observed for the isomeric complexes **7f** and **7j** (Table 3, entries 6 and 11).

In terms of selectivity, the best results were obtained for those complexes with R = Cy (Table 3, entries 1, 7, 8 and 10), producing preferentially the *R*-isomer. The same selectivity was obtained with complex **7e** (R, R' = Cy), although with lower ee (Table 3, entry 5). The best results were obtained with complex **7h** (Table 3, entry 8 and 9), so it was selected for the screening with different ketones (Table 4).

Table 4. Results for the transfer hydrogenation of ketones using complex **7h** as catalyst.

Entry[a]	Ketone	Yield (%)[b]	ee[c] (%)
1	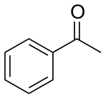	97	43(*R*)
2	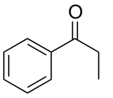	89	50(*R*)
3	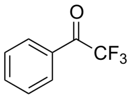	>99	19(*S*)
4	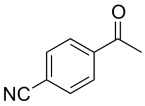	30	58(*R*)
5	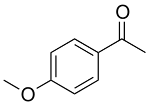	91	44(*R*)
6	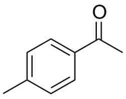	94	27
7	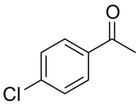	98	55
8	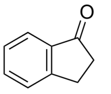	75	0

9	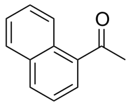	99	53(*R*)
10	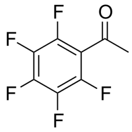	>99	46

[a] Reaction conditions: Conc. of substrate 0.4M; Catalyst prepared *in situ*, 1% of ligand and 1% of [$ReOCl_3(AsPh_3)_2$]; ca. 20% of TEA; 80 °C, 20 h. [b] Calculated by integration of the signals in ^1H NMR. [c] Determined by chiral HPLC.

For these reactions the catalyst was generated *in situ* as it showed similar selectivity and a little higher yield than the isolated complex. For all of the substrates tested the reaction proceeded cleanly and in general with good to excellent yields. The only exception was for 4-cyanophenylmethylketone (Table 4, entry 4), due probably to coordination of the cyano moiety to the metal centre, hampering the reactivity of the catalyst. The same substrate gave conversely the highest enantioselectivity, due most likely, to steric factors.

2.3.2. Mechanistic considerations

Transfer hydrogenation (TH) of ketones has been shown to proceed via different pathways, depending heavily on the metal, ligands and reaction conditions.[1a, 1c] Since this is the first report using a rhenium catalyst in this kind of reaction, no prediction can be made concerning their preferred *modus operandi.* Nevertheless, assessing the geometry, reactivity and coordination behavior of our Re^V complexes, a plausible reaction pathway is proposed (vide infra). After completion of the TH of acetophenone in 2-propanol using complex *exo*-**7a**, a very stable rhenium isopropoxide complex, [$ReOCl_2$(*i*-PrO)(**2a**)] **18**, was isolated and characterized. The X-Ray structure of **18** is presented in Figure 20. Complex **18**, just as its ethoxy analog (**12**), exhibits a slightly distorted octahedral geometry with the oxo and alkoxo ligands in a *trans* arrangement. Remarkably, it also shows an inverted configuration relative to the starting material, **7a**.

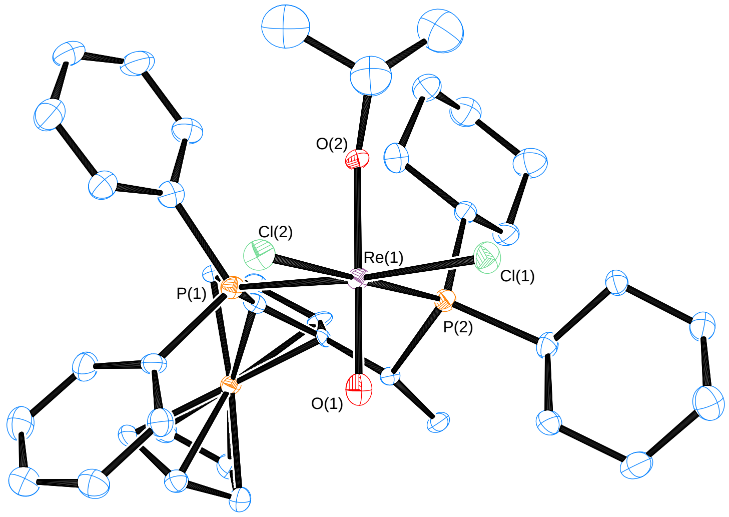

Figure 20. ORTEPIII drawing of complex **18.** Ellipsoids at 50% probability. Relevant distances and angles (Å and deg.): Re-P(1) 2.458(3), Re-P(2) 2.457(3), Re-O(1) 1.727(7), Re-O(2) 1.875(6), Re-Cl(1) 2.456(2), ReCl(2) 2.477(3), P(1)-Re-P(2) 92.29(9), O(1)-Re-O(2) 178.4(3).

Metal alkoxide complexes are common intermediates in transfer hydrogenation reactions, namely those that proceed either through a inner-sphere monohydridic route or through a Meerwein-Ponndorf-Verley-type hydrogen transfer.[1c] These complexes are rather stable and have been proposed to serve simply as inactive catalyst reservoirs in Ru-catalized TH[48] or as the resting state of the catalyst in Rh-catalyzed TH.[49] The fact that the isolated alkoxy intermediate **18** still contains two equatorial chloride ligands suggest that the mechanism does not proceed through a metal-hydride pathway since, as observed by Bäckvall and co-workers for the $RuCl_2(PPh_3)_3$-catalyzed TH,[50] in basic media the successive alkoxide displacement-β-elimination reactions lead to the formation of metal-dihydride species, which in our case, have not been observed. Taking these observations into account, the reaction mechanism depicted in Scheme 12 is proposed.

The first step of the mechanism is the dissociation of a phosphine ligand in **A**, to allow the coordination of the incoming alcohol. The assumption that the Josiphos ligand could alternate between monodentate and bidentate coordination is supported by the observed thermal isomerization of the complexes (*vide supra*) and by the fact that the alkoxo complex **18** exhibits an inverted configuration as compared to the parent complex *exo*-**7a**. Of the two phosphorus donors of the bidentate Josiphos ligand, the one which is more likely to dissociate first is the one directly attached to the ferrocene, being less electron-rich and thus, a weaker σ-donor. The resulting alcohol-complex **B** eliminates HX with the aid of the added base to give the alkoxo-complex **C**. Upon coordination of the ketone substrate (complex **D**), a direct hydrogen transfer from the coordinated alkoxide to the ketone takes place. This bears a strong resemblance to the mechanism found for the TH with Ir-COD derivates.[51] The resulting complex **E** releases an acetone molecule upon coordination of another alcohol ligand and this complex (**F**) undergoes intramolecular proton exchange and dissociation of the reduced ketone to regenerate the metal alkoxide **C**.

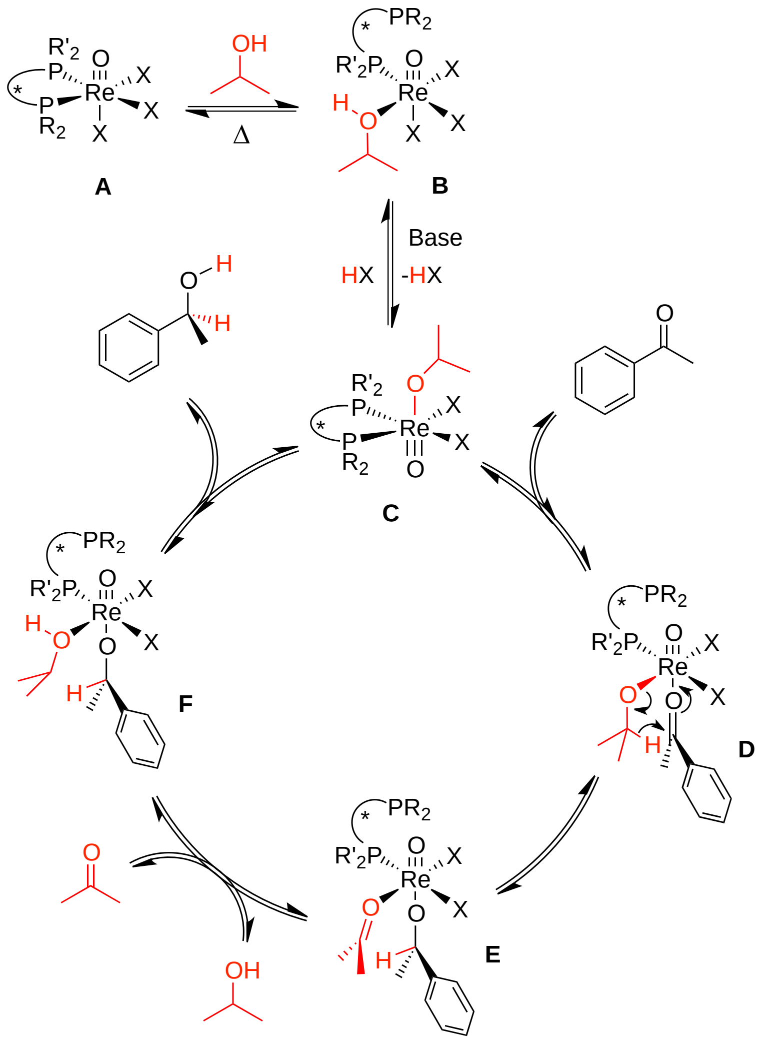

Scheme 12

The stereochemical outcome of the reaction is believed to depend heavily on steric factors (as the proposed mechanism depicts). However, considering that several factors (solvation, dispersion, steric and electrostatic interactions) have been reported to determine the degree of enantioselectivity,[1c] a definite conclusion can not be drawn.

2.4. Conclusion

In summary, we have developed an asymmetric transfer hydrogenation reaction of ketones using novel rhenium(V)-complexes with chiral bidentate ferrocenylphosphine ligands. The reaction uses 2-propanol as solvent and as the sole hydrogen source requiring the addition of substoichiometric amounts of a base. The reaction is clean and gives generally good to excellent yields (up to >99%), although the enantioselectivity is still moderate (up to 58%). The new rhenium(V) complexes are bench stable and easy to handle. An alkoxo-complex was isolated after completion of the reaction with catalyst *exo*-**7a**. Based on this, and considering the previously proposed reaction pathways, a plausible reaction mechanism was proposed in which the reduction occurs via the direct hydrogen transfer between the simultaneously coordinated alkoxy and ketone substrate. To the best of our knowledge, this is the first example of a transfer hydrogenation reaction catalyzed by rhenium complexes.

References

[1] a) G. Zassinovich, G. Mestroni, S. Gladiali, *Chem. Rev.* **1992**, *92*, 1051-1069; b) S. Gladiali, E. Alberico, *Chem. Soc. Rev.* **2006**, *35*, 226-236; c) J. S. M. Samec, J.-E. Bäckvall, P. G. Andersson, P. Brandt, *Chem. Soc. Rev.* **2006**, *35*, 237-248.

[2] R. Spogliarich, J. Kaspar, M. Graziani, F. Morandini, O. Piccolo, *Journal of Catalysis* **1985**, *94*, 292-296.

[3] H. Brunner, M. Kunz, *Chem. Ber.* **1986**, *119*, 2868-2873.

[4] A. Fujii, S. Hashiguchi, N. Uematsu, T. Ikariya, R. Noyori, *J. Am. Chem. Soc.* **1996**, *118*, 2521-2522.

[5] X. Wu, X. Li, A. Zanotti-Gerosa, A. Pettman, J. Liu, A. J. Mills, J. Xiao, *Chem. Eur. J.* **2008**, *14*, 2209-2222.

[6] a) N. Uematsu, A. Fujii, S. Hashiguchi, T. Ikariya, R. Noyori, *J. Am. Chem. Soc.* **1996**, *118*, 4916-4917; b) P. Barbaro, C. Bianchini, A. Togni, *Organometallics* **1997**, *16*, 3004-3014; c) J. S. M. Samec, J.-E. Bäckvall, *Chem. Eur. J.* **2002**, *8*, 2955-2961; d) S. E. Clapham, A. Hadzovic, R. H. Morris, *Coord. Chem. Rev.* **2004**, *248*, 2201-2237; e) J. Wu, F. Wang, Y. Ma, X. Cui, L. Cun, J. Zhu, J. Deng, B. Yu, *Chem. Commun.* **2006**, 1766-1768.

[7] G. Zassinovich, G. Mestroni, *J. Mol. Cat.* **1987**, *42*, 81-90.

[8] S. Kuhl, R. Schneider, Y. Fort, *Organometallics* **2003**, *22*, 4184-4186.

[9] a) W. Baratta, M. Ballico, G. Chelucci, K. Siega, P. Rigo, *Angew. Chem. Int. Ed.* **2008**, *47*, 4362-4365; b) W. Baratta, M. Ballico, A. D. Zotto, K. Siega, S. Magnolia, P. Rigo, *Chem. Eur. J.* **2008**, *14*, 2557-2563.

[10] a) N. Meyer, A. J. Lough, R. H. Morris, *Chem. Eur. J.* **2009**, *15*, 5605-5610; b) S. Zhou, S. Fleischer, K. Junge, S. Das, D. Addis, M. Beller, *Angew. Chem.* **2010**, *122*, 8298-8302; c) A. Mikhailine, A. J. Lough, R. H. Morris, *J. Am. Chem. Soc.* **2009**, *131*, 1394-1395; d) P. O. Lagaditis, A. J. Lough, R. H. Morris, *Inorg. Chem.* **2010**, *49*, 10057-10066; e) V. V. K. M. Kandepi, J. M. S. Cardoso, E. Peris, B. Royo, *Organometallics* **2010**, *29*, 2777-2782.

[11] J. Noddack, W. Noddack, *Z. Anorg. Allg. Chem.* **1929**, *183*, 353-375.

[12] a) R. Hua, J.-L. Jiang, *Curr. Org. Syn.* **2007**, *4*, 151-174; b) Y. Kuninobu, K. Takai, *Chem. Rev.* **2010**, *111*, 1938-1953; c) W. A. Herrmann, F. E. Kühn, *Acc. Chem. Res.* **1997**, *30*, 169-180.

[13] a) N. Greenwood, A. Earnshaw, *Chemistry of the Elements*, 2 ed., Butterworth-Heinemann, Oxford, **1998**; b) B. Royo, C. C. Romão, in *Comprehensive Organometallic Chemistry III, Vol. 5* (Eds.: R. H. Crabtree, D. M. P. Mingos), Elsevier, **2007**, pp. 855-960.

[14] a) K. Nolin, R. Ahn, Y. Kobayashi, J. Kennedy-Smith, F. Toste, *Chem. Eur. J.* **2010**, *16*, 9555-9562; b) K. A. Nolin, R. W. Ahn, F. D. Toste, *J. Am. Chem. Soc.* **2005**, *127*, 12462-12463.

[15] C.-T. Yeung, P.-F. Teng, H.-L. Yeung, W.-T. Wong, H.-L. Kwong, *Org. Biomol. Chem.* **2007**, *5*, 3859-3864.

[16] a) E. A. Ison, J. E. Cessarich, G. Du, P. E. Fanwick, M. M. Abu-Omar, *Inorg. Chem.* **2006**, *45*, 2385-2387; b) G. Du, P. E. Fanwick, M. M. Abu-Omar, *J. Am. Chem. Soc.* **2007**, *129*, 5180-5187; c) E. A. Ison, E. R. Trivedi, R. A. Corbin, M. M. Abu-Omar, *J. Am. Chem. Soc.* **2005**, *127*, 15374-15375; d) G. Du, M. M. Abu-Omar, *Organometallics* **2006**, *25*, 4920-4923.

[17] B. Royo, C. C. Romão, *J. Mol. Cat. A: Chem.* **2005**, *236*, 107-112.

[18] a) Y. Nishibayashi, I. Takei, S. Uemura, M. Hidai, *Organometallics* **1999**, *18*, 2291-2293; b) Y.-M. Zhang, P. Liu, H.-L. Zhang, *Synth. React. Inorg., Met.-Org., Nano-Met. Chem.* **2008**, *38*, 778-780; c) Y.-M. Zhang, P. Liu, H.-L. Zhang, Z.-M. Zhou, *Synth. React. Inorg., Met.-Org., Nano-Met. Chem.* **2008**, *38*, 577-579.

[19] a) W. Baratta, G. Chelucci, E. Herdtweck, S. Magnolia, K. Siega, P. Rigo, *Angew. Chem. Int. Ed.* **2007**, *46*, 7651-7654; b) W. Baratta, F. Benedetti, A. Del Zotto, L. Fanfoni, F. Felluga, S. Magnolia, E. Putignano, P. Rigo, *Organometallics* **2010**, *29*, 3563-3570.

[20] a) T. P. Yoon, E. N. Jacobsen, *Science* **2003**, *299*, 1691-1693; b) H.-U. Blaser, B. Pugin, F. Spindler, E. Mejía, A. Togni, in *Privileged Chiral Ligands and Catalysts*, 1 ed. (Ed.: Q.-L. Zhou), Wiley-VCH, Weinheim, **2011**, pp. 93-136.

[21] T. J. Kealy, P. L. Pauson, *Nature* **1951**, *168*, 1039-1040.

[22] A. Togni, T. Hayashi, *Ferrocenes: Homogeneous Catalysis, Organic Synthesis, Materials Science*, VCH Publishers, Weinheim, **1995**.

[23] G. Wilkinson, M. Rosenblum, M. C. Whiting, R. B. Woodward, *J. Am. Chem. Soc.* **1952**, *74*, 2125-2126.

[24] A. Togni, *Angew. Chem. Int. Ed.* **1996**, *35*, 1475.

[25] a) G. Gokel, D. Marquarding, I. Ugi, *J. Org. Chem.* **1972**, *37*, 3052-3058; b) D. Marquarding, H. Klusacek, G. Gokel, P. Hoffmann, I. Ugi, *J. Am. Chem. Soc.* **1970**, *92*, 5389-5393.

[26] a) T. Hayashi, T. Mise, M. Fukushima, M. Kagotani, N. Nagashima, Y. Hamada, A. Matsumoto, S. Kawakami, M. Konishi, K. Yamamoto, M. Kumada, *Bull. Chem. Soc. Jpn.* **1980**, *53*, 1138-1151; b) T. Hayashi, K. Yamamoto, M. Kumada, *Tetrahedron Lett.* **1974**, *15*, 4405-4408.

[27] A. Togni, C. Breutel, A. Schnyder, F. Spindler, H. Landert, A. Tijani, *J. Am. Chem. Soc.* **1994**, *116*, 4062-4066.

[28] H.-U. Blaser, W. Brieden, B. Pugin, F. Spindler, M. Studer, A. Togni, *Top. Catal.* **2002**, *19*, 3-16.

[29] R. Koller, Thesis No. 19219, ETH Zürich (Zürich), **2010**.

[30] B. Aechter, K. Polborn, W. Beck, *Z. Anorg. Allg. Chem.* **2001**, *627*, 43-54.

[31] A. M. Bond, R. Colton, R. W. Gable, M. F. Mackay, J. N. Walter, *Inorg. Chem.* **1997**, *36*, 1181-1193.

[32] a) R. J. Angelici, F. Basolo, *J. Am. Chem. Soc.* **1962**, *84*, 2495-2499; b) J. D. Atwood, T. L. Brown, *J. Am. Chem. Soc.* **1975**, *97*, 3380-3385; c) J. D. Atwood, T. L. Brown, *J. Am. Chem. Soc.* **1976**, *98*, 3155-3159.

[33] D. M. Kimari, A. M. Duzs-Moore, J. Cook, K. E. Miller, T. A. Budzichowski, D. M. Ho, S. K. Mandal, *Inorg. Chem. Commun.* **2005**, *8*, 14-17.

[34] a) C. Bianchini, A. Marchi, L. Marvelli, M. Peruzzini, A. Romerosa, R. Rossi, A. Vacca, *Organometallics* **1995**, *14*, 3203-3215; b) C. Bianchini, A. Marchi, L. Marvelli, M. Peruzzini, A. Romerosa, R. Rossi, *Organometallics* **1996**, *15*, 3804-3816.

[35] P. Bergamini, F. F. DeBiani, L. Marvelli, N. Mascellani, M. Peruzzini, R. Rossi, P. Zanello, *New J. Chem.* **1999**, 207-217.

[36] N. P. Johnson, J. L. Lock, G. Wilkinson, *J. Chem. Soc.* **1964**, 1054-1066.

[37] M. L. Parr, C. Perez-Acosta, J. W. Fallerb, *New J. Chem.* **2005**, *29*, 613-619.

[38] a) S. Bolaño, J. Bravo, R. Carballo, E. Freijanes, S. García-Fontán, P. Rodríguez-Seoane, *Polyhedron* **2003**, *22*, 1711-1717; b) L. Suescun, A. W. Mombru, R. A. Mariezcurrena, H. Pardo, S. Russi, C. Kremer, M. Rivero, E. Kremer, *Acta Cryst.* **2000**, *C56*, 930-931.

[39] J. M. Mayer, *Inorg. Chem.* **1988**, *27*, 3899-3903.

[40] G. F. Ciani, G. D'Alfonso, P. F. Romiti, A. Sironi, M. Freni, *Inorg. Chim. Acta.* **1983**, *72*, 29-37.

[41] U. Abram, in *Comprehensive Coordination Chemistry II, Vol. 5*, Second ed. (Eds.: J. A. McCleverty, T. J. Meyer), Elsevier, **2003**, pp. 271-402.

[42] L. Wei, J. W. Babich, J. Zubieta, *Inorg. Chem.* **2004**, *43*, 6445-6454.

[43] S. Schmidt, J. Strähle, *Z. Krist.* **1991**, *196*, 243-253.

[44] F. Tisato, F. Refosco, M. Porchia, G. Bandoli, G. Pilloni, L. Uccelli, A. Boschi, A. Duatti, *J. Organomet. Chem.* **2001**, *637-639*, 772-776.

[45] B. P. Sullivan, J. C. Brewer, H. B. Gray, D. Linebarrier, J. M. Mayer, *Inorg. Synth.* **1992**, *29*, 146-150.

[46] a) S. Abram, U. Abram, E. Schulz-Lang, J. Strähle, *Acta Cryst.* **1995**, *C51*, 1078-1080; b) F. o. Baril-Robert, A. Beauchamp, *Can. J. Chem.* **2003**, *81*, 1326-1340.

[47] J. Chatt, G. A. Rowe, *J. Chem. Soc.* **1962**, 4019-4033.

[48] M. Yamakawa, H. Ito, R. Noyori, *J. Am. Chem. Soc.* **2000**, *122*, 1466-1478.

[49] V. Guiral, F. o. Delbecq, P. Sautet, *Organometallics* **2000**, *19*, 1589-1598.

[50] A. Aranyos, G. Csjernyik, K. J. Szabo, J.-E. Backvall, *Chem. Commun.* **1999**, 351-352.

[51] J.-W. Handgraaf, J. N. H. Reek, E. J. Meijer, *Organometallics* **2003**, *22*, 3150-3157.

3. Chiral Rhenium Hydrido Complexes and Catalytic Hydrogenation[*]

3.1. Introduction

The importance of hydrogenation reactions in organic chemistry was early recognized in 1912 when the French chemist Paul Sabatier was awarded the Nobel Prize in chemistry (shared with his fellow countryman Victor Grignard) "for his method of hydrogenating organic compounds in the presence of finely disintegrated metals whereby the progress of organic chemistry has been greatly advanced in recent years".[1] Heterogeneous catalysts present obvious advantages in terms of stability, separation and reusability. However, the homogeneous systems allow easy fine-tuning of their chemo-, regio- and stereoselectivity properties. Asymmetric homogeneous hydrogenation is, by far, the most popular industrial method for the introduction of tertiary carbon stereocenters. Different substrates are subject to these processes, including C=C, C=O and C=N bonds, making use of several metals, rhodium, iridium and ruthenium being the most popular .[2] In 2001, R. Noyori and W. Knowles received the Nobel prize in chemistry (shared with B. Sharpless) "for their work on chirally catalysed hydrogenation reactions",[3] accenting the crucial role of hydrogenation reactions in organic synthesis.

The use of Re in homogeneous catalysis, in particular asymmetric catalysis, is still relatively underdeveloped. Nevertheless, in the last twenty years there has been an increasing development of transition metal-catalyzed organic syntheses using rhenium-based catalysts (see section 1.3.). However, in the field of hydrogenation, most of the recently reported rhenium catalysts are bimetallic, having the rhenium atom as part of the ligand.[4] There are only few reports of “truly” rhenium-catalyzed hydrogenation processes[5] from which, the recent contributions by Berke and his group are, perhaps, the most significant.[5e, 6] Moreover, to the best of our knowledge, there is only one reported asymmetric process.[7] For a deeper survey on this topic, see section 1.3.5.

---

[*] Part of the experimental work described in this chapter was carried out in the frame of Undergraduate Semester Projects by Nikolas Huwyler in spring 2008 and Pascal Engl in spring 2010, both in ETH Zürich.

3.1.1. Pigiphos ligands

Chiral ferrocenylphosphine ligands, as discussed in Chapter 2, have found several applications in asymmetric catalysis both in academia and industry, the bidentate ligands of the Josiphos type being particularly successful.[8] Soon after the invention of *Josiphos*, the methodology for its synthesis was further developed to give rise to a novel kind of chiral tridentate bis-ferrocenylphosphine ligands nicknamed *Pigiphos* after Pierluigi Barbaro, the chemist who first synthesized them (Scheme 1). The Pigiphos scaffold, analogous to Josiphos, features high modularity, allowing tailoring of its sterical and electronic properties by changing the nature of the residues on the phosphorus atoms.

This kind of ligands are a notable example of still rare chiral tridentate phosphines.[9] The first Pigiphos ligand to be synthesized and still the one with the best performance in catalysis is bis-{(*R*)-1-[(*S*)-2-(diphenylphosphino)ferrocenyl]ethyl}cyclohexylphosphine) (**19a**).

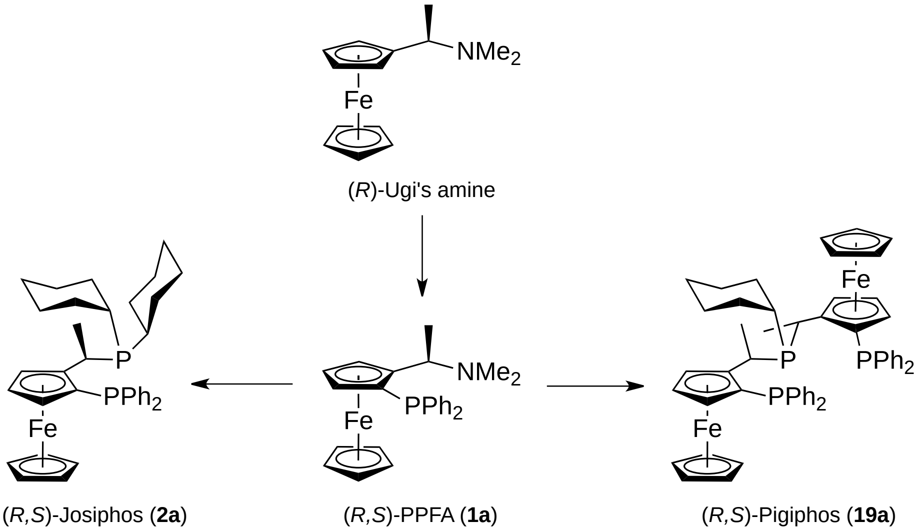

Scheme 1

This versatile ligand can adopt both *meridional* and *facial* coordination geometries[10] and various neutral and cationic complexes with Pd, Ni, Ru, Rh and Ir have been reported, as well as several applications in asymmetric catalysis such as transfer hydrogenations,[10] hydroaminations,[11] phosphinations,[12] and Nazarov cyclizations.[13]

3.2. Synthesis and Characterization of the Complexes

3.2.1. Ligand synthesis

The bis-ferrocenyl triphosphine ligands of the Pigiphos type (**19**) were synthesized following the reported procedure with slight modifications.[14] The starting material, as for the synthesis of the ligands of the Josiphos family, was (*R*)-[1-(dimethylamino)ethyl]ferrocene (Ugi's amine) (Scheme 2).

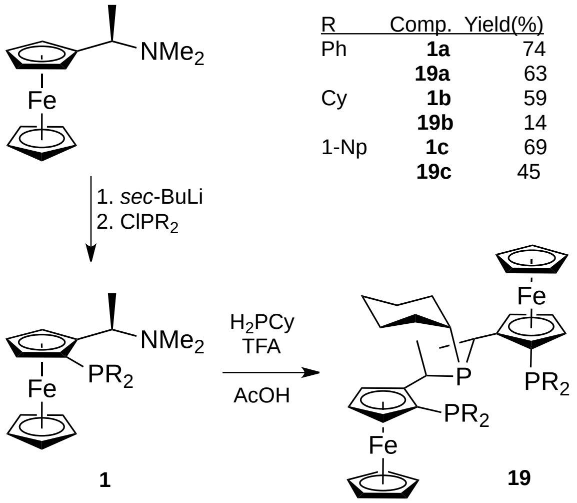

R	Comp.	Yield(%)
Ph	**1a**	74
	19a	63
Cy	**1b**	59
	19b	14
1-Np	**1c**	69
	19c	45

Scheme 2

3.2.2. Synthesis of rhenium(I) derivatives of **19a**

The chemistry of Re^I complexes with tridentate triphosphine ligands is practically confined to that of the $[Re(triphos)(CO)_2]^+$ moiety (triphos = $MeC(CH_2PPh_2)_3$), which displays a rich chemistry.[15] It is synthesized from $[ReCl(CO)_3(PPh_3)_2]$ by thermal ligand substitution. The resulting chloride, $[ReCl(triphos)(CO)_2]$, can be easily converted to the corresponding mono- or trihydride (Figure 1) by reaction with $LiAlH_4$ in the presence or absence of CO, respectively. The hydride atom from [ReH(triphos)(CO)$_2$] can be easily abstracted by treatment with Meerwein's salt to afford the cationic, coordinativelly unsaturated [Re(triphos)(CO)$_2$]$^+$ which stabilizes itself by an agostic interaction of a C-H bond from the ligand. It can coordinate several different donors like CO, MeCN, acetylenes, etc., and can activate molecular hydrogen.[15b] Triphos dicarbonyl complexes display a *facial* geometry (see Figure 1),[15b] while analogous η^3 complexes with the potentially tetradentate ligand P(CH$_2$CH$_2$PPh$_2$)$_3$ have been reported to have a *cis,meridional* geometry. The latter complexes are synthesized by thermal decarbonylation of [ReX(CO)$_5$].[16]

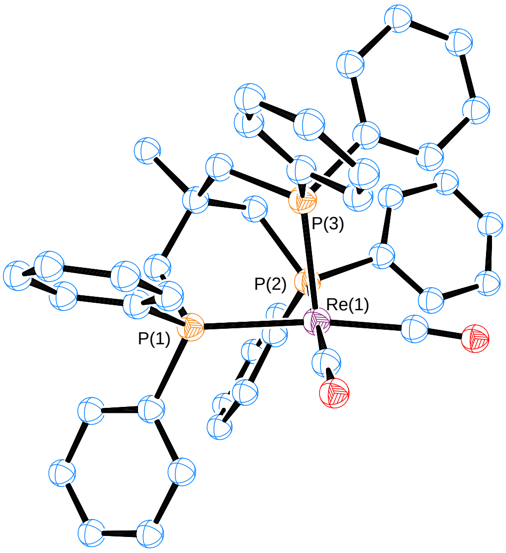

Figure 1. ORTEPIII drawing of the crystal structure of [ReH(CO)$_2$(triphos)]. The hydride ligand *trans* to P(3) was not located.[15b]

By a modification of a reported procedure[17] and analogously to the synthesis of the Josiphos derivatives **3** and **4**, the preparation of the Pigiphos complexes [ReBr(CO)$_2$(**19a**)] (**20**) and [ReCl(CO)$_2$(**19a**)] (**21**) was carried out successfully, giving the desired products in good yields (Scheme 3). The remarkable stability of both, the ligand and the complexes is evidenced by the good yields (>85%) obtained in spite of the harsh reaction conditions (180 - 200 °C, overnight). Lower temperatures and/or shorter reaction times led to complex product mixtures, presumably resulting from incomplete ligand substitution.

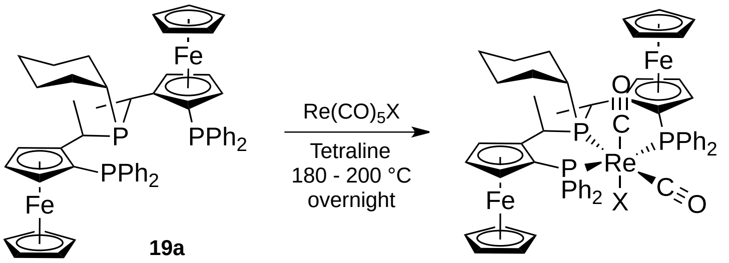

X	Comp.	Yield(%)
Br	**20**	88
Cl	**21**	85

Scheme 3

Contrary to their Josiphos counterparts **3** and **4**, both complexes **20** and **21** were obtained as a single isomer, as evidenced by NMR analysis. The ^{31}P NMR spectra of both complexes (Figure 2) show an AMX spin pattern.[10] The magnitude of the coupling constants is consistent with a *meridional* coordination (see experimental part). The two CO ligands could be assumed to be in a *cis* situation due to the substitution mechanism observed for rhenium (and manganese pentacarbonyl halides), as it was already discussed in section 2.2.2. (see Scheme 3 in Chapter 2). As observed for the Josiphos analogs **3** and **4**, the bromine derivative **20** shows a low-field shift with respect to **21**, due to the higher polarizability (lower electronegativity) of the bromide ligand.

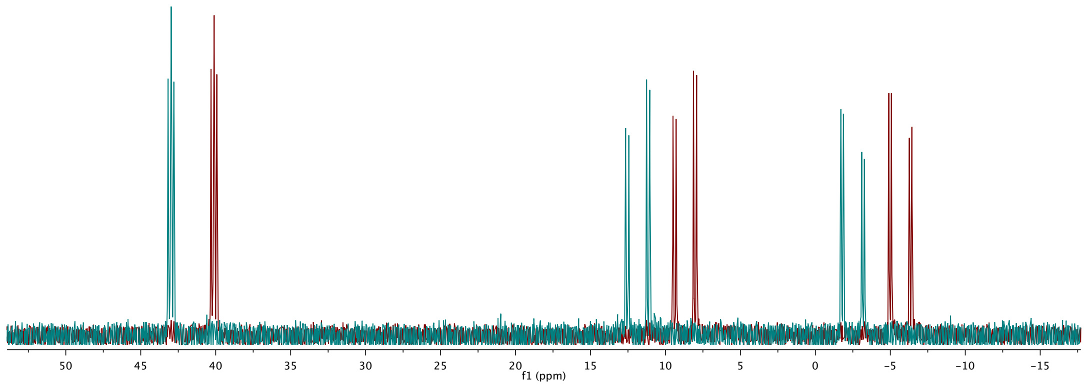

Figure 2. ^{31}P NMR spectra (121.5 MHz, $CDCl_3$) for complexes **20** (red) and **21** (green).

X-ray structural analysis of complex **20** revealed that the obtained isomer is *exo*-[$ReBr(CO)_2$(**19a**)] (Figure 3), with the bromide ligand in a transoid position with respect to the cyclohexyl ring. Considering the strong structural analogy between **20** and **21**, it is possible to assume that the same isomer is also formed for the chloride analog **21**. Unfortunately, due to the poor quality of the measured crystal, the accurate determination of angles and distances was precluded.

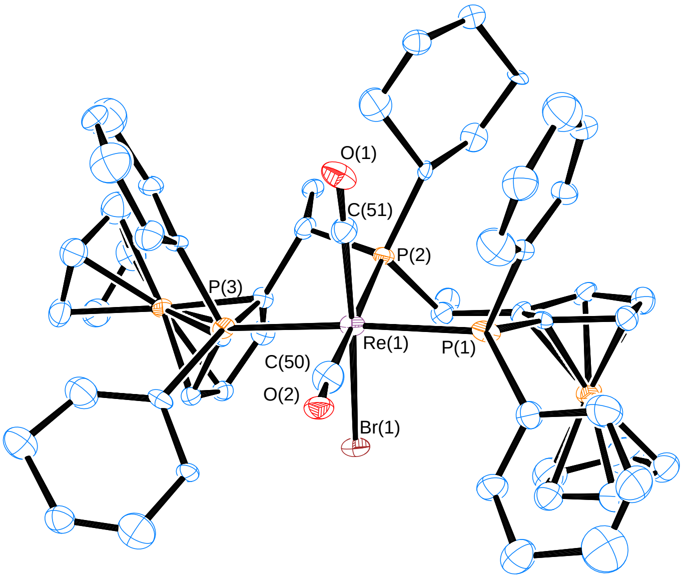

Figure 3. ORTEPIII drawing of the crystal structure for complex **20**. Ellipsoids at 30% probability. For the synthesis of this sample (*S*,*R*)-**19a** was used.

Several attempts to abstract the halide ligand either from **20** or **21** were unsuccessful. Typical reagents like AgOTf or $TlPF_6$ led to formation of unidentified oxidation products it the former case or simply did not react at all, in the latter case. The use of MeOTf as halide scavenger,[18] which proved to be effective for the Josiphos complex **3**, was also unsuccessful in this case. Complexes **20** and **21** also showed to be inert against $NaBH_4$ while with $LiAlH_4$ only minute amounts of the desired hydride [ReH(CO)$_2$(**19a**)] were observed by ^{1}H NMR spectroscopy.

There is a strong contrast between these results and those reported for the Triphos analogues for which the halide is reported to be easily abstracted and substituted by the aforementioned procedures.[15b, 18] This difference in reactivity is, logically, a consequence of the different geometry; in the triphos derivatives (see Figure 1) the monoanionic ligand has a phospine group in the *trans* position, while for **20** and **21** this position is occupied by a CO ligand.

The carbonyl group is much milder σ-donor than the phosphine and hence, has a lower labilizing effect on the Re-X bond.

3.2.3. Synthesis of rhenium(V)-oxo derivatives

Following an analogous procedure as for the synthesis of [ReO_2I(**2a**)] (**10**), the corresponding Pigiphos derivative [ReO_2I(**19a**)] (**22**) was obtained by thermal ligand substitution from [$ReO_2I(PPh_3)_3$] at room temperature in good yield (Scheme 4).

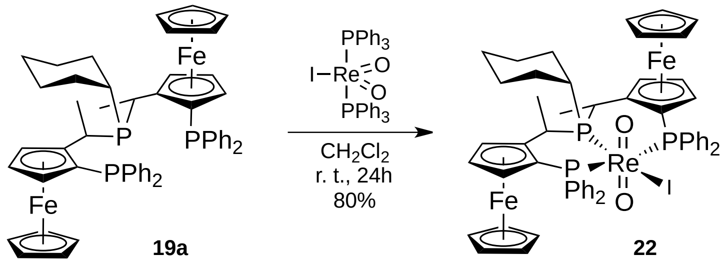

Scheme 4

The resulting paramagnetic complex **22** was characterized by elemental analysis and HR-MS confirming the proposed stoichiometry. In the FT-IR spectra the expected stretching frequency for the *trans*-[ReO_2] moiety at 784.6 cm^{-1} was observed.

After several crystallization attempts, single crystals were obtained from an hexane/pentane saturated solution of **22**. The solved X-ray structure (Figure 4) confirmed the proposed ligand arrangement (*mer-trans*). Unfortunately, due to the poor quality of the measured crystal (twined and with several disordered solvent molecules), the accurate determination of bond lengths and angles was not possible.

Contrary to its Josiphos counterpart (**10**), complex **22** does not possess a free coordination position due, of course, to the tridentate nature of Pigiphos. Attempts to activate the electronically (and coordinatively) saturated complex **22** by abstraction of the iodine atom were unsuccessful. The use of NaOTf, AgOTf or AgOAc as halide scavengers resulted only in the formation of dark reaction mixtures out of which no identifiable product could be isolated. The impossibility of isolate or, at least, identify the activated species, discouraged us to use these complex as hydrogenation (pre)catalyst.

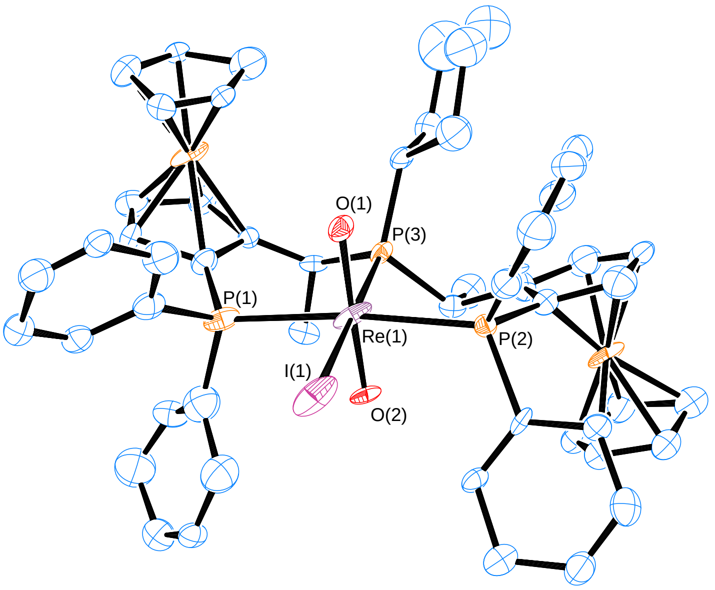
O(1)
P(3)
P(1)
Re(1)
P(2)
I(1)
O(2)

Figure 4. ORTEPIII drawing of the crystal structure fof complex **22**. Ellipsoids at 30% probability. For the synthesis of this sample (*S*,*R*)-**19a** was used.

3.2.4. *Synthesis of the rhenium(III) derivatives [ReCl$_3$(**19**)] (**23**)*

The method of choice for the synthesis of this complexes was the direct ligand substitution reaction of the parent complex [ReCl$_3$(NCMe)(PPh$_3$)$_2$] with the corresponding Pigiphos ligand (Scheme 5) adapting the reported procedure used for the synthesis of [ReCl$_3$(triphos)].[19] The products were obtained in good yields as a dark brown-green microcrystalline solids.

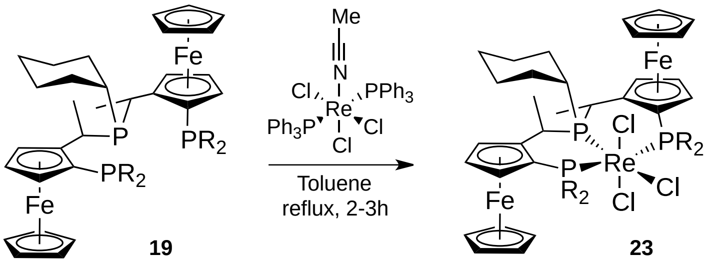
Fe
P
PR2
PR2
Fe
19
Me
N
Cl
PPh3
Re
Ph3P
Cl
Cl
Toluene
reflux, 2-3h
Fe
P
Cl
PR2
P
R2
Re
Cl
Cl
Fe
23

R	Comp.	Yield(%)
Ph	**23a**	98
Cy	**23b**	67
1-Np	**23c**	73

Scheme 5

Compounds **23** are octahedral rhenium(III) d^4 complexes which exhibit a second-order paramagnetism as it is usual the case for [ReX_3L_3] species.[19-20] The large reduction of μ_{eff} due to their strong spin-orbit coupling[20b] actually allows the measurement of Knight-shifted ^{1}H NMR spectra of difficult interpretation. This feature, along with their silent ^{31}P NMR spectra, precludes the usefulness of NMR-techniques in this case. The complexes were then characterized by elemental analysis and by high-resolution mass spectroscopy. Single crystals of complex **23a** were obtained, making the confirmation of the proposed structure by X-ray analysis possible (Figure 5).

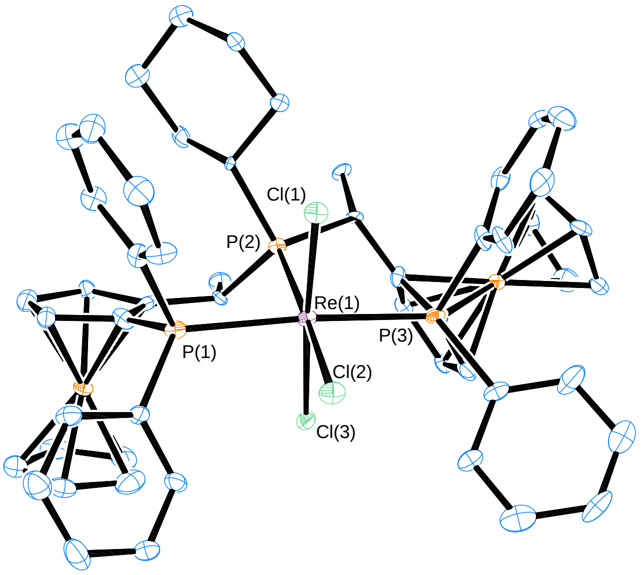

Figure 5. ORTEPIII drawing of the crystal structure of complex **23a**. Ellipsoids at 50% probability. Relevant distances and angles (Å and deg.): Re-P(1) 2.452(2), Re-P(2) 2.421(2), Re-P(3) 2.444(2), Re-Cl(1) 2.3271(19), Re-Cl(2) 2.4429(19), Re-Cl(3) 2.3684(19), P(1)-Re-P(2) 87.87(6), P(2)-Re-P(3) 92.92(6), P(1)-Re-P(3) 175.57(7), Cl(1)-Re-Cl(2) 86.36(6), Cl(2)-Re-Cl(3) 176.22(7), Cl(1)-Re-Cl(3) 91.78(7), P(1)-Re-Cl(2) 88.89(6), Cl(2)-Re-P(3) 90.52(6).

The coordination around the metal center is approximately octahedral with the three chloride ligands in *meridional* configuration. It is noteworthy that in spite of the bulkiness of the Pigiphos ligand, the distortion from the ideal geometry is rather small if compared with other *mer*-(trisphosphine)$ReCl_3$ complexes: in complex **23a** the Re atom is only 0.092 Å away from the plane defined by the three phosphorus atoms and the angle between the two phosphines in *trans* and the Re atom is fairly close to 180°, i.e., 175.57(7). In *mer*-$(PPh_2Me)_3ReCl_3$[21] and *mer*-$(PPhEt_2)_3ReCl_3$[22] this distances are 0.105 Å and 0.139 Å while the corresponding angles are 165.8(2) and 167.7(1) respectively. A direct comparison of the structural features of **23a** and other metal complexes bearing the Pigiphos ligand is less straightforward since this is the first reported X-ray structure for an octahedral complex with this ligand.

3.2.5. Synthesis of rhenium(V) and -(VII) polyhydrides

Metal hydrides are ubiquitous in several catalytic transformations being either the catalyst precursors, the active species or elusive intermediates.[23] Among the most stable and hence more studied metal-hydride complexes are the rhenium polyhydrides, especially rhenium(V) penta-[24] and rhenium(VII) heptahydrides.[25] In spite of their rich chemistry, facile synthesis and ease of handling, the potential of these kind of derivatives in catalysis still has not been exploited. With this precedent in mind, the synthesis of rhenium polyhydrides with Pigiphos and Josiphos ligads was pursued.

Upon treatment with $NaBH_4$ in refluxing ethanol, the trichloride complex **23a** produces compound **24** in almost quantitative yield (Scheme 6). This procedure is similar to that used to obtain [ReH_5(Triphos)].[19, 26] The product is an orange solid, stable to air and moisture even in solution, though it decomposes slowly in chlorinated solvents to give various still unidentified products.

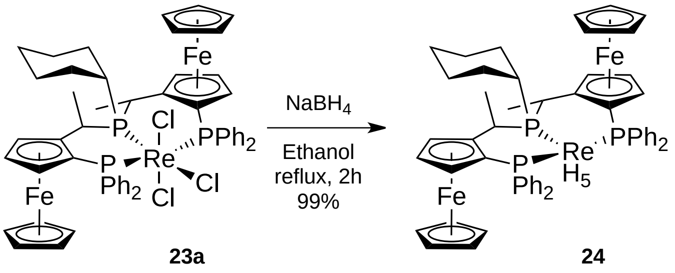

Scheme 6

In the FTIR spectrum of **24**, apart from the bands corresponding to the ligand vibration modes, ν(Re-H) absorptions are observed at 1931 and 1896 cm^{-1}, similar to those reported for [$ReH_5(PhP(CH_2CH_2CH_2PCy_2)_2)$].[24b]

The ^{31}P NMR spectrum (Figure 6) shows the expected ABX spin system with coupling constants $^{cis}J_{PP}$ = 10.6 and $^{trans}J_{PP}$ = 68.3 Hz. This is consistent with the presence of two diastereotopic ferrocenylphosphine moieties. It is noteworthy that the magnitude of the $^{trans}J_{PP}$ coupling constant is rather small if compared with Pd, Ni, Rh and Ir complexes with the same ligand in a *meridional* arrangement in which it varies from 131 to 411 Hz.[9, 27] This is a consequence of a decrease in the angle between the wing phosphorous atoms and the Re center, departed from the ideal *trans* situation as it will be shown later.

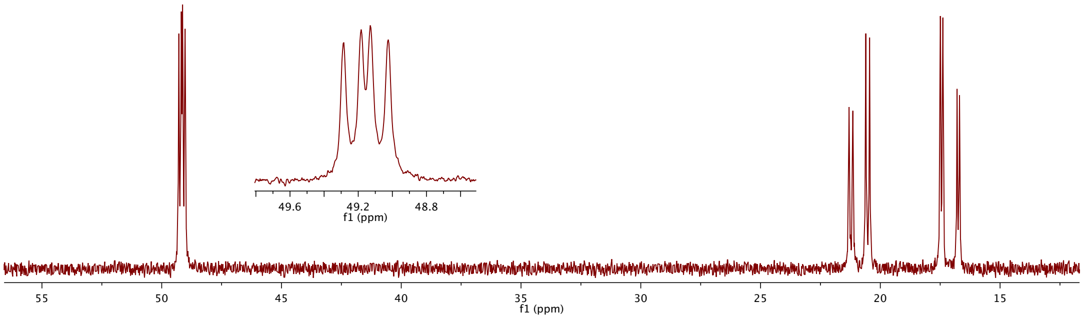

Figure 6. ^{31}P NMR spectrum (room temp., 101.3 MHz, C_6D_6) for complex **24**.

In the ^{1}H NMR spectra at room temperature (either in CD_2Cl_2, C_6D_6, toluene-D_8 or chlorobenzene-D_5) the five hydride protons are equivalent and appear at δ -6.05 as a broad featureless singlet indicating a fast fluxional behavior. Upon heating the toluene-D_8 solution to 323 K the fast movement regime is attained and the hydride signal is resolved in what could be described as a quartet, suggesting equivalence of the five hydrides and a similar coupling constant with the three different phosphorus atoms. Upon cooling the sample, the hydride resonance start to decoalesce at 273 K, being completely resolved at 213 K in three signals, a triplet at δ -5.5, a quadruplet at δ -6.2 and a singlet at δ -6.5 with a relative intensity of 2:2:1, respectively. Further cooling to 173 K leads to almost complete disappearance of the signals without further decoalescence. These spectra are shown in Figure 7.

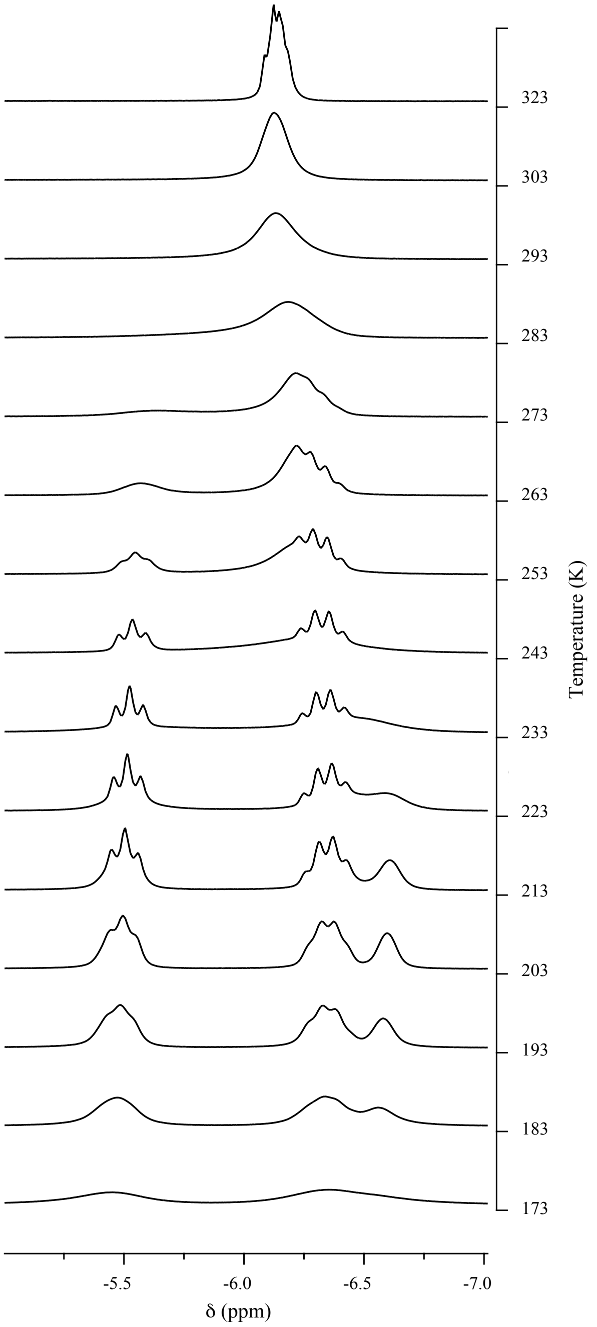

Figure 7. Variable-temperature ^{1}H NMR spectra (500 MHz, Tol-D_8) for complex **24** (hydride region only).

With respect to the nature of the Re-H bond, X-Ray and neutron diffraction studies on different rhenium-pentahydrides containing chelating[24b] triphosphine- or monodentate[28] phosphine ligands have shown that these kind of complexes do not show H-H distances short enough to be considered as η^2-H_2 ligands or "non classical" hydrides. The same complexes can be also addressed as "classical" in solution based on the measurement of the spin-lattice relaxation times, T_1,[29] in spite of the ambiguous results given by this method, specially for crowded polyhydrides with bulky ligands[30] and for hydrides of metals with high gyromagnetic ratio (like rhenium) in which metal-hydride dipole-dipole contributions to relaxation are significant.[29b]

To rule out the possible presence or formation of η^2-H_2 ligands (i.e. as intermediates in the exchange process), variable-temperature T_1 measurements were carried out for complex **24** at 500 MHz, suggesting a "classical" structure. The plot of ln(T_1) vs. 1000/T (K) for the three resonances observed after decoalescence (Figure 8) shows the same behavior for all the hydridic protons with an estimated T_1 minimum value of 158 ms which is in good agreement with the reported values for all-terminal rhenium-pentahydride complexes.[29b]

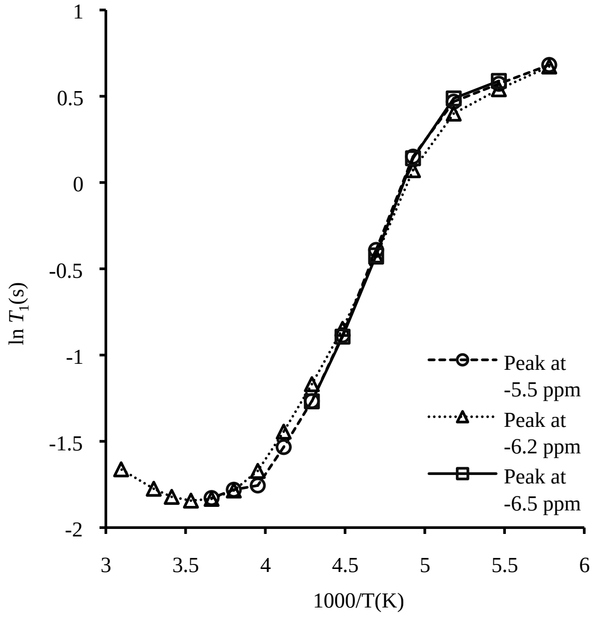

Figure 8. Plot of the temperature dependence of T_1 for complex **24** (^{1}H NMR spectra at 500 MHz, Tol-D_8). T_1 (min) = 158 ms.

X-Ray quality crystals of complex **24**, which co-crystallizes along with two benzene molecules, were obtained. An ORTEP view of **24**•2(C_6H_6) is shown in Figure 9.

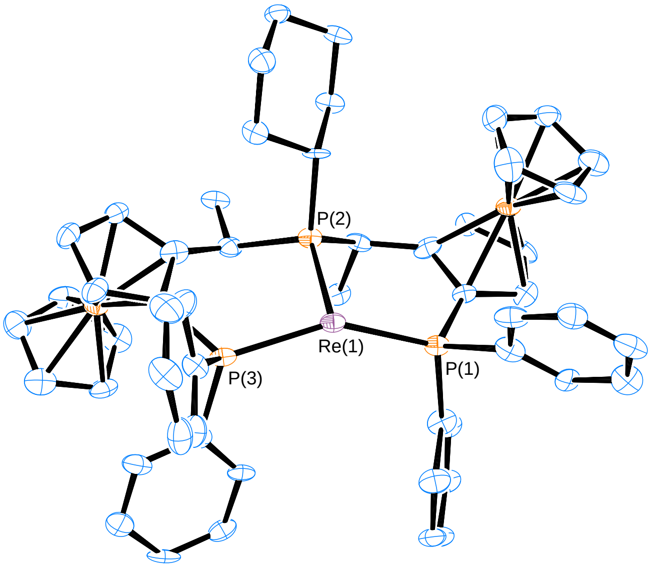

Figure 9. ORTEPIII drawing of the crystal structure of complex **24**•2(C_6H_6). Solvent molecules are omitted for clarity. Ellipsoids at 50% probability. Relevant distances and angles (Å and deg.): Re-P(1) 2.355(3), Re-P(2) 2.387(2), Re-P(3) 2.353(3), P(1)-Re-P(2) 96.20(10), P(2)-Re-P(3) 97.45(10), P(1)-Re-P(3) 148.76(9). The hydridic protons were not located.

Even though the hydrides could not be located by X-Ray measurements, one can assess the overall coordination geometry around the metal center in the complex by analysis of the geometries of the Re-P bonds.[31] The important parameters to take into account are the P-Re-P bond angles (see Figure 9) and the distance of the rhenium atom to the plane determined by the three phosphorus atoms (0.498 Å). This set of parameters are consistent with a triangulated dodecahedral geometry[32] as shown in Figure 10 and are also in accordance with the values obtained for the related compound [$ReH_5(PhP(CH_2CH_2CH_2PCy_2)_2$] (95.10°, 95.10°, 151.80° and 0.486 Å) in which the hydridic protons were actually located.[24b]

The triangulated dodecahedral geometry around the rhenium atom in **24** could be described by two mutually orthogonal trapezoids BAAB.[33] In complex **24** (see Figure 10), one of these planes would contain the central phosphorus atom, P1, and the hydridic protons H1, H2 and H3. The rhenium atom would be also included in this plane. The second plane would be defined by the wing phosphorus atoms, P1 and P3, and the hydrides H4 and H5. With this geometry there would be three different types of hydride ligands: two pairs of hydrides occupying the four-neighbor A positions, H1, H2, H3 and H4 (being the two latter at the same side with respect the cyclohexyl substituent) and one hydride, H3, occupying the remaining five-neighbor B position. This spatial arrangement accounts for the observed decoalescence pattern in ^{1}H NMR when the slow movement regime is attained upon cooling to 213 K (Figure 7).

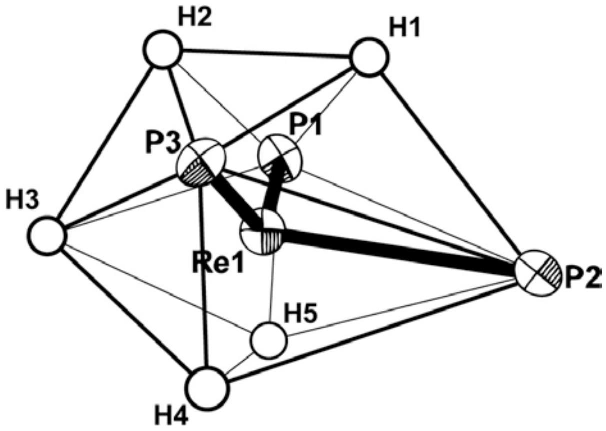

Figure 10. Coordination sphere of Re in [ReH_5(**19a**)] (**24**). The Re-P core is taken from the actual crystal structure of **24**•2(C_6H_6) (50% probability ellipsoids) and the hydride ligands (represented by spheres of arbitrary size) are placed assuming an idealized triangulated dodecahedral geometry.

Rhenium(VII) heptahydrides of the type [ReH_7(**2**)] (**25**) were obtained by a slight modification of the method reported by Crabtree,[25b] starting from the Re^V oxo-halide derivatives [$ReOCl_3$(**2**)] (**7**) which upon reaction with hydride sources like $LiAlH_4$ or $NaBH_4$ at room temperature followed by hydrolysis, yielded the corresponding nonacoordinated heptahydrides (Scheme 7).

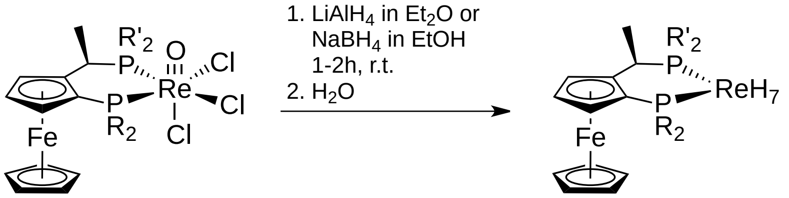

7 **25**

R	R'	Comp.	Yield(%)
Ph	Cy	**25a**	76
Cy	Ph	**25b**	31
CF_3	Cy	**25c**	36

Scheme 7

These compounds are orange solids, moderately stable to moisture and air during several days in the solid state but not in solution, giving dark brown decomposition mixtures. In the ^{1}H NMR spectrum at room temperature all the hydridic protons are magnetically equivalent (on the NMR time scale), giving a triplet by coupling with the two phosphorus atoms with the same coupling constant (vide infra). In the proton-decoupled ^{31}P NMR spectra the expected AB coupling pattern was observed. For **25a**, selective hydride coupling experiments in ^{31}P NMR spectroscopy (for the signal corresponding to *P*Ph$_2$) showed an octet, confirming the presence of seven hydride ligands equivalent at room temperature (Figure 11).

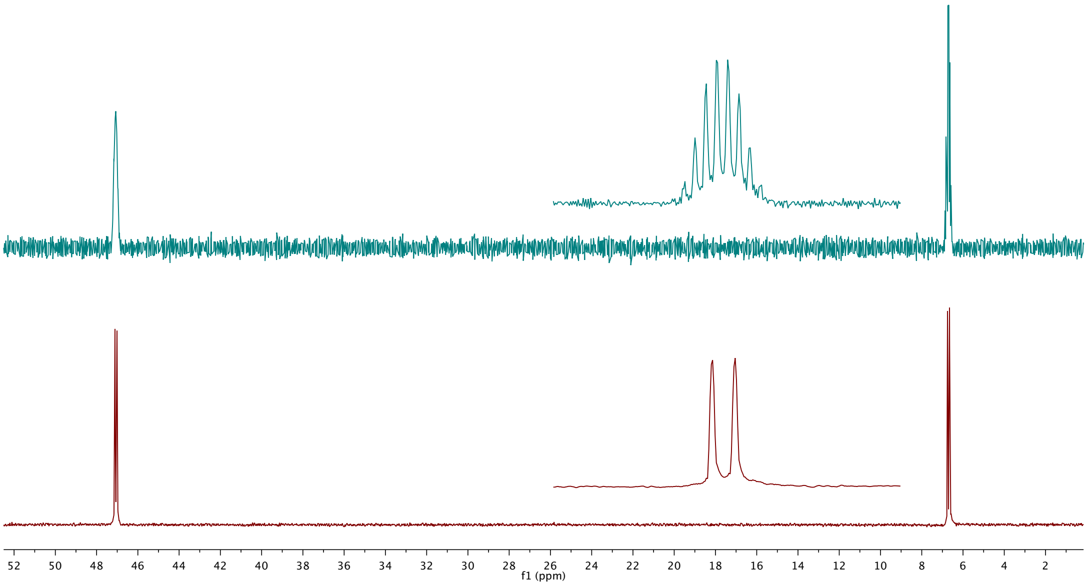

Figure 11. ^{31}P NMR spectra for complex **25a** (room temp., 283.4 MHz, Tol-D$_6$). The "Simple" H-decoupled spectrum is shown in the lower part (red) and the selectively hydride-coupled in the upper part (green).

The coordination geometry around the metal center is expected to be a tricapped trigonal prism (Figure 12) as it has been determined for the closely related [ReH$_7$(dppe)] by means of single crystal neutron diffraction experiments.[25a]

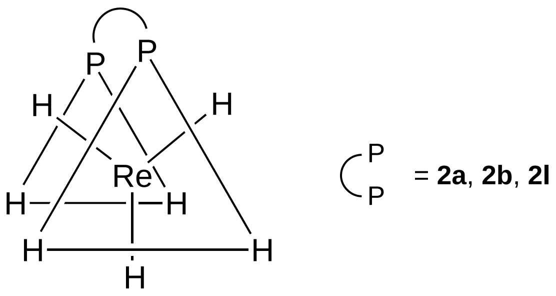

Figure 12. Assumed coordination sphere of Re in [ReH$_7$(**2**)] (**25**). The coordination geometry is a tricapped trigonal prism (TTP). The lines of the triangular faces represent the edges of the polyhedron, not chemical bonds.

In our case, the chelating phosphorus atoms in **25** are expected to occupy the eclipsed prism positions (as depicted in Figure 12) and not the equatorial positions capping two of the prism faces since, in the ideal geometry, the required P-Re-P angles are 90° and 120°, respectively.[25b] This assumption is made taking into account the bite angles reported for several different Josiphos complexes for which an average value of 92.7° is observed,[8] the highest of the series being 104.1°, reported for [CuBr(**2a**)].[34] Thus, with this precedent it appears very unlikely to expect a different coordination geometry.

Complexes of the type [ReH$_7$L$_2$] are reported to be highly fluxional (as expected for a nonacoordinated complex),[35] a fact that hampers the ^{1}H NMR T_1 analysis since it is first necessary to freeze out the fluxionality in order to measure the ratio and relaxation times for the different kinds of hydrides present in the molecule.[25b] Experimental evidence of the occurrence of all-terminal (classic) TTP structures in solution has been found for several rhenium heptahydrides containing "conformationally restrictive" chelating diphosphines like dppf, dppb and (+)-diop.[25b]

Variable temperature ^{1}H NMR experiments for complex [ReH$_7$(**2a**)] (**25a**) in toluene-D$_8$ at 700 MHz are presented in Figure 13. At 293 K the seven hydrides are magnetically equivalent, giving a triplet resonance (δ -6.11 ppm, $^2J_{PH}$ = 14.7 Hz). Upon cooling, the triplet showed no decoalescence down to 183 K, becoming only a broad, featureless singlet. Only at 173 K decoalescence starts to be noticeable. However, complete resolution of the signals could not be observed at any accessible temperature. This observation speaks not only for the high fluxionality of the complex but also for the astonishing conformational nonrigidity of the Josiphos scaffold in solution in spite of its apparent steric bulk and complexity.

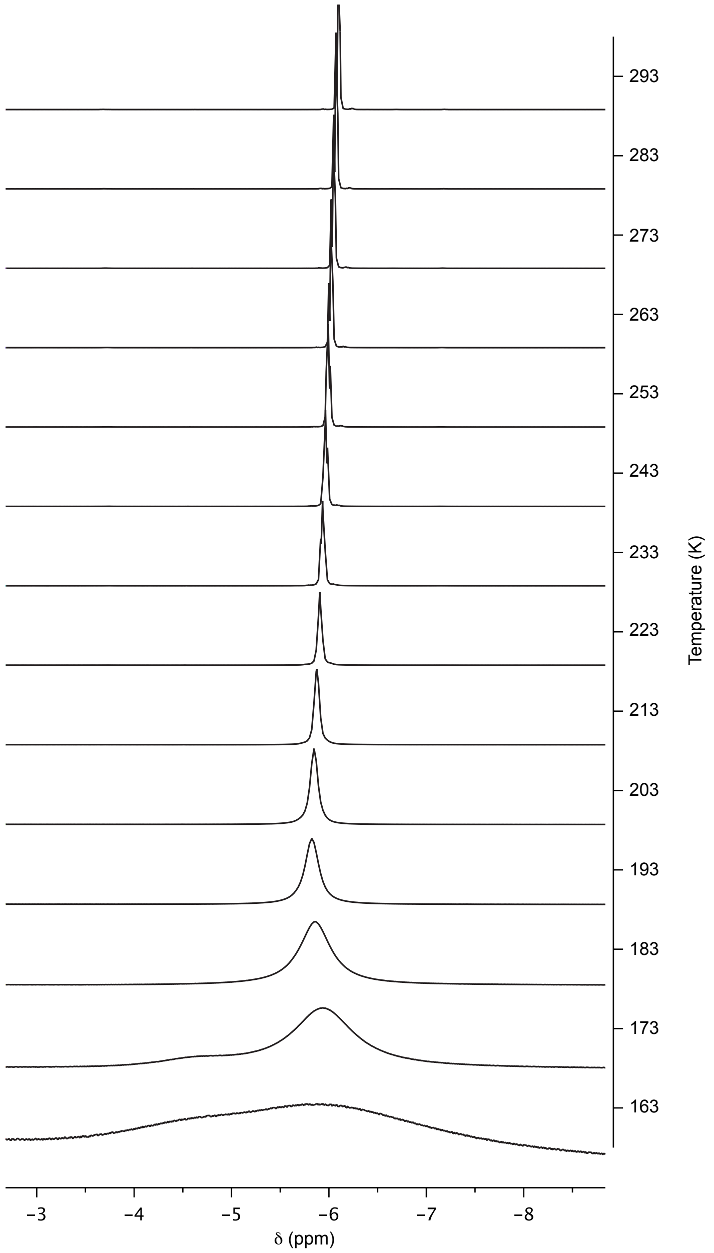

Figure 13. Variable-temperature ^{1}H NMR spectra (700 MHz, Tol-D$_8$) for complex **25a** (hydride region only).

As stated before, if clear decoalesence could not be attained, that is, if the fluxionality could not be frozen out, it is difficult to distinguish between the classical and non classical formulation by T_1 arguments. If there is, at any point, an η^2-H_2 ligand, its fast relaxation would be "diluted" by exchange with the more numerous terminal hydrides which relax much slower.[25b] As for complex **24**, variable-temperature (293-173 K) ^{1}H NMR T_1 measurements were carried out for the heptahydride **25a** in toluene-D_8 at 700 MHz. The resulting plot of ln T_1 vs 1000/T (K) for the hydridic resonance (Figure 14) has a similar shape as for **24** and an estimated T_1 (min) value of 163 ms, which is also in good agreement with the classical TTP formulation.[25b]

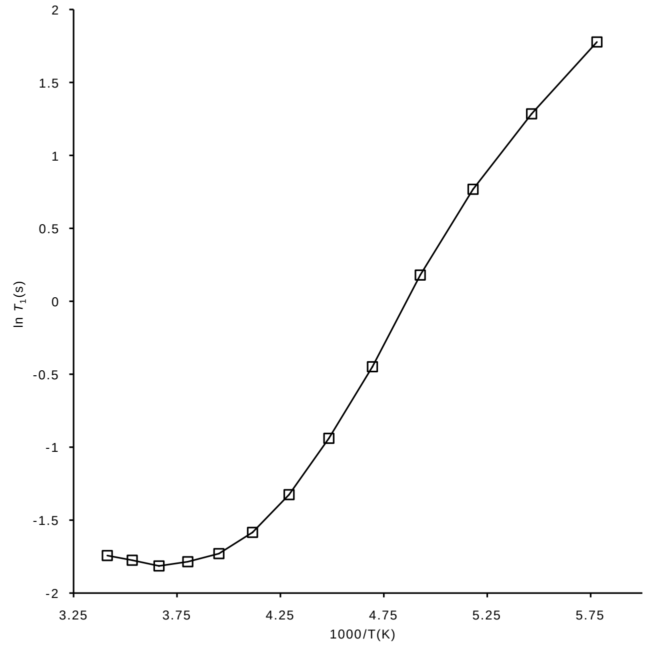

Figure 14. Plot of the temperature dependence of T_1 for complex **25a** (^{1}H NMR spectra at 700 MHz, Tol-D_8). T_1 (min) = 163 ms.

3.3. Reactions of the Rhenium Polyhydrides with Brønsted Acids and Hydride Scavengers

It has been observed that complexes of the type [ReH_5L_3] react with Brønsted acids to give [ReH_6L_3]$^+$ species, some times also described as [$Re(H_2)H_4L_3$]$^+$ (L = PPh_3,[36] PMe_2Ph,[37] $PhP(CH_2CH_2CH_2PCy_2)_2$[29a]). The stability of these complexes is dependent on the nature of the accompanying phosphine ligands: with monodentate phosphines the cationic complexes react readily with σ-donor ligands releasing molecular hydrogen[36] while with the tripodal phosphine $PhP(CH_2CH_2CH_2PCy_2)_2$ the resulting η^2-H_2 complex "exhibits a remarkable lack of reactivity" being practically inert to substitution with common $2e^-$ donor ligands.[29a] In contrast, complex **24** reacts in quantitative yield with either HBF_4•Et_2O or $H[BAr^F]$•$2.3Et_2O$ at room temperature in CD_2Cl_2 to give the corresponding cationic tetrahydride $[ReH_4($**19a**$)]^+A^-$ (**26**$[BF_4]$ and **26**[BArF]). The η^2-H_2 intermediates $[Re(H_2)H_4($**19a**$)]^+A^-$ were never observed, decomposing immediately at room temperature by releasing molecular hydrogen also visually indicated by the evolution of H_2 bubbles. This striking lability towards H_2 dissociation could be due to the enhanced π-acceptor qualities of ferrocenylphosphine ligands compared with tertiary alkyl- or arylphosphines. Since the η^2-H_2 ligand acts not only as a σ-donor but also as a π-acceptor, the increased π-acidity of Pigiphos leads to much less accessible π-electron density at the metal center to populate the σ^* orbital of H_2 through back-donation, indispensable requisite to strengthen its binding.[38] The reaction of **24** with the hydride-ion abstractor $CPh_3[BAr^F]$ gives the cationic tetrahydride $[ReH_4($**19**$)]^+(BAr^F)^-$ (**26**) as expected[36]. A comparison of the ^1H NMR spectra confirms the formation of **26** which was identified by a clear down-field shift of the hydride resonance from δ -6.67 to -4.72 ppm in all the cases. These spectra are presented in Figure 15.

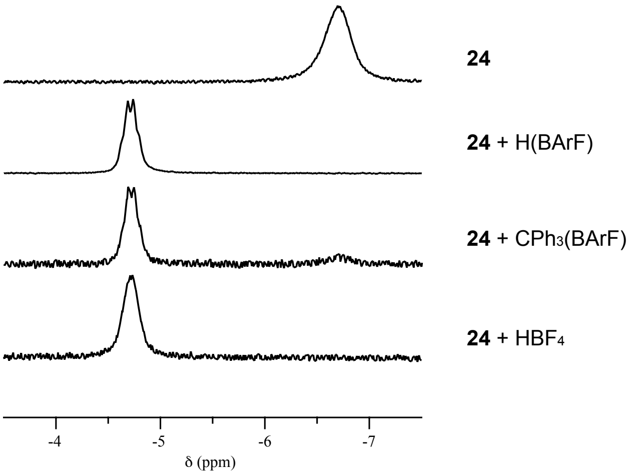

Figure 15. Comparison of ^1H NMR spectra at room temperature (250 MHz, CD_2Cl_2) for complex **24** upon reaction with different acids (hydride region only).

Rhenium(VII) heptahydrides have shown to readily undergo hydrogen exchange in the presence of water or protic solvents presumably through an associative mechanism with the intermediacy of cationic η^2-H_2 complexes of the type $[ReH_6(H_2)L_2]^+$.[39] The basic character of this kind of complexes was somehow neglected by Chatt and Coffey in their pioneering report,[35b] arguing that the absence of non-bonding *d* electrons in the Re^{VII} core would preclude the protonation and hence, the observed hydrogen exchange reactions should proceed by a dissociative mechanism. The simple protonation of a hydride ligand could not be considered since at that time the dihydrogen ligand was still unkown.[39]

As already shown and discussed for the rhenium(V) pentahydrides with Pigiphos ligands (**24**), the heptahydrides supported by ligands of the Josiphos type, such as [ReH_7(**2**)] (**25**) undergo hydride abstraction upon reaction with either Meerwein's salt $Et_3O(PF_6)$ or with the tritylium cation $Ph_3C(BAr^F)$ to give (presumably) the corresponding cationic species [ReH_6(**2**)]$^+$ (**27**). This was evidenced by ^1H NMR for complex **25a** as presented in figure 16.

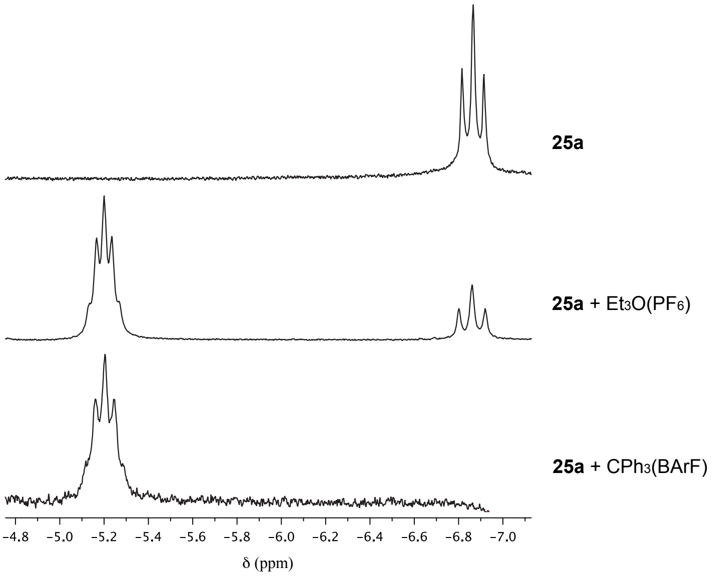

Figure 16. Comparison of ^1H NMR spectra at room temperature (300 and 250 MHz, CD_2Cl_2) for complex **25a** upon reaction with different hydride scavengers (hydride region only).

Attempts to isolate and fully characterize the cationic complexes **26** and **27** were unsuccessful due to the reactive nature of these compounds.

3.4. Catalytic Hydrogenation of Dimethyl Itaconate

3.4.1. Development of the method

After the observation that the obtained polyhydride complexes **24** and **25** could be easily deprotonated by reaction with acids to give the corresponding "activated species" **26** and **27**, and that these complexes are not prone to bind strongly with molecular hydrogen, it was envisioned that these 16e$^-$ species could catalyze the hydrogenation of olefins, and by virtue of the chirality of the ligands, the product could show enantiomeric enrichment. The prochiral substrate of choice was the rather standard dimethyl itaconate. The reaction is outlined in Scheme 8 and the obtained results presented in Table 1.

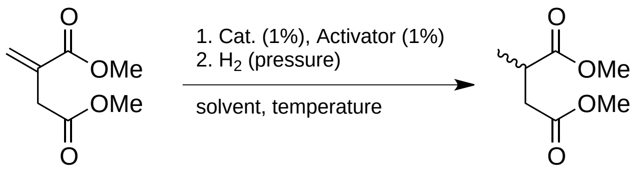

Catalyst: **24**, **25a**, **25b**
Activator: $CPh_3(BAr^F)$, HBF_4•Et_2O
$Et_3O(PF_6)$

Scheme 8

Table 1. Results for the hydrogenation of dimethyl itaconate under different reaction conditions.

Entry[a]	Catalyst	Activator	Solvent	Yield (%)[b]
1	**24**	-	DCM	0
2[c]	**24**	$CPh_3(BAr^F)$	DCM	17
3	**24**	$CPh_3(BAr^F)$	DCM	46
4	**24**	$CPh_3(BAr^F)$	THF	22
5[c][d][e]	**25a**	HBF_4•Et_2O	MeOH	Trace
6[c][e]	**25a**	HBF_4•Et_2O	MeOH	Trace
7[c]	**25a**	HBF_4•Et_2O	MeOH	7.6[f]
8[c]	**25a**	HBF_4•Et_2O	DCM	26
9[c]	**25a**	$CPh_3(BAr^F)$	DCM	27
10	**25a**	$CPh_3(BAr^F)$	DCM	26

11[c]	**25a**	$CPh_3(BAr^F)$	DMF	0
12[c]	**25a**	$Et_3O(PF_6)$	DCM	0
13	**25a**	-	DCM	0
14	**25b**	$CPh_3(BAr^F)$	DCM	21

[a] Concentration of substrate ca. 0.04M. Catalyst loads ca. 1%. Pressure of H_2 = 100 bar. Reaction overnight [b] Determined by ^1H NMR. [c] Transfer of the reaction mixture into the steel autoclave with rigorous exclusion of air and moisture. In all the other cases the transfer was made under "open flask" conditions. [d] 30 bar oh H_2. [e] Room temperature. [f] Determined by GC.

It was in fact observed that the reaction takes place in modest yields and without any enantiomeric excess. These experiments showed that the catalysis could be set up in air and that the careful exclusion of air and moisture results in lower yields when **24** was used (Table 1, entry 2). When the heptahydrides **25** were used, the presence or absence of air and moisture showed almost no effect on the catalytic performance.

3.4.2. Mechanistic considerations

As discussed before, upon hydride abstraction from **24** or **25**, a cationic, activated complex with a free coordination position is generated (**26** and **27** respectively). This open coordination site can be filled either by an H_2 molecule or by the olefin substrate. In the case of the Re^V pentahydride **24**, once the alkene is coordinated, it can insert into a Re-H bond to give an alkyl derivative which can first undergo reductive elimination to release the hydrogenation product plus a reactive Re^{III} intermediate. This would be followed by oxidative addition of H_2 to regenerate the Re^V cationic catalyst. An alternative route would be of course the prior oxidative addition of H_2 to give a Re^{VII} intermediate which could then reductively eliminate the product to regenerate the Re^V catalyst. The latter pathway seems more likely considering the reluctance of rhenium to form coordinativelly unsaturated species and the high pressure of H_2 under which the reactions are carried out. The proposed reaction mechanism with catalyst **24** is outlined in Scheme 9. An analogous pathway is expected for the hydrogenation with the Re^{VII}

heptahydrides **25**. In this case an analogous Re^{VII}-Re^{V}-Re^{VII} cycle could be operative.

The lack of enantioselectivity could be attributed either to a small or vanishing energy difference between the two diastereomeric intermediates resulting from the coordination of the olefin. The effect of coordinating solvents showed to be deleterious (i.e. THF, Table 1, entry 4, MeOH, entries 5-7 or DMF, entry 11), probably competing with the incoming olefin for the free coordination site in **26** and **27** and/or hampering the coordination of H_2.

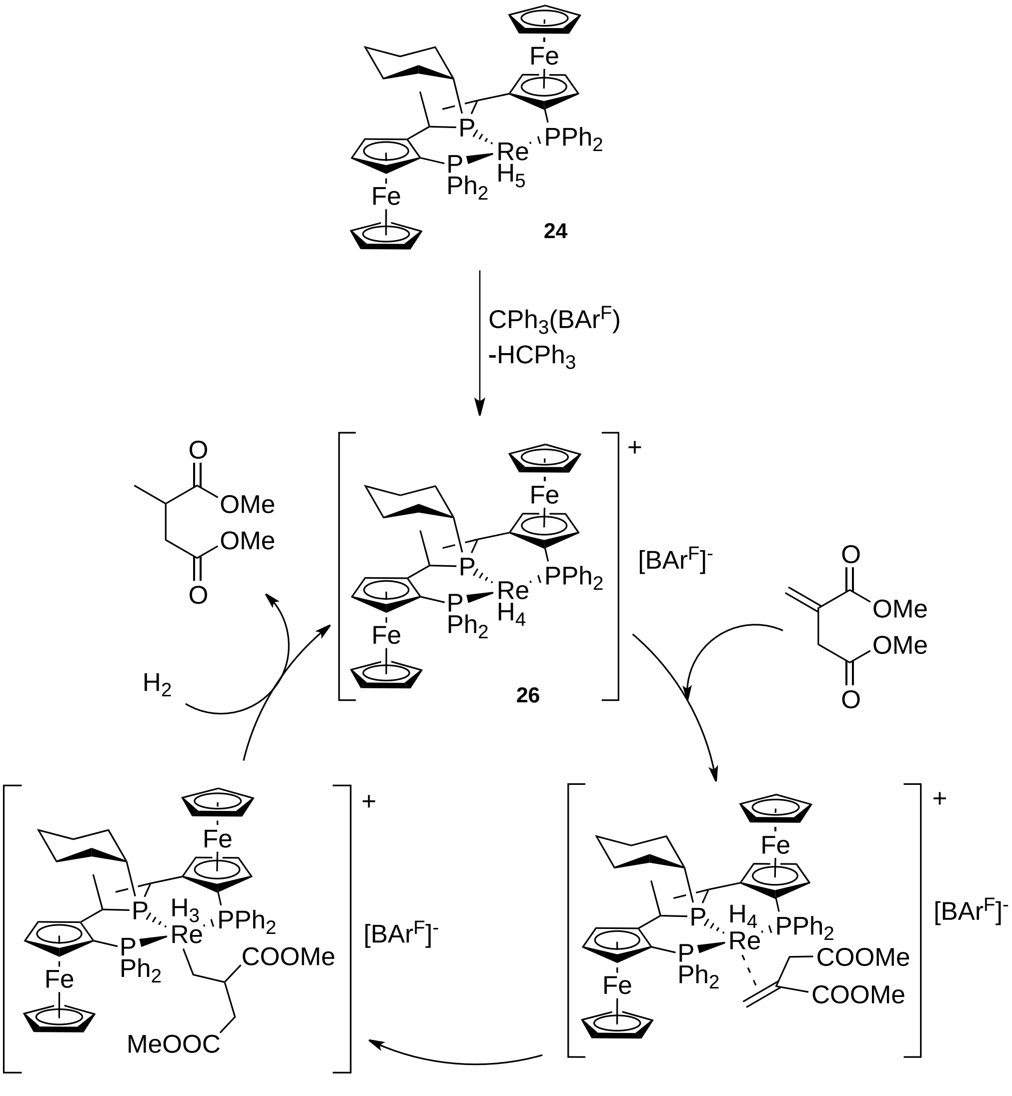
Fe
Fe
P
PPh2
Re
P
Ph2
H5
24
CPh3(BArF)
-HCPh3
26
H4
[BArF]-
+
H2
OMe
OMe
H3
COOMe
MeOOC
COOMe
COOMe

Scheme 9

3.5. Conclusion

In summary, new chiral, non-racemic rhenium complexes containing the tripodal phosphine ligand (*R*)-(*S*)-Pigiphos have been synthesized and fully characterized, namely the Re^{III}-trichloride- (**23**) and Re^{V}-pentahydrido (**24**) derivates. Both complexes showed to be markedly stable to ambient conditions, even in solution. X-Ray structural analysis of complex [$ReCl_3$(**19a**)] (**23c**) showed an almost undistorted octahedral geometry around the metal center in spite of the tridentate nature and bulkiness of the Pigiphos ligand **19**, while the pentahydride [ReH_5(**19**)] (**24**) could be better described as a triangulated dodecahedron. The latter was subjected to variable temperature ^{1}H NMR studies showing a decoalescence pattern that supports the above statement. The "classical" nature of the hydride ligands in solution was assessed by means of spin-lattice relaxation time (T_1) measurements. Upon reaction with either Brønsted acids or hydride scavengers [ReH_5(**19**)] (**24**) readily reacts at room temperature to give in all cases the same cationic tetrahydride complex, a 16e^- species which showed to be able to catalyze the hydrogenation of dimethylitaconate under high pressure but without any enantiomeric excess. These new complexes are the first of their kind containing a chiral tridentate ligand. Rhenium(VII) heptahydrides of the type [ReH_7(**2**)] (**25**) were also synthesized from the corresponding rhenium(V) oxotrichloride derivatives (**7**) and characterized by NMR techniques. For **25a** selective-coupling, variable-temperature and T_1 NMR experiments were carried out and the obtained results support the proposed TTP geometry with all the hydridic protons in a terminal (classical) situation. After hydride abstraction, complexes **25** also showed to be active in the hydrogenation of dimethylithaconate. Although still non-asymmetric, the potential applications of rhenium polyhydrides as catalyst in hydrogenation reactions were unveiled.

References

[1] Nobel-Fundation, *Nobel Lectures - Chemistry : 1901-1921*, Elsevier Publishing Company, Amsterdam, **1966**.

[2] J. F. Hartwig, *Organotransition Metal Chemistry: From Bonding to Catalysis*, First ed., University Science Books, **2010**.

[3] a) W. S. Knowles, *Angew. Chem.* **2002**, *114*, 2096-2107; b) R. Noyori, *Angew. Chem.* **2002**, *114*, 2108-2123.

[4] a) B. D. Zwick, A. M. Arif, A. T. Patton, J. A. Gladysz, *Angew. Chem. Int. Ed.* **1987**, *26*, 910; b) O. Delacroix, J. A. Gladysz, *Chem. Commun.* **2003**, 665-675; c) K. Kromm, B. D. Zwick, O. Meyer, F. Hampel, J. A. Gladysz, *Chem. Eur. J.* **2001**, *7*, 2015-2027; d) K. Kromm, F. Hampel, J. A. Gladysz, *Organometallics* **2002**, *21*, 4264-4274; e) K. Kromm, P. L. Osburn, J. A. Gladysz, *Organometallics* **2002**, *21*, 4275-4280.

[5] a) V. I. Bakhmutov, E. V. Vorontsov, D. Y. Antonov, *Inorg. Chim. Acta.* **1998**, *278*, 122-126; b) V. M. Belousov, T. A. Palchevskaya, L. V. Bogutskaya, L. A. Zyuzya, *J. Mol. Cat.* **1990**, *60*, 165-172; c) V. M. Belousov, T. A. Palchevskaya, O. M. Negomedzyanova, K. V. Kotegov1, *React. Kinet. Catal. Lett.* **1985**, *28*, 41-46; d) M. A. Ryashentseva, L. V. Borisova, *Russ. Chem. Bull. Int. Ed.* **2000**, *49*, 1732-1734; e) X.-Y. Liu, K. Venkatesan, H. W. Schmalle, H. Berke, *Organometallics* **2004**, *23*, 3153-3163.

[6] a) A. Choualeb, E. Maccaroni, O. Blacque, H. W. Schmalle, H. Berke, *Organometallics* **2008**, *27*, 3474-3481; b) B. Dudle, K. Rajesh, O. Blacque, H. Berke, *J. Am. Chem. Soc.* **2011**, *133*, 8168-8178; c) Y. Jiang, J. Hess, T. Fox, H. Berke, *J. Am. Chem. Soc.* **2010**, *132*, 18233-18247.

[7] W. D. Klobucar, C. H. Kolich, T. Manimaran*, Vol. 5187136*, Ethyl Corporation, Richmond, Va., United States, **1993**.

[8] H.-U. Blaser, B. Pugin, F. Spindler, E. Mejía, A. Togni, in *Privileged Chiral Ligands and Catalysts*, 1 ed. (Ed.: Q.-L. Zhou), Wiley-VCH, Weinheim, **2011**, pp. 93-136.

[9] P. Barbaro, A. Togni, *Organometallics* **1995**, *14*, 3570-3573.

[10] P. Barbaro, C. Bianchini, A. Togni, *Organometallics* **1997**, *16*, 3004-3014.

[11] a) L. Fadini, A. Togni, *Chem. Commun.* **2003**, 30-31; b) L. Fadini, A. Togni, *Chimia* **2004**, *58*, 208-211; c) L. Fadini, A. Togni, *Helv. Chim. Acta* **2007**, *90*, 411-424.

[12] a) A. D. Sadow, I. Haller, L. Fadini, A. Togni, *J. Am. Chem. Soc.* **2004**, *126*, 14704-14705; b) A. D. Sadow, A. Togni, *J. Am. Chem. Soc.* **2005**, *127*, 17012-17024; c) P. Butti, R. Rochat, A. D. Sadow, A. Togni, *Angew. Chem. Int. Ed.* **2008**, *47*, 4878-4881.

[13] I. Walz, A. Togni, *Chem. Commun.* **2008**, 4315-4317.

[14] L. Fadini, A. Togni, *Tetrahedron Asymmetry* **2008**, *19*, 2555-2562.

[15] a) C. Bianchini, A. Marchi, L. Marvelli, M. Peruzzini, A. Romerosa, R. Rossi, *Organometallics* **1996**, *15*, 3804-3816; b) C. Bianchini, A. Marchi, L. Marvelli, M.

Peruzzini, A. Romerosa, R. Rossi, A. Vacca, *Organometallics* **1995**, *14*, 3203-3215; c) E. S. Shubina, N. V. Belkova, E. V. Bakhmutova, E. V. Vorontsov, V. I. Bakhmutov, A. V. Ionidis, C. Bianchini, L. Marvelli, M. Peruzzini, L. M. Epstein, *Inorg. Chim. Acta.* **1998**, *280*, 302-307.

[16] A. M. Bond, R. Colton, A. van den Bergen, J. N. Walter, *Inorg. Chem.* **2000**, *39*, 4696-4703.

[17] A. M. Bond, R. Colton, R. W. Gable, M. F. Mackay, J. N. Walter, *Inorg. Chem.* **1997**, *36*, 1181-1193.

[18] P. Bergamini, F. F. DeBiani, L. Marvelli, N. Mascellani, M. Peruzzini, R. Rossi, P. Zanello, *New J. Chem.* **1999**, 207-217.

[19] C. Bianchini, M. Peruzzini, F. Zanobini, *J. Organomet. Chem.* **1993**, *451*, 97-106.

[20] a) K. A. Conner, R. A. Walton, in *Comprehensive Coordination Chemistry, Vol. 4* (Eds.: G. Wilkinson, R. Gillard, J. A. McCleverty), Pergamon, **1987**, pp. 125-203; b) J. E. Fergusson, *Coord. Chem. Rev.* **1966**, *1*, 459-530.

[21] F. A. Cotton, R. L. Luck, *Inorg. Chem.* **1989**, *28*, 2181-2186.

[22] C. A. Mitsopoulou, N. Mahieu, M. Motevalli, E. W. Randall, *J. Chem. Soc. Dalton Trans.* **1996**, 4563-4566.

[23] B. Gschwend, B. Pugin, A. Bertogg, A. Pfaltz, *Chem. Eur. J.* **2009**, *15*, 12993-13007.

[24] a) Y. Kim, J. C. Gallucci, A. Wojcicki, *Organometallics* **1992**, *11*, 1963-1967; b) Y. Kim, H. Deng, J. C. Gallucci, A. Wojcicki, *Inorg. Chem.* **1996**, *35*, 7166-7173; c) S. Bolaño, L. Gonsalvi, P. Barbaro, A. Albinati, S. Rizzato, E. Gutsul, N. Belkova, L. Epstein, E. Shubina, M. Peruzzini, *J. Organomet. Chem.* **2006**, *691*, 629-637.

[25] a) J. A. K. Howard, S. A. Mason, O. Johnson, I. C. Diamond, S. Crennell, P. A. Keller, J. L. Spencer, *J. Chem. Soc., Chem. Commun.* **1988**, 1502-1503; b) X.-L. Luo, R. H. Crabtree, *J. Am. Chem. Soc.* **1990**, *112*, 4813-4821; c) S. Bolaño, J. Bravo, S. García-Fontán, *Inorg. Chim. Acta.* **2001**, *315*, 81-87.

[26] M. T. Costello, P. E. Fanwick, M. A. Green, R. A. Walton, *Inorg. Chem.* **1992**, *31*, 2359-2365.

[27] L. Hintermann, M. Perseghini, P. Barbaro, A. Togni, *Eur. J. Inorg. Chem.* **2003**, 601-609.

[28] T. J. Emge, T. F. Koetzle, J. W. Bruno, K. G. Caulton, *Inorg. Chem.* **1984**, *23*, 4012-4017.

[29] a) Y. Kim, H. Deng, D. W. Meek, A. Wojcicki, *J. Am. Chem. Soc.* **1990**, *112*, 2798-2800; b) P. J. Desrosiers, L. Cai, Z. Lin, R. Richards, J. Halpern, *J. Am. Chem. Soc.* **1991**, *113*, 4173-4184.

[30] C. Ammann, F. Isaia, P. S. Pregosin, *Magn. Reson. Chem.* **1988**, *26*, 236-238.

[31] R. G. Teller, W. E. Carroll, R. Bau, *Inorg. Chim. Acta.* **1984**, *87*, 121-127.

[32] S. J. Lippard, in *Progress in Inorganic Chemistry, Vol. 8* (Ed.: F. A. Cotton), John Wiley & Sons, **1967**, pp. 109-193.

[33] J. L. Hoard, J. V. Silverton, *Inorg. Chem.* **1963**, *2*, 235-242.

[34] S. R. Harutyunyan, F. Lopez, W. R. Browne, A. Correa, D. Pena, R. Badorrey, A. Meetsma, A. J. Minnaard, B. L. Feringa, *J. Am. Chem. Soc.* **2006**, *128*, 9103-9118.

[35] a) J. P. Jesson, in *Transition Metal Hydrides* (Ed.: E. L. Muetterties), Marcel Dekker Inc., New York, **1971**, p. 75; b) J. Chatt, R. S. Coffey, *J. Chem. Soc. (A)* **1969**, 1963-1972.

[36] G. A. Moehring, R. A. Walton, *J. Chem. Soc. Dalton Trans.* **1987**, 715-720.

[37] P. G. Douglas, B. L. Shaw, E. R. Wonchoba, G. W. Parshall, in *Inorg. Synth., Vol. 17* (Ed.: G. M. Alan), McGraw-Hill, **1977**, pp. 64-66.

[38] D. M. Heinekey, C. E. Radzewich, M. H. Voges, B. M. Schomber, *J. Am. Chem. Soc.* **1997**, *119*, 4172-4181.

[39] J. A. Wazio, V. Jimenez, S. Soparawalla, S. John, G. A. Moehring, *Inorg. Chim. Acta.* **2009**, *362*, 159-165.

4. Aromatic Trifluoromethylation

4.1. Introduction

4.1.1. Trifluoromethylation

In recent years organofluorine compounds have played a major role not only on the pharmaceutical industry, with hundreds of F-containing drugs on the market,[1] but also in the agrochemical industry and in materials science. Among the plethora of fluorinated organic compounds available, those containing a perfluoroalkyl group deserve special attention due to their high stability, electronegativity and remarkable solubility properties.[2] Nevertheless, amenable methods for the introduction of fluorine into organic compounds are still scarce and are the subject of current research. Among these, direct trifluoromethylation, either radical, nucleophilic or electrophilic is one of the most powerful and straightforward methodologies.[3]

Introduction of the CF_3 moiety into aromatic or heteroaromatic compounds is not a trivial task. It has been typically carried out by radical trifluoromethylation using, for example, $(CF_3)_2E$ (E=Te, Hg),[4] Umemoto's *N*-trifluoromethyl-*N*-nitrosotrifluoromethanesulfonamide (TNS-Tf),[5] bis-(trifluoroacetyl)peroxide,[6] trifluoroacetic acid in the presence of XeF_2,[7] or more recently CF_3I in the presence of Fe(II) compounds,[8] albeit in moderate yields. An overview of the "state of the art" of direct aromatic trifluoromethylation is given in Scheme 1.

One way to achieve aromatic trifluoromethylation is the copper-mediated substitution of functionalized aromatic substrates (i.e. iodides[9] or boronic acids[10]), which require stoichiometric amounts of metal, or the more elegant palladium-catalyzed version which gives excellent results with less than 0.1 equivalents of catalyst.[11] The main drawback in the cases mentioned above is that the corresponding functionalized precursor is required. Thus, a simple method for the direct trifluoromethylation of non-functionalized arenes (and heteroarenes) under mild conditions is desirable.

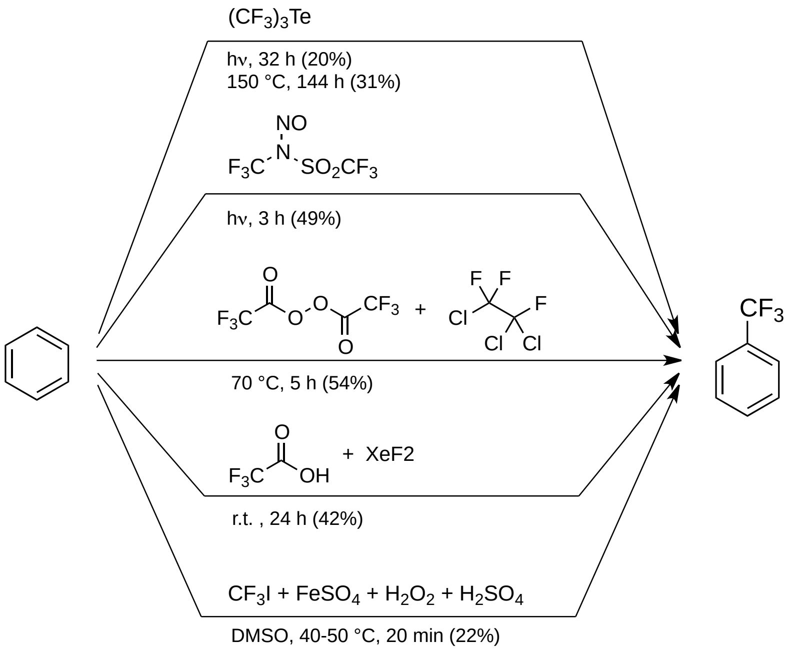
(CF3)3Te
hν, 32 h (20%)
150 °C, 144 h (31%)
NO
N
F3C
SO2CF3
hν, 3 h (49%)
O
F3C
O
O
CF3
O
+
F F
Cl
F
Cl Cl
70 °C, 5 h (54%)
O
F3C
OH
+ XeF2
r.t. , 24 h (42%)
CF3I + FeSO4 + H2O2 + H2SO4
DMSO, 40-50 °C, 20 min (22%)
CF3

Scheme 1

In 2006, Togni developed a new class of electrophilic trifluoromethylating reagents based on hypervalent iodine, including 1-(trifluoromethyl)-1,2-benziodoxol-3(1*H*)-one (**28**) and trifluoromethyl-1,3-dihydro-3,3-dimethyl-1,2-benziodoxole (**29**)[12] both easily accessible in high yields from *o*-iodobenzoic acid.[13] The key step of both procedures is the umpolung of the CF_3^- group introduced via ligand displacement at the hypervalent iodine atom using the commercially available CF_3TMS (Ruppert-Prakash reagent) yielding a formal CF_3^+ source.

Reagents **28** and **29** have been used successfully in our laboratories for the direct electrophilic trifluoromethylation of β-keto esters,[12a] sulphur centred nucleophiles,[14] α-nitro carbonyls,[14] phosphines,[15] phenolates,[16] alcohols[17] and for the Ritter-type N-trifluoromethylation of nitriles[18] (Scheme 2). Recently, MacMillan and co-workers reported the use of reagent **29** for the enantioselective α-trifluoromethylation of aldehydes.[19]

Also recently, Togni reported the electrophilic trifluoromethylation of N-heteroarenes and activated arenes under mild conditions. These transformation commonly require the use of substoichiometric amounts of tris(trimethylsilyl)silyl chloride or a zinc salt as additives.[20] The reaction was further explored by Sodeoka and co-workers who reported the trifluoromethylation of indole derivatives catalyzed by CuOAc.[21]

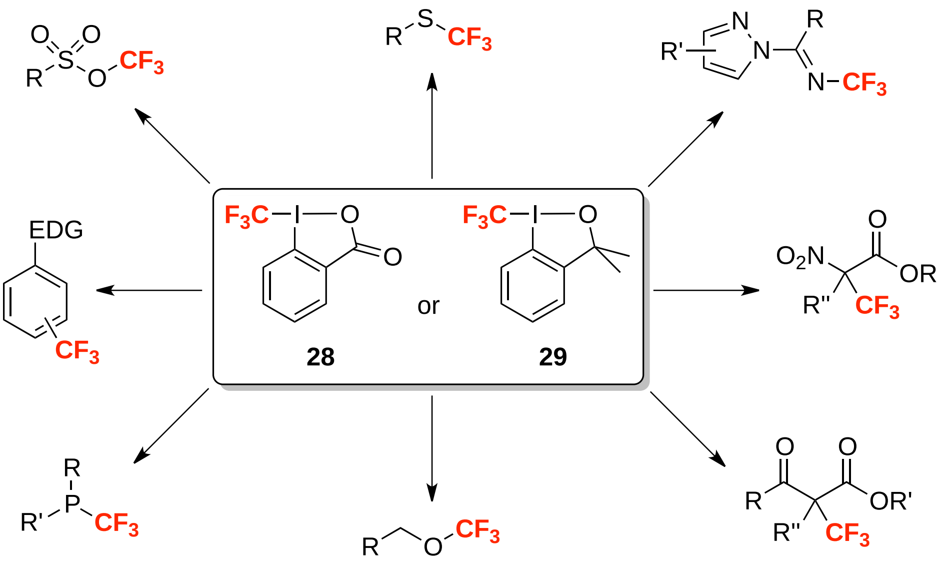
F3C–I–O
O
or
F3C–I–O
28
29
R–S(O2)–O–CF3
R–S–CF3
R'
N
N
R
N–CF3
EDG
CF3
O2N
O
OR
R''
CF3
R
R'–P–CF3
R
O
CF3
O
O
R
OR'
R''
CF3

Scheme 2

Using the commercially available reagent **29**, Liu and Shen reported the successful copper-catalyzed electrophilic substitution of aryl boronic acids in the presence of a base and a chelating bidentate nitrogen-based ligand (Scheme 3).

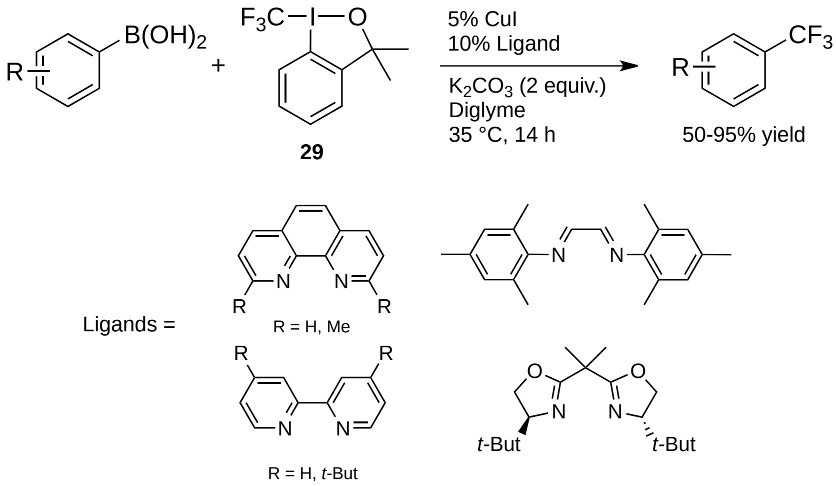
R
B(OH)2
+
F3C–I–O
29
5% CuI
10% Ligand
K2CO3 (2 equiv.)
Diglyme
35 °C, 14 h
R
CF3
50-95% yield
Ligands =
N
N
R
R
R = H, Me
N
N
R
R
N
N
R = H, t-But
O
N
O
N
t-But
t-But

Scheme 3

4.1.2. Methyltrioxorhenium (MTO)

Methyltrioxorhenium, or MTO (**30**), is arguably the most important organo-rhenium compound. It has by far the widest range of applications in catalysis of all known rhenium complexes. It was briefly introduced in Section 1.2.9.

MTO is the first and the simplest of a large family of derivatives of the [ReO_3] core including a wide variety of alkyl, aryl and alkenyl substituents.[22] It was first observed serendipitously in 1979 by Beattie and Jones in the air oxidation products of residues from the synthesis of Me_3ReO_2.[23] In this seminal report the authors already pointed out the remarkable stability of the new compound to air and moisture. The synthesis developed at that time required several weeks and the yields were modest.[23]

In 1988, Herrmann reported the improved synthesis of MTO based on the methylation of dirheniumheptoxide with tetramethyltin. For the synthesis of other alkyl and aryl derivatives, organozinc reagents were (and still are) preferred.[24] This reactions are very straightforward, giving almost quantitative yields, as high as 50% relative to the quantity of rhenium added. The other half ends as unreactive tin or zinc complexes (Scheme 4). Another drawback is that the common precursor, Re_2O_7, is extremely sensitive to moisture.[25]

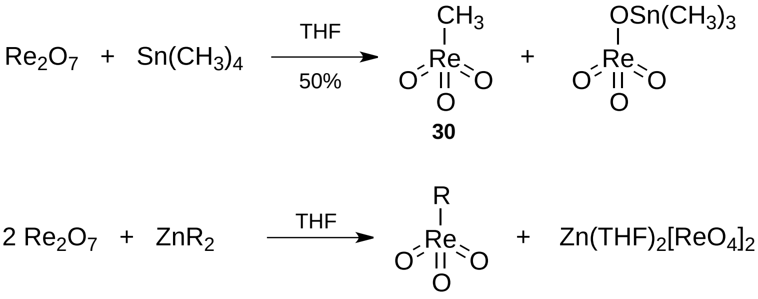

Scheme 4

The method for the synthesis of alkyltrioxorhenium derivatives was further improved by Herrmann using the more accessible perrhenates M[ReO_4] (M = Ag, K, Na, Zn, Ca, NH_4) as starting materials (Scheme 5).

These one-pot reactions do not require the careful exclusion of air and moisture and make use of all the added rhenium, thus giving higher yields.[26]

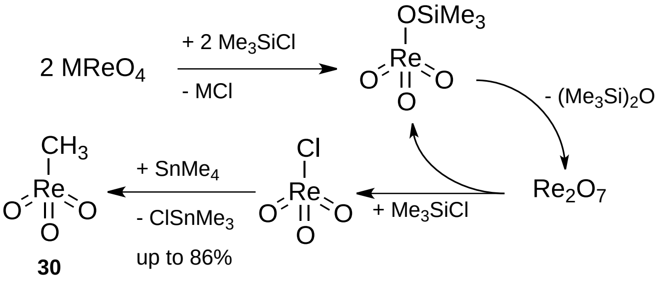

Scheme 5

The MTO molecule has a pseudotetrahedral geometry with a Re-C bond slightly shorter than a single bond (2.063 Å) but still longer than a double bond.[22b] It has formally a 14-electron metal core and hence, displays a pronounced Lewis acidity, readily forming adducts with halide ions and a considerable number of nitrogen and oxygen donors. Pyridine and amine adducts account for the majority of examples.[22] Organyltrioxorhenium compounds easily form trigonal bipiramidal adducts with monodentate ligands and octahedral complexes with bidentate donors (Scheme 6). These adducts are sensitive to moisture and are thermally unstable.[22b]

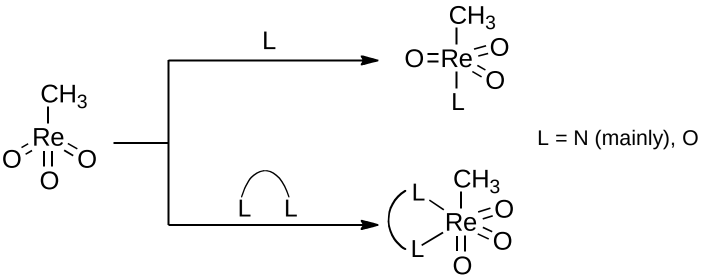

Scheme 6

Its high catalytical activity, ease of handling and the deep understanding of its reactivity and coordination properties, make MTO (**30**) perhaps the most versatile and widely used rhenium catalyst. Some of the multiple applications of MTO as catalyst in C-C bond forming reactions and in oxidations are presented in Section 1.3.

4.2. Rhenium-Catalyzed Aromatic Trifluoromethylation

4.2.1. Reaction discovery and development: a case of serendipity

In an attempt to synthesize a trifluoromethylated derivate of methyltrioxorhenium (MTO, **30**)[26] using reagent **29** in benzene-D_6, we observed the formation of deuterated benzotrifluoride (**31**) as the main trifluorometylated product (Scheme 7).

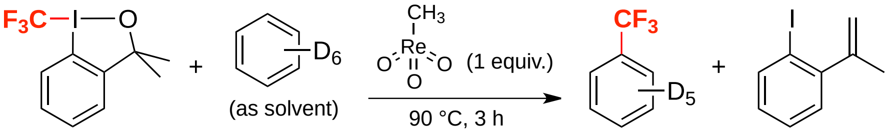

29 **31**

Scheme 7

Further experiments showed that reagent **28** effected this transformation even faster and in higher yields of **31**. Therefore, we chose it along with benzene-D_6 as substrate to optimize the reaction conditions (Scheme 8, Table 1). It is important to note that the reaction with either reagent **28** or **29** does not proceed in the absence of the rhenium catalyst, showing only in some cases trace amounts of product. The reactions were conducted overnight in order to guarantee full conversion although they were normally complete after circa two hours, as indicated by the darkening of the reaction mixture. The main side product of the reaction is the trifluoromethyl ester of *o*-iodobenzoic (**32**) which is the decomposition product of **28** in presence of either Lewis or Brønsted acids, as reported previously.[27]

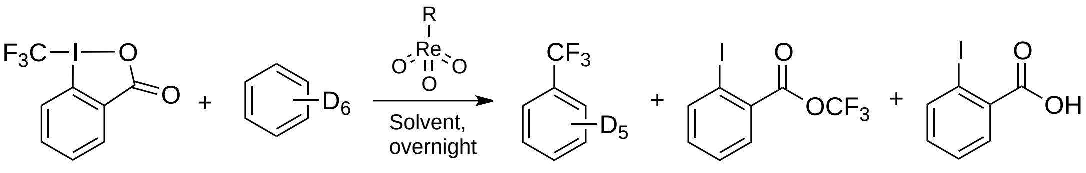

28 **31** **32**

Scheme 8

In most cases CF_3I, CF_3H and CF_3D were obtained as main by-products but the exact amounts were not determined due to their volatility. It was observed that better results were achieved when a slight excess of substrate was used. The optimal catalyst loading was between 5 and 10 mol-%. The solvent of choice was chloroform in which decomposition of **28** to **32** was minimized to less than 1% (Table 1, entry 7).

Another rhenium complex, namely mesityltrioxorhenium (**33**) was synthesized following the "zinc route" (Scheme 9).[28] This compound has a higher Lewis acidity than MTO and is thermally stable (it is the only aryltrioxorhenium compound stable at room temperature without additional ligands). Complex **33** was tested as catalyst in the aromatic trifluoromethylation of benzene where it also showed to be active although less than MTO (Table 1, entry 10).

Table 1. Screening of the reaction conditions for the trifluoromethylation of benzene-D_6 with reagent **28** (Scheme 6).

Entry[a]	Solv.	T (°C)	C_6D_6 (eq.)	**28** (eq.)	Cat. (eq.)	**3**[b] (%)	**31**:**32**[b]
1	CD_2Cl_2	70	1	1	0.08	41	14:1
2	CD_2Cl_2	70	1.5	1	0.09	53	18:1
3	CD_2Cl_2	70	3	1	0.08	54	11:1
4	CD_2Cl_2	70	1	1.5	0.09	48	7:1
5	CD_2Cl_2	40	1.5	1	0.08	trace	-
6	CD_2Cl_2	70	1.5	1	0.24	47	16:1
7	$CDCl_3$	70	1.5	1	0.08	54	108:1
8	$CDCl_3$	70	1.5	1	0.02	51	17:1
9	$CDCl_3$	70	1.5	1	0.01	31	4:1
10[c]	$CDCl_3$	70	1.5	1	0.07	44	11:1

[a] Reaction conditions: Limiting reagent (1 eq.) ca. 0.1 M in a closed Young-type NMR tube; R = Methyl (**30**). [b] Calculated by ^{19}F NMR using perfluoronaphthalene as internal standard. [c] R = Mesity (**33**).

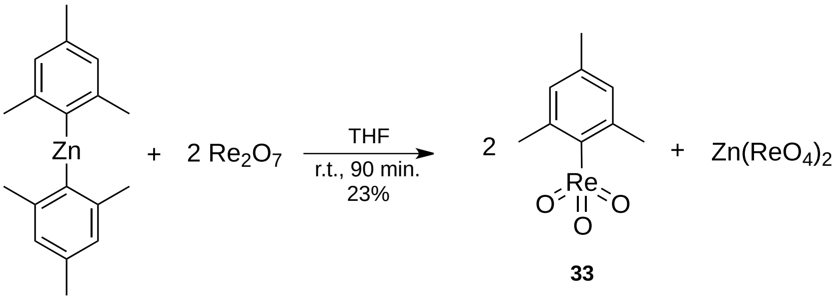

Scheme 9

4.2.2. Substrate screening and reaction scope

Once the best reaction conditions were established (Table 1, entry 7), the trifluoromethylation of several arenes bearing different functional groups was examined (Table 2). The reaction proceeded in all cases, giving higher yields when electron-donor groups were attached to the aromatic rings. The best results were obtained for anisol derivatives (Table 2, entries 4 to 7). Contrary to what has been reported previously,[20] the electrophilic trifluoromethylation of non-activated or electron-poor aromatic systems was possible, though in moderate yields (Table 2, entries 10 to 15). Under the reaction conditions mentioned above, the first direct trifluoromethylation of ferrocene was carried out (Table 2, entry 16). It is also worth mentioning that traces of bistrifluoromethylated products were observed by GC-MS analysis for several substrates (see the experimental part).

Table 2. Trifluoromethylation of arenes with reagent **28** and MTO (**30**) as catalyst.

Entry[a]	Substrate	Total yield (%)[b]	Isomer ratio[b]		
			o-	*m-*	*p-*
1	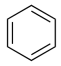	54	-	-	-
2	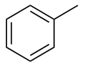	58	1.3	1	2.4
3	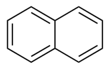	58	5.4(α)	1(β)	-
4	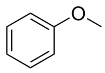	62	2.6	1	1.3

5	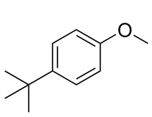	63	1	n.d.	-
6	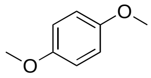	70	-	-	-
7	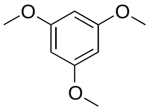	77	-	-	-
8	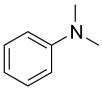	49	5.5	1	9.1
9	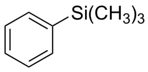	45	n.d.	n.d	n.d
10	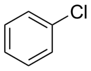	42	1.6	1	1.1
11	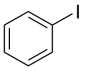	41	1.3	1	1
12	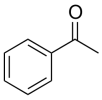	32	1.3	1	1.9
13	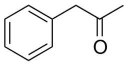	31	1	1	1
14	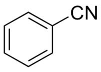	~15	1	n.d.	1
15	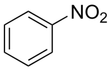	13	1	3.5	10
16	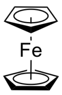	33	-	-	-

[a] Reaction conditions: Reagent **28** (1 eq.) ca. 0.1 M in $CDCl_3$ in a closed Young-type NMR tube; 1.5 eq. of substrate; 70 °C, overnight; MTO (5-8%) used as catalyst; n.d. = not determined. [b] Calculated by ^{19}F NMR using perfluoronaphthalene as internal standard.

The scope of the reaction was further extended to O-, S-, and N-heteroaromatic substrates (Table 3). The highly electron-rich 1-benzofuran and 1-benzothiophene showed moderate yields probably due to strong coordination of the substrate to the catalyst. Better results were obtained for 1H-indole and its derivates (Table 3, entries 3-5) and in the case of 3-methylindole the regioselective trifluoromethylation at the more electron-rich 2- position yielded 75%. Also pyridines were successfully trifluoromethylated under these conditions, albeit with modest yields when electron-withdrawing or bulky substituents were present (Table 3, entries 6-18). The introduction of methoxy groups showed two competing effects: electron-enrichment that, as seen before, favours the electrophilic triflouromethylation, and an increase of the basicity of the substrate[29] which could lead to decomposition of the catalyst (Table 3, entries 15-18).

Table 3. Trifluoromethylation of heteroarenes with reagent **28** and MTO (**30**) as catalyst.

Entry[a]	Substrate	Total yield (%)[b]	Isomer ratio[b]		
			2-	*3-*	*7-* or *4-*
1[c]	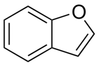	43	2.4	1	-
2	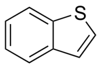	45	1.1	1	1
3	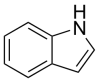	59	3.4	1	1.5
4[d]	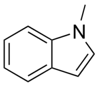	64	2.8	1.2	1
5	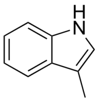	75	1	-	n.d.
6	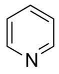	38	4.3	3.0	1
7	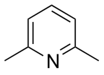	~25	-	n.d.	1
8[d]	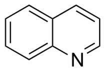	50	n.d.	n.d.	n.d.
9[e]	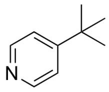	20	1	n.d.	-

10[d]	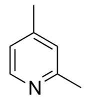	36	1(6-)	1.5(5-)	2.8(3-)
11[f]	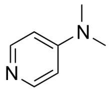	24	1	n.d.	-
12	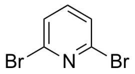	11	-	n.d.	1
13	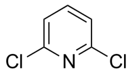	14	-	n.d.	1
14[g]	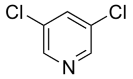	18	1	-	n.d.
15	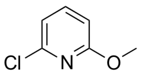	48	-	1	3.3(5-)
16	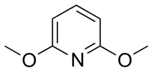	60	-	13	1
17	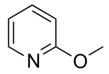	33	1(6-)	1.6(5-)	7(3-)
18	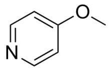	Trace	n.d.	n.d.	-

[a] Reaction conditions: Reagent **28** (1 eq.) ca. 0.1 M in $CDCl_3$ in a closed Young-type NMR tube; 1.5 eq. of substrate; 70 °C, overnight; MTO (5-8%) used as catalyst; n.d. = not determined. [b] Calculated by ^{19}F NMR using perfluoronaphthalene as internal standard. [c] 23% of CF_3H formed. [d] 36-39 hours. [e] ca. 300 hours. [f] 95 hours. [g] 24 hours.

4.3. Mechanistic Studies

4.3.1. ^{17}O NMR

Extensive ^{17}O NMR studies on alkyl and aryl [$RReO_3$] derivatives and their Lewis base adducts have been performed by Herrmann and his group.[30] It has been observed that chemical shifts have a strong solvent and added base dependence. The observed effects correlate with the Lewis basicity (Gutmann donor number) of the solvent and added bases, so stronger donors shift the resonances to lower fields.[31] This results could be considered as counterintuitive taking into account that an electron enrichment of the metal core should shield the oxo ligands and hence, a high-field shift is expected. In this case, the effect responsible for the ^{17}O NMR low-field shift is the structural change of the tetrahedral complex upon coordination of a fifth ligand to give the corresponding trigonal bipyramidal adduct (see Scheme 6). The magnitude of the shift correlates then directly with the ability of the donor to form the adduct and with the stability of the latter.[30]

A possible first step in the reaction mechanism for the trifluoromethalation of aromatics would be the activation of the trifluoromethylating reagent **28** by coordination with the Lewis acid MTO (**30**), as depicted in Scheme 10. This kind of Lewis-pair adducts such as **34** from reagents **28** and **29** have been postulated before. Upon coordination, the polarized O-I bond should be weakened and the electrophilicity of the iodine atom enhanced, propitiating the concomitant CF_3 transfer to the substrate.[21, 27]

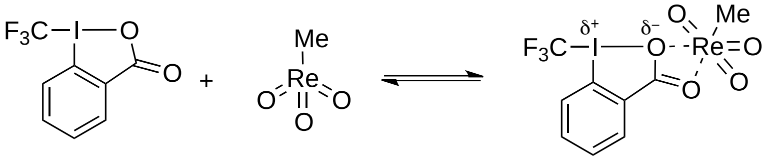

28 **30** **34**

Scheme 10

The formation of the activated intermediate **34** was monitored by ^{17}O NMR at 64.8 MHz in $CDCl_3$. Equimolar amounts of the hypervalent iodine reagent **28** and MTO (**30**) were mixed at room temperature and the spectrum recorded during ca. 60 hours (Figure 1). In the region were the MTO signal was expected, between 600 and 1000 ppm, only one resonance was observed at δ 830.56. This chemical shift corresponds almost exactly with the reported value for free MTO in the same solvent (δ 829).[30] This results does not preclude the formation of **34** but indicates that, if formed, it has a life time to short for the NMR time scale or simply that the equilibrium postulated in Scheme 10 is shifted to the left and there is not an effective concentration of the adduct in solution high enough to be observed.

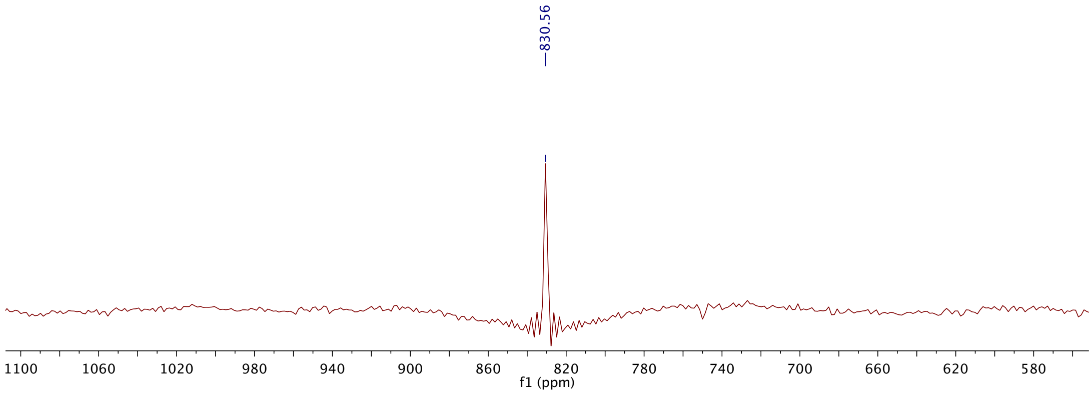

Figure 1. ^{17}O NMR (64.8 MHz, $CDCl_3$. 60 h, 2'597.945 scans, room temp.) of the equimolar mixture of reagent **28** and MTO (**30**).

4.3.2. *Time dependent ^{19}F NMR*

The trifluoromethylation of benzene-D_6 (1.5 equivalents, ca. 0.1 M) in $CDCl_3$ with 1 equivalent of reagent **28** in the presence of a catalytic amount of MTO (0.08 eq.) was monitored at 70 °C for 3 hours by ^{19}F NMR spectroscopy (Figure 2).

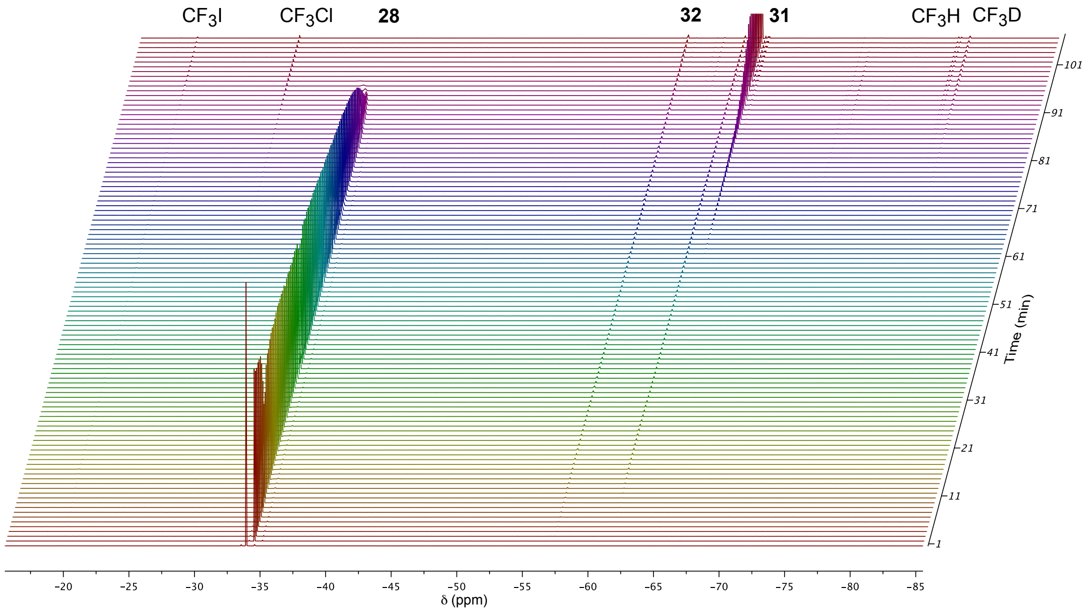

Figure 2. Time dependent ^{19}F NMR spectra for the trifluoromethylation of benzene-D_6 with **28** at 70°C (376 MHz, $CDCl_3$).

From simple observation of the time dependent spectra in Figure 2, it appears clear that the formation of the product **31** (δ -62.95), along with the consumption of the reagent **28** (δ -34.22) occurs only after a certain induction time. Also noteworthy is that the decomposition product of **28**, the trifluoromethylester **32** (δ -57.3), appears at an early stage of the reaction and its concentration remains almost constant. Interestingly, other secondary products, i. e. CF_3I (δ -4.46), CF_3Cl (δ -27.63), CF_3H (δ -78.02) and CF_3D (δ -78.78) make their appearance only near to the reaction completion. A closer look into the changes concerning the resonance of the CF_3 group in **28**, reveals a rather interesting behavior (Figure 3). In the first stage of the reaction, during the induction period (C, Figure 3), the signal is broaden and shifted, suggesting the possible formation of an adduct or intermediate of dynamic nature. Once the reaction starts, the signal is shifted back to its initial position (D, Figure 3). During the consumption of **28** its resonance undergoes a low-field shift, likely due to the increasing concentration of *o*-iodobenzoic acid product of the trifluoromethyl transfer to the aromatic substrate (Scheme 8). This is in good agreement with previous observations.[32]

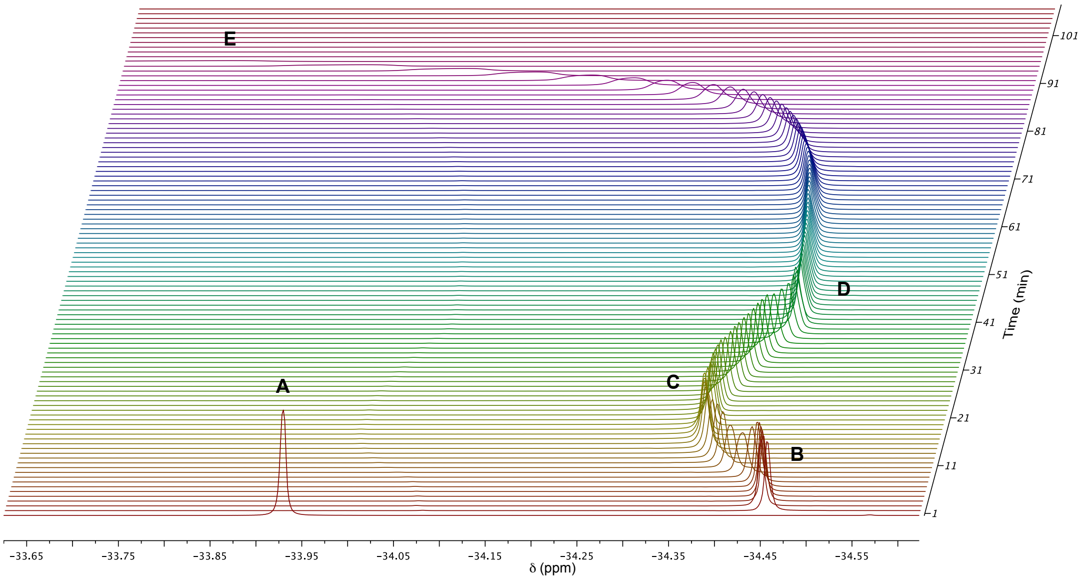

Figure 3. Time dependent ^{19}F NMR spectra for the trifluoromethylation of benzene-D_6 at 70°C (376 MHz, $CDCl_3$). Only the region between -34.5 and -33.6 ppm is presented. **A**: room temperature; **B**: 70°C; **C**: formation of an adduct or intermediate?; **D**: beginning of the reaction; **E**: end of the reaction.

The observed time vs. yield profiles show (as already discussed) a long induction period of ca. one hour where after the reaction goes to completion within 20 minutes (Figure 4). These sigmoid curves suggest a mechanism which involves autocatalysis and/or radical processes.

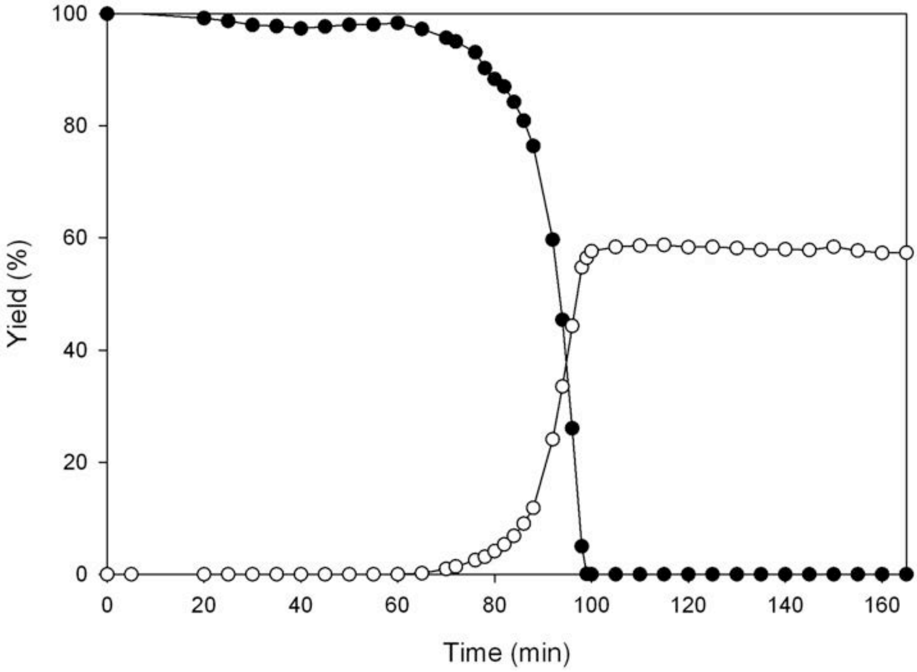

Figure 4. Reaction profile for the trifluoromethylation of benzene-D_6 as monitored by ^{19}F NMR, showing the consumption of **28** (filled circles) and the formation of benzotrifluoride (**31**) (hollow circles). Reaction conditions: reagent **28** ca. 0.1 M in $CDCl_3$; 1.5 equiv. of substrate; 0.08 equiv. of MTO; 70 °C. Perfluoronaphthalene was used as internal standard.

The same experiment, under the same conditions, was carried out with 4-*t*-butylanisole. The results showed that the trifluoromethylation of this electron-enriched arene proceed faster than for benzene, having a shorter induction time of ca. 15 min. after which, exactly as observed for benzene, the trifluoromethylating reagent **28** is consumed within ca. 20 min (Figure 5). Thus, appears clear that the influence of electronic factors is (at least apparently) more significant in the first stage of the reaction. The electron enrichment of the aromatic ring thus "facilitates" the formation of the reactive intermediate(s) needed for the trifluoromethyl transfer to take place. This conclusion, of course, needs further experimental support.

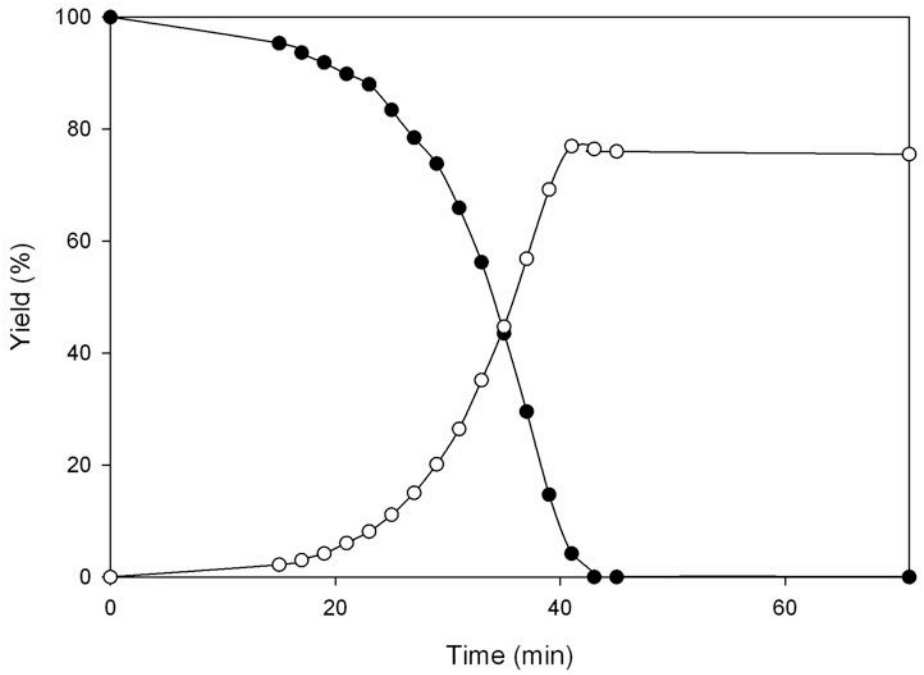

Figure 5. Reaction profile for the trifluoromethylation of 4-*t*-butylanisole as monitored by ^{19}F NMR, showing the consumption of **28** (filled circles) and the formation of 2-trifluoromethyl-4-*t*-butylanisole (hollow circles). Reaction conditions: reagent **28** ca. 0.1 M in $CDCl_3$; 1.5 equiv. of substrate; 0.08 equiv. of MTO; 70 °C. Perfluoronaphthalene was used as internal standard.

4.3.3. EPR

Careful analysis of the reaction product mixtures by NMR and CG-MS showed that in most of the cases CF_3H, CF_3D, CF_3Cl and CF_3I are formed in considerable quantities. Moreover, for certain substrates, coupling and cyclization products were detected (Scheme 11).

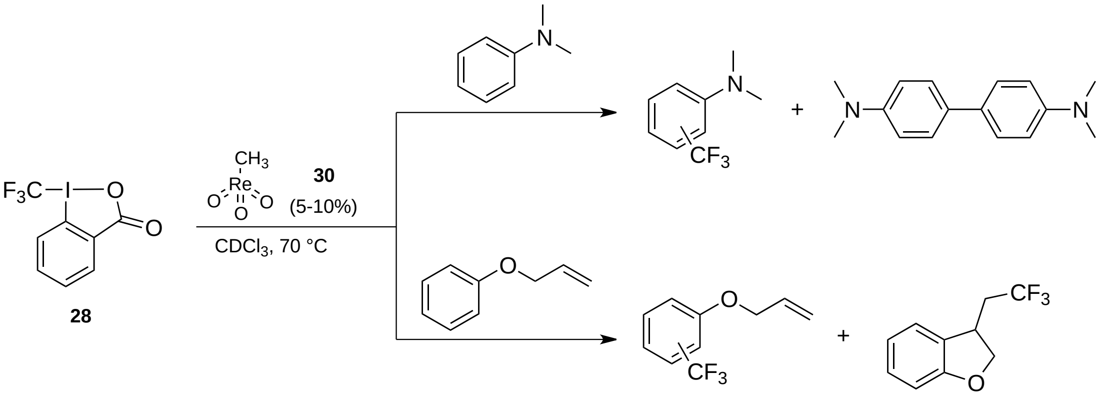

Scheme 11

The only (or the simplest) explanation to these observations is the intermediacy of radical species in the reaction mechanism. In order to check this, EPR monitoring of the reaction was made, selecting 4-*t*-butylanisol as substrate due to the enhanced stability of its radicals which would lead to better detection.[33] The time-dependent EPR spectra shows an increase of the concentration of radicals in solution followed by their consumption (Figure 6). The most intense signal (after 72 min) appears to be a broad doublet with a *g* factor of 2 and an isotropic splitting a_X of 13.5 G.

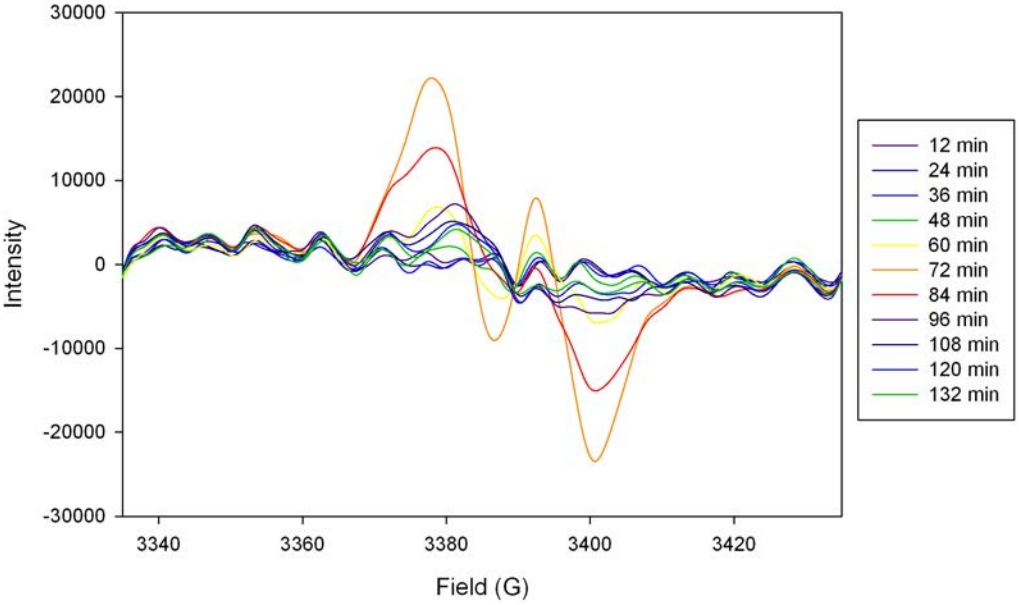

Figure 6. Time-dependent EPR spectra for the trifluoromethylation of 4-*t*-butylanisole in $CDCl_3$ at 70°C. Reaction conditions: reagent **28** 0.17M, 3.3 equiv. of substrate and 0.86 equiv. of MTO (**30**). Further details of the experimental set up are given in the experimental part.

In order to have a clearer view of the progress of the reaction, the first integral of the EPR spectra in Figure 6 was plotted as a function of time and field to obtain the tridimensional reaction profile presented in Figure 7. The reaction profile shows an induction period of ca. 1 hour after which the concentration of radical species rises suddenly and is consumed within ca. 30 minutes. It is noteworthy that the shape of the EPR signal also changes during the reaction, being at the beginning a pseudo-doublet which rapidly collapses in to a singlet, meaning that the composition of the radical mixture changes during the course of the reaction.

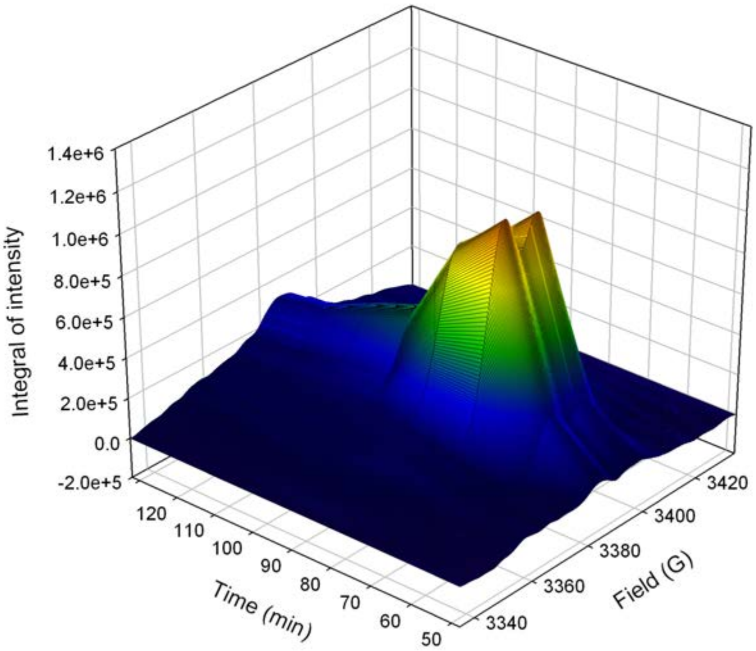

Figure 7. Reaction profile for the trifluoromethylation of 4-*t*-butylanisole in $CDCl_3$ at 70°C as monitored by EPR.

A direct comparison between the ^{19}F NMR and EPR profiles (Figure 8) gives more clues about the course of the reaction. It can be seen that, the fast accumulation of radicals in solution takes place only after consumption of the trifluoromethylating reagent **28**. This suggests that if a radical chain reaction mechanism is involved, the observed accumulation of radicals occurs in the termination step rather than in the propagation stage, when the trifluoromethylation should take place.

A high modulation EPR experiment was made for which the trifluoromethylation of 4-*t*-buthylanisole in $CDCl_3$ was run at 70°C for one hour and then the system was rapidly frozen by immersion in liquid nitrogen. The obtained EPR spectrum is presented in Figure 9. It features a hyperfine splitting with a coupling constant a_X of ca. 2 G. This values of a_X rule out the possibility that the observed radical species were inorganic (for example $I^{\bullet}$ or derivatives of MTO) or $CF_3^{\bullet}$.

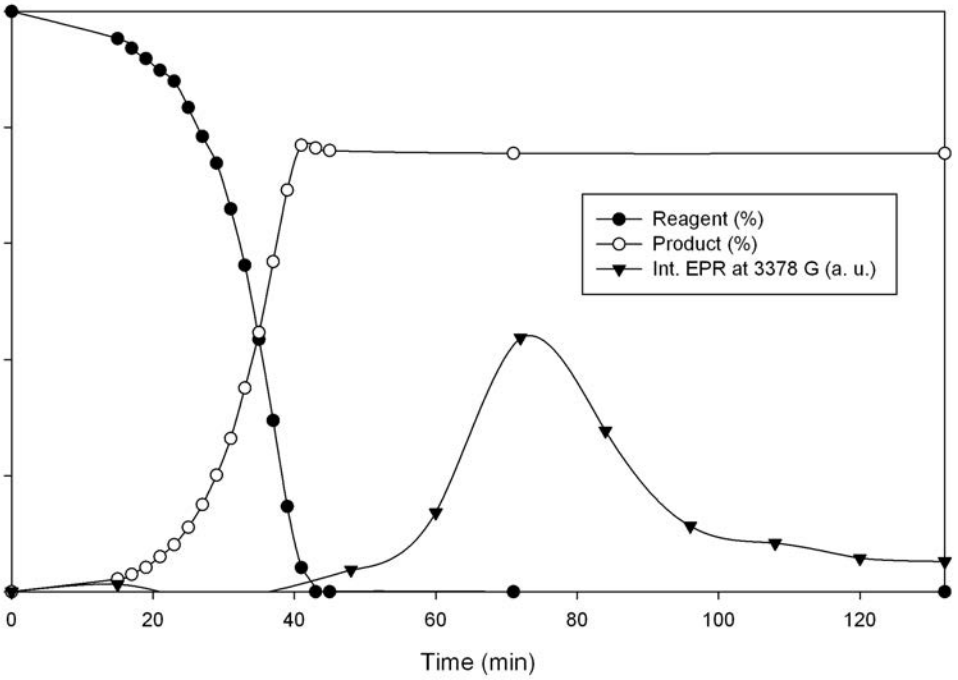

Figure 8. Superimposition of the reaction profiles for the trifluoromethylation of 4-*t*-butylanisole as monitored by ^{19}F NMR (circles) and EPR (triangles).

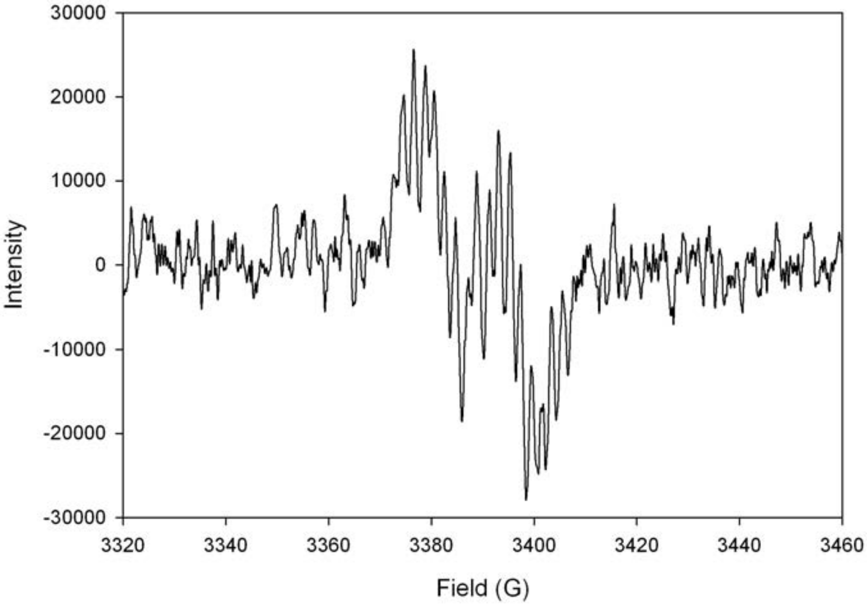

Figure 9. High modulation EPR spectra at room temperature for the trifluoromethylation of 4-*t*-butylanisole with **28** in the presence of MTO (**30**) in $CDCl_3$ after 1 h at 70°C followed by fast cooling with liquid nitrogen. Further details of the experimental set up are given in the experimental part.

The observed splitting pattern indicates ^{1}H-coupling, which could be explained as follows. After addition of the CF_3 moiety, the formed radical intermediate (see Section 4.3.6.) would have the delocalized structure presented in Scheme 12 and the resulting EPR spectrum would be the sum of the spectra of the contributing species. For structures **B** and **C** in Scheme 12, with the unpaired electron located in the *meta* positions (relative to the methoxy group) a doublet is expected. Due to the fact that the chemical environment of these two protons is very similar, the two signals would overlap giving as a result one broad doublet, which in this case is observed with a coupling constant $a_{\text{H-}meta}$ of 13.5 G. In all cases (**A**, **B** and **C**), the unpaired electron displays long-range ^{1}H-couplings (through two bonds) with the protons in the *ortho* positions with a coupling constant $a_{\text{H-}ortho}$ of ca. 2 G. These values are in good agreement with those reported in the literature.[34]

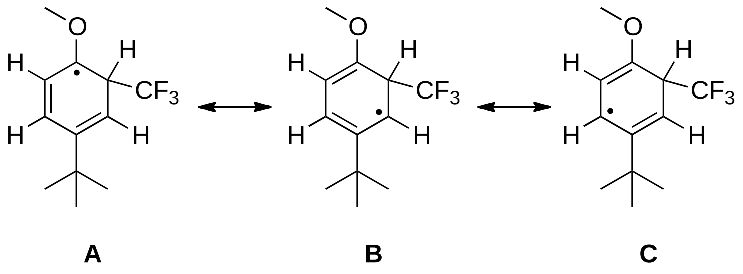

Scheme 12

4.3.4. *Deuterium kinetic isotope effect*

Deuterium kinetic isotope effect for the Re-catalyzed trifluoromethylation with **28** was evaluated by a direct competition reaction between equimolar amounts of benzene and benzene-D_6 used as solvent mixture (Scheme 13). In this case, the reaction required longer times to reach completion than when chloroform was used.

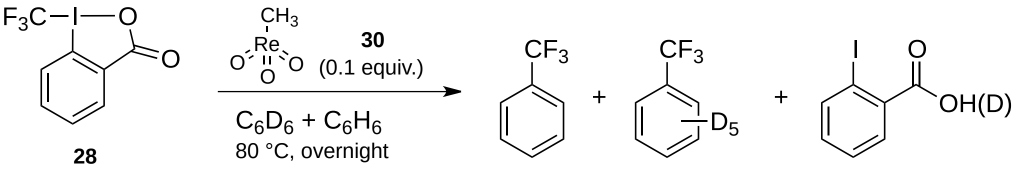

Scheme 13

After completion of the reaction, the relative amounts of benzotrifluoride and its deuterated analogue were determined by integration of the signals in the ^{19}F NMR spectrum (Figure 10). The signal assignment was made by subsequent addition of a small amount of commercial benzotrifluoride to the reaction mixture. The ratio k_H/k_D = 1.3 represent a small primary or secondary KIE, suggesting that the C-H bond breaking is somehow involved in the rate determining step.

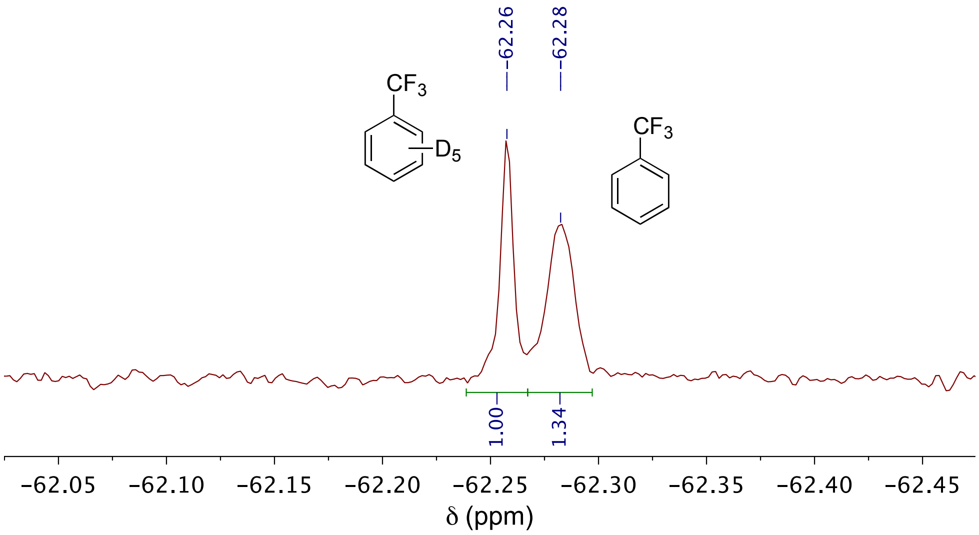

Figure 10. ^{19}F NMR spectra (376 MHz) for the trifluoromethylation of C_6H_6 and C_6D_6 at 80°C.

4.3.5. UV-Vis

From all the assayed aromatic trifluoromethylation reactions with **28** in presence of MTO (**30**), only those in which an effective CF_3-transfer to the substrate occurred resulted in strongly dark brown-colored reaction mixtures. This observation is somewhat striking since the "expected" reaction products are colorless. The formation of these unidentified side products is then substrate dependent and seems also to depend on the formation of the reactive intermediate(s) that trigger(s) the trifluoromethylation reaction, rather than on the mere activation and/or decomposition of **28**. The trifluoromethylation of 4-*t*-butylanisole was monitored by UV-Vis spectroscopy showing that, in fact, the appearance of colored side products starts at a late stage of the reaction, after the observed induction period. The obtained reaction profile is presented in Figure 11. Further conclusions can not be drawn from this experiment, since the nature of this colored material remains unknown.

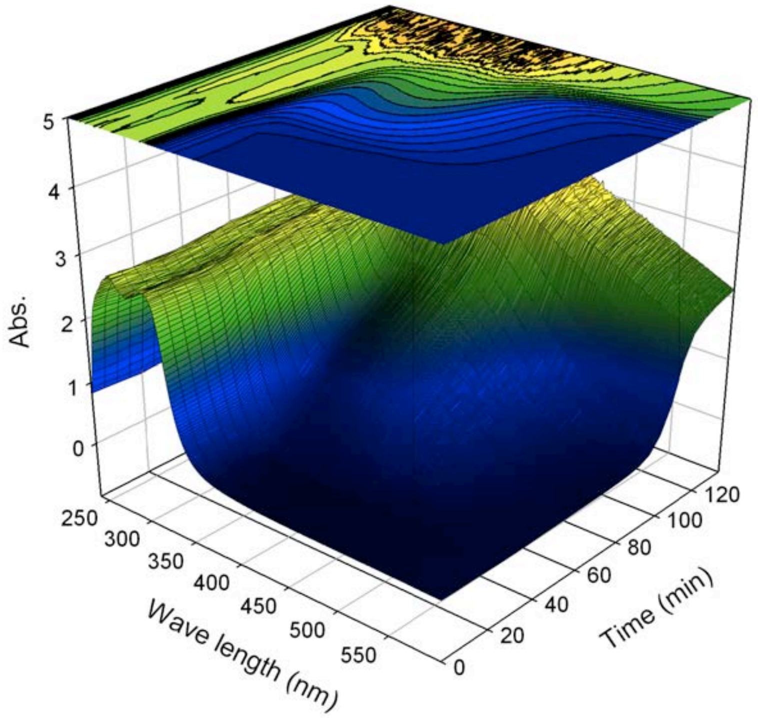

Figure 11. Reaction profile for the trifluoromethylation of 4-*t*-butylanisole in $CDCl_3$ at 70°C as monitored by UV-Vis.

4.3.6. *Mechanistic proposal*

Taking the observations above into account along with previous kinetic studies on these kind of reactions,[27, 35] we propose the radical chain mechanism depicted in Scheme 14 using benzene as model substrate.

The first stage of the reaction, or initiation step (Scheme 14, A), starts with the activation of **28** by coordination to the Lewis acid (MTO, **30**),[21, 27] making the hypervalent iodine(III) a better oxidant and thus promoting the single electron transfer (SET) from the benzene molecule in the encounter complex **35**.[36] This generates an aromatic cation radical species antiferromagnetically coupled with the reduced reagent **28** (singlet diradical **36**).[16] This caged pair would then react via ion-pair collapse[37] with an effective transfer of a CF_3^- moiety to give the radical intermediate **37**.

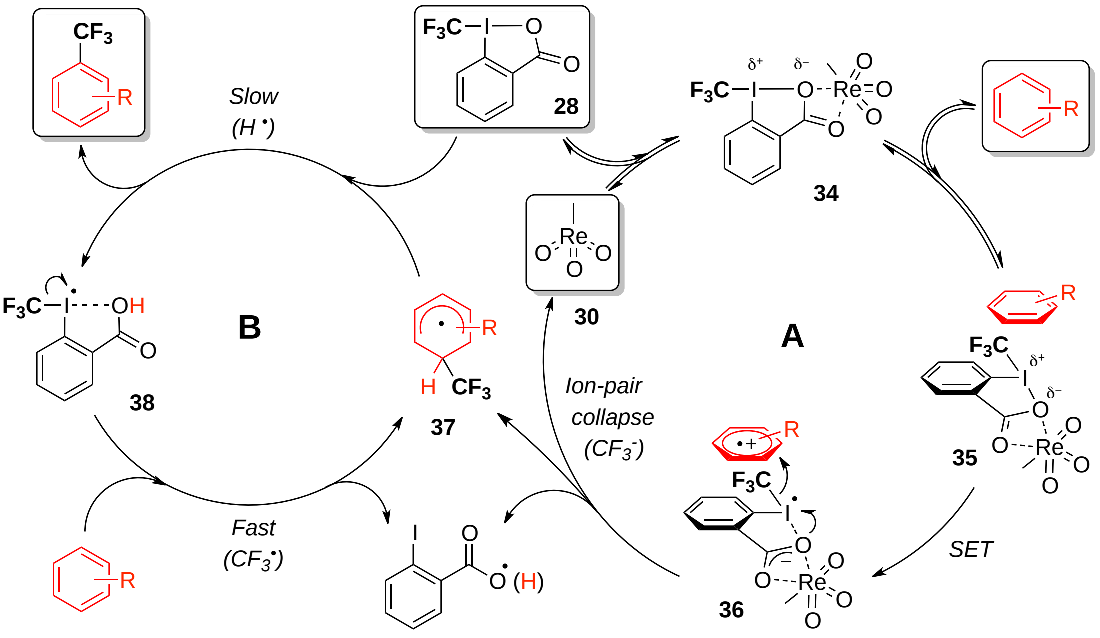

Scheme 14

The propagation step (Scheme 14, B) starts with the slow deprotonation of **37**, probably by **28** leading to the reactive intermediate **38** which is rapidly consumed by transfer of a $CF_3^{\bullet}$ unit to the substrate, closing the cycle. The termination step would be the decomposition of the radical **37** (after consumption of **28**) leading to the formation of CF_3H, CF_3D, CF_3Cl, CF_3I and the unidentified dark brown products, all of them formed only in the latest stage of the reaction as verified by NMR and UV-Vis.

4.4. Conclusion

In summary, a novel methodology for the direct trifluoromethylation of both activated and unactivated arenes and heteroarenes was developed using an easily accessible, shelf-stable hypervalent iodine(III) trifluoromethylating reagent (**28**) and MTO (**30**) as catalyst. Only a small excess of substrate and 5-10 mol-% of catalyst are required. To the best of our knowledge, this is the direct aromatic trifloromethylation procedure with the broadest substrate scope so far.

References

[1] K. Müller, C. Faeh, F. Diederich, *Science* **2007**, *317*, 1881-1886.

[2] P. Kirsch, *Modern Fluoroorganic Chemistry*, WILEY-VCH Verlag GmbH & Co. KGaA, Weinheim, **2004**.

[3] a) J.-A. Ma, D. Cahard, *J. Fluorine Chem.* **2007**, *128*, 975-996; b) M. A. McClinton, D. A. McClinton, *Tetrahedron* **1992**, *48*, 6555-6666; c) T. Umemoto, *Chem. Rev.* **1996**, *96*, 1757-1778; d) N. Shibata, A. Matsnev, D. Cahard, *Beilstein J. Org. Chem.* **2010**, *6, doi:10.3762/bjoc.6.65*

[4] D. Naumann, B. Wilkes, J. r. Kischkewitz, *J. Fluorine Chem.* **1985**, *30*, 73-87.

[5] T. Umemoto, A. Ando, *Bull. Chem. Soc. Jpn.* **1986**, *59*, 447-452.

[6] H. Sawada, M. Nakayama, M. Yoshida, T. Yoshida, N. Kamigata, *J. Fluorine Chem.* **1990**, *46*, 423-431.

[7] T. B. Patrick, S. Khazaeli, S. Nadji, K. Hering-Smith, D. Reif, *J. Org. Chem.* **1993**, *58*, 705-708.

[8] T. Kino, Y. Nagase, Y. Ohtsuka, K. Yamamoto, D. Uraguchi, K. Tokuhisa, T. Yamakawa, *J. Fluorine Chem.* **2010**, *131*, 98-105.

[9] a) V. C. R. McLoughlin, J. Thrower, *Tetrahedron* **1969**, *25*, 5921-5940; b) C.-P. Zhang, Z.-L. Wang, Q.-Y. Chen, C.-T. Zhang, Y.-C. Gu, J.-C. Xiao, *Angew. Chem. Int. Ed.* **2011**, *50*, 1896-1900.

[10] T. D. Senecal, A. T. Parsons, S. L. Buchwald, *J. Org. Chem.* **2011**, *76*, 1174-1176.

[11] E. J. Cho, T. D. Senecal, T. Kinzel, Y. Zhang, D. A. Watson, S. L. Buchwald, *Science* **2010**, *328*, 1679-1681.

[12] a) P. Eisenberger, S. Gischig, A. Togni, *Chem. Eur. J.* **2006**, *12*, 2579-2586; b) I. Kieltsch, P. Eisenberger, K. Stanek, A. Togni, *Chimia* **2008**, *62*, 260–263.

[13] a) K. Stanek, R. Koller, I. Kieltsch, P. Eisenberger, A. Togni, *e-EROS* **2009**, Article-Rn01121; b) K. Stanek, R. Koller, I. Kieltsch, P. Eisenberger, A. Togni, *e-EROS* **2009**, Article-Rn01120.

[14] I. Kieltsch, P. Eisenberger, A. Togni, *Angew. Chem. Int. Ed.* **2007**, *46*, 754-757.

[15] P. Eisenberger, I. Kieltsch, N. Armanino, A. Togni, *Chem. Commun.* **2008**, 1575-1577.

[16] K. Stanek, R. Koller, A. Togni, *J. Org. Chem.* **2008**, *73*, 7678-7685.

[17] R. Koller, K. Stanek, D. Stolz, R. Aardoom, K. Niedermann, A. Togni, *Angew. Chem. Int. Ed.* **2009**, *48*, 4332-4336.

[18] K. Niedermann, N. Früh, E. Vinogradova, M. S. Wiehn, A. Moreno, A. Togni, *Angew. Chem.* **2011**, *123*, 1091-1095.

[19] A. E. Allen, D. W. C. MacMillan, *J. Am. Chem. Soc.* **2010**, *132*, 4986-4987.

[20] M. S. Wiehn, E. V. Vinogradova, A. Togni, *J. Fluorine Chem.* **2010**, *131*, 951-957.

[21] R. Shimizu, H. Egami, T. Nagi, J. Chae, Y. Hamashima, M. Sodeoka, *Tetrahedron Lett.* **2010**, *51*, 5947-5949.

[22] a) W. A. Herrmann, F. E. Kühn, *Acc. Chem. Res.* **1997**, *30*, 169-180; b) C. C. Romão, F. E. Kühn, W. A. Herrmann, *Chem. Rev.* **1997**, *97*, 3197-3246.

[23] I. R. Beattie, P. J. Jones, *Inorg. Chem.* **1979**, *18*, 2318-2319.

[24] a) W. A. Herrmann, M. Ladwig, P. Kiprof, J. Riede, *J. Organomet. Chem.* **1989**, *371*, C13-C17; b) W. A. Herrmann, C. C. Romão, R. W. Fischer, P. Kiprof, C. d. M. de Bellefon, *Angew. Chem.* **1991**, *103*, 183-185.

[25] W. A. Herrmann, J. G. Kuchler, J. K. Felixberger, E. Herdtweck, W. Wagner, *Angew. Chem.* **1988**, *100*, 420-422.

[26] W. A. Herrmann, R. M. Kratzer, R. W. Fischer, *Angew. Chem. Int. Ed.* **1997**, *36*, 2652-2654.

[27] S. Fantasia, J. M. Welch, A. Togni, *J. Org. Chem.* **2010**, *75*, 1779-1782.

[28] C. De Meric de Bellefon, W. A. Herrmann, P. Kiprof, C. R. Whitaker, *Organometallics* **1992**, *11*, 1072-1081.

[29] a) I. I. Grandberg, G. K. Faizova, A. N. Kost, *Chem. Heterocycl. Comp.* **1967**, *2*, 421-425; b) A. Gero, J. J. Markham, *J. Org. Chem.* **1951**, *16*, 1835-1838.

[30] W. A. Herrmann, F. E. Kühn, P. W. Roesky, *J. Organomet. Chem.* **1995**, *485*, 243-251.

[31] V. Gutmann, *Coord. Chem. Rev.* **1976**, *18*, 225-255.

[32] R. Koller, No. 19219 thesis, ETH Zürich (Zürich), **2010**.

[33] Y. Kita, H. Tohma, K. Hatanaka, T. Takada, S. Fujita, S. Mitoh, H. Sakurai, S. Oka, *J. Am. Chem. Soc.* **1994**, *116*, 3684-3691.

[34] a) M. J. Perkins, *Radical Chemistry*, Ellis Horwood Limited, Hertfordshire, **1994**; b) F. Gerson, W. Huber, *Electron Spin Resonance Spectroscopy of Organic Radicals*, Wiley-VCH, Weinheim, **2003**.

[35] M. Tobisu, Y. Kita, Y. Ano, N. Chatani, *J. Am. Chem. Soc.* **2008**, *130*, 15982-15989.

[36] a) T. Dohi, M. Ito, K. Morimoto, M. Iwata, Y. Kita, *Angew. Chem. Int. Ed.* **2008**, *47*, 1301-1304; b) T. Dohi, M. Ito, N. Yamaoka, K. Morimoto, H. Fujioka, Y. Kita, *Tetrahedron* **2009**, *65*, 10797-10815.

[37] S. Sankararaman, W. A. Haney, J. K. Kochi, *J. Am. Chem. Soc.* **1987**, *109*, 7824-7838.

5. General Conclusion and Outlook

Here we described the synthesis and characterization of 33 new rhenium complexes in different oxidation states, namely 1, 3, 5, 6 and 7, all of them containing chiral ferrocenyl phosphine ligands and several different accompanying ligands including halides (Cl, Br, I), hydrides, oxo, alkoxo, nitrido and carbonyl.

The majority of these novel compounds exhibit remarkable stabilities to atmospheric conditions, a desirable feature in catalysis. Moreover, most of them showed to be active as catalysts in the asymmetric transfer hydrogenation of ketones, giving excellent yields up to >99% and moderate to good enantioselectivities, up to 58%. Although this is not a new reaction, this is the first report using rhenium-based catalysts. The rhenium polyhydrides described in this work displayed moderate activities in the high-pressure hydrogenation of dimethyl itaconate. Although no enantioselectivity was observed, the applicability of this kind of complexes in hydrogenation catalysis was demonstrated for the first time.

Making use of the (perhaps) most popular rhenium complex and hence readily available methyltrioxorhenium (MTO), we developed a novel methodology to tackle a difficult and still unsolved problem: the direct trifluoromethylation of aromatic and heteroaromatic substrates. This was achieved using 1-(trifluoromethyl)-1,2-benziodoxol-3(1*H*)-one, a hypervalent iodine-based reagent developed in our laboratories, as trifluoromethylating agent. This new method avoids the use of previously functionalized substrates, shows good functional groups tolerance and a broad substrate scope.

In all the above mentioned reactions corresponding mechanistic studies were carried out. Several reaction intermediates were characterized (in some cases also isolated) and different spectrometric and spectroscopic techniques were used. Consequently, for each reaction type a possible reaction mechanism was proposed and discussed.

In order to achieve higher catalytic performances (in all the cases) it is necessary to find more effective ways to activate the catalysts, not an easy task due precisely to inherent stability of the complexes. Different ligand abstraction methods should be tested and the use of more reactive rhenium precursors, like Re^{II} and Re^{IV} derivatives, would be advisable.

Having unveiled the capability of rhenium complexes containing ferrocenyl phosphine ligands, other kind of reactions could be tested using these catalysts: hydrosylilations and transfer hydrogenation of imines using the Re^{V}-oxo and nitrido complexes, as well as hydroaminations and C-H activations using the Re^{V} and Re^{VII} polyhydrides.

As discussed in the previous chapters, rhenium catalysis is a field still in progress where a lot remains to be explored and discovered. The unique properties of this rare metal make it suitable for the development of new catalysts and methods to which this work serves as a small but important contribution.

6. Experimental Part

6.1. General Methods

6.1.1. Starting materials

All the reactions were carried out under inert argon atmosphere using standard Schlenk techniques. Solvents were distilled and dried prior utilization using reported procedures.[1] All commercially available reagents were used as received without further purification. (*R*)-[1-(Dimethylamino)ethyl]ferrocene (Ugi's amine) was kindly provided by SOLVIAS AG as the tartrate salt. The ligand precursors dimethyl{(*R*)-1-[(*S*)-2-(diphenylphosphino)ferrocenyl]-ethyl}amine (**1a**) and dimethyl{(*R*)-1-[(*S*)-2-(dicyclohexylphosphino)-ferrocenyl]ethyl}amine (**1b**) were synthesized as described previously.[2] The Josiphos ligand (*R*)-1-[(S_P)-2-(diphenylphosphino)ferrocenyl]ethyl-dicyclohexylphosphine (**2a**) was prepared as previously reported.[3] The ligands (*R*)-1-[(S_P)-2-(dicyclohexylphosphino)ferrocenylethyl]diphenyl-phosphine (**2b**), (*R*)-1-[(S_P)-2-(diphenylphosphino)ferrocenyl]ethyldi(3,5-xylyl)phosphine (**2d**), (*R*)-1-[(S_P)-2-(dicyclohexylphosphino)ferrocenyl]-ethyldicyclohexylphosphine (**2e**), (*R*)-1-[(S_P)-2-(diphenylphosphino)ferrocenyl]ethyldi-*tert*-butylphosphine (**2f**), (*R*)-1-[(S_P)-2-(dicyclohexylphosphino)ferrocenyl]ethyldi-*tert*-butylphosphine (**2g**), (*R*)-1-[(S_P)-2-(di-*tert*-butylphosphino)ferrocenyl]ethyldiphenylphosphine (**2j**), (*R*)-1-{(R_P)-2-[2-(diphenylphosphino)phenyl]ferrocenyl}ethylbis[3,5-bis-(trifluoromethyl)phenyl]phosphine (**13a**) and (*R*)-1-{(R_P)-2-[2-(diphenylphosphino)-phenyl]ferrocenyl}ethyldiphenylphosphine (**13b**) were purchased from Aldrich (Solvias Chiral Ligands Kit) and used as received. The Pigiphos ligands bis-{(*R*)-1-[(*S*)-2-(diphenylphosphino)ferrocenyl]ethyl}cyclohexylphosphine) (**19a**), bis-{(*R*)-1-[(*S*)-2-(dicyclohexylphosphino)ferrocenyl]ethyl}cyclohexylphosphine) (**19b**) and bis-{(*R*)-1-[(*S*)-2-(di(1-naphthyl)phosphino)ferrocenyl]ethyl}-cyclohexylphosphine) (**19c**) were prepared as previously reported[4] starting from (*R*)-[1-(dimethylamino)ethyl]ferrocene (Ugi's amine).

The parent Re complexes $[ReOCl_3(PPh_3)_2]$,[5] $[Re(NCMe)Cl_3(PPh_3)_2]$,[6] $[ReOCl_3(AsPh_3)_2]$ (X = Cl, Br)[7] and $[NBu_4][ReNCl_4]$[8] were synthesized following literature procedures. Complex [ReOCl$_3$(*S*-BINAP)] (**17**) was prepared as previously reported.[9]

Commercial methyltrioxorhenium (MTO, **30**) was sublimed prior to use. Mesityltrioxorhenium (**33**)[10] and a second batch of MTO[11] were synthesized following published procedures. Trifluoromethylating reagents **28** and **29** were synthesized by Ms. Elisabeth Maenel, Mr. Václav Matoušek and Mr. Nico Santschi as previously reported.[12]

6.1.2. Analytical methods and instruments

NMR: Spectra were recorded on Bruker Avance 700, 500, 400, 300, 250 and 200 MHz instruments. The δ chemical shifts are reported in parts per million (ppm). In ^{1}H and ^{13}C spectra, shifts are referred to TMS and calibrated with the residual solvent peak and in ^{31}P NMR relative to H_3PO_4 (85%) as an external reference. ^{19}F NMR spectra were referenced to external $CFCl_3$ (δ = 0.0). NMR-Yields were determined by integration on ^{1}H or ^{19}F NMR with 90° pulse width = 3.33 μs and relaxation delay between scans = 3 s. In ^{19}F NMR perfluoronaphthalene was used as internal standard.[13] In ^{1}H NMR the yields were determined by the relative amounts of starting materials and products. Coupling constants *J* are given in Hertz (Hz). *High-resolution MS:* ESI-MS and MALDI-MS measurements were performed by the MS-service of the "Laboratorium für Organische Chemie der ETH Zürich". Values are given as *m/z*. *EA:* Elemental analyses were performed by the microelemental analysis service of the "Laboratorium für Organische Chemie der ETH Zürich". *IR:* FTIR-measurements were performed in a Perkin-Elmer Specrtum BX Series spectrometer in solid state using an ATR Golden Gate sampling accessory. *HPLC:* Agilent Series 1100 or HP 1050 with UV-detector (DAD); flow in mL/min and eluent (hexane:*i*PrOH-ratio) are given in each case; columns: Chiralcel OD-H, OB, AD-H (4.6 x 250 mm, particle 5 μm) or Chiralcel OJ (4.6 x 250 mm, particle 10 μm). Retention times are given in minutes. *GC-MS:* Analysis were carried out in a Thermo Finnigan Trace MS, EI-MS, column: Zebron ZB-5 (30m x 0.25mm x 0.25 μm). Temperature program (unless otherwise stated): 5 min at 30 °C, then up to 60 °C (1 °C/min), then up to 250 °C (20 °C/min) and finally 20 min at 250 °C. *X-ray:* structural measurements were carried out on a Siemens CCD diffractometer (Siemens SMART PLATFORM, with CCD detector, graphite monochromator, Mo-Kα-radiation). Data were collected using the program SMART. Integration was performed with SAINT. Structure solution (direct methods) was accomplished with SHELXTL 97.

6.2. Asymmetric Transfer Hydrogenation (Chapter 2)

6.2.1. Synthesis of ligands and complexes

General Method for the Synthesis of (*R,S*)-PPFA analogs (1)

In an oven-dried Schlenk tube, (*R*)-[1-(dimethylamino)ethyl]ferrocene (Ugi's amine) (1 equiv.) was dissolved in dry diethyl ether (to a concentration of 1 - 2 molar) and this solution cooled to -78 °C. To this solution *t*-butyllithium (1,6 M) in pentane (1.2 equiv.) was added dropwise with a syringe. The reaction mixture was stirred at this temperature for 30 minutes. Then the cooling bath was removed to allow the mixture to warm to room temperature. It was stirred for further 60 minutes leading to the formation of a red-orange precipitate. The same amount of ether used before was added and the mixture was stirred for another 60 minutes giving a clear solution. The solution was cooled again to -78 °C and the corresponding secondary phosphine chloride (1.1 equiv.) was added dropwise with a syringe. The reaction was allowed to warm to room temperature overnight. To the resulting orange suspension a saturated solution of Na_2CO_3 was added slowly to quench the reaction. The biphasic mixture was separated in a separatory funnel and the organic phase was washed with water and brine and dried over $MgSO_4$, then filtered and concentrated to dryness *in vacuo* to give a sticky orange solid. The crude product was purified by either column chromatography or by recrystallization to give pure **1** as an orange solid.

Dimethyl{(*R*)-1-[(*S*)-2-(diphenylphosphino)ferrocenyl]ethyl}amine (1a)[2]

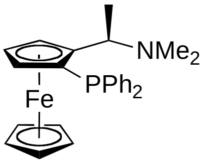

From 4.024 g of Ugi's amine (15.652 mmol, 1 equiv.), 12 mL of *t*-butyllithium (1,6 M in pentane) (19.2 mmol, 1.2 equiv.) and 3 mL of clorodiphenylphosphine (16.652 mmol, 1.1 equiv.), according to the general method. Recrystallized at -20 °C from a saturated dichloromethane/hexane solution to give orange crystals. Yield 5.133 g (74%). ^{1}H NMR (250 MHz, $CDCl_3$) δ 7.66 (m, 2H, Ph), 7.48 – 7.39 (m, 3H), 7.27 (m, 5H), 4.45 (s, 1H, *H*Cp), 4.32 (t, *J* = 2.3 Hz, 1H, *H*Cp), 4.23 (ddd, *J* = 13.2, 6.4, 2.3 Hz, 1H, *H*CMe), 4.02 (s, 5H, Cp), 3.93 (s, 1H, *H*Cp), 1.84 (s, 6H, N*Me*), 1.34 (d, *J* = 6.7 Hz, 3H, HC*Me*). ^{31}P NMR (101 MHz, $CDCl_3$) δ -22.82 (s).

Dimethyl{(*R*)-1-[(*S*)-2- (dicyclohexylphosphino)ferrocenyl]-ethyl}amine (1b)[2]

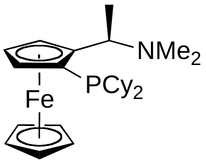

From 1.821 g of Ugis's amine (7.08 mmol, 1 equiv.), 5.4 mL of *t*-butyllithium (1,6 M in pentane) (8.5 mmol, 1.2 equiv.) and 1.8 mL of clorodicyclohexylphosphine (8.15 mmol, 1.1 equiv.), according to the general method. Flash chromatography through silica, eluting with a mixture of *n*-hexane/ethyl acetate, 5:1. Recrystallized at -20 °C from a saturated ethanol solution to give an orange powder. Yield 1.896 g (59%). ^{1}H NMR (300 MHz, CD_2Cl_2) δ 4.28 (s, 1H, *H*Cp), 4.24 (t, *J* = 2.1 Hz, 1H, *H*Cp), 4.10 (s, 1H, *H*Cp), 4.05 (s, 5H, Cp), 3.98 (m, 1H, *H*CMe), 2.34 (bs, Cy), 2.09 (bs, Cy), 2.00 (bs, Cy), 1.84 (bs, Cy), 1.68 (m, Cy), 1.48 – 1.33 (m, Cy), 1.28 (d, *J* = 6.7 Hz, 3H, Me), 1.23 – 1.01 (m, Cy). ^{31}P NMR (121 MHz, CD_2Cl_2) δ -11.84 (s).

General Method for the Synthesis of the Josiphos Ligands (2)

In an oven-dried Schlenk tube, **1** (1 equiv.) was dissolved in degassed glacial acetic acid (to a concentration of 0,5 - 1 molar). To this solution, the corresponding secondary phosphine (1.1 equiv.) was added and the mixture was stirred at 80 °C for three hours. The solvent and volatiles were removed *in vacuo* to give an orange sticky solid. It was dissolved in dichloromethane and washed successively with a saturated Na_2CO_3 solution, brine and water, dried over $MgSO_4$ and filtered. It was concentrated to dryness with a rotavapor to give the crude product. The crude was purified either by column chromatography or by recrystallization to give pure **2** as an orange solid.

(*R*)-1-[(S_P)-2-(Diphenylphosphino)ferrocenyl]ethyldicyclohexylphosphine (2a)[3]

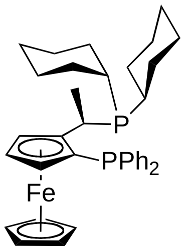

From 1.394 g of **1a** (3.1614 mmol, 1 equiv.) and 0.7 mL of dicyclohexylphosphine (3.4597 mmol, 1.1 equiv.), according to the general procedure. Recrystallized from a saturated dichloromethane solution at -20 °C to give orange crystals. Yield: 1.813 g (96%). ^{1}H NMR (300 MHz, CD_2Cl_2) δ 7.73 – 7.58 (m, 2H, Ph), 7.46 – 7.33 (m, 3H, Ph), 7.16 (d, *J* = 3.2 Hz, 5H, Ph), 4.36 (s, 1H, *H*Cp), 4.32 (t, *J* = 2.2 Hz, 1H, *H*Cp), 4.07 (s, 1H, *H*Cp), 3.79 (s, 5H, Cp), 3.30 (dd, *J* = 7.0, 2.0 Hz, 1H, *H*CMe), 1.77 (bs, Cy), 1.70 (bs, Cy), 1.63 (bs, Cy), 1.59 (dd, *J* = 7.2, 4.7 Hz, 3H, Me), 1.55 – 1.43 (m, Cy), 1.35 – 0.91 (m, Cy). ^{31}P NMR (121 MHz, CD_2Cl_2) δ 15.46 (d, *J* = 37.6 Hz), -25.76 (d, *J* = 37.6 Hz).

(*R*)-1-[(S_P)-2-(Dicyclohexylphosphino)ferrocenyl]ethyldiadamantylphosphine (2c)

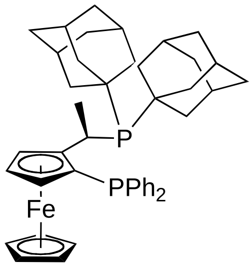

This compound was synthesized by Mr. Phillip Battaglia according to the general method, from 500.6 mg of **1a** (1.13 mmol, 1 equiv.), 412.8 mg of bisadamantylphosphine[14] (1.36 mmol, 1.2 equiv.) and with the addition of 0.08 mL of trifluoroacetic acid. Purification by flash chromatography in silica eluting with a mixture of *c*-hexane/ethanol 10:1, to give an orange powder. Yield 268.3 mg (34%). ^{1}H NMR (250 MHz, CD_2Cl_2) δ 7.67 – 7.57 (m, 2H, Ph), 7.40 – 7.31 (m, 3H, Ph), 7.26 – 7.12 (m, 5H, Ph), 4.43 (d, *J* = 1.2 Hz, 1H, *H*Cp), 4.23 (t, *J* = 2.3 Hz, 1H, *H*Cp), 4.01 – 3.95 (m, 1H, *H*Cp), 3.81 (s, 5H, Cp), 3.43 (dt, *J* = 7.0, 5.5 Hz, 1H, *H*CMe), 2.00 (bs, Adamantyl), 1.93 (dd, *J* = 7.2, 3.0 Hz, 3H, Me), 1.79 (bs, Adamantyl), 1.73 (bs, Adamantyl), 1.64 (bs, Adamantyl). ^{13}C NMR (63 MHz, CD_2Cl_2) δ 143.22 (dd, *J* = 8.0, 1.7 Hz), 140.96 (dd, *J* = 12.2, 5.3 Hz), 136.45 (d, *J* = 23.4 Hz), 133.50 (dd, *J* = 16.7, 3.0 Hz), 129.21 (s), 128.27 (d, *J* = 8.0 Hz), 127.58 (d, *J* = 6.0 Hz), 127.11 (s), 103.45 (dd, *J* = 25.1, 24.4 Hz), 74.93 (dd, *J* = 12.3, 4.3 Hz), 72.17 (dd, *J* = 5.0, 0.9 Hz), 70.92 (dd, *J* = 4.4, 2.5 Hz), 69.97 (s), 68.67 (s), 42.96 (dd, *J* = 11.0, 3.0 Hz), 42.52 (d, *J* = 12.0 Hz), 40.19 (d, *J* = 2.8 Hz), 39.84 (s), 39.62 (d, *J* = 2.7 Hz), 39.35 (s), 37.63 (s), 29.88 – 29.29 (m), 19.10 (s). ^{31}P NMR (101 MHz, CD_2Cl_2) δ 49.79 (d, *J* = 54.1 Hz), -26.35 (d, *J* = 54.1 Hz). HR-MALDI MS: Monoisotopic mass ([M+H]$^+$) *m/z*, calcd: 699.2967, found: 699.2973.

(*R*)-1-[(*S*$_P$)-2-(Dicyclohexylphosphino)ferrocenyl]ethyldi(3,5-bis-(trifluoro-methyl)pheny)phosphine (2h)

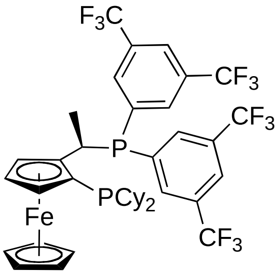

From 106.6 mg of **1b** (0.235 mmol, 1 equiv.) and 111 mg of bis[3,5-bis(trifluoromethyl)phenyl]-phosphine[15] (0.242 mmol, 1 equiv.), according to the general procedure. Purification by recrystallization from methanol at -20 °C, to give an orange powder. Yield 141 mg (69%). ^{1}H NMR (300 MHz, CD_2Cl_2) δ 7.97 (s, Ph), 7.93 (s, Ph), 7.85 (s, Ph), 7.80 (s, Ph), 7.71 (s, Ph), 7.69 (s, Ph), 4.30 (s, Cp, minor comformer), 4.22 (s, 5H, Cp, major conformer), 4.12 (s, *H*Cp), 4.07 (s, *H*Cp), 3.93 (bs, 1H, *H*CMe), 3.64 (s, *H*Cp), 2.66 – 2.52 (m, Cy), 2.44 (dd, *J* = 16.5, 8.8 Hz, Cy), 2.22 (d, *J* = 8.5 Hz, Cy), 1.90 (bs, Cy), 1.84 – 1.68 (m, Cy), 1.53 (dd, *J* = 37.7, 22.3 Hz, Cy), 1.43 – 1.32 (m, 3H, Me), 1.28 (d, *J* = 7.6 Hz, Cy), 1.19 (d, *J* = 16.4 Hz, Cy), 1.01 – 0.70 (m, Cy). ^{13}C NMR (63 MHz, CD_2Cl_2) δ 135.94 (dd, *J* = 21.8, 2.8 Hz), 132.16 (dd, *J* = 19.0, 3.6 Hz), 131.78 (d, *J* = 3.1 Hz), 131.45 (d, *J* = 7.0 Hz), 125.99 (d, *J* = 5.7 Hz), 124.17 (s), 122.46 (s), 121.65 (d, *J* = 5.6 Hz), 95.93 (dd, *J* = 23.1, 18.5 Hz), 72.97 (s), 70.70 (s), 70.62 (s), 70.05 (s), 69.20 (s), 67.94 (s), 38.26 (s), 35.55 (s), 33.90 (s), 32.03 (s), 30.63 (d, *J* = 10.2 Hz), 30.40 (s), 30.24 (s), 29.92 (s), 28.88 (s), 28.61 (s), 28.03 (s), 27.87 (s), 27.67 (d, *J* = 11.3 Hz), 26.88 (d, *J* = 8.0 Hz), 17.50 (s). ^{31}P NMR (121 MHz, CD_2Cl_2) δ 11.96 (s, minor comformer), 8.31 (bs, major comformer), -11.77 (s, minor comformer), -16.16 (bs, major comformer). ^{19}F NMR (282 MHz, CD_2Cl_2) δ -63.24 (d, *J* = 28.9 Hz, minor comformer), -63.34 (d, *J* = 26.5 Hz, major comformer). HR-MALDI MS: Monoisotopic mass ([M+H]$^+$) *m/z*, calcd: 867.1836, found: 867.1826.

(*R*)-1-[(S_P)-2-(Dicyclohexylphosphino)ferrocenyl]ethyldi(3,5-xylyl)-phosphine (2i)

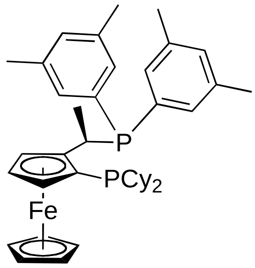

From 200.7 mg of **1b** (0.443 mmol, 1 equiv.) and 120 μL of bis(3,5-xylyl)phosphine (0.529 mmol, 1.2 equiv.), according to the general procedure. Purification by flash chromatography in silica eluting with a mixture of *n*-hexane/ethyl acetate 20:1 and 5% of TEA, to give an orange powder. Yield 155 mg, 95% purity (53%). ^{1}H NMR (250 MHz, CD_2Cl_2) δ 7.00 (s, 1H, Xyl), 6.98 (s, 2H, Xyl), 6.95 (s, 2H, Xyl), 6.89 (s, 1H, Xyl), 4.19 (s, 2H, *H*Cp), 4.16 (s, 5H, Cp), 3.89 (s, 1H, *H*Cp), 3.52 (ddd, *J* = 13.8, 6.9, 3.5 Hz, 1H, *H*CMe), 2.27, (s, 6H, *Me*(Xyl)), 2.26, (s, 6H, *Me*(Xyl)), 1.87 (bs, Cy), 1.70 (dd, *J* = 24.2, 15.9 Hz, 3H, HC*Me*), 1.40 (m, Cy), 1.28 (bs, Cy), 1.14 (bs, Cy), 0.89 (bs, Cy). ^{13}C NMR (63 MHz, CD_2Cl_2) δ 138.97 (d, *J* = 18.1 Hz), 138.06 (d, *J* = 5.0 Hz), 137.67 (d, *J* = 7.8 Hz), 136.27 (d, *J* = 19.9 Hz), 133.70 (d, *J* = 21.1 Hz), 131.20 (s), 130.02 (d, *J* = 16.0 Hz), 129.69 (s), 99.25 (dd, *J* = 22.4, 19.4 Hz), 78.94 (dd, *J* = 22.5, 3.3 Hz), 71.70 (s), 69.71 (s), 69.17 (dd, *J* = 9.7, 3.9 Hz), 68.07 (s), 37.34 (d, *J* = 13.0 Hz), 35.91 (dd, *J* = 12.3, 3.5 Hz), 33.82 (d, *J* = 22.6 Hz), 32.15 (dd, *J* = 13.5, 3.5 Hz), 31.60 (d, *J* = 13.9 Hz), 30.49 (d, *J* = 4.4 Hz), 28.77 (d, *J* = 14.9 Hz), 27.86 (d, *J* = 9.9 Hz), 27.09 (d, *J* = 4.9 Hz), 21.61 (d, *J* = 6.9 Hz), 19.84 (t, *J* = 3.9 Hz). ^{31}P NMR (101 MHz, CD_2Cl_2) δ 3.66 (d, *J* = 8.4 Hz), -14.61 (d, *J* = 7.6 Hz). HR-MALDI MS: Monoisotopic mass ($[M+H]^+$) *m/z*, calcd: 651.2967, found: 651.2968.

[ReBr(CO)$_3$(2a)] (3)

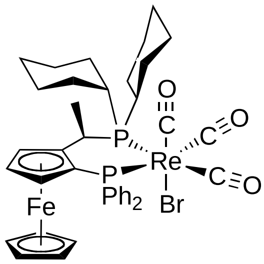

In an oven-dried Schlenk tube, 115 mg of [ReBr(CO)$_5$] (0.283 mmol, 1 equiv.) and 170 mg of **2a** (0.286 mmol, 1 equiv.) were mixed in 5 mL of degassed tetralin. The mixture was heated at 180 °C and stirred under argon for 4 hours. The system was then allowed to cool to room temperature and the orange solution was filtered through a cannula-filter. The solvent was removed by passing the solution through a plug of silica gel, washing thoroughly with *n*-hexane. The product was eluted with DCM. This solution was concentrated to dryness with a rotavapor to give product **3** as an orange solid. Yield 259.1 mg (96.9%). X-ray quality crystals were obtained by layering a saturated toluene solution with pentane. ^{1}H NMR (250 MHz, CD_2Cl_2) δ 8.49 – 8.29 (m, 2H, Ph), 7.55 (s, 3H, Ph), 7.33 (s, 3H, Ph), 7.23 (dd, *J* = 13.1, 5.0 Hz, 2H, Ph), 5.25 (p, *J* = 7.4 Hz, 1H, *H*CMe), 4.70 (s, 1H, *H*Cp), 4.54 (d, *J* = 2.5 Hz, 1H, *H*Cp), 4.51 (d, *J* = 1.0 Hz, 1H, *H*Cp), 3.76 (s, 5H, Cp), 2.37 (d, *J* = 9.4 Hz, 1H, Cy), 2.07 (m, Cy), 1.76 (dd, *J* = 10.2, 7.5 Hz, 3H, Me), 1.70 – 1.51 (m, Cy), 1.40 (m, Cy), 1.14 (m, Cy), 1.05 – 0.79 (m, Cy). ^{13}C NMR (63 MHz, CD_2Cl_2) δ 193.30 – 189.16 (m, 3C, CO), 140.99 (d, *J* = 51.8 Hz), 137.54 (dd, *J* = 48.2, 2.0 Hz), 136.23 (d, *J* = 10.7 Hz), 132.61 (d, *J* = 10.2 Hz), 131.18 (d, *J* = 2.4 Hz), 129.49 (d, *J* = 1.9 Hz), 128.36 (d, *J* = 10.2 Hz), 128.00 (d, *J* = 9.5 Hz), 95.10 (dd, *J* = 20.6, 3.3 Hz), 74.69 (d, *J* = 0.7 Hz), 71.65 (s), 71.03 (dd, *J* = 8.5, 1.9 Hz), 70.45 (d, *J* = 5.3 Hz), 69.01 (dd, *J* = 42.7, 4.0 Hz), 38.39 (d, *J* = 21.1 Hz), 37.86 (d, *J* = 14.1 Hz), 31.07 (d, *J* = 4.9 Hz), 30.91 (d, *J* = 1.7 Hz), 30.16 (s), 28.61 (s), 27.95 (d, *J* = 11.4 Hz), 27.73 (d, *J* = 1.8 Hz), 27.72 (d, *J* = 7.9 Hz), 27.53 (d, *J* = 7.2 Hz), 26.63 (d, *J* = 1.2 Hz), 26.56 (d, *J* = 0.9 Hz). 16.38 (d, *J* = 6.5 Hz). ^{31}P NMR (101 MHz, CD_2Cl_2) δ 18.98 (d, *J* = 26.6 Hz, *exo*), 14.65 (d, *J* = 28.4 Hz), -0.19 (d, *J* = 28.7 Hz, *exo*), -14.66 (d, *J* = 28.4 Hz). HR-ESI MS: Monoisotopic mass (M^+) *m/z*, calcd: 944.0837, found: 944.0834. EA: Anal. calcd. for $C_{39}H_{44}O_3P_2FeBrRe$ (%): C, 49.59; H, 4.69; P, 6.56. Found: C, 50.35; H, 4.58; P, 6.48. FTIR (neat): cm^{-1} 2923.56, 2850.79, 2014.69, 1926.79, 1900.00, 1866.33, 1681.19, 1433.01, 697.52

[ReCl(CO)$_3$(2a)] (4)

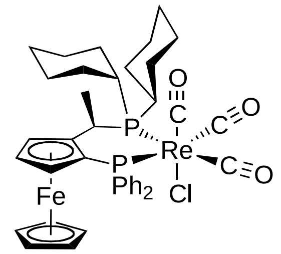

In an analogous procedure as for the synthesis of **3**, 104 mg of **2a** (0.175 mmol, 1.2 equiv.) and 54 mg of [ReCl(CO)$_5$] (0.149 mmol, 1 equiv.) were dissolved in 5 mL of degassed tetralin and stirred at 180 °C overnight. The resulting solution was passed through a short column of silica gel, eluting out first the solvent with *n*-hexane and then the product with a mixture *n*-hexane/ethyl acetate 4:1. The solution was concentrated *in vacuo* and the resulting sticky solid was carefully washed with *n*-hexane and pentane and dried again under high vacuum to give the product as an orange solid. Yield 70 mg (74%). ^{1}H NMR (250 MHz, CD_2Cl_2) δ 8.38 – 8.23 (m, 2H, Ph), 7.51 (dd, *J* = 5.5, 2.6 Hz, 3H, Ph), 7.29 (t, *J* = 3.4 Hz, 3H, Ph), 7.24 (d, *J* = 2.6 Hz, 1H, Ph), 7.19 (dd, *J* = 6.6, 3.6 Hz, 1H, Ph), 5.16 – 4.98 (m, 1H, *H*CMe), 4.66 (s, 1H, *H*Cp), 4.49 (t, *J* = 2.5 Hz, 1H, *H*Cp), 4.46 (s, 1H, *H*Cp), 3.68 (s, 5H, Cp), 2.35 (dd, *J* = 22.1, 11.1 Hz, 1H, Cy), 1.93 (bs, Cy), 1.72 (dd, *J* = 10.1, 7.5 Hz, 3H, Me), 1.60 (m, Cy), 1.47 – 1.23 (m, Cy), 1.23 – 1.00 (m, Cy), 1.00 – 0.77 (m, Cy). ^{31}P NMR (101 MHz, CD_2Cl_2) δ 25.19 (d, *J* = 28.3 Hz, *exo*), 18.71 (d, *J* = 28.5 Hz, *endo*), 3.58 (d, *J* = 28.3 Hz, *exo*), -11.21 (d, *J* = 28.5 Hz, *endo*). HR-ESI MS: Monoisotopic mass (M^+) *m/z*, calcd: 900.1350, found: 900.1338.

[ReH(CO)$_3$(2a)], mixture of isomers (5)

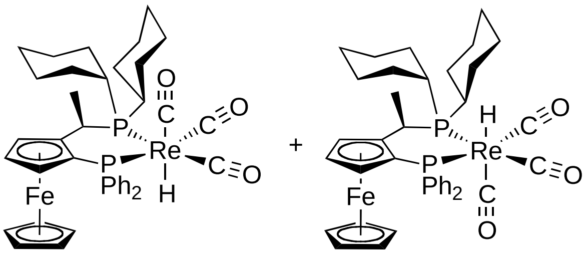

In an oven-dried Schlenk tube, 133.3 mg of **2a** (0.224 mmol, 1 equiv.) and 74 mg of [$Re_2(CO)_{10}$] (0.113 mmol, 1 equiv.) were dissolved in 7 mL of dry 1-pentanol and refluxed under argon overnight. The solvent was removed by bulb-to-bulb distillation under high vacuum at 80 °C. The resulting sticky solid was washed with *n*-hexane (3 x 5 mL) and dried at 60 °C under high vacuum to give the product as an orange solid. Yield 159.7 mg (82%). ^{1}H NMR (500 MHz, CD_2Cl_2) δ 8.34 – 8.24 (m, 2H, Ph, *endo*), 8.00 – 7.93 (m, Ph, *exo*), 7.59 – 7.51 (m, Ph), 7.51 – 7.45 (m, Ph), 7.38 – 7.23 (m, Ph), 4.56 (s, *H*Cp, *exo*), 4.53 (s, 1H, *H*Cp, *endo*), 4.48 (dt, *J* = 2.7, 1.4 Hz, 1H, *H*Cp, *endo*), 4.38 – 4.35 (m, *H*CMe), 4.13 (dt, *J* = 2.7, 1.4 Hz, *H*Cp, *exo*), 3.72 (s, Cp, *exo*), 3.51 (s, 5H, Cp, *endo*), 2.31 – 2.24 (m, Cy), 2.19 (dd, *J* = 22.0, 11.8 Hz, Cy), 2.05 (s, Cy), 1.91 (s, Cy), 1.85 (s, Cy), 1.79 (s, Cy), 1.76 (s, Cy), 1.67 (dd, *J* = 9.9, 7.5 Hz, Me), 1.59 (m, Cy), 1.53 (s, Cy), 1.38 (s, Cy), 1.36 – 1.31 (m, Cy), 1.31 – 1.22 (m, Cy), 1.16 (m, Cy), 1.06 (m, Cy), 0.95 – 0.86 (m, Cy), -4.87 (t, *J* = 25.8 Hz, 1H, *H*Re, *endo*), -5.38 (dd, *J* = 26.8, 22.9 Hz, *H*Re, *exo*). ^{31}P NMR (101 MHz, CD_2Cl_2) δ 34.04 (d, *J* = 29.6 Hz, *endo*), 31.98 (d, *J* = 29.3 Hz, *exo*), 0.21 (d, *J* = 29.2 Hz, *endo*), -1.98 (d, *J* = 29.4 Hz, *exo*). HR-MALDI MS:

Monoisotopic mass ($[M\text{-}H]^+$) *m/z*, calcd: 865.1670, found: 865.1671. FTIR (neat): cm^{-1} 3053.67, 2927.04, 2851.29, 1991.23, 1891.30, 1729.56, 1433.87, 1260.82, 1161.54, 1093.75, 1001.27, 818.17, 743.49, 694,88.

[Re(CO)$_3$(2a)]OTf, mixture of isomers (6)

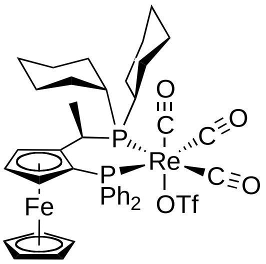

One equivalent of either **4**, **5** or **6** was dissolved in dry DCM under argon and this mixture was cooled to -78 °C in a 2-propanol/dry ice cooling bath. To this solution an excess of MeOTf was added with a syringe and the resulting solution was allowed to slowly warm to room temperature. The solvent and volatiles were eliminated *in vacuo* to give the product as a yellow solid. Any attempts to purify the crude product led only to decomposition. ^{1}H NMR (250 MHz, Tol) δ 8.77 (dd, *J* = 11.4, 7.9 Hz, Ph), 8.59 – 8.43 (m, Ph), 8.19 – 8.04 (m, Ph), 7.91 (dd, *J* = 16.5, 9.1 Hz, Ph), 7.65 (m, Ph), 4.99 – 4.74 (m, *H*Cp), 4.55 – 4.36 (m, *H*Cp), 4.22 (s, Cp, major isomer), 4.18 (s, Cp, minor isomer), 3.20 (bs), 2.91 (t, *J* = 8.7 Hz), 2.80 – 2.65 (m), 2.65 – 2.37 (m, Cy), 2.27 (s, Cy), 2.15 (dd, *J* = 9.7, 7.4 Hz, HC*Me*), 1.93 (d, *J* = 9.0 Hz, Cy), 1.86 – 1.43 (m, Cy). ^{31}P NMR (101 MHz, Tol) δ 29.21 (d, *J* = 26.4 Hz, major isomer), 26.24 (d, *J* = 27.1 Hz, minor isomer), 8.88 (d, *J* = 27.1 Hz, minor isomer), -3.48 (d, *J* = 26.4 Hz, major isomer). ^{19}F NMR (188 MHz, Tol) δ -71.15 (d, *J* = 17.0 Hz, minor isomer), -71.35 (d, *J* = 38.6 Hz, major isomer).

General Method for the Synthesis of [ReOX$_3$(2)] (7)

In an oven-dried Schlenk tube, [ReOX$_3$(AsPh$_3$)$_2$] (X = Cl, Br)[7] (1 equiv.) and the corresponding Josiphos ligand (**2**) were dissolved in dry dichloromethane (to a concentration of ca. 0.1 M). The mixture was then stirred at room temperature for 3-12 hours. It was then concentrated *in vacuo* to a fourth of its original volume and to the resulting brown solution *n*-hexane was added (two- or three-fold of the initial volume) to afford the precipitation of a brown solid. This was decanted and washed thoroughly with hexane and finally with diethylether. The product was then dried *in vacuo* and purified (when necessary) by recrystallization.

[ReOCl$_3$(2a)] (7a)

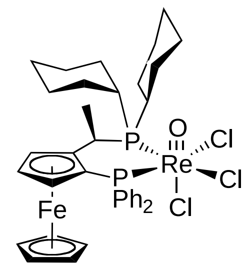

From 298.5 mg of [ReOCl$_3$(AsPh$_3$)$_2$] (0.324 mmol, 1 equiv.) and 194.3 mg of **2a** (0.327 mmol, 1 equiv.) according to the general method to give a brown-green solid. Yield 274 mg (94%). X-ray quality crystals were obtained by layering a saturated dichloromethane solution with benzene. ^{1}H NMR (250 MHz, CD$_2$Cl$_2$) δ 8.28 – 8.10 (m, 2H, Ph), 7.57 (m, 3H, Ph), 7.50 – 7.37 (m, 2H, Ph), 7.27 (m, 3H, Ph), 4.90 (s, 1H, *H*Cp), 4.60 (d, *J* = 7.6 Hz, 1H, *H*Cp), 3.73 (s, 5H, Cp), 3.41 (s, 1H, *H*Cp), 2.52 (bs, 1H, *H*CMe), 2.07 (dd, *J* = 12.0, 7.4 Hz, 3H, Me), 2.00 – 1.74 (m, Cy), 1.74 – 1.31 (m, Cy), 1.22 (s, Cy), 1.05 – 0.80 (m, Cy), 0.74 – 0.44 (m, Cy). ^{13}C NMR (63 MHz, CD$_2$Cl$_2$) δ 141.28 (d, *J* = 53.5 Hz), 135.98 (d, *J* = 8.4 Hz), 133.67 (d, *J* = 61.3 Hz), 132.63 (d, *J* = 8.9 Hz), 131.97 (d, *J* = 2.6 Hz), 130.88 (d, *J* = 2.4 Hz), 128.37 (d, *J* = 10.6 Hz), 128.02 (d, *J* = 10.1 Hz), 92.78 (d, *J* = 15.5 Hz), 76.47 (d, *J* = 2.8 Hz), 72.44 (d, *J* = 7.7 Hz), 71.97 (s), 71.33 (d, *J* = 6.5 Hz), 39.86 (d, *J* = 19.2 Hz), 37.67 (d, *J* = 19.1 Hz), 31.04 (d, *J* = 21.7 Hz), 29.91 (s), 29.80 (s), 28.68 (d, *J* = 8.7 Hz), 28.17 (s), 27.84 (s), 27.42 (s), 27.23 (s), 26.80 (s), 26.28 (s).17.54 (d, *J* = 6.7 Hz). ^{31}P NMR (101 MHz, CD$_2$Cl$_2$) δ 3.06 (d, *J* = 15.5 Hz), -34.81 (d, *J* = 15.6 Hz). HR-ESI MS: Monoisotopic mass ([M-Cl]$^+$) *m/z*, calcd: 867.1133, found: 867.1138. EA: Anal. calcd. for $C_{36}H_{44}OP_2Cl_3FeRe$ (%): C, 47.88; H, 4.91; P, 6.86. Found: C, 48.15; H, 4.93; P, 6.82.

[ReOCl$_3$(2b)] (7b)

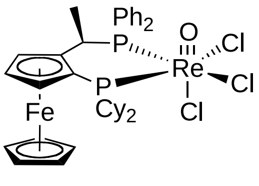

From 37.7 mg of [ReOCl$_3$(AsPh$_3$)$_2$] (0.041 mmol, 1 equiv.) and 25.9 mg of **2b** (0.043 mmol, 1 equiv.) according to the general method to give a brown solid. Yield 29 mg (78%).^{1}H NMR (250 MHz, CD$_2$Cl$_2$) δ 7.84 (s, Ph), 7.74 (s, Ph), 7.73 – 7.60 (m, Ph), 7.53 (bs, Ph), 7.41 (d, *J* = 6.9 Hz, Ph), 7.37 – 7.18 (m, Ph), 4.90 (s, 1H, *H*Cp), 4.74 (s, 1H, *H*Cp), 4.69 (s, 1H, *H*Cp), 4.56 (s, 1H, *endo*), *H*Cp, 4.38 (s, 5H, Cp, *exo*), 4.34 (s, 5H, *endo*), 4.04 – 3.81

(m, 1H, *H*CMe), 3.40 (s, Cy), 3.17 (q, *J* = 12.2 Hz, Cy), 2.76 (dd, *J* = 24.5, 11.9 Hz, Cy), 2.48 (d, *J* = 28.1 Hz, Cy), 2.20 – 1.99 (m, Cy), 1.98 – 1.77 (m, Cy), 1.69 (dd, *J* = 12.7, 6.9 Hz, 3H, Me), 1.62 – 1.33 (m, Cy), 1.33 – 1.07 (m, Cy), 0.94 – 0.76 (m, Cy). ^{13}C NMR (63 MHz, CD_2Cl_2) δ 135.21 (d, *J* = 6.9 Hz), 134.27 (d, *J* = 7.2 Hz), 132.02 (d, *J* = 2.1 Hz), 131.59 (d, *J* = 3.1 Hz), 129.09 (d, *J* = 9.2 Hz), 127.85 (d, *J* = 10.3 Hz), 91.32 – 90.61 (m), 75.61 (d, *J* = 4.4 Hz), 71.64 (s), 70.68 (s), 70.38 (d, *J* = 6.5 Hz), 40.91 (d, *J* = 23.2 Hz), 38.28 (d, *J* = 22.2 Hz), 30.22 (s), 29.23 (s), 29.07 (s), 28.74 (s), 28.34 (s), 27.85 (s), 27.73 – 27.09 (m), 26.77 (s), 26.09 (s), 16.72 (d, *J* = 6.4 Hz). ^{31}P NMR (101 MHz, CD_2Cl_2) δ 1.43 (bs, *endo*), -2.86 (d, *J* = 13.4 Hz, *exo*), -12.19 (bs, *exo*), -19.89 (bs, *endo*). HR-MALDI MS: Monoisotopic mass ($[M-Cl]^+$) *m/z*, calcd: 867.1134, found: 867.1128.

[ReOCl$_3$(2c)], mixture of isomers (7c)

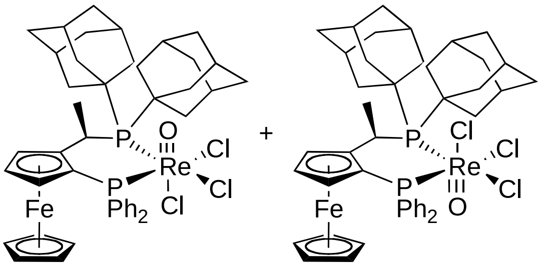

From 122 mg of [ReOCl$_3$(AsPh$_3$)$_2$] (0.132 mmol, 1 equiv.) and 99 mg of **2c** (0.142 mmol, 1.1 equiv.) according to the general method to give a brown solid. Yield 113 mg (85%).^{1}H NMR (250 MHz, CD_2Cl_2) δ 8.43 – 8.28 (m, Ph), 8.28 – 8.13 (m, Ph), 8.02 (dd, *J* = 18.7, 10.2 Hz, Ph), 7.71 – 7.39 (m, Ph), 7.34 (t, *J* = 9.0 Hz, Ph), 5.21 (dd, *J* = 10.9, 7.6 Hz, *H*CMe), 4.86 (s, *H*Cp), 4.78 (s, *H*Cp), 4.75 – 4.67 (m, *H*Cp), 4.57 (s, *H*Cp), 4.47 (s, *H*Cp), 4.40 (s, *H*Cp), 4.36 (s, Cp), 4.33 (s, *H*Cp), 3.78 (s, Cp), 3.49 (s, Adamantyl), 2.97 (bs, Adamantyl), 2.70 (bs, Adamantyl), 2.49 (bs, Adamantyl), 2.38 (dd, *J* = 9.1, 7.2 Hz, Me), 2.33 (bs, Adamantyl), 2.29 (bs, Adamantyl), 2.19 (bs, Adamantyl), 2.07 (d, *J* = 8.1 Hz, Adamantyl), 1.96 (bs, Adamantyl), 1.88 (bs, Adamantyl), 1.80 (bs, Adamantyl), 1.75 (bs, Adamantyl), 1.69 (bs, Adamantyl), 1.65 (bs, Adamantyl), 1.52 (bs, Adamantyl), 1.46 (bs, Adamantyl), 1.39 (bs, Adamantyl), 1.34 (bs, Adamantyl), 1.26 (bs, Adamantyl), 0.73 (bs, Adamantyl). ^{31}P NMR (101 MHz, CD_2Cl_2) δ 26.88 (d, *J* = 11.3 Hz, *exo*), 8.50 (d, *J* = 14.4 Hz, *endo*), -28.08 (d, *J*

= 11.5 Hz, *exo*), -32.99 (d, *J* = 14.5 Hz, *endo*). HR-MALDI MS: Monoisotopic mass ([M-Cl]$^+$) *m/z*, calcd: 971.1761, found: 971.1739

[ReOCl$_3$(2d)], both isomers (7d)

From 61 mg of [ReOCl$_3$(AsPh$_3$)$_2$] (0.066 mmol, 1 equiv.) and 43 mg of **2d** (0.067 mmol, 1 equiv.) according to the general method to give a brown solid. Yield 54 mg (71%). The obtained *endo* isomer isomerizes slowly in solution at room temperature to give the *exo* isomer. X-ray quality crystals of *exo*-**7d** were obtained by layering a saturated chloroform solution with *n*-hexane.

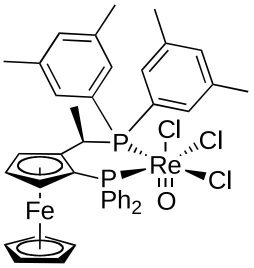

Endo-isomer: δ 8.18 – 8.02 (m, Ar), 7.66 (dd, *J* = 11.0, 7.2 Hz, Ar), 7.58 – 7.38 (m, Ar), 7.32 (m, Ar), 7.06 (s, 1H, Xyl), 6.97 (s, 1H, Xyl), 4.78 (s, 1H, *H*Cp), 4.60 (t, *J* = 2.4 Hz, 1H, *H*Cp), 4.22 (s, 1H, *H*Cp), 4.19 (m, *H*CMe), 3.79 (s, 5H, Cp), 2.30 (s, 6H, *Me*(Xyl)), 2.22 (s, 6H, *Me*(Xyl)), 1.49 (dd, *J* = 13.1, 7.2 Hz, 3H, HC*Me*). ^{31}P NMR (101 MHz, CDCl$_3$) δ -9.27 (bs), -22.00 (d, *J* = 14.8 Hz). HR-MALDI MS: Monoisotopic mass ([M-Cl]$^+$) *m/z*, calcd: 911.0821, found: 911.0820. ^{13}C NMR (63 MHz, CDCl$_3$).

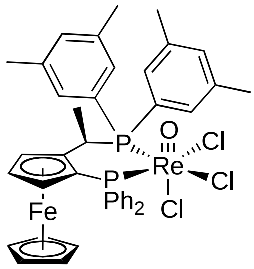

Exo-isomer: δ 140.46 (s), 139.59 (s), 137.51 (d, *J* = 8.2 Hz), 137.34 (d, *J* = 7.4 Hz), 135.56 (d, *J* = 8.4 Hz), 134.81 (s), 133.37 (s), 132.80 (s), 132.28 (d, *J* = 8.2 Hz), 131.94 (d, *J* = 9.5 Hz), 131.62 (d, *J* = 7.4 Hz), 130.01 (s), 129.42 (s), 128.63 (s), 128.03 (d, *J* = 11.1 Hz), 127.27 (d, *J* = 11.1 Hz), 92.54 (dd, *J* = 17.6, 3.5 Hz), 77.30 (s), 75.99 – 75.72 (m), 73.70 (s), 72.77 (s), 71.54 (s), 70.99 (s), 70.23 (d, *J* = 6.9 Hz), 32.70 (d, *J* = 29.9 Hz), 21.70 (s), 21.29 (s), 15.28 (dd, *J* = 4.9, 1.7 Hz). ^{31}P NMR (101 MHz, CDCl$_3$) δ 1.33 (d, *J* = 15.7 Hz), -30.73 (d, *J* = 15.9 Hz).

[ReOCl$_3$(2e)] (7e)

From 67 mg of [ReOCl$_3$(AsPh$_3$)$_2$] (0.073 mmol, 1 equiv.) and 45 mg of **2e** (0.074 mmol, 1 equiv.) according to the general method to give a brown

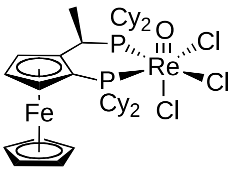

powder. Yield 48 mg (73%). X-ray quality crystals were obtained by layering a saturated dichloromethane solution with diethylether. ^{1}H NMR (250 MHz, CD_2Cl_2) δ 4.74 (s, 1H, *H*Cp), 4.55 (s, 1H, *H*Cp), 4.46 (s, 1H, *H*Cp), 4.30 (s, 5H, Cp), 3.50 (s, 1H, Cy), 3.01 (s, 1H, Cy), 2.80 (q, *J* = 13.3 Hz, 1H, *H*C(Me)), 2.48 (s, 2H, Cy), 2.30 (d, *J* = 9.4 Hz, 1H, Cy), 2.10 (d, *J* = 7.4 Hz, 3H), 2.05 (d, *J* = 7.4 Hz, 3H), 1.85 (m, Cy), 1.53 (m, Cy), 1.39 (m, Cy), 1.25 – 0.97 (m, Cy), 0.85 (m, Cy). ^{13}C NMR (63 MHz, CD_2Cl_2) δ 91.75 (bs), 71.27 (s), 70.50 (s), 70.39 (s), 70.09 (s), 70.00 (s), 40.53 (d, *J* = 16.8 Hz), 36.94 (d, *J* = 23.3 Hz), 32.17 (d, *J* = 34.6 Hz), 30.02 (d, *J* = 5.5 Hz), 29.71 (d, *J* = 7.1 Hz), 28.96 (s), 28.89 – 28.38 (m), 27.98 (d, *J* = 9.6 Hz), 27.69 (d, *J* = 2.9 Hz), 27.50 (d, *J* = 1.8 Hz), 26.74 (d, *J* = 4.1 Hz), 26.55 (d, *J* = 4.4 Hz). ^{31}P NMR (101 MHz, CD_2Cl_2) δ 6.19 (d, *J* = 13.4 Hz), -27.57 (d, *J* = 13.7 Hz). HR-MALDI MS: Monoisotopic mass ($[M-Cl]^+$) *m/z*, calcd: 879.20849, found: 879.2065.

[ReOCl$_3$(2f)], mixture of isomers (7f)

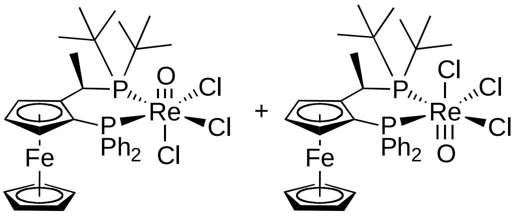

From 49.1 mg of [ReOCl$_3$(AsPh$_3$)$_2$] (0.053 mmol, 1 equiv.) and 31.5 mg of **2f** (0.058 mmol, 1.1 equiv.) according to the general method to give a brown powder. Yield 44 mg (97%). X-ray quality crystals of *endo*-**7f** were obtained by layering a saturated chloroform solution of the isomer mixture with *n*-hexane. ^{1}H NMR (300 MHz, $CDCl_3$) δ 8.46 – 8.32 (m, Ph), 8.25 – 8.13 (m, Ph), 8.13 – 7.96 (m, Ph), 7.85 (d, *J* = 7.4 Hz, Ph), 7.80 – 7.71 (m, Ph), 7.64 (t, *J* = 7.3 Hz, Ph), 7.45 (bs, Ph), 7.33 (bs, Ph), 5.38 (dt, *J* = 12.9, 6.9 Hz, 1H, *H*CMe), 4.79 (s, 1H, *H*Cp), 4.70 (s, 1H, *H*Cp), 4.66 (s, 1H, *H*Cp), 4.44 (s, 1H, *H*Cp), 4.33 (s, 5H, Cp (*exo*)), 4.09 (s, 1H, *H*Cp), 3.87 (dt, *J* = 17.0, 7.2 Hz, 1H, *H*CMe), 3.76 (s, 5H, Cp (*endo*)), 3.56 (s, 1H, *H*Cp), 2.29 (dd, *J* = 9.2, 7.5 Hz, 3H, HC*Me* (*exo*)), 2.19 (dd, *J* = 9.9, 7.6 Hz, 3H, HC*Me* (*endo*)), 1.56 (s, 9H, *Me*(*t*-but) (*exo*)), 1.51 (s, 9H, *Me*(*t*-but) (*exo*)), 1.15 (s, 9H, *Me*(*t*-but) (*endo*)), 1.10 (s, 9H, *Me*(*t*-but) (*endo*)). ^{13}C NMR (63 MHz, $CDCl_3$) δ 138.05 (d, *J* = 50.0 Hz), 136.08 (d, *J* = 8.4 Hz), 135.20 (d, *J* = 8.1 Hz), 135.05 (d, *J* = 47.5 Hz), 133.80

(s), 133.39 (d, *J* = 8.9 Hz), 132.98 (d, *J* = 10.4 Hz), 132.36 (s), 131.46 (d, *J* = 2.6 Hz), 131.20 (s), 130.69 (d, *J* = 2.3 Hz), 130.51 (s), 130.17 (s), 128.74 (s), 128.55 (s), 128.11 (d, *J* = 4.5 Hz), 127.97 (s), 127.89 (d, *J* = 2.4 Hz), 127.69 (d, *J* = 1.5 Hz), 127.51 (d, *J* = 1.0 Hz), 93.62 (s), 82.11 (s), 77.36 (s), 75.91 (s), 75.70 (d, *J* = 6.6 Hz), 72.22 (s), 71.67 (s), 71.06 (d, *J* = 8.1 Hz), 70.63 (s), 69.92 (d, *J* = 7.8 Hz), 45.33 (d, *J* = 8.9 Hz), 44.02 (d, *J* = 6.5 Hz), 43.24 (d, *J* = 9.7 Hz), 41.55 (d, *J* = 10.4 Hz), 39.04 (d, *J* = 10.0 Hz), 33.19 (s), 32.11 (s), 30.52 (s), 19.71 (s), 18.67 (s). ^{31}P NMR (101 MHz, $CDCl_3$) δ 27.61 (d, *J* = 12.0 Hz, *exo*), 23.14 (d, *J* = 14.6 Hz, *endo*), -27.55 (d, *J* = 11.9 Hz, *exo*), -33.81 (d, *J* = 14.7 Hz, *endo*). HR-MALDI MS: Monoisotopic mass ($[M-Cl]^+$) *m/z*, calcd: 815.0820, found: 815.0826

[ReOCl$_3$(2g)], mixture of isomers (7g)

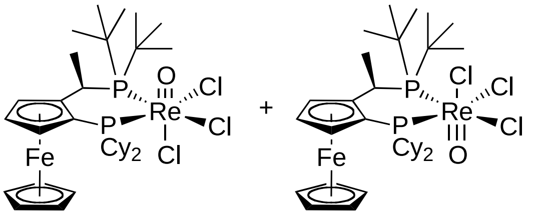

From 49 mg of [ReOCl$_3$(AsPh$_3$)$_2$] (0.053 mmol, 1 equiv.) and 32 mg of **2g** (0.058 mmol, 1.1 equiv.) according to the general method to give a brown solid. Yield 39 mg (85%). X-ray quality crystals were obtained by layering a saturated dichloromethane solution with *n*-hexane. ^{1}H NMR (250 MHz, CD_2Cl_2) δ 4.71 (s, 1H, *H*Cp), 4.65 (s, 1H, *H*Cp), 4.63 (s, 1H, *H*Cp), 4.59 (s, 1H, *H*Cp), 4.56 (s, 1H, *H*Cp), 4.50 (s, 1H, *H*Cp), 4.37 (s, 5H, Cp), 4.32 (s, 5H, Cp), 3.82 (dt, *J* = 13.2, 5.5 Hz, 1H, *H*CMe), 3.64 – 3.41 (m, 1H, *H*CMe), 3.09 (bs, Cy), 2.99 – 2.50 (m, Cy), 2.44 (bs, Cy), 2.25 (dd, *J* = 10.0, 7.2 Hz, HC*Me*), 2.16 (dd, *J* = 9.9, 7.2 Hz, HC*Me*), 1.94 (bs, Cy), 1.79 (bs, Cy), 1.75 (bs, Cy), 1.53 (d, *J* = 12.2 Hz, *t*-But), 1.41 (d, *J* = 13.3 Hz, *t*-But), 1.33 – 1.16 (m, *t*-But), 0.94 – 0.81 (m, Cy). ^{31}P NMR (101 MHz, CD_2Cl_2) δ 24.89 (s), 23.61 (d, *J* = 10.4 Hz), -23.29 (s), -37.56 (s). HR-MALDI MS: Monoisotopic mass ($[M-2Cl]^+$) *m/z*, calcd: 792.2077, found: 792.2085; ($[M-Cl]^+$) calcd: 827.1759, found: 827.1758

[ReOCl$_3$(2h)], mixture of isomers (7h)

From 25 mg of [ReOCl$_3$(AsPh$_3$)$_2$] (0.027 mmol, 1 equiv.) and 25 mg of **2h** (0.029 mmol, 1.1 equiv.) according to the general method to give a brown

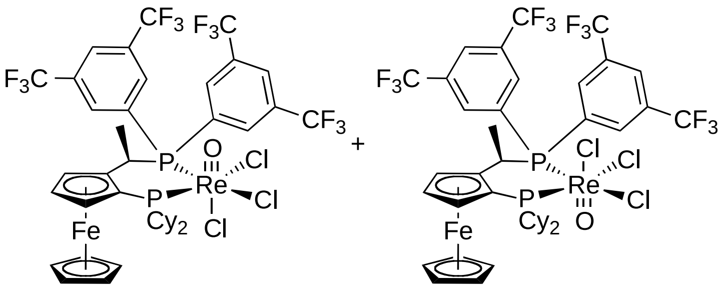

powder. Yield 5.3 mg (16%).^{1}H NMR (300 MHz, CD_2Cl_2) δ 8.22 (d, *J* = 8.4 Hz, Ar), 8.13 (d, *J* = 7.4 Hz, Ar), 7.98 (bs, Ar), 7.61 (bs, Ar), 4.99 (s, 1H, *H*Cp), 4.78 (d, *J* = 8.5 Hz, 1H, *H*Cp), 4.64 (s, 1H, *H*Cp), 4.58 (s, 1H, *H*Cp), 4.41 (s, 5H, Cp), 4.40 (s, 5H, Cp), 4.30 (d, *J* = 8.8 Hz, 1H, *H*Cp), 4.25 (s, 1H, *H*Cp), 3.95 – 3.83 (m, 1H, *H*CMe), 3.48 (m, 1H, *H*CMe), 2.90 (d, *J* = 12.1 Hz, Cy), 2.82 (bs, Cy), 2.57 (bs, Cy), 2.34 (bs, Cy), 2.12 (bs, Cy), 2.07 – 1.78 (m, Cy), 1.70 (dd, *J* = 13.2, 6.7 Hz, 3H, Me), 1.64 (dd, *J* = 13.8, 7.0 Hz, 3H, Me), 1.53 (bs, Cy), 1.47 – 1.20 (m, Cy), 0.92 – 0.83 (m, 1H, Cy). ^{31}P NMR (121 MHz, CD_2Cl_2) δ 2.71 (s), -4.26 (s), -10.27 (s), -18.27 (s). ^{19}F NMR (188 MHz, CD_2Cl_2) δ -63.30 (s), -63.43 (s), -63.46 (s), -63.47 (s). HR-MALDI MS: Monoisotopic mass ($[M-Cl]^+$) *m/z*, calcd: 1139.0629, found: 1139.0646.

[ReOCl$_3$(2i)] (7i)

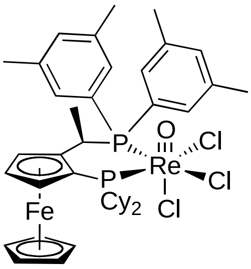

From 61.8 mg of [ReOCl$_3$(AsPh$_3$)$_2$] (0.067 mmol, 1 equiv.) and 44.9 mg of **2i** (0.069 mmol, 1 equiv.) according to the general method to give a brown solid. Yield 65 mg (>99%). X-ray quality crystals were obtained by layering a saturated dichloromethane solution with *n*-hexane. ^{1}H NMR (250 MHz, CD_2Cl_2) δ 7.39 (s, 1H, Xyl), 7.35 (s, 1H, Xyl), 7.17 (s, 1H, Xyl), 6.98 (s, 1H, Xyl), 6.94 (s, 1H, Xyl), 4.61 (bs, 1H, *H*CMe), 4.54 (bs, 2H, *H*Cp), 4.35 (s, 1H, *H*Cp), 4.33 (s, 5H, Cp), 3.12 (dd, *J* = 22.8, 11.6 Hz, 1H, Cy), 2.88 (bs, 1H, Cy), 2.72 (d, *J* = 11.4 Hz, 1H, Cy), 2.35 (s, 6H, *Me*(Xyl)), 2.13 (s, 6H, *Me*(Xyl)), 2.08 (d, *J* = 8.9 Hz, Cy), 1.97 – 1.67 (m, Cy), 1.57 (dd, *J* = 13.3, 7.1 Hz, 3H, HC*Me*), 1.49 – 1.13 (m, Cy), 1.13 – 0.71 (m, Cy), 0.38 (bs, Cy). ^{13}C NMR (63 MHz, CD_2Cl_2) δ 137.95 (s), 137.79 (s), 137.61 (s), 133.39 (d, *J* = 2.0 Hz), 133.35 (d, *J* = 1.4 Hz), 133.09 (d, *J* = 7.5 Hz), 132.48 (d, *J* = 6.6 Hz), 129.96 (s), 129.13 (s), 91.34 (s), 76.44 (s), 71.62 (s), 70.27 (d, *J* = 5.8 Hz), 42.62 (d, *J* = 27.5 Hz), 34.33 (d, *J* = 28.2 Hz), 30.05 (d, *J* = 3.3 Hz), 28.99 (s), 28.81 (s), 28.50 (s), 28.06 (s), 27.89 (s),

27.65 (s), 27.46 (s), 27.01 (d, *J* = 2.0 Hz), 26.90 (d, *J* = 1.3 Hz), 26.33 (s), 21.87 (s), 21.37 (s), 15.66 (d, *J* = 5.3 Hz). ^{31}P NMR (101 MHz, CD_2Cl_2) δ 1.45 (bs), -20.41 (bs). HR-MALDI MS: Monoisotopic mass ($[M-Cl]^+$) *m/z*, calcd: 923.1777, found: 923.1776; ($[M+Na]^+$) calcd: 981.1341, found: 981.1340

[ReOCl$_3$(2j)] (7j)

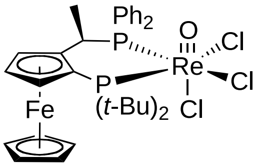

From 47 mg of $[ReOCl_3(AsPh_3)_2]$ (0.051 mmol, 1 equiv.) and 30.6 mg of **2j** (0.056 mmol, 1.1 equiv.) according to the general method to give a brown solid. Yield 31.4 mg (72%). ^{1}H NMR (250 MHz, CD_2Cl_2) δ 7.91 – 7.21 (m, Ph), 5.08 (s, 1H, *H*Cp), 5.00 (dd, *J* = 15.4, 7.4 Hz, 1H, *H*CMe), 4.84 (s, 1H, *H*Cp), 4.76 (s, 1H, *H*Cp), 4.28 (s, 5H, Cp), 2.07 (s, 9H, *t*-but), 2.02 (s, 9H, *t*-but), 1.64 (dd, *J* = 13.2, 7.3 Hz, 3H, HC*Me*). ^{13}C NMR (63 MHz, CD_2Cl_2) δ 134.95 (d, *J* = 7.3 Hz), 134.60 (d, *J* = 7.1 Hz), 131.98 (d, *J* = 2.6 Hz), 131.63 (d, *J* = 2.9 Hz), 128.63 (d, *J* = 3.8 Hz), 128.47 (d, *J* = 4.6 Hz), 90.82 (dd, *J* = 12.7, 5.1 Hz), 78.61 (s), 76.32 (d, *J* = 29.0 Hz), 72.75 (s), 71.57 (s), 71.18 (d, *J* = 5.3 Hz), 45.21 (d, *J* = 16.8 Hz), 43.71 (d, *J* = 16.6 Hz), 34.50 (d, *J* = 28.7 Hz), 32.76 (s), 31.05 (s), 16.66 (d, *J* = 6.1 Hz). ^{31}P NMR (101 MHz, CD_2Cl_2) δ 18.12 (d, *J* = 12.8 Hz), 2.97 (d, *J* = 13.2 Hz), -8.18 (d, *J* = 13.3 Hz), -8.69 (d, *J* = 13.0 Hz). HR-MALDI MS: Monoisotopic mass ($[M-Cl]^+$) *m/z*, calcd: 815.0820, found: 815.0816.

[ReOBr$_3$(2k)], mixture of isomers (7k)

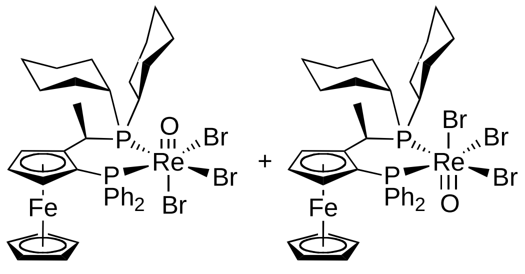

From 138.7 mg of $[ReOBr_3(AsPh_3)_2]$ (0.131 mmol, 1 equiv.) and 82.6 mg of **2a** (0.139 mmol, 1 equiv.) according to the general method to give a greenish-brown solid. Yield 132 mg (97%). ^{1}H NMR (250 MHz, CD_2Cl_2) δ 8.31 (dd, *J* = 16.7, 8.7 Hz, Ph), 8.15 – 7.97 (m, Ph), 7.64 – 7.52 (m, Ph), 7.48 (s, Ph), 7.35 (bs, Ph), 7.34 (s, Ph), 7.26 (m, Ph), 5.29 – 5.13 (m, 1H, *H*CMe), 4.94 (s, 1H, *H*Cp), 4.74 (s, 1H, *H*Cp), 4.65 – 4.59 (m, 1H, *H*Cp), 4.56 (d, *J* = 1.9 Hz, 1H, *H*Cp), 4.47 (s, 1H, *H*Cp), 4.27 (s,

5H, Cp), 4.25 (s, 1H, *H*Cp), 3.78 (s, 5H, Cp), 3.72 – 3.49 (m, 1H, *H*Cp), 2.82 – 2.58 (m, Cy), 2.44 – 2.22 (m, Cy), 2.13 (dd, *J* = 12.2, 7.5 Hz, 3H, Me), 2.05 (dd, *J* = 12.0, 8.4 Hz, 3H, Me), 1.98 – 1.46 (m, Cy), 1.42 (d, *J* = 8.6 Hz, Cy), 1.34 – 0.83 (m, Cy), 0.82 – 0.60 (m, Cy), 0.58 – 0.33 (m, Cy). ^{13}C NMR (63 MHz, CD_2Cl_2) δ 142.13 (d, *J* = 52.8 Hz), 136.28 (d, *J* = 8.0 Hz), 135.93 (d, *J* = 8.2 Hz), 135.70 (d, *J* = 9.7 Hz), 133.24 (d, *J* = 61.4 Hz), 133.09 (d, *J* = 9.9 Hz), 132.31 (d, *J* = 8.6 Hz), 131.94 (d, *J* = 2.6 Hz), 131.78 (s), 131.29 (s), 130.75 (d, *J* = 2.1 Hz), 128.23 (s), 128.05 (s), 127.94 (s), 127.83 (d, *J* = 5.7 Hz), 92.10 (dd, *J* = 17.8, 2.3 Hz), 91.13 (d, *J* = 14.4 Hz), 76.83 (d, *J* = 7.2 Hz), 76.36 (d, *J* = 2.4 Hz), 73.03 (d, *J* = 5.7 Hz), 72.67 (d, *J* = 9.0 Hz), 71.95 (s), 71.85 (s), 71.63 (s), 71.47 – 71.23 (m), 71.03 (s), 70.15 (d, *J* = 8.9 Hz), 65.92 (s), 41.54 (d, *J* = 19.7 Hz), 38.74 (d, *J* = 18.5 Hz), 36.69 (d, *J* = 16.3 Hz), 32.69 (d, *J* = 22.8 Hz), 31.00 (d, *J* = 5.4 Hz), 30.67 (d, *J* = 4.0 Hz), 30.42 (d, *J* = 4.1 Hz), 30.25 (s), 28.61 (s), 28.41 (d, *J* = 6.7 Hz), 28.15 (s), 27.99 (s), 27.86 (s), 27.64 (s), 27.50 (s), 27.22 (s), 27.04 (s), 26.92 (s), 26.72 (s), 26.60 (s), 26.50 (s), 26.18 (s), 26.08 (s), 18.21 (d, *J* = 6.8 Hz), 17.31 (s). ^{31}P NMR (101 MHz, CD_2Cl_2) δ -0.56 (s, *endo*), -3.73 (d, *J* = 14.8 Hz, *exo*), -29.68 (s, *endo*), -43.80 (d, *J* = 14.7 Hz, *exo*). HR-MALDI MS: Monoisotopic mass ([M-Br]$^+$) *m/z*, calcd: 957.0110, found: 957.0088.

[ReOCl$_3$(2l)], mixture of isomers (7l)

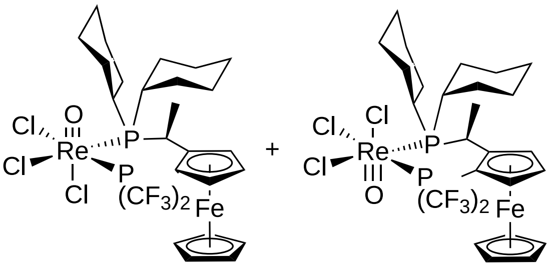

From 150.5 mg of [ReOCl$_3$(AsPh$_3$)$_2$] (0.1628 mmol, 1 equiv.) and 106.8 mg of **2l** (0.1833 mmol, 1.1 equiv.) according to the general method to give a brown solid. Yield 126 mg (87%). X-ray quality crystals of *exo*-**7l** were obtained by layering a saturated dichloromethane solution of the isomer mixture with *n*-hexane. ^{1}H NMR (250 MHz, CD_2Cl_2) δ 5.10 (s, 1H, *H*Cp), 5.07 (s, 1H, *H*Cp), 4.87 (d, *J* = 2.9 Hz, 2H, *H*Cp), 4.80 (bs, 2H, *H*Cp), 4.71 (dd, *J* = 14.2, 7.1 Hz, 1H, *H*CMe), 4.47 (s, 5H, Cp), 4.33 (s, 5H, Cp), 3.69 (dd, *J* = 21.8, 11.5 Hz, 1H, Cy), 3.59 – 3.43 (m, 1H, *H*CMe), 2.64 (q, *J* = 12.0 Hz, 1H, Cy), 2.36 (bs, Cy), 2.20 (bs, Cy), 2.11

(dd, *J* = 12.1, 7.3 Hz, 3H, Me), 2.01 (dd, *J* = 11.4, 7.1 Hz, 3H, Me), 1.89 (bs, Cy), 1.84 (bs, Cy), 1.67 (bs, Cy), 1.63 – 1.32 (m, Cy), 1.32 – 1.08 (m, Cy), 1.01 (bs, Cy). ^{13}C NMR (63 MHz, CD_2Cl_2) δ 94.16 (d, *J* = 23.0 Hz), 90.96 (d, *J* = 17.1 Hz), 77.23 (s), 76.89 (s), 75.17 (d, *J* = 2.0 Hz), 74.99 (d, *J* = 1.8 Hz), 74.15 (d, *J* = 7.7 Hz), 73.93 (d, *J* = 10.9 Hz), 73.09 (s), 72.19 (s), 38.42 (d, *J* = 18.2 Hz), 38.06 (d, *J* = 17.0 Hz), 36.88 (d, *J* = 20.8 Hz), 35.89 (d, *J* = 20.1 Hz), 31.13 (d, *J* = 5.1 Hz), 30.95 (d, *J* = 4.7 Hz), 30.73 (s), 30.20 (s), 29.84 (s), 29.63 (d, *J* = 7.7 Hz), 29.49 (d, *J* = 4.3 Hz), 28.81 (d, *J* = 9.3 Hz), 28.41 (d, *J* = 10.8 Hz), 28.04 (d, *J* = 10.5 Hz), 27.68 (d, *J* = 2.4 Hz), 27.61 (d, *J* = 2.1 Hz), 27.46 (d, *J* = 5.0 Hz), 27.43 (d, *J* = 5.9 Hz), 27.32 (s), 27.19 (s), 26.76 (d, *J* = 1.5 Hz), 26.55 (d, *J* = 1.5 Hz), 26.33 (d, *J* = 1.1 Hz), 26.18 (d, *J* = 1.4 Hz), 17.42 (d, *J* = 5.4 Hz), 17.01 (d, *J* = 5.6 Hz). ^{31}P NMR (101 MHz, CD_2Cl_2) δ 14.12 (d, *J* = 13.5 Hz), 12.57 (septd, *J* = 65.0, 12.9 Hz), 10.73 (d, *J* = 12.6 Hz), -3.55 (septd, *J* = 62.8, 13.3 Hz). ^{19}F NMR (188 MHz, CD_2Cl_2) δ -46.89 (dq, *J* = 66.9, 8.5 Hz), -49.09 (dq, *J* = 66.7, 7.7 Hz), -56.07 (dq, *J* = 63.3, 8.5 Hz), -57.60 (dq, *J* = 62.4, 7.7 Hz). HR-MALDI MS: Monoisotopic mass ([M-Cl]$^+$) *m/z*, calcd: 851.0254, found: 851.0244. EA: Anal. calcd. for $C_{26}H_{34}OF_6P_2Cl_3FeRe$ (%): C, 35.21; H, 3.86; P, 6.98. Found: C, 35.33; H, 3.85; P, 6.84.

[ReO$_2$I(2a)] (10)

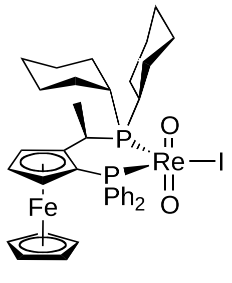

In a nitrogen-filled glove-box, 116.2 mg of **2a** (0.195 mmol, 1.1 equiv.) and 154 mg of [ReO$_2$I(PPh$_3$)$_2$] (0.177 mmol, 1 equiv.) were dissolved in 3 mL of dichloromethane. The resulting deep dark red solution was stirred at room temperature overnight. To this solution *n*-hexane was added until the precipitation of an orange solid occurred. The crude product was decanted, washed thoroughly with *n*-hexane and diethylether and dried *in vacuo* to afford an orange-brown paramagnetic powder. Yield 140 mg (84%). HR-ESI MS: Monoisotopic mass ([M-I]$^+$) *m/z*, calcd: 813.1720, found: 813.1750. FTIR (neat): *cm^{-1}* 3052.48, 2923.36, 2848.79, 1433.99, 1559.78, 1096.27, 908.60, 790.73, 744.09, 692.46. EA:

Anal. calcd. for $C_{36}H_{44}O_2P_2FeIRe$ (%): C, 46.02; H, 4.72; P, 6.59. Found: C, 45.85; H, 4.92; P, 6.44.

[ReNCl$_2$(2a)] (11)

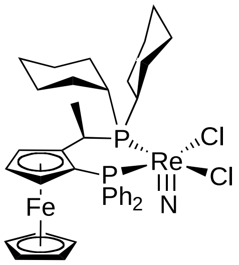

In an oven-dried Schlenk tube, 59.3 mg of **2a** (0.099 mmol, 1 eqiv.) and 52.8 mg of [NBu_4][$ReNCl_4$][8] were dissolved in 5 mL of dry toluene. The orange solution was stirred at 90 °C for two hours to give a dark brown solution. It was then allowed to cool to room temperature and 10 mL of *n*-hexane were added with a syringe leading to the precipitation of a brown solid. The solid was decanted and washed with *n*-hexane (3x10 mL) and dried *in vacuo* to give a green-brown solid. The crude product was dissolved in dichloromethane, filtered through celite and concentrated to dryness to give the product as a greenish-black solid. Yield 40.2 mg (47%). X-ray quality crystals (*endo*-isomer) were obtained by recrystallization from a saturated dichloromethane/*n*-hexane solution at -20 °C. ^{1}H NMR (250 MHz, CD_2Cl_2) δ 8.16 (dd, *J* = 12.1, 7.7 Hz, 2H, Ph), 7.65 (dd, *J* = 15.0, 6.9 Hz, 5H, Ph), 7.35 (dt, *J* = 13.2, 6.5 Hz, 3H, Ph), 4.82 (s, 1H, *H*Cp), 4.60 (s, 1H, *H*Cp), 4.45 (s, 1H, *H*Cp), 4.11 – 3.95 (m, 1H, *H*CMe), 3.68 (s, 5H, Cp), 3.05 (dd, *J* = 24.2, 11.9 Hz, 1H, Cy), 2.78 (dd, *J* = 24.9, 12.2 Hz, 1H, Cy), 2.28 (m, Cy), 1.94 (m, Cy), 1.73 (dd, *J* = 11.8, 7.5 Hz, 3H, Me), 1.36 – 1.20 (m, Cy), 1.14 (m, Cy), 1.00 – 0.77 (m, Cy), 0.24 (m, Cy), 0.08 (bs, Cy). ^{13}C NMR (63 MHz, CD_2Cl_2) δ 135.07 (d, *J* = 11.3 Hz), 134.29 (d, *J* = 9.2 Hz), 134.18 (d, *J* = 61.2 Hz), 131.32 (d, *J* = 2.8 Hz), 131.18 (d, *J* = 2.0 Hz), 129.95 (d, *J* = 51.6 Hz), 128.63 (d, *J* = 7.3 Hz), 128.46 (d, *J* = 9.0 Hz), 92.36 (d, *J* = 17.0 Hz), 75.26 (s), 72.33 (s), 70.60 (d, *J* = 15.3 Hz), 68.30 (s), 43.47 (d, *J* = 28.2 Hz), 36.27 (d, *J* = 21.0 Hz), 33.97 (d, *J* = 23.9 Hz), 30.94 (s), 29.15 (s), 28.84 (s), 28.13 (s), 27.47 – 25.80 (m), 25.18 (s), 24.84 (s), 23.35 (s), 16.03 (s). ^{31}P NMR (101 MHz, CD_2Cl_2) δ 31.37 (d, *J* = 11.9 Hz), 15.82 (d, *J* = 12.0 Hz).

[ReOCl$_2$(OEt)(2a)] (12)

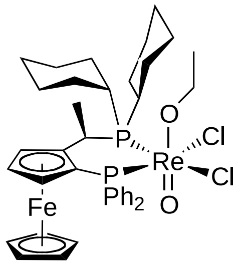

An attempted synthesis of **11** resulted in the formation of **12** as the major product. In an Schlenk tube, 6.5 mg of phenylhydrazine•HCl (0.045 mmol, 1 equiv.), 24.3 mg of triphenylphosphine (0.093 mmol, 2 equiv.) and 40.7 mg of **7a** (0.045 mmol, 1 equiv.) were mixed under argon and 2 mL of absolute ethanol along with 40 µL of water were added. The greenish suspension was refluxed for 2 hours under argon. The resulting orange suspension was allowed to cool to room temperature and filtered trough a glass fritte. The remaining solid was washed thoroughly with ethanol and water and dried *in vacuo* to give **12** as an orange powder. Yield 25.3 mg (62%). X-ray quality crystals were obtained by layering a saturated dichloromethane solution with diethyl ether. ^{1}H NMR (250 MHz, CD_2Cl_2) δ 8.20 (bs, 2H, Ph), 7.57 (m, 5H, Ph), 7.33 (bs, 3H, Ph), 4.76 (bs, 1H, *H*Cp), 4.63 (bs, 1H, *H*Cp), 4.59 (t, *J* = 2.5 Hz, 1H, *H*Cp), 3.81 – 3.71 (m, 1H, *H*CMe), 3.57 (s, 5H, Cp), 3.43 (m, 1H, OCH_2CH_3), 2.62 (td, *J* = 13.9, 7.1 Hz, 1H, Cy), 2.42 (dt, *J* = 18.9, 6.8 Hz, 1H, Cy), 2.19 (bs, Cy), 2.07 (bs, Cy), 1.96 (dd, *J* = 11.3, 7.4 Hz, 3H, HC*Me*), 1.82 (bs, Cy), 1.60 (bs, Cy), 1.49 – 1.38 (m, Cy), 1.33 – 1.19 (m, Cy), 1.15 (t, *J* = 7.0 Hz, Cy), 0.97 (m, Cy), 0.31 (t, *J* = 7.0 Hz, 3H, OCH_2CH_3). ^{13}C NMR (63 MHz, CD_2Cl_2) δ 135.95 (d, *J* = 9.2 Hz), 134.73 (d, *J* = 8.9 Hz), 131.80 (d, *J* = 2.5 Hz), 130.90 (d, *J* = 2.5 Hz), 128.54 (d, *J* = 10.6 Hz), 127.93 (d, *J* = 10.2 Hz), 93.45 (dd, *J* = 19.3, 1.8 Hz), 76.34 (s), 71.49 (s), 71.20 (d, *J* = 6.7 Hz), 70.84 (d, *J* = 6.4 Hz), 66.86 (s), 37.70 (d, *J* = 20.8 Hz), 36.18 (dd, *J* = 20.7, 3.3 Hz), 29.00 (dd, *J* = 22.1, 4.9 Hz), 28.27 (d, *J* = 9.8 Hz), 28.19 (s), 27.87 (d, *J* = 11.9 Hz), 27.77 (d, *J* = 10.1 Hz), 27.01 (d, *J* = 13.4 Hz), 26.46 (s), 22.88 (s), 18.18 (d, *J* = 6.0 Hz), 15.31 (s). ^{31}P NMR (101 MHz, CD_2Cl_2) δ 18.45 (s), -10.65 (d, *J* = 13.0 Hz). HR-ESI MS: Monoisotopic mass ($[M-OEt]^+$) *m/z*, calcd: 867.1151, found: 867.1140.

[ReOCl$_3$(13a)] (14)

In an oven-dried Schlenk tube, 27.7 mg of [ReOCl$_3$(AsPh$_3$)$_2$] (0.030 mmol, 1 equiv.) and 30 mg of **13a** (0.032 mmol, 1.1 equiv.) were dissolved in 2 mL of dry dichloromethane under argon. The mixture was stirred at room temperature overnight. The resulting dark green solution was concentrated to

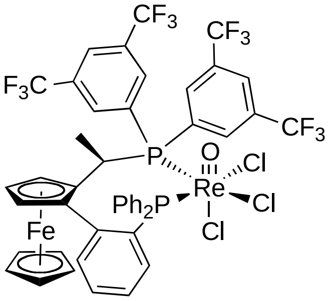

a minimum of its volume by blowing a stream of N$_2$ at room temperature and 10 mL of *n*-pentane were added. The mixture was cooled down in a 2-propanol/dry ice bath. The precipitate was decanted, washed with *n*-pentane and dried *in vacuo* to give a green solid. Yield 38 mg (>99%). ^{1}H NMR (250 MHz, CD$_2$Cl$_2$) δ 8.60 – 8.46 (m, Ph), 8.18 (s, Ph), 8.04 (d, *J* = 8.0 Hz, Ph), 7.99 (bs, Ph), 7.94 – 7.73 (m, Ph), 7.70 – 7.42 (m, Ph), 7.37 (m, Ph), 7.27 (m, Ph), 4.23 (s, 5H, Cp), 4.17 (s, Cp, minor isomer), 3.90 – 3.82 (m, 1H, *H*Cp), 3.52 – 3.37 (m, 1H, *H*CMe), 3.42 (s, 1H, *H*Cp), 3.08 (d, *J* = 1.8 Hz, 1H, *H*Cp), 1.85 (dd, *J* = 12.9, 7.6 Hz, Me, minor isomer), 1.47 (dd, *J* = 12.1, 7.1 Hz, 3H, Me). ^{31}P NMR (121 MHz, CD$_2$Cl$_2$) δ 53.66 (d, *J* = 8.6 Hz, minor isomer), -6.02 (d, *J* = 10.0 Hz), -24.16 (d, *J* = 8.0 Hz, minor isomer), -30.04 (d, *J* = 10.3 Hz). ^{19}F NMR (188 MHz, CD$_2$Cl$_2$) δ -63.14 (s, minor isomer), -63.31 (s), -63.43 (s, minor isomer), -63.48 (s). HR-MALDI MS: Monoisotopic mass (M+H$^+$) *m/z*, calcd: 1238.9766, found: 1238.9758.

[ReOCl$_3$(13b)] (15)

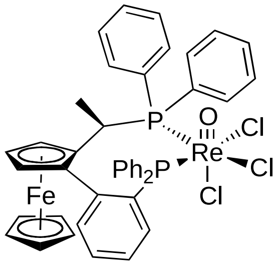

In a Schlenk tube, 2 mL of dry dichloromethane were added to a mixture of 30 mg of **13b** (0.0455 mmol, 1 equiv.) and 40 mg of [ReOCl$_3$(AsPh$_3$)$_2$] (0.043 mmol, 1 equiv.). The mixture was stirred at room temperature overnight. To the resulting dark green solution, 15 mL of *n*-hexane were added leading to the precipitation of a green solid. It was decanted and washed thoroughly with *n*-hexane and dried *in vacuo* giving a light green solid. Yield 28 mg (66%). ^{1}H NMR (250 MHz, CD$_2$Cl$_2$) δ 8.50 (bs, Ph), 8.01 – 7.84 (m, Ph), 7.74 (s, Ph), 7.47 (m, Ph), 7.26 (m, Ph), 4.18 (s, 5H, Cp), 3.77 (s, 1H, *H*Cp), 3.57 (s, 1H, *H*Cp), 3.48 – 3.33 (m, 1H, *H*CMe), 2.99 (s, 1H, *H*Cp), 1.52 (dd, *J* = 11.4, 6.9 Hz, 3H, Me). ^{13}C NMR (63 MHz, CD$_2$Cl$_2$) δ 140.29 (d, *J* = 1.3 Hz), 140.14 (d, *J* = 2.3 Hz), 137.22 (d, *J* = 6.8 Hz), 136.91 (d, *J* = 7.5 Hz), 136.52 (d, *J* = 45.4 Hz), 135.78 (s), 135.23 (d, *J* = 5.4 Hz), 133.70 (s), 133.57 (s), 133.48 (d, *J* =

68.1 Hz), 131.98 (d, *J* = 2.2 Hz), 131.75 (s), 131.12 (d, *J* = 2.5 Hz), 131.03 (d, *J* = 57.8 Hz), 130.64 (d, *J* = 2.4 Hz), 130.45 (d, *J* = 50.8 Hz), 128.81 (d, *J* = 9.7 Hz), 128.20 (d, *J* = 9.7 Hz), 127.88 (d, *J* = 9.5 Hz), 127.72 (d, *J* = 38.6 Hz), 126.93 (d, *J* = 10.0 Hz), 92.98 (d, *J* = 8.0 Hz), 72.55 (s), 70.08 (s), 66.48 (s), 64.47 (d, *J* = 2.5 Hz), 29.78 (d, *J* = 18.7 Hz), 21.76 (d, *J* = 5.7 Hz). ^{31}P NMR (121 MHz, CD_2Cl_2) δ -3.90 (d, *J* = 10.6 Hz), -33.90 (d, *J* = 10.5 Hz). HR-MALDI MS: Monoisotopic mass (M+H$^+$) *m/z*, calcd: 967.03, found: 967.0.

[ReOCl$_2$(*i*-PrO)(2a)] (18)

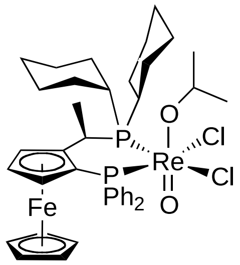

After the transfer-hydrogenation catalysis (*vide infra*) the product is extracted with *n*-hexane and the remaining insoluble orange solid is dried *in vacuo*. It is then dissolved in dichloromethane and this solution filtered through a plug of silica eluting with the same solvent. The solution is concentrated to dryness to give the product as a light orange powder. X-ray quality crystals were obtained by layering a saturated dichloromethane solution with *n*-hexane. ^{1}H NMR (300 MHz, CD_2Cl_2) δ 8.16 (s, 2H, Ph), 7.87 – 7.69 (m, 2H, Ph), 7.52 (s, 3H, Ph), 7.41 – 7.22 (m, 3H, Ph), 4.76 (s, 1H, *H*Cp), 4.71 (s, 1H, *H*Cp), 4.64 (s, 1H, *H*Cp), 3.83 – 3.66 (m, 1H, *H*C(Me)$_2$), 3.56 (s, 5H, Cp), 3.27 (dd, *J* = 12.1, 5.8 Hz, 1H, *H*CMe), 3.18 (dd, *J* = 24.4, 11.9 Hz, 1H, Cy), 2.85 (s, 1H, Cy), 2.63 (dd, *J* = 22.9, 12.3 Hz, 1H, Cy), 2.11 – 1.94 (m, Cy), 1.89 (dd, *J* = 10.2, 7.6 Hz, 3H, HC*Me*), 1.75 (bs, Cy), 1.55 (bs, Cy), 1.49 – 1.32 (m, Cy), 1.19 – 0.99 (m, Cy), 0.85 (dd, *J* = 24.3, 11.8 Hz, Cy), 0.66 (s, Cy), 0.61 (d, *J* = 6.0 Hz, 3H, HC(*Me*)$_2$), 0.05 (d, *J* = 6.0 Hz, 3H, HC(*Me*)$_2$). ^{13}C NMR (63 MHz, CD_2Cl_2) δ 137.94 (d, *J* = 58.8 Hz), 135.84 (d, *J* = 9.3 Hz), 135.33 (d, *J* = 8.8 Hz), 133.80 (d, *J* = 55.9 Hz), 131.49 (d, *J* = 2.5 Hz), 130.98 (d, *J* = 2.4 Hz), 128.31 (d, *J* = 10.5 Hz), 127.91 (d, J = 10.3 Hz), 93.63 (d, J = 19.0 Hz), 76.21 (d, J = 2.0 Hz), 75.49 (s), 71.38 (s), 70.86 (s), 70.71 (s), 37.66 (d, J = 20.5 Hz), 36.92 (d, J = 21.4 Hz), 36.02 (d, J = 19.5 Hz), 29.99 (s), 29.06 (d, J = 6.0 Hz), 28.24 (s), 28.09 (d, J = 3.9 Hz), 27.81 (s), 27.64 (s), 27.46 (s), 27.14 (s), 26.44 (d, J = 6.6 Hz), 25.92 (s), 23.24 (s), 22.52 (s), 17.32 (d, J = 5.4 Hz). ^{31}P NMR (101

MHz, CD_2Cl_2) δ 15.03 (bs), -11.44 (d, J = 12.7 Hz). HR-MALDI MS: Monoisotopic mass ($[M-Cl]^+$) *m/z*, calcd: 891.1949, found: 891.1935

6.2.2. Transfer hydrogenation catalysis

General procedure for the catalytic transfer hydrogenation of ketones

In an oven-dried Young-Schlenk tube, the corresponding amount of catalyst (ca. 1%) was dissolved in dry 2-propanol at room temperature. When the catalyst was synthesized *in situ*, the ligand and the corresponding rhenium precursor were mixed in a 1:1 ratio (ca. 1% each). To this solution 1 equiv. of the ketone substrate is added (final concentration ca. 0.4 M). Then an excess of triethylamine (8 - 20 %) is added and the system heated for 20 - 24 hours at 80 °C. The mixture is then allowed to cool to room temperature and the solvent and volatiles are removed *in vacuo*. *n*-Hexane is then added and the solution filtered through a plug of silica eluting with *n*-hexane and concentrated in the rotavapor to give the crude product. The yields were determined by integration on ^{1}H NMR with 90° pulse width = 3.33 µs and relaxation delay between scans = 3 s. The ee% was measured by chiral HPLC. In every case the absolute configuration of the product was determined by comparison of the retention time with that of an authentic sample of a pure enantiomer.

1-Phenylethanol (Table 2, Table 3 and Table 4, entry 1)

^{1}H NMR (300 MHz, $CDCl_3$) δ 7.23 (dd, *J* = 8.8, 3.2 Hz, Ph), 7.20 – 7.12 (m, Ph), 4.78 (q, *J* = 6.4 Hz, 1H, HCMe), 1.80 (bs, 1H, OH), 1.39 (d, *J* = 6.5 Hz, 3H, Me). HPLC OD-H, *n*-Hex/*i*-PrOH 90:10, 0.5 mL/min. Ret. time (min): *R* 12.256, *S* 13.811.

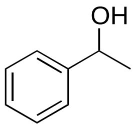

1-Phenylpropan-1-ol (Table 4, entry 2)

^{1}H NMR (300 MHz, $CDCl_3$) δ 7.27 (bs, Ph), 7.20 (dd, *J* = 8.6, 4.3 Hz, Ph), 4.51 (t, *J* = 6.6 Hz, 1H, HCH_2CH_3), 1.85 (bs, 1H, O*H*), 1.81 – 1.63 (m, 2H, HCH_2CH_3), 0.84 (t, *J* = 7.4 Hz,

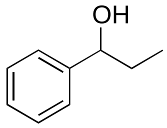

3H, HCH_2CH_3). HPLC OB-H, *n*-Hex/*i*-PrOH 90:10, 0.5 mL/min. Ret. time (min): *S* 10.216, *R* 11.663.

2,2,2-Trifluoro-1-phenylethanol (Table 4, entry 3)

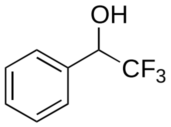

^1H NMR (300 MHz, $CDCl_3$) δ 7.39 (bs, Ph), 7.37 – 7.29 (m, Ph), 4.93 (dd, *J* = 13.2, 6.5 Hz, 1H, $HCCF_3$), 3.30 (bs, 1H, O*H*). ^{19}F NMR (188 MHz, $CDCl_3$) δ -78.29 (d, *J* = 6.7 Hz). HPLC OB-H, *n*-Hex/*i*-PrOH 99:1, 0.8 mL/min. Ret. time (min): *R* 24.266, *S* 26.508.

4-(1-Hydroxyethyl)benzonitrile (Table 4, entry 4)

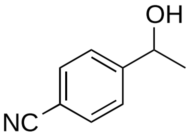

^1H NMR (250 MHz, $CDCl_3$) δ 7.57 (d, *J* = 8.2 Hz, 2H, Ph), 7.43 (d, *J* = 8.2 Hz, 2H, Ph), 4.90 (dd, *J* = 12.5, 6.2 Hz, 1H, *H*CMe), 2.20 (bs, 1H, O*H*), 1.43 (d, *J* = 6.5 Hz, 3H, Me). HPLC OJ, *n*-Hex/*i*-PrOH 90:10, 0.7 mL/min. Ret. time (min): *S* 21.604, *R* 25.542.

1-(4-Methoxyphenyl)ethanol (Table 4, entry 5)

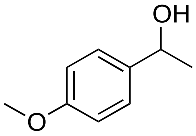

^1H NMR (250 MHz, $CDCl_3$) δ 7.23 (d, *J* = 8.6 Hz, 2H, Ph), 6.81 (d, *J* = 8.7 Hz, 2H, Ph), 4.79 (q, *J* = 6.4 Hz, 1H, *H*CMe), 3.73 (s, 3H, O*Me*), 1.72 (bs, 1H, O*H*), 1.41 (d, *J* = 6.4 Hz, 3H, HC*Me*). HPLC OB-H, *n*-Hex/*i*-PrOH 90:10, 0.5 mL/min. Ret. time (min): *S* 24.127, *R* 29.531.

1-(*p*-Tolyl)ethanol (Table 4, entry 6)

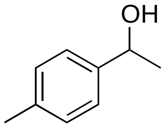

^1H NMR (300 MHz, $CDCl_3$) δ 7.19 (d, *J* = 7.9 Hz, 2H, Ph), 7.08 (d, *J* = 7.9 Hz, 2H, Ph), 4.78 (q, *J* = 6.4 Hz, 1H, *H*CMe), 2.27 (s, 3H, Ph*Me*), *1*.84 (bs, 1H, O*H*), 1.40 (d, *J* = 6.4 Hz, 3H, HC*Me*). HPLC OB-H, *n*-Hex/*i*-PrOH 90:10, 0.5 mL/min. Ret. time (min): 12.408, 13.813.

1-(4-Chlorophenyl)ethanol (Table 4, entry 7)

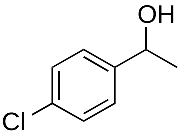

^{1}H NMR (250 MHz, $CDCl_3$) δ 7.23 (bs, 4H, Ph), 4.79 (q, *J* = 6.4 Hz, 1H, *H*CMe), 1.93 (bs, 1H, O*H*), 1.39 (d, *J* = 6.4 Hz, 3H, HC*Me*). HPLC OB-H, *n*-Hex/*i*-PrOH 98:2, 0.5 mL/min. Ret. time (min): 29.230, 31.707.

2,3-Dihydro-1*H*-inden-1-ol (Table 4, entry 8)

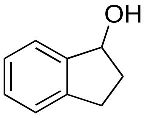

^{1}H NMR (300 MHz, $CDCl_3$) δ 7.37 – 7.31 (m, Ph), 7.18 (bs, Ph), 5.17 (t, *J* = 6.0 Hz, 1H, *H*COH), 2.96 (dd, *J* = 8.5, 4.9 Hz, 1H, $CH(OH)CH_2CH_2$), 2.76 (dd, *J* = 15.6, 8.0 Hz, 1H, $CH(OH)CH_2CH_2$), 2.42 (ddd, *J* = 13.1, 7.4, 5.1 Hz, 1H, $CH(OH)CH_2CH_2$), 1.87 (ddd, *J* = 13.7, 8.4, 6.3 Hz, 1H, $CH(OH)CH_2CH_2$), 1.79 (bs, 1H, O*H*). HPLC OB-H, *n*-Hex/*i*-PrOH 90:10, 0.5 mL/min. Ret. time (min): 11.472, 17.103.

1-(Naphthalen-1-yl)ethanol (Table 4, entry 9)

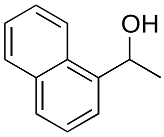

^{1}H NMR (300 MHz, $CDCl_3$) δ 8.02 (d, *J* = 8.3 Hz, 1H, Ar), 7.85 – 7.75 (m, 1H, Ar), 7.69 (d, *J* = 8.2 Hz, 1H, Ar), 7.58 (d, *J* = 7.1 Hz, 1H, Ar), 7.50 – 7.34 (m, 3H, Ar), 5.55 (q, *J* = 6.3 Hz, 1H, *H*CMe), 2.09 (bs, 1H, O*H*), 1.57 (d, *J* = 6.5 Hz, 3H, Me). HPLC OB-H, *n*-Hex/*i*-PrOH 90:10, 0.5 mL/min. Ret. time (min): *S* 17.372, *R* 20.052.

1-(Perfluorophenyl)ethanol (Table 4, entry 10)

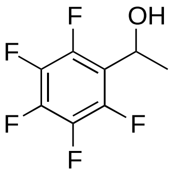

^{1}H NMR (200 MHz, $CDCl_3$) δ 5.56 – 4.78 (m, 1H, *H*CMe), 1.58 (d, *J* = 6.7 Hz, 3H, Me), 1.20 (bs, 1H, O*H*). ^{19}F NMR (188 MHz, $CDCl_3$) δ -144.61 (dd, *J* = 22.1, 8.1 Hz), -155.56 (t, *J* = 20.8 Hz), -161.92 (dt, *J* = 22.2, 8.3 Hz). HPLC AD-H, *n*-Hex/*i*-PrOH 98:2, 0.5 mL/min. Ret. time (min): 20.765, 24.905

6.3. Chiral Rhenium Hydrido Complexes and Catalytic Hydrogenation (Chapter 3)*

6.3.1. Synthesis of ligands and complexes

---

* Compounds **1c**, **19b**, **19c**, **23b**, **23c** and **25b** were synthesized by Mr. Pascal Engl as part of his Undergraduate Research Project in ETH Zürich under the supervision of the author.

Dimethyl{(*R*)-1-[(*S*)-2-(di(1-naphthyl)phosphino)ferrocenyl]-ethyl}amine (1c)[2]

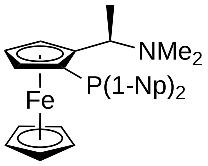

From 505.9 mg of Ugis's amine (1.986 mmol, 1 equiv.), 1.5 mL of *t*-butyllithium (1,6 M in pentane) (2.4 mmol, 1.2 equiv.) and 643.6 mg of chlorodi(1-naphthyl)phosphine (2.008 mmol, 1 equiv.), according to the general method (see section 5.2.1). It was purified by flash chromatography through silica, eluting with a mixture of *n*-hexane/ethyl acetate, 3:1 with 5% of NEt_3. Recrystallized at -20 °C from a saturated ethanol solution to give an orange solid. Yield 598.9 mg (69%). ^{1}H NMR (300 MHz, CD_2Cl_2) δ 9.70 (t, *J* = 7.6 Hz, 1H, Ar), 8.23 (dd, *J* = 8.4, 3.6 Hz, 1H, Ar), 7.95 (d, *J* = 8.1 Hz, 1H, Ar), 7.86 (d, *J* = 8.1 Hz, 1H, Ar), 7.83 – 7.70 (m, Ar), 7.61 (t, *J* = 7.5 Hz, 1H, Ar), 7.43 (dd, *J* = 6.0, 4.4 Hz, 1H, Ar), 7.34 (m, Ar), 7.29 – 7.16 (m, Ar), 4.50 (s, 1H, *H*Cp), 4.35 (s, 1H, *H*Cp), 4.06 (s, 1H, *H*Cp), 3.64 (s, 5H, Cp), 1.81 (s, 6H, N*Me*), 1.33 (d, *J* = 6.8 Hz, 3H, HC*Me*). ^{31}P NMR (121 MHz, CD_2Cl_2) δ -49.94 (s). HR-ESI MS: Monoisotopic mass (M-NMe_2) *m/z*, calcd: 497.12, found: 497.1.

General Method for the Synthesis of the Pigiphos Ligands (19)

In an oven-dried Schlenk tube, **1** (1 equiv.) was dissolved in degassed glacial acetic acid (to a concentration of 0,5 - 1 molar) and trifluoroacetic acid (TFA) was added (at least one equivalent). This mixture was heated to 50 °C. To this solution, the corresponding secondary phosphine (1.1 equiv.) was added and the mixture was stirred at 80 °C for four hours. The solvent and volatiles were removed *in vacuo* to give an orange sticky solid. It was dissolved in ethyl acetate and washed successively with a saturated $NaHCO_3$ solution, brine and water, dried over $MgSO_4$ and filtered. This was concentrated to dryness with a rotavapor to give the crude product. The crude was purified by either column chromatography or by recrystallization to give pure **19** as an orange solid.

Bis-{(*R*)-1-[(*S*)-2-(diphenylphosphino)ferrocenyl]ethyl}-cyclohexyl-phosphine), (*R*)-(*S*)-Pigiphos, (19a)[4a]

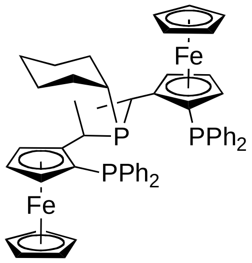

From 1396 mg of (*R,S*)-PPFA (**1a**) (3.163 mmol, 1 equiv.), 2.5 mL of TFA and 0.24 mL of cyclohexylphosphine (1.808 mmol, 1.1 equiv.) according to the general procedure. Purified by recrystallization from a saturated solution in dichloromethane/ethanol at -20 °C. Yield 913 mg (63%). ^{1}H NMR (300 MHz, CD_2Cl_2) δ 7.73 – 7.57 (m, 4H, Ph), 7.39 (s, 6H, Ph), 7.25 (d, *J* = 1.2 Hz, 5H, Ph), 7.19 (s, 5H, Ph), 4.27 (s, 1H, *H*Cp), 4.27 (s, 1H, *H*Cp), 4.24 (d, *J* = 2.3 Hz, 1H, *H*Cp), 4.09 (s, 1H, *H*Cp), 4.01 (s, 2H, *H*Cp), 3.90 (s, 1H, *H*Cp), 3.84 (s, 5H, Cp), 3.80 (s, 5H, Cp), 3.17 (qd, *J* = 6.9, 2.6 Hz, 1H, *H*CMe), 2.97 – 2.84 (m, 1H, *H*CMe), 1.64 (dd, *J* = 7.8 Hz, 3H, Me), 1.55 (dd, *J* = 7.1, 5.1 Hz, 3H, Me), 1.50 (s, Cy), 1.39 (dd, *J* = 25.9, 11.4 Hz, Cy), 1.29 – 1.15 (m, Cy), 1.01 (d, *J* = 6.1 Hz, Cy), 0.72 (t, *J* = 11.9 Hz, 1H, Cy). ^{31}P NMR (121 MHz, CD_2Cl_2) δ 17.57 (dd, *J* = 29.8, 11.1 Hz, *P*Cy), -25.52 (d, *J* = 17.4 Hz, *P*Ph_2), -25.69 (bs, *P*Ph_2).

Bis-{(*R*)-1-[(*S*)-2-(dicyclohexylphosphino)ferrocenyl]ethyl}cyclohexylphosphine)[4b] (19b)

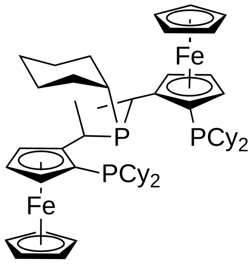

From 350 mg of **1b** (0.773 mmol, 1 equiv.), 60 µL of TFA (0.773 mmol, 1 equiv.) and 53.6 µL of cyclohexylphosphine (0.386 mmol, 1 equiv.) according to the general procedure. Purified by column chromatography over silica eluting with a mixture of *n*-hexane/ethyl acetate 12:1 and subsequent recrystallization from ethanol at -20°C. Yield 49 mg (14%). ^{1}H NMR (250 MHz, CD_2Cl_2) δ 4.51 (s, *H*Cp), 4.30 (s, *H*Cp), 4.18 (s, 5H, Cp), 4.14 (s, 5H, Cp), 4.07 (s, *H*Cp), 4.04 (s, *H*Cp), 3.02 (m, 1H, *H*CMe), 2.89 (m, 1H, *H*CMe), 2.14 (m, Cy), 1.97 – 0.79 (m, Cy). ^{31}P NMR (101 MHz, CD_2Cl_2) δ 10.42 (s), -14.93 (s), -16.02 (s).

Bis-{(*R*)-1-[(*S*)-2-(di(1-naphthyl)phosphino)ferrocenyl]ethyl}-cyclohexylphosphine)[4b] (19c)

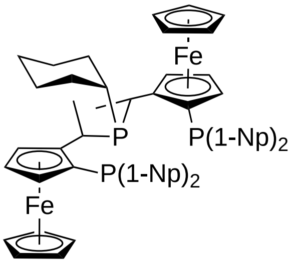

From 250 mg of **1c** (0.462 mmol, 1 equiv.), 34 µL of TFA (0.462 mmol, 1 equiv.) and 31 µL of cyclohexylphosphine (0.231 mmol, 1 equiv.) according to the general procedure. Purified by column chromatography over silica eluting with a mixture of *n*-hexane/ethyl acetate 14:1. Yield 112.5 mg (45%). ^{1}H NMR (250 MHz, CDCl$_3$) δ 9.69 (t, *J* = 7.6 Hz, 1H, Ar), 9.57 (t, *J* = 7.4 Hz, 1H, Ar), 8.20 (dd, *J* = 8.4, 3.0 Hz, 1H, Ar), 8.14 – 8.04 (m, 1H, Ar), 7.91 (t, *J* = 7.2 Hz, Ar), 7.86 – 7.67 (m, Ar), 7.65 – 7.52 (m, Ar), 7.52 – 7.39 (m, Ar), 7.39 – 7.14 (m, Ar), 4.30 (s, 2H, *H*Cp), 4.13 (s, 1H, *H*Cp), 3.83 (s, 3H, *H*Cp), 3.54 (s, 5H, Cp), 3.45 – 3.33 (m, 1H, *H*CMe), 3.24 (s, 5H, Cp), 2.91 – 2.76 (m, 1H, *H*CMe), 1.74 (t, *J* = 7.7 Hz, 3H, HC*Me*), 1.56 (s, Cy), 1.49 (dd, *J* = 6.8, 4.7 Hz, 3H, HC*Me*), 1.43 (s, Cy), 1.42 – 1.30 (m, Cy), 1.26 (s, Cy), 1.16 (d, *J* = 10.4 Hz, Cy), 1.02 – 0.78 (m, Cy), 0.75 – 0.55 (m, Cy). ^{31}P NMR (101 MHz, CDCl$_3$) δ 14.68 (dd, *J* = 35.6, 7.0 Hz), -51.28 (d, *J* = 7.4 Hz), -52.56 (d, *J* = 35.6 Hz).

[ReBr(CO)$_2$(19a)] (20)

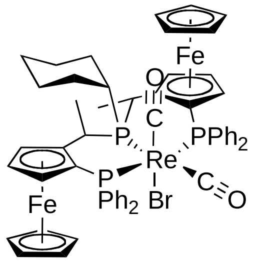

In an oven-dried Schlenk tube 51.6 mg of **19a** (0.057 mmol, 1.1 equiv.) and 21.3 mg of [ReBr(CO)$_5$] (0.025 mmol, 1 equiv.) were dissolved in 10 mL of dry tetralin and stirred at 200 °C overnight. The resulting solution was filtered out with a cannula to another Schlenk tube were 30 mL were added. The slurry mixture was stored at -20 °C overnight. The orange precipitate was decanted and washed with *n*-hexane until the washings were colorless. The solid was dried under high vacuum giving **20** as an orange-brown solid. Yield 57.1 mg (88%). ^{1}H NMR (300 MHz, CDCl$_3$) δ 8.48 – 8.34 (m, 2H, Ph), 8.22 – 8.10 (m, 2H, Ph), 8.04 – 7.91 (m, 2H, Ph), 7.47 (bs, 6H, Ph), 7.37 (t, *J* = 7.0 Hz, 2H, Ph), 7.23 – 7.16 (m, 3H, Ph), 7.16 – 7.04 (m, 3H, Ph), 5.28 – 5.16 (m, 1H, *H*CMe), 4.49 (s, 2H, *H*Cp), 4.33 (s, 2H, *H*Cp), 4.30 (s, 1H, *H*Cp), 4.25 (s, 5H, Cp), 3.70 (s, 3H, Cp), 3.32 (s, 1H, *H*Cp), 3.23 – 3.10 (m, 1H, *H*CMe), 2.08 – 1.96 (m, 3H, Me), 1.93 – 1.79 (m, Cy), 1.79 – 1.67 (m, 3H, Me), 1.53 (m, Cy), 1.32 – 1.11 (m, Cy), 1.10 – 0.75 (m, Cy), 0.46 (dd, *J* = 23.6, 12.6 Hz, 1H, Cy). ^{13}C

NMR (75 MHz, $CDCl_3$) δ 142.80 (d, *J* = 53.1 Hz), 138.69 (d, *J* = 47.6 Hz), 137.63 (d, *J* = 47.9 Hz), 136.17 (d, *J* = 10.9 Hz), 135.90 (d, *J* = 10.5 Hz), 133.84 (dd, *J* = 49.3, 3.0 Hz), 132.21 (d, *J* = 11.1 Hz), 130.21 (d, *J* = 1.8 Hz), 129.94 (d, *J* = 1.8 Hz), 128.76 (d, *J* = 1.0 Hz), 128.21 (d, *J* = 1.1 Hz), 127.97 (d, *J* = 9.9 Hz), 127.57 (d, *J* = 10.0 Hz), 127.22 (d, *J* = 9.6 Hz), 127.09 (d, *J* = 9.7 Hz), 94.90 (dd, *J* = 20.6, 3.5 Hz), 92.01 (dd, *J* = 15.0, 7.7 Hz), 77.36 (s), 76.08 (d, *J* = 5.8 Hz), 73.88 (s), 69.64 (d, *J* = 13.3 Hz), 69.55 (s), 69.23 (d, *J* = 7.8 Hz), 68.89 (d, *J* = 4.6 Hz), 67.90 (d, *J* = 8.3 Hz), 40.36 (d, *J* = 19.0 Hz), 32.33 – 32.04 (m), 30.67 (d, *J* = 7.6 Hz), 28.47 (d, *J* = 8.3 Hz), 27.64 (s), 27.35 (d, *J* = 7.3 Hz), 26.53 (s), 26.40 (d, *J* = 10.9 Hz), 18.36 (d, *J* = 6.6 Hz), 17.91 (d, *J* = 6.5 Hz). ^{31}P NMR (121 MHz, $CDCl_3$) δ 40.94 – 39.16 (m), 8.71 (dd, *J* = 166.0, 25.7 Hz), -5.67 (dd, *J* = 166.2, 21.0 Hz). HR-MALDI MS: Monoisotopic mass (M^+) *m/z*, calcd: 1230.0840, found: 1230.0854. FTIR (neat): cm^{-1} 3055.7, 2927.9, 2850.7, 1939.6, 1863.4, 1434.0, 1157.9, 1092.4, 822.8, 742.9, 698.9. EA: Anal. calcd. for $C_{56}H_{55}O_2P_3Fe_2BrRe$ (%): C, 54.56; H, 4.50; P, 7.55. Found: C, 54.63; H, 4.66; P, 7.56.

[ReCl(CO)$_2$(19a)] (21)

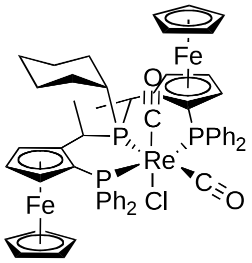

From 224 mg of **19a** (0.247 mmol, 1.1 equiv.) and 82.4 mg of [ReCl(CO)$_5$] (0.228 mmol, 1 equiv.) in a procedure analogous to the synthesis of **20**, but heating to 180 °C. Yield 229 mg (85%). ^1H NMR (300 MHz, $CDCl_3$) δ 8.38 – 8.27 (m, 2H, Ph), 8.15 – 8.06 (m, 2H, Ph), 8.06 – 7.95 (m, 2H, Ph), 7.48 (m, 6H, Ph), 7.38 (t, *J* = 7.1 Hz, 3H, Ph), 7.25 – 7.16 (m, 2H, Ph), 7.13 (d, *J* = 7.1 Hz, 3H, Ph), 5.08 – 4.94 (m, 1H, *H*CMe), 4.49 (d, *J* = 6.2 Hz, 2H, *H*Cp), 4.30 (d, *J* = 7.3 Hz, 1H, *H*Cp), 4.29 (s, 2H, *H*Cp), 4.25 (s, 5H, Cp), 3.67 (s, 5H, Cp), 3.29 (s, 1H, *H*Cp), 3.23 – 3.10 (m, 1H, *H*CMe), 2.01 (dd, *J* = 7.9 Hz, 3H, Me), 1.93 – 1.79 (m, 1H, Cy), 1.79 – 1.68 (m, 3H, Me), 1.55 (bs, Cy), 1.19 (d, *J* = 11.3 Hz, Cy), 1.13 – 0.76 (m, Cy), 0.46 (dd, *J* = 24.1, 12.1 Hz, Cy). ^{13}C NMR (63 MHz, CD_2Cl_2) δ 199.54 (d, *J* = 64.2 Hz), 194.49 (s), 142.53 (d, *J* = 54.4 Hz), 139.66 (d, *J* = 46.3 Hz), 137.82 (d, *J* = 47.8 Hz), 136.28 (d, *J* = 11.0 Hz), 136.06 (d, *J* = 10.3 Hz), 134.65 (d, *J* = 49.6 Hz), 132.49 (d, *J* = 11.1 Hz), 130.63 (d, *J* = 2.0 Hz), 130.30 (d, *J* = 1.7 Hz), 129.08 (d, *J* = 1.2 Hz), 128.52 (d, *J* = 1.7 Hz), 128.27 (d, *J* = 9.7 Hz), 127.90 (d, *J* = 9.7 Hz), 127.65 (d, *J* = 10.0 Hz), 127.47 (d, *J* = 9.8 Hz), 95.27 (d, *J* = 20.3 Hz), 92.68 – 91.84 (m), 77.83 (s), 77.21 (s), 75.99 (d, *J* = 5.6 Hz), 74.24 (d, *J* = 2.5 Hz), 71.40 (s), 71.15 (d, *J* = 6.1 Hz), 70.45 (d, *J* = 8.7 Hz), 70.01 (s), 69.69 (s), 68.30 (d, *J* = 8.5 Hz), 40.76 (d, *J* = 19.1 Hz), 32.63 (s), 30.81 (s), 27.75 (s), 27.60 (s), 26.87 (s), 26.70 (s), 26.16 (d, *J* = 7.4 Hz), 18.22 (d, *J* = 6.6 Hz), 18.08 (d, *J* = 7.3 Hz). ^{31}P NMR (121 MHz, Acetone) δ 44.05 – 42.16 (m), 11.85 (dd, *J* = 169.8, 25.9 Hz), -2.49 (dd, *J* = 169.4, 21.0 Hz). HR-MALDI MS: Monoisotopic mass (M^+) *m/z*, calcd: 1186.1352, found: 1186.1347. FTIR (neat): *cm^{-1}* 3048.52, 2918.11, 1928.56, 1850.10, 1433.40, 1091.76, 822.54, 813.91, 741.71, 697.58. EA: Anal. calcd. for $C_{56}H_{55}O_2P_3Fe_2BrRe$ (%): C, 56.70; H, 4.67; Found: C, 56.63; H, 4.57.

[ReO$_2$I(19a)] (22)

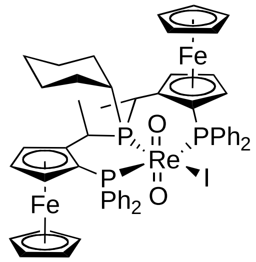

In a Schlenk tube 202.5 mg of [ReO$_2$I(PPh$_3$)$_2$] (0.233 mmol, 1 equiv.) and 220.4 mg of **19a** (0.243 mmol, 1.05 equiv.) were dissolved in 10 mL of degassed dichloromethane. This mixture was stirred at room temperature overnight. To the resulting red solution 40 mL of pentane were added leading to the formation of abundant precipitate. The stirring was continued until the solid agglutinated and the supernatant was clear orange. The solid was decanted and washed thoroughly with *n*-hexane. It was then dried under high vacuum to give the product as a brown powder. Yield 234.5 mg (80%). HR-ESI MS: Monoisotopic mass ([M-I]$^+$) *m/z*, calcd: 1127.1671, found: 1127.1674. FTIR (neat): *cm^{-1}* 3053.6, 2929.7, 1482.9, 1434.4, 1159.8, 1094.9, 904.1, 784.6, 696.1, 510.3, 490.0. EA: Anal. calcd. for $C_{54}H_{55}O_2P_3Fe_2IRe$ (%): C, 51.73; H, 4.42; P, 7.41. Found: C, 51.73; H, 4.70; P, 7.27.

[ReCl$_3$(19a)] (23a)

Ligand **19a** (185 mg, 0.204 mmol, 1 equiv.) and the Re precursor [Re(NCMe)Cl$_3$(PPh$_3$)$_2$][6] (160.3 mg, 0.187 mmol) were dissolved in 30 mL of toluene with stirring. This orange solution was refluxed for two hours. The

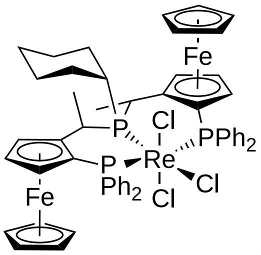

resulting dark brown solution was allowed to cool to room temperature and concentrated to a third of its volume under high vacuum and then 30 mL of *n*-hexane were added leading to the precipitation of a brown solid. The precipitate was decanted and washed thoroughly with *n*-hexane and dried *in vacuo* to afford the pure product as a green paramagnetic powder. Yield 220 mg (98%). X-Ray quality crystals were obtained by layering a saturated solution of **23a** in a mixture of dichloromethane/*n*-hexane with toluene. FTIR: It shows only bands associated with ligand resonance modes, *cm*$^{-1}$ 3052 (s), 2916 (br), 2848 (s), 1433 (s), 822 (s), 740 (s), 693 (s). EA: Anal. Calcd. for $C_{54}H_{55}P_3Cl_3Fe_2Re$: C, 54.00; H, 4.61; P, 7.74. Found: C, 54.09; H, 4.84; P, 7.70. HR-ESI MS: Monoisotopic mass ($[M\text{-}Cl]^+$) *m/z*, calcd: 1165.1136, found: 1165.1162.

[ReCl$_3$(19b)] (23b)

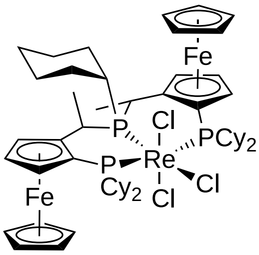

From 28.4 mg (0.031 mmol, 1.2 equiv.) of **19b** and 21.7 mg (0.025 mmol, 1 equiv.) of [Re(NCMe)$Cl_3(PPh_3)_2$], following the same procedure as for the synthesis of **23a**. Yield 28 mg (67%). HR-ESI MS: Monoisotopic mass ($[MH\text{-}Cl]^+$) *m/z*, calcd: 1189.3014, found: 1189.303.

[ReCl$_3$(19c)] (23c)

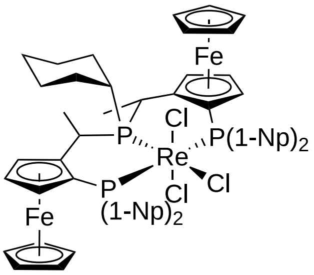

From 100 mg of **19c** (0.091 mmol, 1.2 equiv.) and 64.3 mg of [Re(NCMe)$Cl_3(PPh_3)_2$] (0.075 mmol, 1 equiv.), following the same procedure as for the synthesis of **23a**. Yield 77.1 mg (73%). HR-ESI MS: Monoisotopic mass ($[M\text{-}Cl]^+$) *m/z*, calcd: 1365.18, found: 1365.19.

[ReH$_5$(19a)] (24)

A solution of **23a** (60 mg, 0.05 mmol) and $NaBH_4$ (111,2 mg, 2,92 mmol) in ethanol was refluxed for two hours. The resulting orange suspension

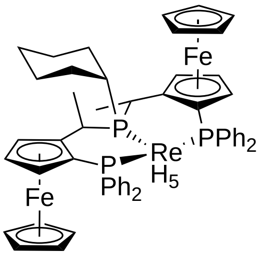

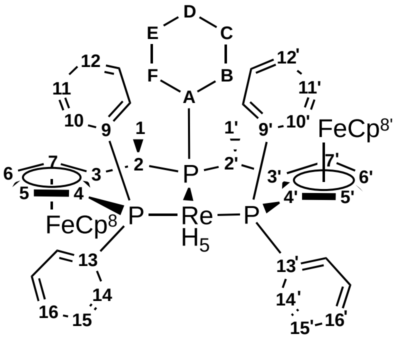

was allowed to settle, cooled to -20 °C and filtered through Celite. The resulting orange solid was washed thoroughly with methanol and then taken up in toluene. The toluene solution was concentrated to dryness *in vacuo* to afford the product as a pale orange powder. Yield 54.4 mg (99%). X-Ray quality crystals were obtained by layering a saturated benzene solution of **24** with *n*-hexane. ^{1}H NMR (500.23 MHz, C_6D_6) δ -6.05 (bs, 5H, Re*H*), 1.12 (m, 1H, H^F *ax*), 1.20-1.30 (m, 5H, H$^{1'}$, H^E *ax*, H^D *ax*), 1.40 (m, 1H, H^C *ax*), 1.50 (dd, 3H, H^1, J_{HH} = J_{HP} = 7.5), 1.60-1.75 (m, 2H, H^D *eq*, H^B *ax*), 1.80-1.95 (m, 2H, H^E *eq*, H^C *eq*), 2.57 (m, 1H, H^B *eq*), 2.75 (m, 1H, H^A), 3.01 (m, 1H, H^F *eq*), 3.15-3.25 (m, 2H, H$^{2'}$, H^2), 3.38 (s, 5H, H^8), 3.90 (s, 5H, H$^{8'}$), 3.91 (m, 1H, H$^{7'}$), 3.98 (dd, 1H, H^6, J_{HH} = J_{HH} = 2.5), 4.06 (dd, 1H, H$^{6'}$, J_{HH} = 2.5, J_{HH} = 4.5), 4.18 (bs, 1H, H$^{5'}$), 4.23 (bs, 1H, H^7), 4.33 (m, 1H, H^5), 6.90-7.02 (m, 3H, H$^{12'}$, H$^{11'}$, H^{12}), 7.03-7.25 (m, 5H, H^{16}, H$^{16'}$, H^{11}, H$^{15'}$, H^{15}), 7.75 (m, 2H, H^{10}), 7.90 (m, 2H, H$^{14'}$), 8.17 (m, 2H, H$^{10'}$), 8.38 (m, 2H, H^{14}). ^{13}C{^{1}H} NMR (125.75 MHz, C_6D_6) δ 16.80 (d, 1C, C^1, $^2J_{PC}$ = 9.9), 22.66 (d, 1C, C$^{1'}$, $^2J_{PC}$ = 2.5), 26.73 (d, 1C, C$^{2'}$, $^1J_{PC}$ = 21.4), 27.47 (s, 1C, C^D), 28.50 (d, 1C, C^C, $^3J_{PC}$ = 6.3), 28.83 (d, 1C, C^E, $^3J_{PC}$ = 12.6), 30.39 (d, 1C, C^F, $^2J_{PC}$ = 1.8), 30.55 (d, 1C, C^B, $^2J_{PC}$ = 6.9), 40.45 (dd, 1C, C^2, $^3J_{PC}$ = 1.2, $^1J_{PC}$ = 20.7), 42.01 (d, 1C, C^A, $^1J_{PC}$ = 17.6), 66.67 (d, 1C, C^6, $^3J_{PC}$ = 5.6), 67.01 (dd, 1C, C$^{6'}$, $^4J_{PC}$ = 1.9, $^3J_{PC}$ = 4.4), 68.99 (dd, 1C, C^7, $^3J_{PC}$ = 1.2, $^3J_{PC}$ = 8.2), 70.51 (s, 5C, C^8), 70.96 (s, 5C, C$^{8'}$), 71.80 (dd, 1C, C$^{7'}$, $^3J_{PC}$ = $^3J_{PC}$ = 7.8), 72.74 (s, 1C, C$^{5'}$), 74.65 (d, 1C, C$^{4'}$, $^1J_{PC}$ = 50.3), 75.60 (d, 1C, C^5, $^2J_{PC}$ = 1.5), 81.15 (d, 1C, C^4, $^1J_{PC}$ = 42.7), 94.88 (dd, 1C, C^3, $^2J_{PC}$ = 7.5, $^2J_{PC}$ = 20.1), 102.23 (dd, 1C, C$^{3'}$, $^2J_{PC}$ = 3.9, $^2J_{PC}$ = 18.8), 126.74 (d, 1C, C$^{15'}$, $^3J_{PC}$ = 9.6), 126.90 (d, 1C, C$^{11'}$, $^3J_{PC}$ = 10.0), 127.17 (d, 1C, C^{11}, $^3J_{PC}$ = 9.5), 127.21 (d, 1C, C^{15}, $^3J_{PC}$ = 8.8), 127.72 (d, 1C, C^{12}, $^4J_{PC}$ = 1.6), 128.29 (1C, C$^{16'}$), 129.03 (d, 1C, C$^{12'}$, $^4J_{PC}$ = 1.7), 129.08 (d, 1C, C^{16}, $^4J_{PC}$ = 1.9), 132.30 (d, 1C, C^{10}, $^2J_{PC}$ = 10.0), 133.30 (d, 1C, C$^{14'}$, $^2J_{PC}$ = 10.9), 136.27 (d, 1C, C$^{10'}$, $^2J_{PC}$ = 11.6), 136.96 (d, 1C, C^{14}, $^2J_{PC}$ = 12.3), 140.53 (d, 1C, C$^{9'}$, $^1J_{PC}$ = 51.5), 143.87 (dd, 1C, C$^{13'}$, $^3J_{PC}$ = 4.6, $^1J_{PC}$ = 46.5), 146.82 (dd, 1C, C^{13}, $^3J_{PC}$ = 3.4, $^1J_{PC}$ = 44.6), 152.27

(d, 1C, C^9, $^1J_{PC} = 57.4$). $^{31}P\{^1H\}$ (202.46 MHz, C_6D_6) δ 17.47 (dd, 1P, *P*Ph$_2$, $^{cis}J_{PP} = 10.6$, $^{trans}J_{PP} = 68.3$), 21.18 (dd, 1P, *P*Ph$_2$, $^{cis}J_{PP} = 16.1$, $^{trans}J_{PP} = 68.3$), 49.56 (dd, 1P, *P*Ph$_2$, $^{cis}J_{PP} = 10.6$, $^{cis}J_{PP} = 16.1$). FTIR: bands associated with ligand resonance modes, *cm^{-1}* 2916 (br), 2847 (s), 1431 (s), 807 (s), 688 (s). Re-H, *cm^{-1}* 1931, 1896. EA: Anal. Calcd. for $C_{54}H_{60}P_3Fe_2Re$: C, 58.97; H, 5.50; P, 8.45. Found: C, 59.37; H, 5.57; P, 8.35. HR-ESI MS: *m/z* 1097.1982 (100, mixture of $[M]^{\bullet+}$, $[M-H]^+$, $[M-2H]^+$, $[M-3H]^+$, $[M-4H]^+$ and $[M-5]^+$).

[ReH$_7$(2a)] (25a)

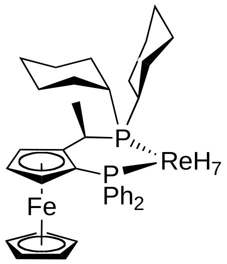

In an oven-dried Schlenk tube 51 mg of **7a** (0.056 mmol, 1 equiv.) were mixed with ca. 40 mg of $LiAlH_4$ (excess) and to this mixture 5 mL of diethylether were added. The resulting yellowish suspension was stirred at room temperature for two hours. The mixture was then filtered through celite and to the filtered yellow solution two drops of distilled water were added with stirring. When the hydrolysis was finished (ceased hydrogen evolution), $MgSO_4$ was added and the organic phase was filtered out to another Schlenk with a cannula. This solution was concentrated to dryness under vacuum giving the product as a pale orange solid. Yield 34 mg (76%). ^{1}H NMR (700 MHz, Tol-D_8) δ 8.42 (dd, *J* = 11.2, 7.6 Hz, 2H, Ph), 7.49 – 7.43 (m, 2H, Ph), 7.20 – 7.15 (m, 2H, Ph), 7.11 (dd, *J* = 7.6, 6.0 Hz, 1H, Ph), 7.04 (td, *J* = 7.8, 2.1 Hz, 2H, Ph), 6.99 – 6.94 (m, 1H, Ph), 4.20 – 4.15 (m, 2H, *H*Cp), 3.97 (t, *J* = 2.5 Hz, 1H, *H*Cp), 3.60 (p, *J* = 7.4 Hz, 1H, *H*CMe), 3.41 (s, 5H, Cp), 2.27 (dd, *J* = 23.8, 12.3 Hz, 1H, Cy), 2.21 (bs, 1H, Cy), 2.12 (dt, *J* = 4.3, 2.2 Hz, 1H, Cy), 2.08 – 1.96 (m, 3H, Cy), 1.89 (d, *J* = 9.9 Hz, 1H, Cy), 1.81 (s, 1H, Cy), 1.73 – 1.58 (m, 3H, Cy), 1.53 (bs, 1H, Cy), 1.50 (dd, *J* = 9.4, 7.5 Hz, 3H, HC*Me*), 1.44 – 1.33 (m, 2H, Cy), 1.32 – 1.22 (m, 1H, Cy), 1.19 – 1.10 (m, 2H, Cy), 1.10 – 0.96 (m, 1H, Cy), 0.92 (dt, *J* = 9.4, 7.2 Hz, 1H, Cy), -6.11 (t, *J* = 14.7 Hz, 7H, Re*H*). ^{31}P NMR (283 MHz, Tol-D_8) δ 47.06 (d, *J* = 27.7 Hz), 6.70 (d, *J* = 27.7 Hz). Not H decoupled, $^2J_{PH}$ = 13 Hz. FTIR (neat): *cm^{-1}* 3054.60, 2924.15, 2851.17, 1979.85, 1914, 1482.53, 1434.06, 1259.94, 1160.59, 1094.21, 1001.42, 809.62, 743.56, 692.88

[ReH$_7$(2b)] (25b)

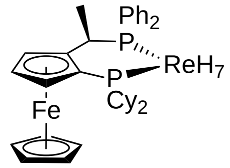

From 103 mg of **7b** (0.114 mmol, 1 equiv.) and 66.4 mg of $LiAlH_4$ (excess). Following the same procedure as for the synthesis of **25a**. Yield 27.4 mg (31%). ^{1}H NMR (300 MHz, CD_2Cl_2) δ 7.60 – 7.29 (m, Ph), 7.24 (d, *J* = 7.5 Hz, Ph), 4.40 (s, 1H, *H*Cp), 4.22 (s, 1H, Cp), 4.17 (s, 1H, *H*Cp), 3.76 (s, 1H, *H*Cp), 3.45 – 3.38 (m, 1H, *H*CMe), 2.44 (bs, Cy), 2.30 (bs, Cy), 2.17 (bs, Cy), 1.88 (m, Cy), 1.45 (m, Cy), 1.38 – 1.30 (m, 3H, HC*Me*), 1.27 (bs, Cy). 0.99 – 0.79 (m, Cy), -6.94 (t, *J* = 14.7 Hz, Cy). ^{31}P NMR (121 MHz, CD_2Cl_2) δ 41.54 (d, *J* = 28.0 Hz), 21.69 (d, *J* = 27.1 Hz).

[ReH$_7$(2l)] (25c)

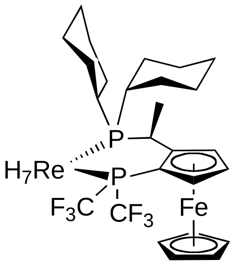

In a Schlenk tube 53 mg of **7l** and an excess of $NaBH_4$ were mixed and 5 mL of absolute ethanol were added with stirring producing gentle bubling. The orange suspension was stirred at room temperature for three hours after which ca. 1 mL of distilled water was added dropwise with a syringe. The system was further stirred for 90 minutes. The resulting suspension was filtered and the solid was washed with ethanol and water and dried *in vacuo* to give the product as an orange powder. Yield 17 mg (36%). ^{1}H NMR (250 MHz, CD_2Cl_2) δ 4.77 (s, 2H, *H*Cp), 4.57 (s, 1H, *H*Cp), 4.27 (s, 5H, Cp), 3.40 – 3.22 (m, 1H, *H*CMe), 2.12 – 1.82 (m, Cy), 1.77 – 1.66 (m, 3H, HC*Me*), 1.49 (m, Cy), 1.24 – 0.98 (m, Cy), 0.97 – 0.77 (m, Cy), -7.34 (t, *J* = 13.9 Hz, 7H, Re*H*). ^{31}P NMR (101 MHz, CD_2Cl_2) δ 55.67 – 51.95 (m, $P(CF_3)_2$), 44.37 (d, *J* = 25.7 Hz, PCy_2). ^{19}F NMR (188 MHz, CD_2Cl_2) δ -62.99 (dq, *J* = 71.1, 8.6 Hz), -64.80 (dq, *J* = 74.4, 8.6 Hz).

6.3.2. Hydrogenation catalysis

General Procedure for the Reactivity Study of Complexes 24 and 25a with Brønsted Acids and Hydride Scavengers

Approximately (0.009 mmol) of the rhenium complex along with one equivalent of the corresponding reactant (HBF_4•Et_2O, H[BAr^F]•2.3Et_2O,

$Et_3O(PF_6)$ or CPh3[BAr^F]) were dissolved in 0.5 mL of CD_2Cl_2 at room temperature in the glove-box. The mixture was allowed to react for a few minutes and then the ^1H and ^{31}P NMR spectra were recorded.

General procedure for the hydrogenation of dimethylitaconate

Hydrogenation experiments were performed in a steel autoclave in the High-Pressure laboratory of the "Institut fur Chemie und Bioingenieurwissenschaften der ETH Zürich". In a typical reaction, 150 mg (0.948 mmol) of dimethylitaconate were dissolved in 10 mL of solvent while, in a separate flask, the catalyst and the corresponding activator (0.009 mmol each) were dissolved together in 10 mL of solvent and stirred at room temperature. After 5 minutes the catalyst’s solution was added onto the substrate's solution and this mixture was injected into the reaction vessel (the final volume was 25 to 30 mL). The atmosphere inside the reactor was changed to hydrogen by several cycles of compression-release, then the autoclave was closed and the system stirred overnight at 80 °C under a pressure of hydrogen of 100 bar. After quenching the reaction by cooling down to room temperature, the solvent was removed under vacuum and the residue dissolved in ethyl acetate and passed through a short silica column eluting with ethyl acetate. The resulting solution was then concentrated under vacuum giving a brown oil.

The yield was determined by ^1H NMR (90° pulse width = 3.33 µs, relaxation delay between scans = 2 s). The enantiomeric excess was determined by Chiral HPLC on an OD-H column (length 25 cm, inner diameter 4.6 mm, particle size 5 µm, flow rate 0.8 mL/min), ratio of hexane/*i*-PrOH (98:2), sample injection volume 10 µL and sample concentration approximately 2 mg/mL.

6.4. Aromatic Trifluoromethylation (Chapter 4)

6.4.1. Trifluoromethylation catalysts

General procedure

A dried Young-type NMR tube was charged with 1-(trifluoromethyl)-1,2-benziodoxol-3(1H)-one (**28**, 12,6 mg, 0,04 mmol), 100 µL of a stock solution of perfluoronaphthalene in $CDCl_3$ containing 0.01 mmol (used as internal standard) and 100 µL of a freshly prepared stock solution of methyltrioxorhenium (MTO, **30**) in $CDCl_3$ containing 0.08 equivalents (0.003 mmol). To the colourless solution 1,5 equivalents (0,06 mmol) of the aromatic substrate were added and $CDCl_3$ was added to afford a final volume of 0,5 mL. The tube was closed and the mixture was heated at 70 °C for a certain amount of time (until the colour changed to dark brown). The mixture was allowed to cool to room temperature and after the corresponding NMR analysis, it was filtered through a plug of alumina-N eluting with acetone. The resulting colourless filtrate was then subject to characterization by GC-MS. Literature references of the NMR data for the known compounds are given.

Benzotrifluoride-D_5 (31)

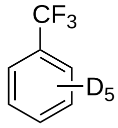

Yield = 54%. ^{19}F NMR: (188 MHz, C_6D_6) δ -62.24 (s). GC-MS: Ret. time = 3.79 min, EI-MS m/z = 151.0 $[M]^+$, 132.0 $[M-F]^+$, 101.0 $[C_6D_5F]^+$, 82.1 $[M-CF_3]^+$.

Benzotrifluoride[16] (Table 2, entry 1)

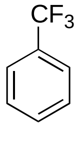

Yield = 54%. ^{19}F NMR (188 MHz, $CDCl_3$) δ -62.68 (s). GC-MS: Ret. time = 3.71 min (monotrifluoromethylated product), EI-MS m/z = 146.0 $[M]^+$, 127.1 $[M-F]^+$, 96.1 $[C_6H_5F]^+$, 77.1 $[M-CF_3]^+$. 3.86 min (ditrifluoromethylated product), EI-MS m/z = 214.1 $[M]^+$, 195.0 $[M-F]^+$, 164.1 $[PhCF_3F]^+$, 145.1 $[M-CF_3]^+$

(Trifluoromethyl)toluene,[17] mixture of isomers (Table 2, entry 2)

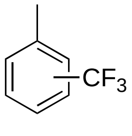

Yield = 58%. ^{19}F NMR (188 MHz, $CDCl_3$) δ -61.66 (s, *para*), -62.24 (s, *meta-*), -62.58 (s, *orto-*). GC-MS: Ret. time = 7.87 min (monotrifluoromethylated product), EI-MS m/z = 160.1 $[M]^+$, 145.0 $[M-CH_3]^+$, 141.1 $[M-F]^+$, 91.1 $[M-CF_3]^+$. 8.19 min (monotrifluoromethylated product). 8.80 min (ditrifluoromethylated product), EI-MS m/z = 228.0 $[M]^+$, 209.1 $[M-F]^+$, 159.0 $[M-CF_3]^+$. 9.25 min (ditrifluoromethylated product).

(Trifluoromethyl)naphthalene,[18] mixture of isomers (Table 2, entry 3)

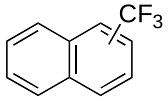

Yield = 58%. ^{19}F NMR (188 MHz, $CDCl_3$) δ -59.70 (d, *J* = 1.5 Hz, α-), -62.21 (s, β-). GC-MS: Ret. time = 38.54 min (ditrifluoromethylated product), EI-MS m/z = 264.0 $[M]^+$, 245.0 $[M-F]^+$, 214.0 $[NpFCF_3]^+$, 195.0 $[M-CF_3]^+$. 38.66 min (monotrifluoromethylated product, β-), EI-MS m/z = 196.0 $[M]^+$, 177.0 $[M-F]^+$, 146.0 $[NpF]^+$, 126.1 $[M-CF_3]^+$. 38.81 min (monotrifluoromethylated product, α-).

(Trifluoromethyl)anisol,[16, 19] mixture of isomers (Table 2, entry 4)

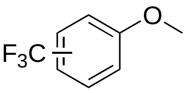

Yield = 62%. ^{19}F NMR (188 MHz, $CDCl_3$) δ -61.42 (s, *para*-), -62.43 (s, *orto*-), -62.67 (s, *meta*-). GC-MS: Ret. time = 19.08 min (monotrifluoromethylated product). 21.75 min (monotrifluoromethylated product). 24.47 min (monotrifluoromethylated product, *orto*-), EI-MS m/z = 176.0 $[M]^+$, 157.0 $[M-F]^+$, 145.0 $[M-OCH_3]^+$.

4-(*Tert*-butyl)-1-methoxy-2-(trifluoromethyl)benzene[20] (Table 2, entry 5)

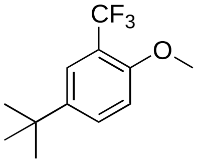

Yield = 63%. ^{19}F NMR (188 MHz, $CDCl_3$) δ -62.08 (s). GC-MS: Ret. time = 39.65 min (monotrifluoromethylated product, *orto*-), EI-MS m/z = 232.0 $[M]^+$, 217.0 $[M-CH_3]^+$, 213.1 $[M-F]^+$. 39.82 min (monotrifluoromethylated product, *meta*-).

1,4-Dimethoxy-2-(trifluoromethyl)benzene[18] (Table 2, Entry 6)

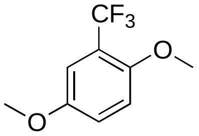

Yield = 70% (5% of ditrifluoromethylated products). ^{19}F NMR (188 MHz, $CDCl_3$) δ -55.11 (s, di-CF_3), -62.37 (s, mono-CF_3), -62.83 (s, di-CF_3). GC-MS: Ret. time = 38.77 min (monotrifluoromethylated product), EI-MS m/z = 206.0 $[M]^+$, 191.0 $[M-CH_3]^+$, 187.0 $[M-F]^+$. 40.15 min (ditrifluoromethylated product), EI-MS m/z = 274.0 $[M]^+$, 259.0 $[M-CH_3]^+$, 255.0 $[M-F]^+$.

1,3,5-Trimethoxy-2-(trifluoromethyl)benzene[21] (Table 2, Entry 7)

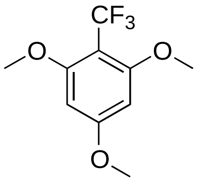

Yield = 77% (4% of ditrifluoromethylated product). ^{19}F NMR (188 MHz, $CDCl_3$) δ -54.11 (s, mono-CF_3), -55.45 (s, di-CF_3). GC-MS: Ret. time = 41.17 min (ditrifluoromethylated product), EI-MS m/z = 304.0 $[M]^+$, 285.0 $[M-F]^+$, 274.0 $[MH-OCH_3]^+$. 41.45 min (monotrifluoromethylated product), EI-MS m/z = 235.9 $[M]^+$, 217.0 $[M-F]^+$, 207.0 $[MH-OCH_3]^+$.

N,N-Dimethyl(trifluoromethyl)aniline,[16, 22] mixture of isomers (Table 2, entry 8)

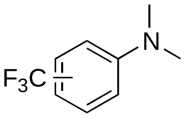

Yield = 49%. ^{19}F NMR (188 MHz, $CDCl_3$) δ -60.03 (s, *para*-), -60.79 (s, *orto*-), -62.56 (s, *meta*-). GC-MS: Ret. time = 38.44 min (monotrifluoromethylated product), EI-MS m/z = 189.1 $[M]^+$, 188.0 $[M-H]^+$, 171.9 $[M-F]^+$, 145.0 $[M-N(CH_3)_2]^+$

Trimethyl((trifluoromethyl)phenyl)silane,[23] mixture of isomers (Table 2, entry 9)

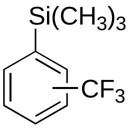

Yield = 45%. ^{19}F NMR (188 MHz, $CDCl_3$) δ -57.10 (s), -57.95 (s), -62.52 (s), -62.83 (s). GC-MS: Ret. time = 28.36 min (monotrifluoromethylated product), EI-MS m/z = 218.0 $[M]^+$, 203.0 $[M-CH_3]^+$. 35.35 min (monotrifluoromethylated product).

Chloro(trifluoromethyl)benzene,[17] mixture of isomers (Table 2, entry 10)

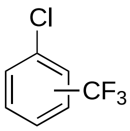

Yield = 42%. ^{19}F NMR (188 MHz, $CDCl_3$) δ -62.54 (s, *para*), -62.62 (s, *orto*-), -62.85 (s, *meta*-). GC-MS: Ret. time = 10.55 min (monotrifluoromethylated product), EI-MS m/z = 180.0 $[M]^+$, 161.0 $[M-F]^+$, 145.0 $[M-Cl]^+$. 10.82 min (monotrifluoromethylated product). 14.85 min (monotrifluoromethylated product).

1-Iodo(trifluoromethyl)benzene,[17] mixture of isomers (Table 2, entry 11)

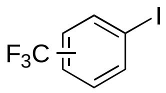

Yield = 41%. ^{19}F NMR (188 MHz, CDCl$_3$) δ -62.78 (s, *para*-), -62.84 (s, *orto*-), -62.93 (s, *meta*-). GC-MS: Ret. time = 30.19 min (monotrifluoromethylated product), EI-MS m/z = 271.9 [M]$^+$, 252.9 [M-F]$^+$, 202.9 [M-CF$_3$]$^+$, 145.0 [M-I]$^+$. 30.32 min (monotrifluoromethylated product). 35.94 min (monotrifluoromethylated product).

1-((Trifluoromethyl)phenyl)ethanone,[16] mixture of isomers (Table 2, entry 12)

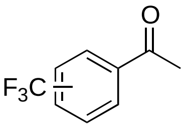

Yield = 32%. ^{19}F NMR (188 MHz, CDCl$_3$) δ -58.12 (s, *orto*-), -62.77 (s, *meta*-), -63.07 (s, *para*-). GC-MS: Temp. Program = 50 °C, 3 min, then up to 250 °C (8 °C/min) and finally 250 °C for 20 min. Ret. time = 9.34 min (monotrifluoromethylated product), EI-MS m/z = 188.1 [M]$^+$, 173.1 [M-CH$_3$]$^+$, 169.1 [M-F]$^+$, 145.0 [M-COCH$_3$]$^+$. 9.37 min (monotrifluoromethylated product).

1-((Trifluoromethyl)phenyl)propan-2-one,[24] mixture of isomers (Table 2, entry 13)

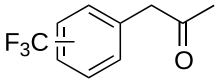

Yield = 31%. ^{19}F NMR (188 MHz, CDCl$_3$) δ -59.92 (s), -62.51 (s), -62.59 (s). GC-MS: Ret. time = 37.76 min (monotrifluoromethylated product). 38.16 min (monotrifluoromethylated product), EI-MS m/z = 202.1 [M]$^+$, 183.1 [M-F]$^+$, 159.1 [M-COCH$_3$]$^+$. 38.34 min (monotrifluoromethylated product).

(Trifluoromethyl)benzonitrile,[16] mixture of isomers (Table 2, entry 14)

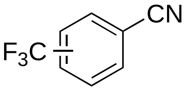

Yield = 15%. ^{19}F NMR (188 MHz, CDCl$_3$) δ -61.92 (s, *orto*-), -63.16 (s, *meta*-), -63.47 (s, *para*-). GC-MS: Ret. time = 22.60 min (monotrifluoromethylated product), EI-MS m/z = 171.0 [M]$^+$, 152.0 [M-F]$^+$, 145.1 [M-CN]$^+$. 22.82 min (monotrifluoromethylated product). 30.55 min (monotrifluoromethylated product).

Nitro(trifluoromethyl)benzene,[25] mixture of isomers (Table 2, entry 15)

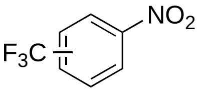

Yield = 13%. ^{19}F NMR (188 MHz, CDCl$_3$) δ -61.13 (s, *orto*-), -62.88 (s, *meta*-), -63.09 (s, *para*-). GC-MS: Ret. time = 31.85 min (monotrifluoromethylated product, *para*-), EI-MS m/z = 191.0 [M]$^+$, 172.0 [M-F]$^+$, 145.1 [M-NO$_2$]$^+$. 22.82 min (monotrifluoromethylated product, *orto*-).

Trifluoromethylferrocene[26] (Table 2, entry 16)

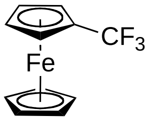

Yield = 33%. ^{19}F NMR (188 MHz, CDCl$_3$) δ -55.53 (s). GC-MS: Ret. time = 39.91 min, EI-MS m/z = 253.9 [M]$^+$, 234.9 [M-F]$^+$, 139.9 [CpFeF]$^+$.

(Trifluoromethyl)benzofuran,[27] mixture of isomers (Table 3, entry 1)

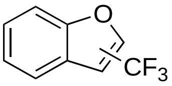

Yield = 43%. ^{19}F NMR (188 MHz, CDCl$_3$) δ -61.33 (s, 3), -64.78 (s, 2-). GC-MS: Ret. time = 23.02 min (monotrifluoromethylated product, 2-), EI-MS m/z = 186.0 [M]$^+$, 167.0 [M-F]$^+$. 26.12 min (monotrifluoromethylated product, 3-).

(Trifluoromethyl)benzo[b]thiophene,[27b] mixture of isomers (Table 3, entry 2)

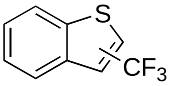

Yield = 45%. ^{19}F NMR (188 MHz, CDCl$_3$) δ -56.25 (s, 2), -60.26 (s, 3-), -61.44 (s, 7-). GC-MS: Ret. time = 37.97 min (monotrifluoromethylated product), EI-MS m/z = 202.0 [M]$^+$, 183.0 [M-F]$^+$. 38.38 min (monotrifluoromethylated product). 38.71 min (monotrifluoromethylated product).

(Trifluoromethyl)-1H-indole,[20, 28] mixture of isomers (Table 3, entry 3)

Yield = 59%. ^{19}F NMR (188 MHz, CDCl$_3$) δ -57.32 (s, 3), -60.46 (s, 2-), -61.42 (s, 7-). GC-MS: Ret. time = 38.43 min (monotrifluoromethylated product), EI-MS m/z = 184.9 [M]$^+$, 166.1 [M-F]$^+$, 165.0 [M-HF]$^+$. 39.02 min

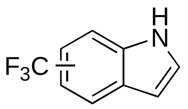

(monotrifluoromethylated product, 2-). 39.70 min (ditrifluoromethylated product), EI-MS m/z = 253.0 $[M]^+$, 234.0 $[M-F]^+$, 233.0 $[M-HF]^+$. 40.65 min (monotrifluoromethylated product, 7-). 40.90 min (monotrifluoromethylated product, 3-).

1-Methyl(trifluoromethyl)indole,[20, 29] mixture of isomers (Table 3, entry 4)

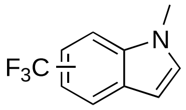

Yield = 64%. ^{19}F NMR (188 MHz, $CDCl_3$) δ -56.70 (s, 3-), -59.54 (s, 2-), -61.36 (s, 7-). GC-MS: Ret. time = 38.84 min (monotrifluoromethylated product, 2-), EI-MS m/z = 199.1 $[M]^+$, 180.1 $[M-F]^+$. 39.85 min (ditrifluoromethylated product), EI-MS m/z = 267.0 $[M]^+$, 248.0 $[M-F]^+$, 198.1 $[M-CH_3]^+$. 40.00 min (monotrifluoromethylated product). 40.20 min (monotrifluoromethylated product, 7-). 40.28 min (monotrifluoromethylated product, 3-).

3-Methyl-2-(trifluoromethyl)-1H-indole[30] (Table 3, entry 5)

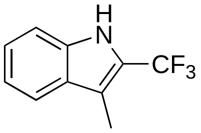

Yield = 75%. ^{19}F NMR (188 MHz, $CDCl_3$) δ -58.57 (d, *J* = 1.5 Hz). GC-MS: Ret. time = 39.94 min (monotrifluoromethylated product, 2-), EI-MS m/z = 200.1 $[M+H]^+$, 199.1 $[M]^+$, 198.4 $[M-H]^+$, 180.1 $[M-F]^+$, 129.9 $[M-CF_3]^+$. 40.52 min (ditrifluoromethylated product), EI-MS m/z = 267.0 $[M]^+$, 248.0 $[M-F]^+$, 198.0 $[M-CH_3]^+$. 41.49 min (monotrifluoromethylated product).

(Trifluoromethyl)pyridine[20] (Table 3, entry 6)

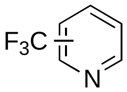

Yield = 38%. ^{19}F NMR (188 MHz, $CDCl_3$) δ -62.96 (s, 3-), -64.92 (s, 4-), -68.07 (s, 2-). GC-MS: Ret. time = 4.19 min (monotrifluoromethylated product), EI-MS m/z = 147.1 $[M]^+$, 128.1 $[M-F]^+$, 78.1 $[M-CF_3]^+$. 4.57 min (monotrifluoromethylated product). 7.01 min (monotrifluoromethylated product).

2,6-Dimethyl-4-(trifluoromethyl)pyridine (Table 3, entry 7)

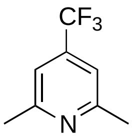

Yield = 25%. ^{19}F NMR (188 MHz, CDCl$_3$) δ -61.83 (s). GC-MS: Ret. time = 14.21 min (monotrifluoromethylated product), EI-MS m/z = 175.1 [M]$^+$, 156.1 [M-F]$^+$, 106.1 [M-CF$_3$]$^+$.

(Trifluoromethyl)quinoline,[25a] mixture of isomers (Table 3, entry 8)

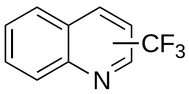

Yield = 50%. ^{19}F NMR (188 MHz, CDCl$_3$) δ -58.57 (d, *J* = 1.5 Hz, major isomer). GC-MS: Ret. time = 38.56 min (monotrifluoromethylated product), EI-MS m/z = 197.0 [M]$^+$, 178.1 [M-F]$^+$, 128.1 [M-CF$_3$]$^+$. 38.81 min (monotrifluoromethylated product). 40.22 min (monotrifluoromethylated product).

4-(*Tert*-butyl)-2-(trifluoromethyl)pyridine (Table 3, entry 9)

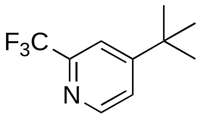

Yield = 20%. ^{19}F NMR (188 MHz, CDCl$_3$) δ -67.76 (s). GC-MS: Ret. time = 36.56 min (monotrifluoromethylated product, 2-), EI-MS m/z = 203.0 [M]$^+$, 188.0 [M-CH$_3$]$^+$, 184.1 [M-F]$^+$. 36.74 min (monotrifluoromethylated product, 3-).

2,4-Dimethyl(trifluoromethyl)pyridine, mixture of isomers (Table 3, entry 10)

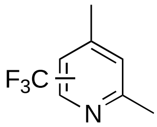

Yield = 36%. ^{19}F NMR (188 MHz, CDCl$_3$) δ -54.73 (m, 3), -61.31 (s, 5-), -67.94 (s, 6-). Signal assignment by analogy with pyridine. GC-MS: Ret. time = 18.00 min (monotrifluoromethylated product), EI-MS m/z = 175.1 [M]$^+$, 156.1 [M-F]$^+$, 106.1 [M-CF$_3$]$^+$. 18.93 min (monotrifluoromethylated product). 21.91 min (monotrifluoromethylated product).

N,N-Dimethyl-2-(trifluoromethyl)pyridin-4-amine (Table 3, entry 11)

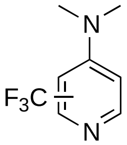

Yield = 24%. ^{19}F NMR (188 MHz, CDCl$_3$) δ -55.73 (s). GC-MS: Temp. Program = 50 °C, 3 min, then up to 250 °C (8 °C/min) and finally 250 °C for 20 min. Ret. time = 11.12 min (ditrifluoromethylated product), EI-MS m/z = 258.1 [M]$^+$, 257.1 [M-H]$^+$, 239.1 [M-F]$^+$, 189.1 [M-CF$_3$]$^+$. 11.72 min (monotrifluoromethylated product), EI-MS m/z = 190.1 [M]$^+$, 189.1 [M-H]$^+$, 171.1 [M-F]$^+$, 146.0 [M-N(CF$_3$)$_2$]$^+$. 13.96 min (monotrifluoromethylated product).

2,6-Dibromo-4-(trifluoromethyl)pyridine[31] (Table 3, entry 12)

Yield = 11%. ^{19}F NMR (188 MHz, CDCl$_3$) δ -63.31 (s). GC-MS: Ret. time = 39.35 min (monotrifluoromethylated product, 4-), EI-MS m/z = 304.8 [M]$^+$, 285.8 [M-F]$^+$, 225.9 [M-Br]$^+$.

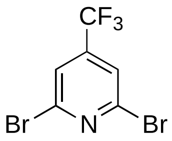

2,6-Dichloro-4-(trifluoromethyl)pyridine[31-32] (Table 3, entry 13)

Yield = 14%. ^{19}F NMR (188 MHz, CDCl$_3$) δ -63.28 (s). GC-MS: Ret. time = 34.19 min (monotrifluoromethylated product, 4-), EI-MS m/z = 214.9 [M]$^+$, 195.9 [M-F]$^+$, 180.0 [M-Cl]$^+$.

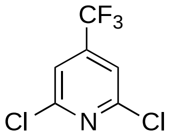

3,5-Dichloro-2-(trifluoromethyl)pyridine (Table 3, entry 14)

Yield = 18%. ^{19}F NMR (188 MHz, CDCl$_3$) δ -65.95 (s). GC-MS: Ret. time = 27.46 min (monotrifluoromethylated product, 4-), EI-MS m/z = 214.9 [M]$^+$, 195.9 [M-F]$^+$, 180.0 [M-Cl]$^+$. 31.03 min (monotrifluoromethylated product, 2-).

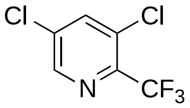

2-Chloro-6-methoxy(trifluoromethyl)pyridine,[33] mixture of isomers (Table 3, entry 15)

Yield = 48%. ^{19}F NMR (188 MHz, CDCl$_3$) δ -61.87 (s, 3-), -63.47 (s, 5-). GC-MS: Ret. time = 32.19 min (monotrifluoromethylated product, 5-), EI-MS m/z = 210.0 [M]$^+$, 192.0 [M-F]$^+$, 180.9 [M-OCH$_3$]$^+$. 33.88 min (monotrifluoromethylated product, 3-).

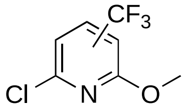

2,6-Dimethoxy(trifluoromethyl)pyridine, mixture of isomers (Table 3, entry 16)

Yield = 60%. ^{19}F NMR (188 MHz, CDCl$_3$) δ -61.86 (s, 3-), -62.23 (s, 4-). GC-MS: Ret. time = 36.36 min

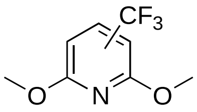

(monotrifluoromethylated product, 3-), EI-MS m/z = 207.1 $[M]^+$, 188.1 $[M\text{-}F]^+$, 178.1 $[MH\text{-}OCH_3]^+$.

2-Methoxy(trifluoromethyl)pyridine,[34] mixture of isomers (Table 3, entry 17)

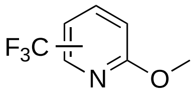

Yield = 33%. ^{19}F NMR (188 MHz, $CDCl_3$) δ -61.48 (s, 5-), -63.90 (s, 3-), -68.46 (s, 6-). GC-MS: Ret. time = 12.94 min (monotrifluoromethylated product, 5-), EI-MS m/z = 177.0 $[M]^+$, 158.0 $[M\text{-}F]^+$, 147.1 $[MH\text{-}OCH_3]^+$, 108.1 $[M\text{-}CF_3]^+$. 14.00 min (monotrifluoromethylated product, 6-). 16.37 min (monotrifluoromethylated product, 3-).

6.4.2. Mechanistic studies

^{19}F NMR monitoring of the trifluoromethylation of benzene-D_6

Trifluoromethylation of benzene-D_6 was monitored by ^{19}F NMR (376 MHz, $CDCl_3$) with a Bruker DRX400 spectrometer. Experimental temperature (343 K) was maintained using a Bruker BVT 3000 temperature control unit calibrated with a digital thermometer fit to a 5mm NMR tube. The reaction was as described in the general procedure using 3.8 mg of perfluoronaphthalene (internal standard), 12.6 mg of **28** (0.0399 mmol, 1 equiv.), 0.8 mg of MTO (0.0032 mmol, 0.08 equiv.) and 5.29 µL of benzene-D_6 (0.0598 mmol, 1.5 equiv). Spectra acquisition was started when the desired temperature (343 K) was reached. A total of 167 experiment were acquired during 3 hours (Chapter 4, Figure 2). Every single spectrum was processed using the software package MestReNova© and the yield (consumption of **28** and formation of **31**) was calculated using the internal standard.

EPR monitoring of the trifluoromethylation of 4-*t*-butylanisol

Trifluoromethylation of 4-*t*-butylanisol was monitored by EPR with a Bruker EMX X-band spectrometer (Bruker Biospin Germany, Ettlingen, GER) 9.5 GHz, magnetic field between 50-400 mT (500-4000 Gauss). Parameters used: Field 333.5-343.5 mT; Modulation Amplitude 0.4 mT; Modulation frequency 100 Hz; Microwave power 2 mW.

The reaction setup was as described in the general procedure using 5.5 mg **28** (0.017 mmol, 1 equiv.), 1.9 mg of MTO (0.0076 mmol, 0.4 equiv.) and 10 µL of 4-*t*-butylanisol (0.057 mmol, 3.3 equiv) dissolved in 0.1 mL of $CDCl_3$.

For the high modulation EPR measurement (Chapter 4, Figure 9) the same experimental conditions were used as in the above mentioned case, using 12.2 mg **28** (0.039 mmol, 1 equiv.), 2.9 mg of MTO (0.011 mmol, 0.29 equiv.) and 20 µL of 4-*t*-butylanisol (0.114 mmol, 2.9 equiv) dissolved in 0.2 mL of $CDCl_3$. The reaction mixture was heated first at 70 °C for 70 min and then quenched by fast cooling with liquid nitrogen. The frozen sample was allowed to warm to room temperature ant the EPR spectra was recorded for two hours using the following set up: Field 328.5-348.5 mT; Modulation Amplitude 0.05 mT; Modulation frequency 100 Hz; Microwave power 2 mW.

Deuterium kinetic isotope effect for the trifluoromethylation of benzene

The deuterium kinetic isotope effect experiment(relative rates) for the trifluoromethylation of benzene with **28** was carried out at 80°C overnight and using one equivalent of MTO. The substrate was used as solvent mixture (1:1 of C_6H_6 and C_6D_6). The technical details are the same as described above for the ^{19}F NMR monitoring of the trifluoromethylation of benzene-D_6. The experiment was made by duplicate and the reported value of KIE is the arithmetic mean value for the two measurements.

UV-Vis measurements

The UV-Vis kinetic measurements were performed in a diode-array spectrophotometer Analitik Jena Specord 100 (Analitik Jena, Jena, GER). The spectra were recorded between 240-260 nm and the light exposition for each measure was 100 ms. Wavelength resolution was 0.85 nm. In a typical procedure, 50.5 mg **28** (0.16 mmol, 1 equiv.), 6.5 mg of MTO (0.026 mmol, 0.16 equiv.) and 100 µL of 4-*t*-butylanisol (0.57 mmol, 3.5 equiv) were dissolved in 2 mL of $CDCl_3$ and this mixture heated at 70 °C for two hours while the UV-Vis spectra were recorded.

References

[1] W. L. F. Amarego, C. L. L. Chai, *Purification of Laboratory Chemicals*, Fifth ed., Cornwal, **2003**.

[2] U. Burckhardt, L. Hintermann, A. Schnyder, A. Togni, *Organometallics* **1995**, *14*, 5415-5425.

[3] A. Togni, C. Breutel, A. Schnyder, F. Spindler, H. Landert, A. Tijani, *J. Am. Chem. Soc.* **1994**, *116*, 4062-4066.

[4] a) L. Fadini, A. Togni, *Tetrahedron Asymmetry* **2008**, *19*, 2555-2562; b) P. Butti, Thesis No. 18839, ETH Zürich (Zürich), **2009**.

[5] G. W. Parshall, L. W. Shive, F. A. Cotton, *Inorg. Synth.* **1977**, *17*, 110-112.

[6] G. Rouschias, G. Wilkinson, *J. Chem. Soc. (A)* **1967**, 993-1000.

[7] N. P. Johnson, J. L. Lock, G. Wilkinson, *J. Chem. Soc.* **1964**, 1054-1066.

[8] U. Abram, M. Braun, S. Abram, R. Kirmse, A. Voigt, *J. Chem. Soc. Dalton Trans.* **1998**, 231-238.

[9] M. L. Parr, C. Perez-Acosta, J. W. Fallerb, *New J. Chem.* **2005**, *29*, 613-619.

[10] a) C. De Meric de Bellefon, W. A. Herrmann, P. Kiprof, C. R. Whitaker, *Organometallics* **1992**, *11*, 1072-1081; b) W. Seidel, I. Bürger, *Z. Anorg. Allg. Chem.* **1981**, *473*, 166-170.

[11] W. A. Herrmann, R. M. Kratzer, R. W. Fischer, *Angew. Chem. Int. Ed.* **1997**, *36*, 2652-2654.

[12] a) K. Stanek, R. Koller, I. Kieltsch, P. Eisenberger, A. Togni, *e-EROS* **2009**, Article-Rn01121; b) K. Stanek, R. Koller, I. Kieltsch, P. Eisenberger, A. Togni, *e-EROS* **2009**, Article-Rn01120.

[13] J. A. Magee, A. C. Herd, *J. Chem. Educ.* **1999**, *76*, 252.

[14] a) J. R. Goerich, R. Schmutzler, *Phosphorus Sulfur Silicon Relat. Elem.* **1993**, *81*, 141-148; b) J. R. Goerich, A. Fischer, P. G. Jones, R. Schmutzler, *Z. Naturforsch.* **1994**, *49b*, 801-811.

[15] C. A. Busacca, J. C. Lorenz, P. Sabila, N. Haddad, C. H. Senanyake, *Organic Synthesis* **2007**, *84*, 242-261.

[16] R. Brownlee, D. Craik, *Aust. J. Chem.* **1980**, *33*, 2555-2559.

[17] D. Naumann, J. Kischkewitz, *J. Fluorine Chem.* **1990**, *47*, 283-299.

[18] T. Umemoto, A. Ando, *Bull. Chem. Soc. Jpn.* **1986**, *59*, 447-452.

[19] Y. Kobayashi, I. Kumadaki, *J. Chem. Soc. Perkin Trans. 1* **1980**, 661-664.

[20] M. S. Wiehn, E. V. Vinogradova, A. Togni, *J. Fluorine Chem.* **2010**, *131*, 951-957.

[21] I. Kieltsch, Thesis No. 17990, ETH Zürich (Zürich), **2008**.

[22] L. M. Yagupolskii, A. V. Matsnev, R. K. Orlova, B. G. Deryabkin, Y. L. Yagupolskii, *J. Fluorine Chem.* **2008**, *129*, 131-136.

[23] M. Tobisu, Y. Kita, Y. Ano, N. Chatani, *J. Am. Chem. Soc.* **2008**, *130*, 15982-15989.

[24] C. He, S. Guo, L. Huang, A. Lei, *J. Am. Chem. Soc.* **2010**, *132*, 8273-8275.

[25] a) M. Oishi, H. Kondo, H. Amii, *Chem. Commun.* **2009**, 1909-1911; b) V. A. Grinberg, S. A. Lundgren, S. R. Sterlin, E. L. Mysov, *Russ. Chem. Bull.* **1997**, *46*, 1131-1135.

[26] T. Akiyama, K. Kato, M. Kajitani, Y. Sakaguchi, J. Nakamura, H. Hayashi, A. Sugimori, *Bull. Chem. Soc. Jpn.* **1988**, *61*, 3531-3537.

[27] a) Y. Kobayashi, I. Kumadaki, Y. Hanzawa, *Chem. Pharm. Bull.* **1977**, *25*, 3009-3012; b) H. Sawada, M. Nakayama, M. Yoshida, T. Yoshida, N. Kamigata, *J. Fluorine Chem.* **1990**, *46*, 423-431.

[28] Q.-Y. Chen, Z.-T. Li, *J. Chem. Soc. Perkin Trans. 1* **1993**, 645-648.

[29] M. M. Bastos, L. M. U. Mayer, E. C. S. Figueira, M. Soares, N. Boechat, W. B. Kover, *J. Heterocyclic Chem.* **2008**, *45*, 969-973.

[30] R. Shimizu, H. Egami, T. Nagi, J. Chae, Y. Hamashima, M. Sodeoka, *Tetrahedron Lett.* **2010**, *51*, 5947-5949.

[31] F. Mutterer, C. D. Weis, *Helv. Chim. Acta* **1976**, *59*, 229-235.

[32] W.-N. Xiong, C.-G. Yang, B. Jiang, *Bioorg. Med. Chem.* **2001**, *9*, 1773-1780.

[33] D. E. Podhorez, *J. Heterocyclic Chem.* **1991**, *28*, 971-976.

[34] R. S. Dainter, T. Jackson, A. H. H. Omar, H. Suschitzky, B. J. Wakefield, N. Hughes, A. J. Nelson, G. Varvounis, *J. Chem. Soc. Perkin Trans. 1* **1989**, 283-287.

7. Appendix

7.1. Crystallographic Information

7.1.1. Experimental details

Intensity data of single crystals glued to a glass capillary were collected at the given temperature (usually 100 K) on a Bruker SMART APEX platform with CCD detector and graphite monochromated Mo-K$_a$-radiation (l = 0.71073 Å). The program SMART served for data collection; integration was performed with the software SAINT.[1] The structures were solved by direct methods or Patterson methods, respectively, using the program SHELXS-97.[2] The refinement and all further calculations were carried out using SHELXL-97.[3] All non-hydrogen atoms were refined anisotropically using weighted full-matrix least-squares on F^2. The hydrogen atoms were included in calculated positions and treated as riding atoms using SHELXL default parameters. In the end absorption correction was applied (SADABS)[4] and weights were optimized in the final refinement cycles. The absolute configuration of chiral compounds was determined on the basis of the Flack parameter.[5, 6] The standard uncertainties (s.u.) are rounded according to the "Notes for Authors" of *Acta Crystallographica*.[7]

[1] *SAINT+*, Software for CCD Diffractometers, v. 6.01; Bruker AXS, Inc., Madison, WI, **2001** and SAINT, v. 6.02.

[2] G. Sheldrick, *Acta Cryst. Sect. A* **1990**, *46*, 467.

[3] G. M. Scheldrick, *SHELXL-97* Program for Crystal Structure Refinement, Universität Göttingen, Göttingen, Germany, **1999**.

[4] R. Blessing, *Acta Cryst. Sect. A* **1995**, *51*, 33.

[5] H. Flack, *Acta Cryst. Sect. A* **1983**, *39*, 876.

[6] G. Bernardinelli, H. D. Flack, *Acta Cryst. Sect. A* **1985**, *41*, 500.

[7] *Acta Cryst.* **2010**, *C66*, e1.

7.1.2. Crystallografic data and tables

[ReBr(CO)$_3$(2a)] (3)

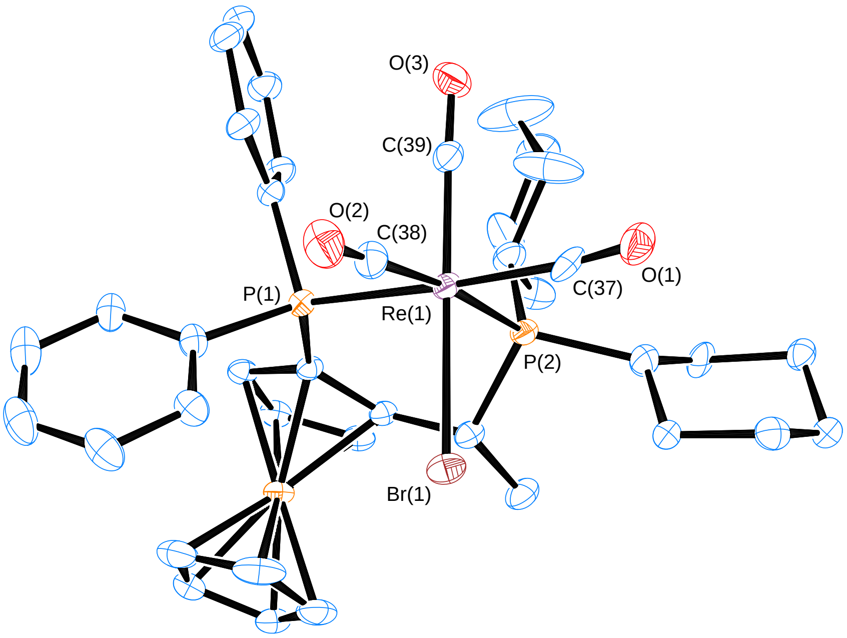

Color, shape	Yellow plates
Empirical formula	$C_{39}H_{33}BrFeO_3P_2Re$
fw	1066.09
Temp, K	100(2)
Wavelenght, Å	0.71073
Cryst syst	Orthorombic
Space group	P 21 21 21
Unit cell dimens (Å/deg)	
a	10.6477(13)
b	11.4576(14)
c	29.923(4)
α	90.0
β	90.0
γ	90.0
V, Å^3	3650.5(8)
Z	4
D (calcd), g/cm^3	1.699
abs coeff, mm^{-1}	4.928
θ range for data collcn, deg	1.36 to 34.40
Index ranges	$-16 \le h \le 16$, $-18 \le k \le 18$, $-47 \le l \le 47$
no. of collcd rflns	137363
Refinement method	Full-matrix least-squares on F^2
no. of data/restraints/params	15322/ 0 / 461
Goodness of fit	1.044
Final R index ($I>2\sigma(I)$)	R1 = 0.0264, wR2 = 0.0587
R indices (all data)	R1 = 0.0295, wR2 = 0.0599
abs structure param	0.002(3)

exo-[ReOCl$_3$(2a)]•C$_6$H$_6$•CH$_2$Cl$_2$ (7a)

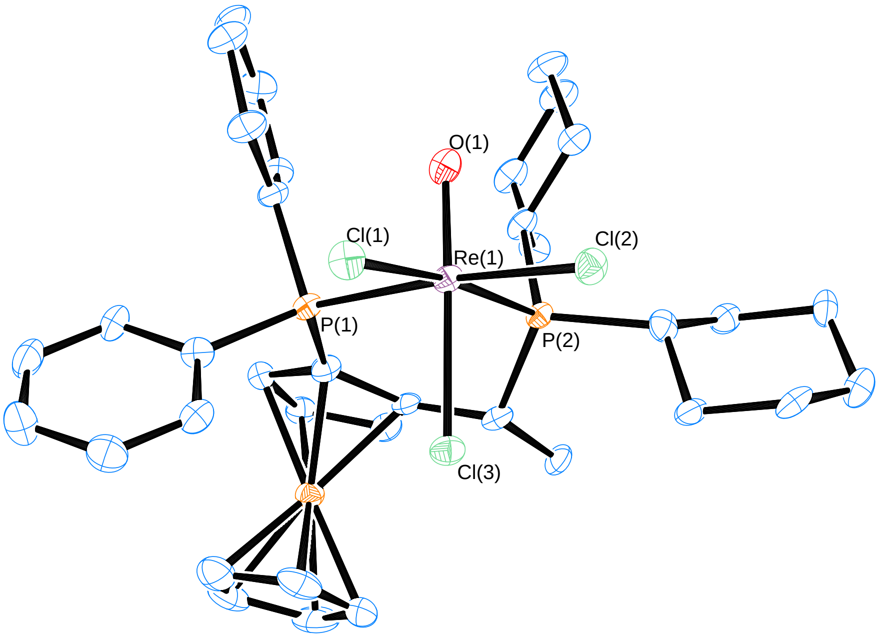

Color, shape	Yellow needles
Empirical formula	C$_{43}$H$_{52}$Cl$_5$FeOP$_2$Re
fw	1066.09
Temp, K	100(2)
Wavelenght, Å	0.71073
Cryst syst	Hexagonal
Space group	P61
Unit cell dimens (Å/deg)	
a	26.1711(14)
b	26.1711(14)
c	11.0896(8)
α	90.0
β	90.0
γ	120.0
V, Å^3	6577.9(7)
Z	6
D (calcd), g/cm^3	1.615
abs coeff, mm^{-1}	3.499
θ range for data collcn, deg	0.90 to 28.44
Index ranges	$-35 \le h \le 34$, $-34 \le k \le 34$, $-14 \le l \le 14$
no. of collcd rflns	61752
Refinement method	Full-matrix least-squares on F^2
no. of data/restraints/params	10906/ 1 / 478
Goodness of fit	0.709
Final *R* index ($I>2\sigma(I)$)	R1 = 0.0361, wR2 = 0.0716
R indices (all data)	R1 = 0.0457, wR2 = 0.0750
abs structure param	-0.006(5)

***exo*-[ReOCl$_3$(2d)]•n(CHC$_3$) (7d)**

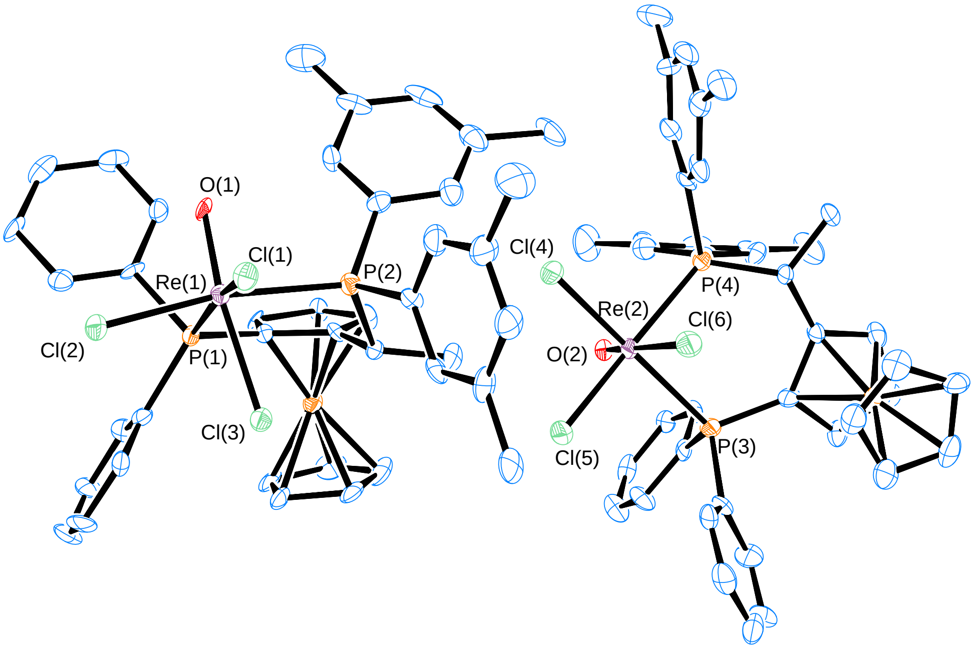

Color, shape	Purple prism
Empirical formula	$C_{81}H_{81}Cl_9Fe_2O_2P_4Re_2$
fw	2013.51
Temp, K	100(2)
Wavelenght, Å	0.71073
Cryst syst	Orthorombic
Space group	P 21 21 21
Unit cell dimens (Å/deg)	
a	14.7813(11)
b	19.1931(15)
c	31.401(3)
α	90.0
β	90.0
γ	90.0
V, Å^3	8908.5(12)
Z	4
D (calcd), g/cm^3	1.501
abs coeff, mm^{-1}	3.411
θ range for data collcn, deg	1.24 to 26.04
Index ranges	$-18 \le h \le 15$, $-23 \le k \le 22$, $-38 \le l \le 38$
no. of collcd rflns	57398
Refinement method	Full-matrix least-squares on F^2
no. of data/restraints/params	17547/ 24 / 911
Goodness of fit	0.953
Final *R* index ($I>2\sigma(I)$)	R1 = 0.0458, wR2 = 0.0910
R indices (all data)	R1 = 0.0621, wR2 = 0.0963
abs structure param	0.004(5)

exo-[ReOCl$_3$(2e)] (7e)

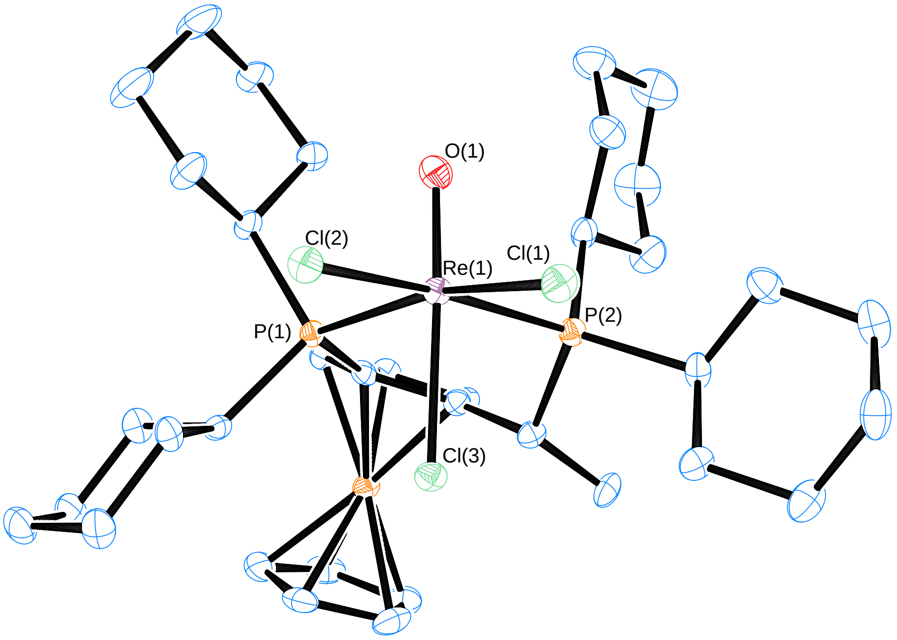

Color, shape	Orange prism
Empirical formula	$C_{36}H_{56}Cl_3FeOP_2Re$
fw	915.15
Temp, K	100(2)
Wavelenght, Å	0.71073
Cryst syst	Orthorombic
Space group	P 21 21 21
Unit cell dimens (Å/deg)	
a	14.0114(17)
b	15.0891(18)
c	17.871(2)
α	90.0
β	90.0
γ	90.0
V, Å^3	3778.3(8)
Z	4
D (calcd), g/cm^3	1.609
abs coeff, mm^{-1}	3.909
θ range for data collcn, deg	1.77 to 28.40
Index ranges	$-18 \le h \le 18$, $-20 \le k \le 20$, $-23 \le l \le 23$
no. of collcd rflns	39477
Refinement method	Full-matrix least-squares on F^2
no. of data/restraints/params	9457/ 0 / 398
Goodness of fit	0.986
Final *R* index ($I>2\sigma(I)$)	R1 = 0.0301, wR2 = 0.0588
R indices (all data)	R1 = 0.0347, wR2 = 0.0603
abs structure param	-0.003(4)

endo-[$ReOCl_3$(2f)]•$CHCl_3$ (7f)

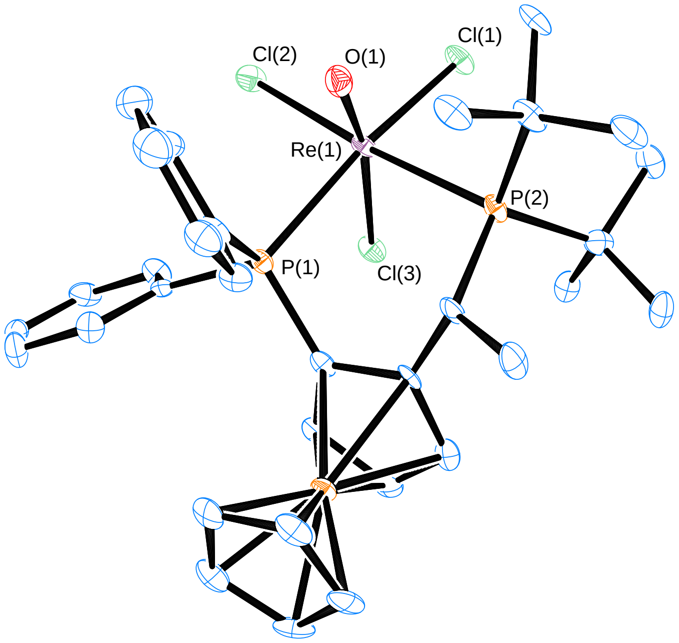

Color, shape	Red prism
Empirical formula	$C_{33}H_{41}Cl_6FeOP_2Re$
fw	970.35
Temp, K	100(2)
Wavelenght, Å	0.71073
Cryst syst	Orthorombic
Space group	P 21 21 21
Unit cell dimens (Å/deg)	
a	9.6809(8)
b	16.9564(14)
c	21.9109(19)
α	90.0
β	90.0
γ	90.0
V, $Å^3$	3596.5(7)
Z	4
D (calcd), g/cm^3	1.792
abs coeff, mm^{-1}	4.328
θ range for data collcn, deg	1.52 to 28.70
Index ranges	$-13 \leq h \leq 13, -22 \leq k \leq 22, -29 \leq l \leq 29$
no. of collcd rflns	38596
Refinement method	Full-matrix least-squares on F^2
no. of data/restraints/params	9302/ 0 / 404
Goodness of fit	1.111
Final *R* index ($I>2\sigma(I)$)	R1 = 0.0426, wR2 = 0.0880
R indices (all data)	R1 = 0.0472, wR2 = 0.0895
abs structure param	0.014(7)

[ReOCl$_3$(2g)] (7g)

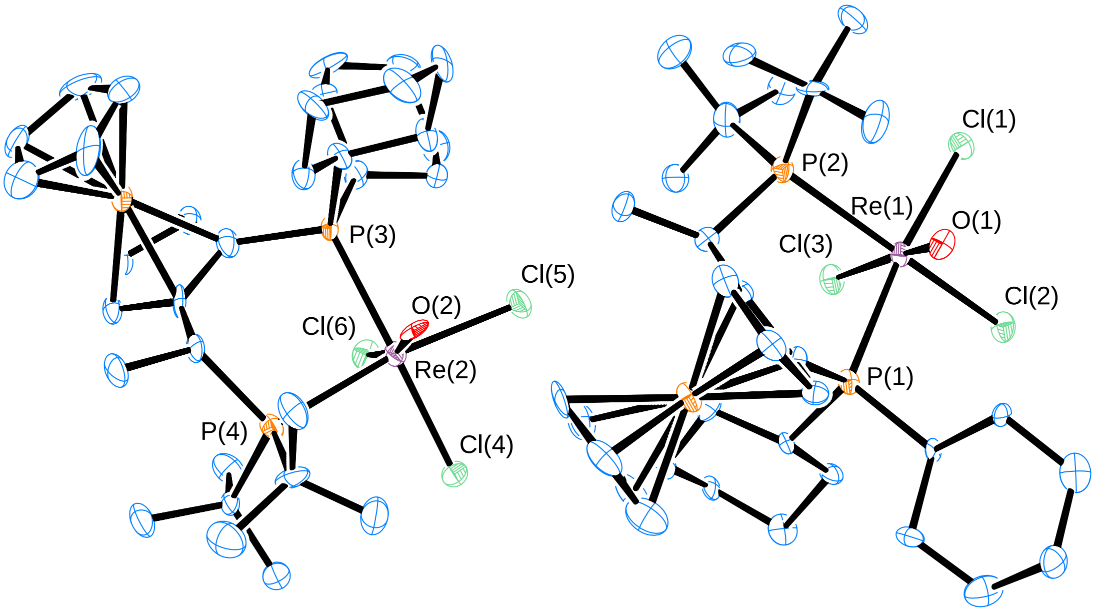

Color, shape	Brown plates
Empirical formula	$C_{32}H_{52}Cl_3FeOP_2Re$
fw	863.08
Temp, K	100(2)
Wavelenght, Å	0.71073
Cryst syst	Orthorombic
Space group	P 21 21 2
Unit cell dimens (Å/deg)	
a	28.090(3)
b	29.380(3)
c	9.7645(11)
α	90.0
β	90.0
γ	90.0
V, Å^3	8058.4(15)
Z	8
D (calcd), g/cm^3	1.423
abs coeff, mm^{-1}	3.661
θ range for data collcn, deg	1.39 to 28.31
Index ranges	$-37 \leq h \leq 37$, $-38 \leq k \leq 39$, $-12 \leq l \leq 13$
no. of collcd rflns	83045
Refinement method	Full-matrix least-squares on F^2
no. of data/restraints/params	20018/ 24 / 721
Goodness of fit	1.079
Final *R* index ($I>2\sigma(I)$)	R1 = 0.0719, wR2 = 0.1742
R indices (all data)	R1 = 0.0956, wR2 = 0.1845
abs structure param	0.021(10)

exo-[ReOCl$_3$(2i)]•CH$_2$Cl$_2$ (7i)

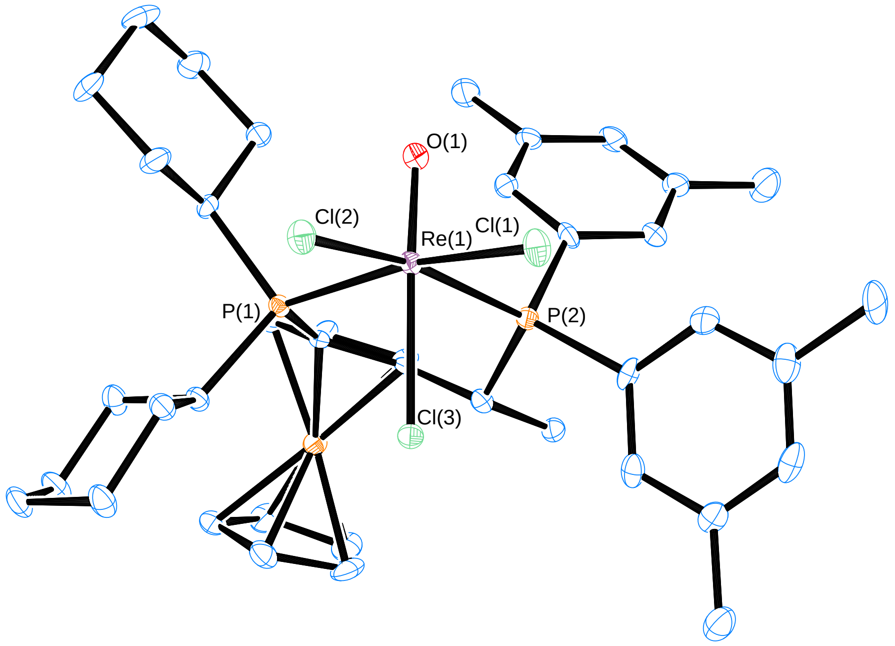

Color, shape	Dark purple prism
Empirical formula	C$_{41}$H$_{54}$Cl$_5$FeOP$_2$Re
fw	1044.08
Temp, K	100(2)
Wavelenght, Å	0.71073
Cryst syst	Orthorombic
Space group	P 21 21 21
Unit cell dimens (Å/deg)	
a	13.462(2)
b	14.816(2)
c	21.347(4)
α	90.0
β	90.0
γ	90.0
V, Å^3	4257.9(12)
Z	4
D (calcd), g/cm^3	1.629
abs coeff, mm^{-1}	3.602
θ range for data collcn, deg	1.67 to 28.31
Index ranges	$-17 \leq h \leq 17$, $-19 \leq k \leq 19$, $-28 \leq l \leq 28$
no. of collcd rflns	44108
Refinement method	Full-matrix least-squares on F^2
no. of data/restraints/params	10542/ 0 / 465
Goodness of fit	1.004
Final R index ($I>2\sigma(I)$)	R1 = 0.0337, wR2 = 0.0707
R indices (all data)	R1 = 0.0365, wR2 = 0.0716
abs structure param	0.003(5)

***exo*-[ReOCl$_3$(2l)] (7l)**

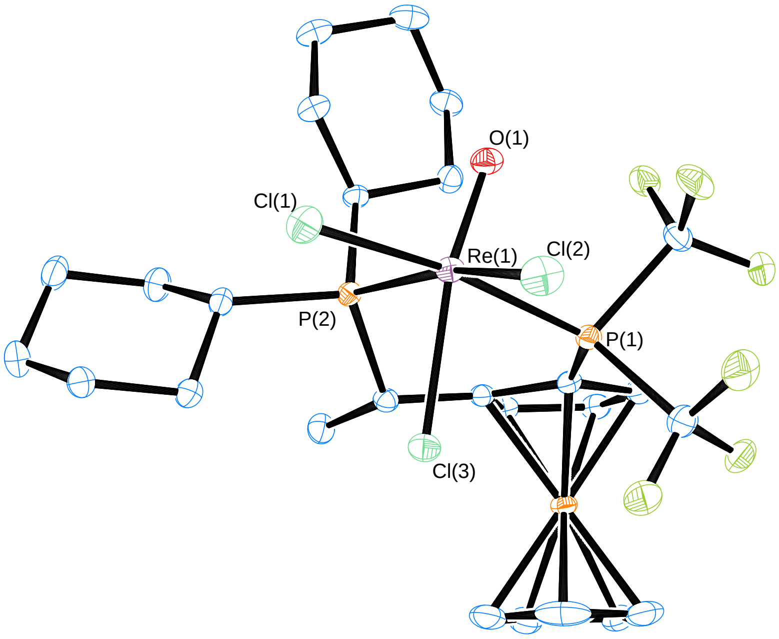

Color, shape	Dark red needles
Empirical formula	$C_{26}H_{34}Cl_3F_6FeOP_2Re$
fw	886.87
Temp, K	100(2)
Wavelenght, Å	0.71073
Cryst syst	Monoclinic
Space group	P 2(1)
Unit cell dimens (Å/deg)	
a	9.2581(4)
b	12.4984(5)
c	13.5508(6)
α	90.0
β	105.1050(10)
γ	90.0
V, Å^3	1513.81(11)
Z	2
D (calcd), g/cm^3	1.946
abs coeff, mm^{-1}	4.902
θ range for data collcn, deg	1.56 to 32.58
Index ranges	$-14 \leq h \leq 14$, $-18 \leq k \leq 18$, $-20 \leq l \leq 20$
no. of collcd rflns	52310
Refinement method	Full-matrix least-squares on F^2
no. of data/restraints/params	11018/ 1 / 361
Goodness of fit	0.990
Final *R* index ($I>2\sigma(I)$)	R1 = 0.0236, wR2 = 0.0497
R indices (all data)	R1 = 0.0248, wR2 = 0.0501
abs structure param	0.056(3)

$[ReOBr_4(2a(\kappa O\text{-}OPPh_2))]\cdot CH_2Cl_2$ (8)

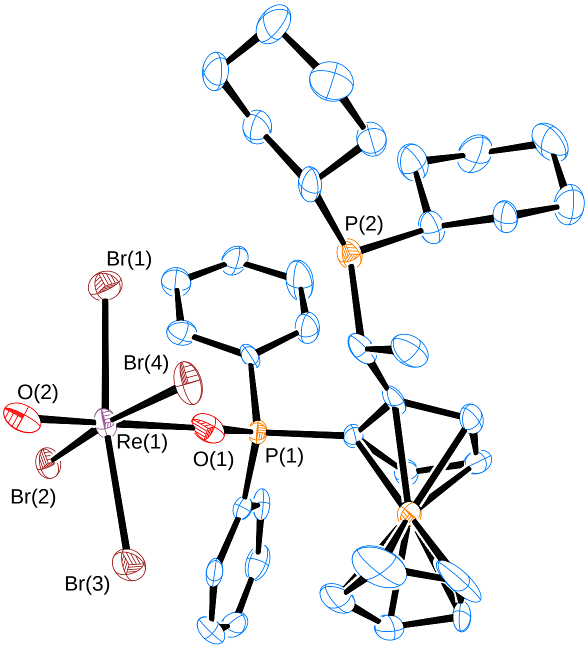

Color, shape	Orange plates
Empirical formula	$C_{37}H_{46}Br_4Cl_2FeO_2P_2Re$
fw	1217.27
Temp, K	100(2)
Wavelenght, Å	0.71073
Cryst syst	Monoclinic
Space group	P 21
Unit cell dimens (Å/deg)	
a	10.3987(8)
b	20.5590(16)
c	11.0074(8)
α	90.0
β	117.509(2)
γ	90.0
V, $Å^3$	2087.2(3)
Z	2
D (calcd), g/cm^3	1.937
abs coeff, mm^{-1}	7.310
θ range for data collcn, deg	1.98 to 28.33
Index ranges	$-13 \leq h \leq 13$, $-27 \leq k \leq 27$, $-14 \leq l \leq 14$
no. of collcd rflns	21650
Refinement method	Full-matrix least-squares on F^2
no. of data/restraints/params	10251/ 37 / 443
Goodness of fit	1.023
Final *R* index ($I>2\sigma(I)$)	R1 = 0.0557, wR2 = 0.1223
R indices (all data)	R1 = 0.0679, wR2 = 0.1282
abs structure param	0.015(10)

$[ReOCl_4(2c(\kappa O\text{-}OPPh_2))]\cdot 2CH_2Cl_2$ (9)

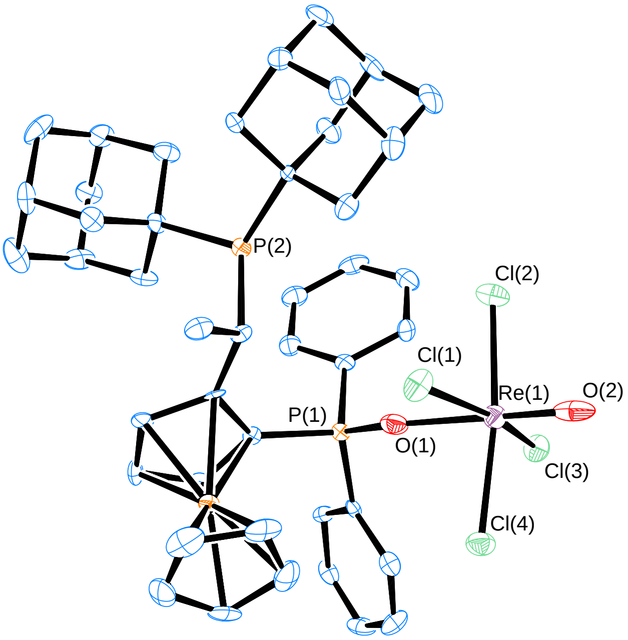

Color, shape	Orange prism
Empirical formula	$C_{46}H_{56}Cl_8FeO_2P_2Re$
fw	1228.50
Temp, K	100(2)
Wavelenght, Å	0.71073
Cryst syst	Triclinic
Space group	P 1
Unit cell dimens (Å/deg)	
a	10.2960(18)
b	11.199(2)
c	11.698(2)
α	76.420(3)
β	76.308(3)
γ	64.342(3)
V, Å^3	1167.7(4)
Z	1
D (calcd), g/cm^3	1.747
abs coeff, mm^{-1}	3.465
θ range for data collcn, deg	1.81 to 28.30
Index ranges	$-13 \le h \le 13, -14 \le k \le 14, -15 \le l \le 15$
no. of collcd rflns	11916
Refinement method	Full-matrix least-squares on F^2
no. of data/restraints/params	10375/ 33 / 542
Goodness of fit	0.861
Final *R* index ($I>2\sigma(I)$)	R1 = 0.0494, wR2 = 0.0984
R indices (all data)	R1 = 0.0527, wR2 = 0.1001
abs structure param	0.002(5)

endo-[ReNCl$_2$(2a)]•CH$_2$Cl$_2$ (11)

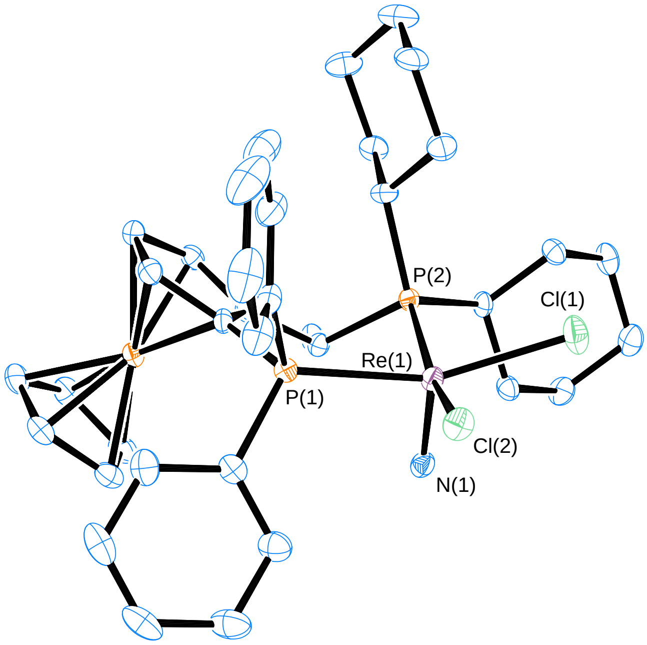

Color, shape	Red prism
Empirical formula	$C_{37}H_{46}Cl_4FeNP_2Re$
fw	950.54
Temp, K	100(2)
Wavelenght, Å	0.71073
Cryst syst	Orthorombic
Space group	P 21 21 21
Unit cell dimens (Å/deg)	
a	14.4860(8)
b	15.1277(9)
c	16.7449(9)
α	90.0
β	90.0
γ	90.0
V, Å^3	3669.5(4)
Z	4
D (calcd), g/cm^3	1.721
abs coeff, mm^{-1}	4.098
θ range for data collcn, deg	1.81 to 28.32
Index ranges	$-19 \leq h \leq 19$, $-20 \leq k \leq 20$, $-22 \leq l \leq 22$
no. of collcd rflns	38022
Refinement method	Full-matrix least-squares on F^2
no. of data/restraints/params	9100/ 0 / 145
Goodness of fit	1.004
Final *R* index ($I>2\sigma(I)$)	R1 = 0.0258, wR2 = 0.0565
R indices (all data)	R1 = 0.0273, wR2 = 0.0569
abs structure param	-0.006(4)

[ReO(OEt)Cl$_2$(2a)] (12)

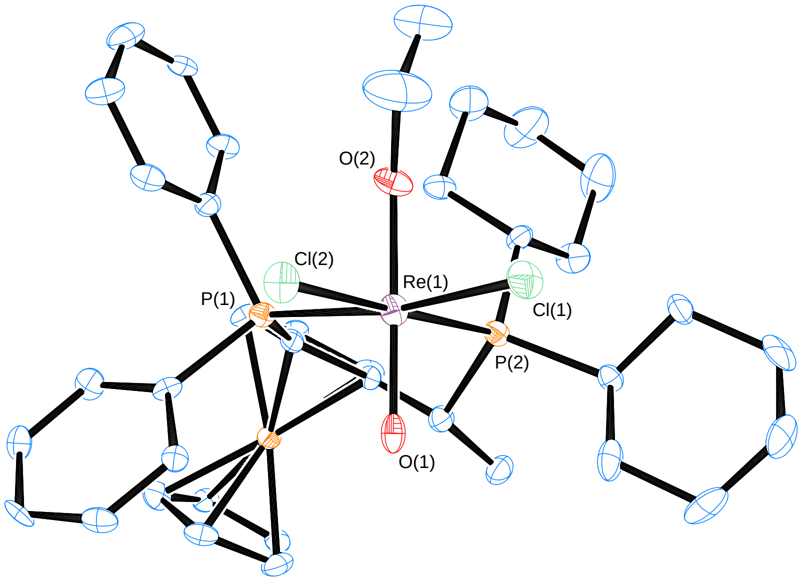

Color, shape	Orange prism
Empirical formula	$C_{38}H_{49}Cl_2FeO_2P_2Re$
fw	912.66
Temp, K	100(2)
Wavelenght, Å	0.71073
Cryst syst	Hexagonal
Space group	P 65
Unit cell dimens (Å/deg)	
a	11.5662(9)
b	11.5662(9)
c	46.144(5)
α	90.0
β	90.0
γ	120.0
V, Å^3	5346.0(8)
Z	6
D (calcd), g/cm^3	1.701
abs coeff, mm^{-1}	4.074
θ range for data collcn, deg	2.03 to 28.44
Index ranges	$-15 \le h \le 15$, $-15 \le k \le 15$, $-61 \le l \le 61$
no. of collcd rflns	49108
Refinement method	Full-matrix least-squares on F^2
no. of data/restraints/params	8865/ 31 / 415
Goodness of fit	1.191
Final *R* index ($I>2\sigma(I)$)	R1 = 0.0603, wR2 = 0.1042
R indices (all data)	R1 = 0.0697, wR2 = 0.1064
abs structure param	0.025(9)

[ReO(*i*-PrO)Cl_2(2a)] (18)

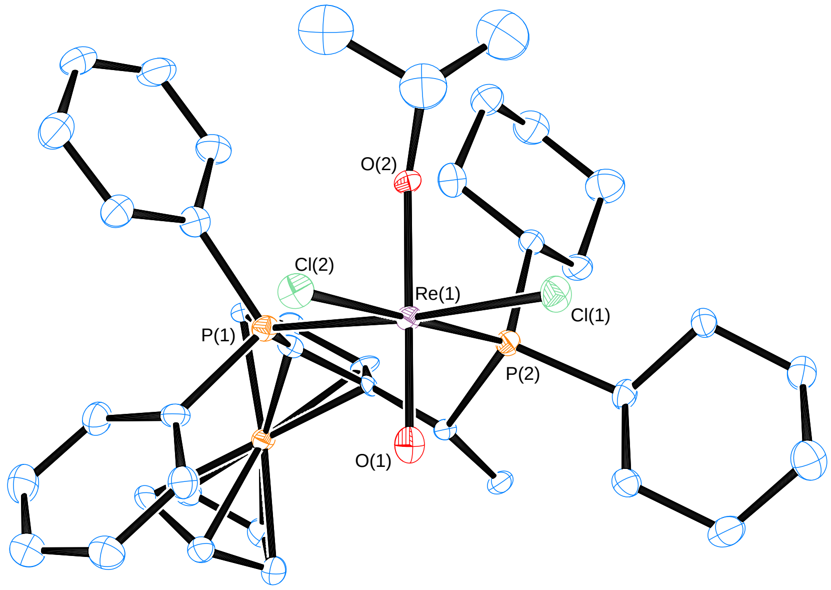

Color, shape	Orange needles
Empirical formula	$C_{39}H_{51}Cl_2FeO_2P_2Re$
fw	926.69
Temp, K	100(2)
Wavelenght, Å	0.71073
Cryst syst	Orthorombic
Space group	P 21 21 21
Unit cell dimens (Å/deg)	
a	14.746(4)
b	14.833(4)
c	16.899(4)
α	90.0
β	90.0
γ	90.0
V, $Å^3$	3706.4(16)
Z	4
D (calcd), g/cm^3	1.661
abs coeff, mm^{-1}	3.919
θ range for data collcn, deg	1.82 to 27.50
Index ranges	$-19 \leq h \leq 19$, $-19 \leq k \leq 19$, $-21 \leq l \leq 21$
no. of collcd rflns	35929
Refinement method	Full-matrix least-squares on F^2
no. of data/restraints/params	8502/ 282 / 427
Goodness of fit	1.070
Final *R* index ($I>2\sigma(I)$)	R1 = 0.0639, wR2 = 0.1150
R indices (all data)	R1 = 0.0776, wR2 = 0.1197
abs structure param	0.012(10)

[ReCl$_3$(19a)] (23a)

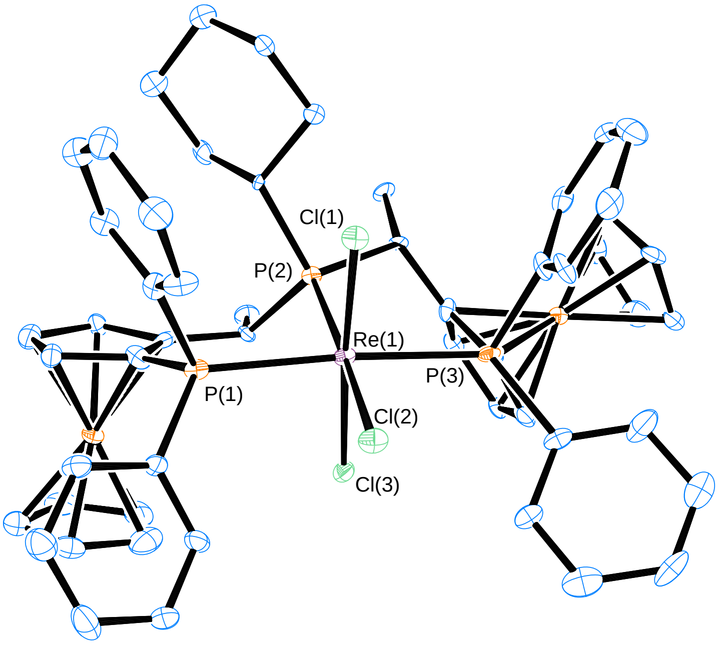

Color, shape	Brown needles
Empirical formula	$C_{54}H_{55}Cl_3Fe_2P_3Re$
fw	1201.14
Temp, K	100(2)
Wavelenght, Å	0.71073
Cryst syst	Orthorombic
Space group	P 21 21 21
Unit cell dimens (Å/deg)	
a	16.041(3)
b	33.811(5)
c	9.8570(16)
α	90.0
β	90.0
γ	90.0
V, Å^3	5346.2(15)
Z	4
D (calcd), g/cm^3	1.492
abs coeff, mm^{-1}	3.068
θ range for data collcn, deg	1.20 to 28.38
Index ranges	$-21 \le h \le 21$, $-44 \le k \le 45$, $-13 \le l \le 13$
no. of collcd rflns	55833
Refinement method	Full-matrix least-squares on F^2
no. of data/restraints/params	13353/ 378 / 571
Goodness of fit	1.123
Final *R* index ($I>2\sigma(I)$)	R1 = 0.0614, wR2 = 0.1211
R indices (all data)	R1 = 0.0733, wR2 = 0.1252
abs structure param	0.036(8)

[ReH_5(19a)]•2C_6H_6 (24)

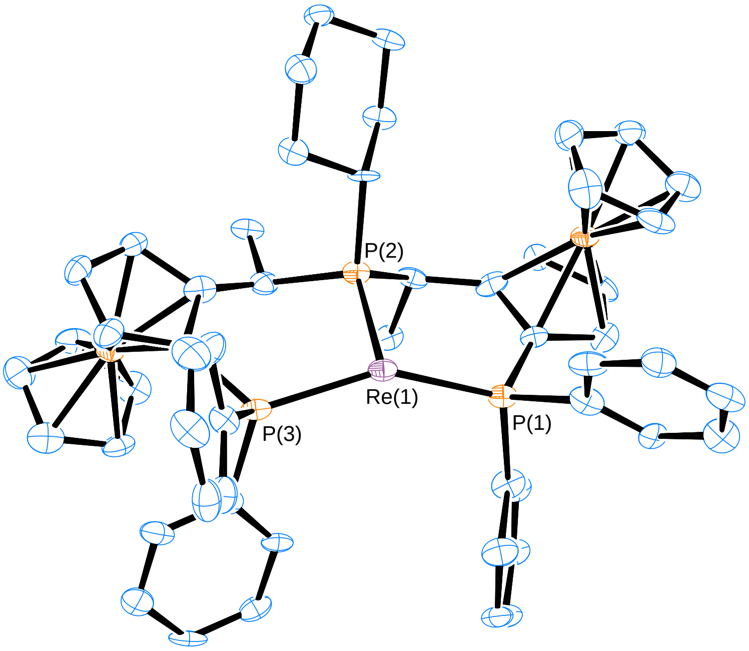

Color, shape	Yellow needles
Empirical formula	$C_{66}H_{67}Fe_2P_3Re$
fw	1251.01
Temp, K	100(2)
Wavelenght, Å	0.71073
Cryst syst	Orthorombic
Space group	P 21 21 21
Unit cell dimens (Å/deg)	
a	9.7567(13)
b	17.805(2)
c	31.703(4)
α	90.0
β	90.0
γ	90.0
V, $Å^3$	5507.5(12)
Z	4
D (calcd), g/cm^3	1.509
abs coeff, mm^{-1}	2.841
θ range for data collcn, deg	1.31 to 25.04
Index ranges	$-11 \leq h \leq 11$, $-21 \leq k \leq 21$, $-37 \leq l \leq 37$
no. of collcd rflns	120974
Refinement method	Full-matrix least-squares on F^2
no. of data/restraints/params	9751/ 24 / 650
Goodness of fit	1.215
Final *R* index ($I>2\sigma(I)$)	R1 = 0.0555, wR2 = 0.1302
R indices (all data)	R1 = 0.0674, wR2 = 0.1359
abs structure param	-0.010(5)

7.2. Publications

Parts of this work are subject of the following paper:

> "Rhenium Chloro- and Polyhydride Complexes with the Chiral Tridentate Ferrocenyl Ligand Pigiphos". E. Mejía and A. Togni. *Organometallics,* **2011**, *30*, 4765-4770

Some of the complexes synthesized in this work have been referenced in:

> "Solvias Josiphos Ligands: From Discovery to Technical Applications". H.-U. Blaser, B. Pugin, F. Spindler, E. Mejía, A. Togni, in *Privileged Chiral Ligands and Catalysts*, 1 ed. (Ed.: Q.-L. Zhou), Wiley-VCH, Weinheim, **2011**, pp. 93-136.

7.3. Participations in Conferences and Symposia

Oral Presentations:

"Rhenium-Catalyzed Trifluoromethylation of Arenes and Heteroarenes by Hypervalent Iodine Reagents"

> SCS Fall Meeting (Fall Meeting and General Assembly of the Swiss Chemical Society), September 9, **2011**. Lausanne, Switzerland.

"New Rhenium Complexes With Chiral Ferrocenyl Ligands: Synthesis and Catalytical Behaviour"

> LAC Mini Symposium (Laboratorium für Anorganische Chemie, ETH Zürich), December 9, **2009**, Zürich, Switzerland.

Posters:

"Rhenium-Catalyzed Trifluoromethylation of Arenes and Heteroarenes by Hypervalent Iodine Reagents"

> OMCOS 16 (16th IUPAC International Symposium on Organometallic Chemistry), July 24–28, **2011**, Shanghai, China.

"New Chiral Rhenium Complexes for Homogeneous Catalysis"

SCS Fall Meeting (Fall Meeting and General Assembly of the Swiss Chemical Society), September 16, **2010**. Zürich, Switzerland. Awards: *Poster Prize* in the area of Inorganic Chemistry.

24th ICOMC (XXIV International Conference on Organometallic Chemistry), July 18-23, **2010**, Taipei, Taiwan.

CaRLa Winter School (Catalysis Research Laboratory, University of Heidelberg - BASF), March **2010,** Heidelgerg, Germany.

"Synthesis of New Rhenium Complexes with Chiral Ferrocenyl Ligands"

SCS Fall Meeting (Fall Meeting and General Assembly of the Swiss Chemical Society), September 4, **2009**, Lausanne, Switzerland.

EuCOMC XVIII (XVIII EuCheMS Conference on Organometallic Chemistry), June 22-25, **2009**, Gothenburg, Sweden.

7.4. Curriculum Vitae

Full name	Oscar Esteban Mejía Vargas
Nationality	Colombian
Date of birth	02.02.1981
Place of birth	Medellín, Colombia
Education	
Dates	January 2008 - December 2011
Title of qualification awarded	Doctor of Sciences
Thesis Advisor	Prof. Dr. Antonio Togni
Institution	Swiss Federal Institute of Technology (ETH Zürich), Wolfgang-Pauli-Strasse 10, 8093 Zurich (Switzerland)
Dates	August 2005 - December 2007
Title of qualification awarded	Master of Sciences - Chemistry
Thesis Advisor	Prof. Dr. Ricardo Fierro
Title of the thesis	“New Organometallic Titanium Compounds with Chalcogen-Ether Type Ligands: Synthesis, Characterization and Use in Styrene Polymerization”
Institution	National University of Colombia, Calle 45 No. 30-02, 111321 Bogotá (Colombia)
Dates	August 1999 - December 2004
Title of qualification awarded	Chemist
Undergraduate Thesis Advisor	Prof. Dr. Ricardo Fierro
Title of the thesis	"Synthesis of a Novel Organometallic Compound With Possible Application in Stereoselective Catalysis"
Awards	Meritorious Mention (National University of Colombia, 2005). National Contest of Best Undergraduate Thesis, 3rd Place in the area of Natural Sciences (National University of Colombia, 2006).
Institution	National University of Colombia, Calle 45 No. 30-02, 111321 Bogotá (Colombia)

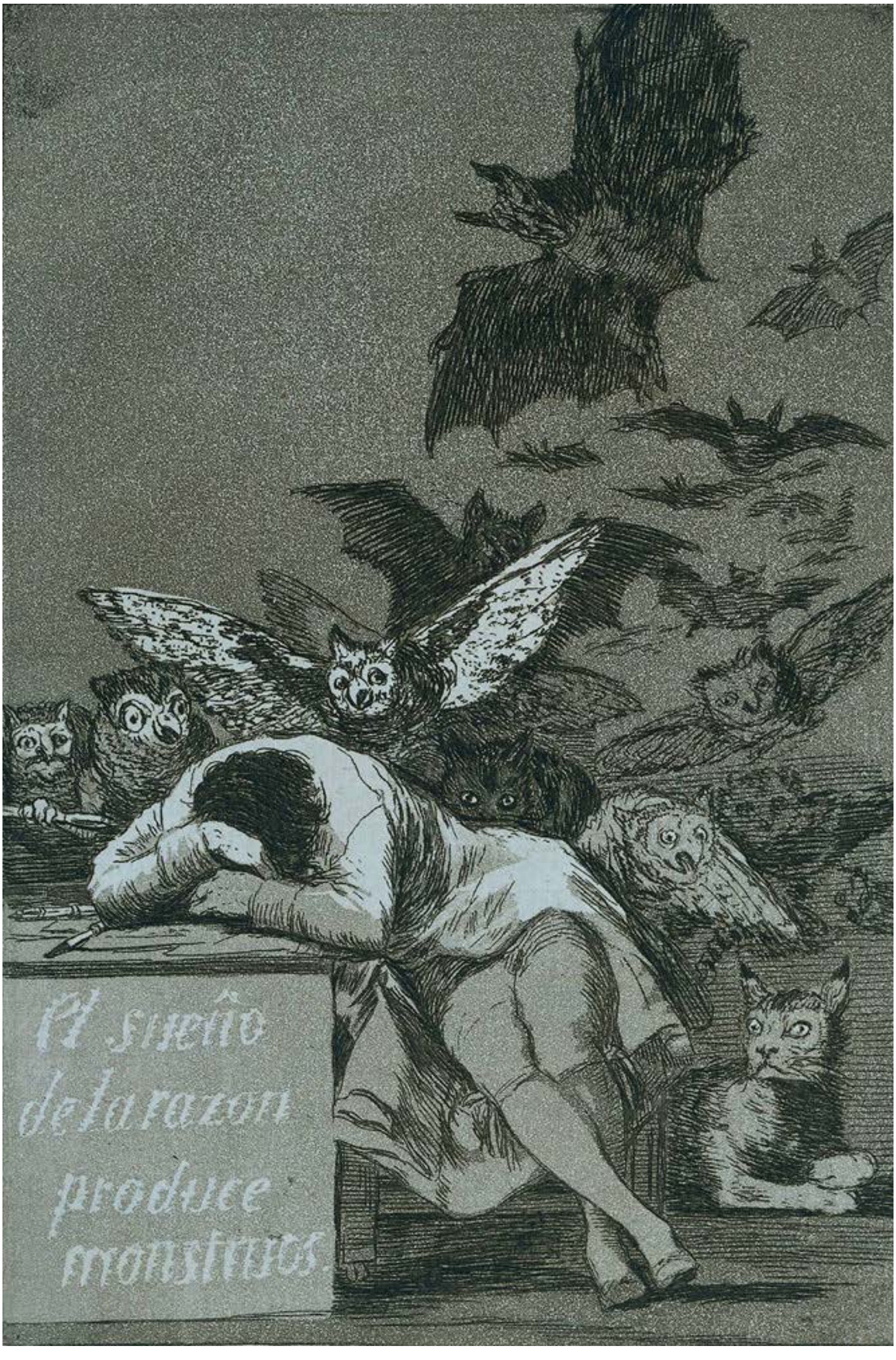
El sueño
de la razon
produce
monstruos.

por Fin